Journal of Thoracic Disease

Volume 6 Number 7 July 2014 Pages 864-1016; E148-E162

Vol 6, No 7 July 2014

ISSN 2072-1439

JOURNAL of THORACIC DISEASE

www.jthoracdis.com

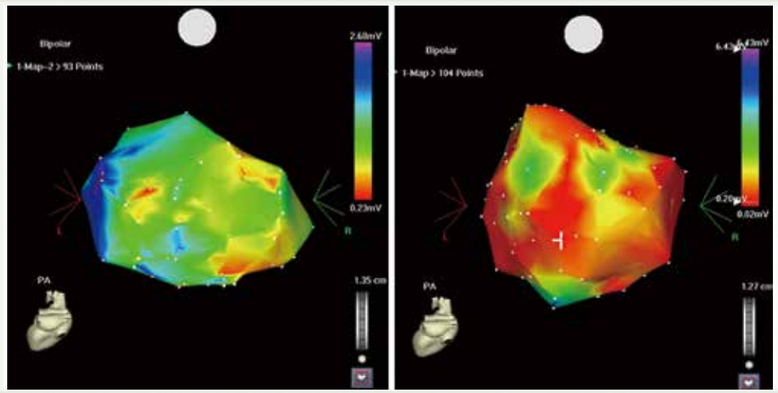

Published by Pioneer Bioscience Publishing Company

Indexed in PubMed, SCI

Indexed in PubMed

Aims and Scope

The *Journal of Thoracic Disease* (JTD, J Thorac Dis, pISSN: 2072-1439; eISSN: 2077-6624) was founded in Dec 2009, indexed in Pubmed/Pubmed Central in Dec 2011, and Science Citation Index (SCI) on Feb 4, 2013. It is published quarterly (Dec 2009- Dec 2011), bimonthly (Jan 2012- Dec 2013), and monthly (Jan 2014-), and openly distributed worldwide. JTD publishes manuscripts that describe new findings in the field to provide current, practical information on the diagnosis and treatment of conditions related to thoracic disease (lung disease, cardiac disease, breast disease and esophagus disease). Original articles are considered most important and will be processed for rapid review by the members of Editorial Board. Clinical trial notes, Cancer genetics reports, Epidemiology notes and Technical notes are also published. Case reports implying new findings that have significant clinical impact are carefully processed for possible publication. Review articles are published in principle at the Editor's request. There is no fee involved throughout the publication process. The acceptance of the article is based on the merit of quality of the manuscripts. All the submission and reviewing are conducted electronically so that rapid review is assured.

The Official Publication of:

- Guangzhou Institute of Respiratory Disease (GIRD)
- China State Key Laboratory of Respiratory Disease
- First Affiliated Hospital of Guangzhou Medical University
- Society for Thoracic Disease (STD)

Endorsed by:

- International COPD Coalition (ICC)

Editorial Correspondence

Daoyuan Wang, MD
Managing Editor
Pioneer Bioscience Publishing Company
Address: 9A Gold Shine Tower, 346-348 Queen's Road Central, Sheung Wan, Hong Kong. Tel: +852 3488 1279; Fax: +852 3488 1279.
Email: jtd@thepbpc.org
www.jthoracdis.com

Note to NIH Grantees

Pursuant to NIH mandate, Pioneer Bioscience Publishing Company will post the accepted version of contributions authored by NIH grant-holders to PubMed Central upon acceptance. This accepted version will be made publicly available 2 months after publication. For further information, see www.thepbpc.org

Conflict of Interest Policy for Editors

The full policy and the Editors' disclosure statements are available online at: www.jthoracdis.com

Disclaimer

The Publisher and Editors cannot be held responsible for errors or any consequences arising from the use of information contained in this journal; the views and opinions expressed do not necessarily reflect those of the Publisher and Editors, neither does the publication of advertisements constitute any endorsement by the Publisher and Editors of the products advertised.

Cover image:

The bronchoscopy procedure(left) is a CARTO map in a normotensive patient. The red color indicates the low-voltage zone (LVZ); (right) is a CARTO map in a hypertensive patient. Comparison of the two maps shows that there is a much larger LVZ in the patient with hypertension (See P916 in this issue).

For submission instructions, subscription and all other information visit www.jthoracdis.com

Table of Contents

Editorial

Original Article

Brief Report

Clinical Nursing

Surgical Technique

Case Report

Letter to the Editor

Editorial

Editorial

Breast cancer in Egypt, China and Chinese: statistics and beyond

Hamdy A. Azim[1], Amal S. Ibrahim[2]

[1]Clinical Oncology Department, Faculty of Medicine, Cairo University, Egypt; [2]Epidemiology Department, National Cancer Institute, Cairo University, Egypt

Correspondence to: Hamdy A. Azim. The Department of Clinical Oncology, Cairo University, Giza, Egypt. Email: azimonc@cairocure.com.

Submitted Jun 11, 2014. Accepted for publication Jun 15, 2014.
doi: 10.3978/j.issn.2072-1439.2014.06.38
View this article at: http://dx.doi.org/10.3978/j.issn.2072-1439.2014.06.38

According to the latest report of The International Agency for Research on Cancer (GLOBOCAN 2012), breast cancer (BC) is by far the world's most common cancer among women, and the most likely cause that a woman will die from cancer worldwide (1).

The disease is reported as the most frequent cancer among women in 140 of 184 countries worldwide including China the world's most populous country (1,2). Notably, the incidence rates of BC varies dramatically across the globe, being always highest in more developed regions, namely North America, Western Europe (more than 90 new cases/10^5 women annually), compared with less than 30/10^5 women annually in regions like Eastern Asia (1). In the current issue of *JTD*, Zeng *et al.* (3), have published the first national dataset on the incidence and mortality of female BC in China, for the year 2010, highlighting also some trends in incidence, and mortality, in different geographical regions within China. The authors should be commended for being the first to provide the literature with a wealth of data regarding BC statistics in China, which harbors around one fifth of all women around the world. According to the authors' estimations, the age standardized incidence rate (ASIR) of BC is 24.2/10^5 and age standardized mortality rate (ASMR) is 6.36/10^5. As such, these figures would confirm the known fact, that the mainland Chinese women have one of lowest BC incidence and mortality rates, when compared to the rest of the world.

Two important questions should be raised with this kind of findings: how far the authors could accurately quantify BC burden (occurrence and outcome) in China? and if their figures are true, then why the mainland Chinese women are so much protected against BC versus Chinese women in other Asian or western counties?

To start with, we need to emphasize that Zeng *et al.* analysis included only 12.96% of the female population of China. This means that the vast majority of Chinese women are not truly represented in their analysis, especially in the western region (less than 10% of their sample size), where the incidence is ~30% less than that reported in other areas. Obviously, "a cautious interpretation" is warranted with this kind of national epidemiological studies, when so many regions in a given country have low or no accurate registry data. Nonetheless, this is a common situation in many countries with emerging population-based registries (4). For instance, in Egypt; with its much smaller scale in geographical and population size, a network of five regional population-based registries, spreading over the whole country, was developed during the last two decades. For the sake of national cancer statistics, Egypt was divided into three regions namely upper, middle and lower Egypt. One or more defined states (governorates), with a regional population-based registry, were selected to represent each region (4). The data evolved on cancer incidence from each cancer registry were extrapolated in a similar methodology like that adopted by Chinese group. BC is estimated to be the most common female cancer in both China and Egypt, despite a marked difference in incidence rates, being much higher among Egyptian women compared to Chinese (ASIR are 48.8/10^5 and 24.2/10^5 respectively) (3,4). In the two countries BC incidence differs considerably among rural and urban populations, with the higher urban incidence being consistent across all women above the age of 45 years (3,5). A similar observation was also found in many developing countries like India, where BC incidence in rural registry of Barshi was 7.2/10^5 compared to 31.3/10^5 in adjoining city of Mumbai (6). In fact, the urban population in developing countries, might suffer from a higher exposure to xenoestrogens, which have been linked to evolution of hormone receptor positive BC in industrialized countries (7).

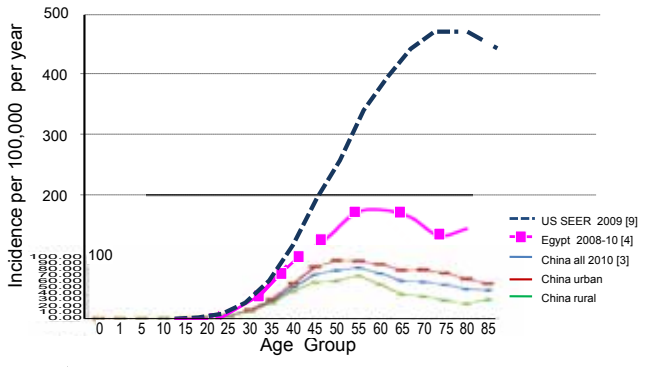

Figure 1 Age specific incidence rates of breast cancer in China, Egypt, and USA.

Pattern of age specific incidence of BC from east to west

Like other countries the age-specific incidence rates in both Egypt and China show a progressive increase after the age of 30 years, to reach a sharp peak of 80/10^5 at the age group of 55-59 years in China, versus a sharp peak of 177.4/10^5 at the age group of 60-64 years in Egypt (3,4). Importantly, in both countries there was a gradually decline in the age-specific incidence thereafter. This pattern of the age specific incidence is in clear contradistinction with western countries, where a continuous rise in BC incidence is observed with increasing age, to reach a peak of ~450/10^5, at the age 80 years, thus rendering the differences in age-specific incidence especially large in elderly women (8-10) (*Figure 1*).

We do not know whether this difference is completely real, or it is partially induced by under-reporting of BC cases specifically among elderly patients, in countries with emerging cancer registry programs. Notably, a pattern of BC age specific incidence, similar to that seen in China and Egypt, has been reported in some Asian countries with a completed national cancer registries like Japan and Singapore (11,12). This would certainly challenge the rule of "The Older the Age; The Higher the BC Risk", which might not be a default hypothesis, when it comes to North African and East Asian women.

Are the mainland Chinese women more protected from BC?

The reasons for the wide international variation in incidence rates of BC are not fully explained. However, it seems true that the low-risk Chinese (and other Asian) populations are enjoying a multitude of biological and lifestyle features that collectively provide a significant protection against the development of BC. In a cross sectional study, Chinese women were found to be significantly less obese (~14 kg less), have their menarche a year later, are more often parous, and consume a lower western diet , compared to Caucasian women (13). The protective effect of Chinese diet was highly emphasized during the last decade. In one study on 1,602 BC women and 1,500 healthy women, all living in Shanghai, it was found that a "meat and sweet" western-style diet was independently associated with a 60% increased risk of BC, compared to a "soy and vegetable" traditional Chinese diet (14). The effect was more significant for estrogen-receptor positive tumors, where the risk of getting this phenotype of BC was almost doubled, among women utilizing western diet (14). A recent meta-analysis, found that the Chinese diet intake is associated with a 41% reduction in BC risk among Asian women (15). This main part explain why Chinese women migrating to North America, adopting a westernized lifestyle, will show a significant rise of BC incidence over a few generations (10,16). Taken together, lifestyle and socio-demographic factors stand as major players in the low BC burden, reported in China and other developing East Asian countries. However and in spite of the major similarities in lifestyle, the incidence rate of BC among Chinese women in the mainland is strikingly lower than that reported for Chinese women in other Asian countries. For example, in Singapore, where a complete national registry coverage is accomplished, an ASIR of 63.7/10^5 has been reported among the Chinese population there (12). Similar figures were also reported in Hong Kong (61/10^5) (17) and Malaysian Chinese (59.9/10^5) (18), with a somewhat lower incidence among Taiwanese women (44.45/10^5) (19) (*Table 1*).

It does not seem that, factors like life expectancy, more urbanization and presence of BC screening programs, can fully explain a 2-3 fold decrease in BC incidence among the mainland Chinese women, compared to Chinese women in other far east countries.

In conclusion, many factors can be directly responsible for the large variation in BC epidemiology across the globe; including life style, life expectancy, wide spread use of screening mammography and accuracy of national cancer statistics. The later factor is specifically crucial in developing countries, where the emerging population—based cancer registries may suffer from under—recording of some of the occurring BC (as well as other cancers). We believe that a wider expansion of the national cancer registries in both

Table 1 Breast cancer ASIR and ASMR for East and West Chinese women

Chinese population	ASIR[+]	ASMR[++]
Chinese Mainland [3]	24.2	6.36
Chinese Singapore [12]	63.7	14.2
Chinese Hong Kong [17]	59.9	NA*
Chinese Malaysia [18]	61	9.1
Chinese Taiwan [19]	44.45	NA*
Chinese US [16]	73.5	11.5 [10]**

[+]ASIR, age standardized incidence rate; [++]ASMR, age standardized mortality rate; *NA, not available in the published reference; **, for all Asian-Americans.

China as well as Egypt, will be able to answer some of the many questions, related to variations in BC statistics in the developing countries.

Acknowledgements

Disclosure: The authors declare no conflict of interest.

References

1. Ferlay J, Soerjomataram I, Ervik M, et al. GLOBOCAN 2012 v1.0, Cancer Incidence and Mortality Worldwide (2013). IARC CancerBase No. 11 Lyon, France: International Agency for Research on Cancer. Available online: http://globocan.iarc.fr/
2. Chen W, Zheng R, Zhang S, et al. Annual report on status of cancer in China, 2010. Chin J Cancer Res 2014;26:48-58.
3. Zeng H, Zheng R, Zhang S, et al. Female breast cancer statistics of 2010 in China: estimates based on data from 145 population-based cancerregistries. J Thorac Dis 2014;6:466-70.
4. Ibrahim A, Khaled H, Mikhail N, et al. Cancer Incidence in Egypt: Results of the National Population-Based Cancer Registry Program. Journal of Cancer Epidemiology 2014. Available online: http://cancerregistry.gov.eg/publications.aspx
5. Dey S, Soliman AS, Hablas A, et al. Urban-rural differences in breast cancer incidence in Egypt (1999-2006). Breast 2010;19:417-23.
6. Risk Factors for Breast Cancer in India: an INDOX Case-Control Study. Available online: INDOX Cancer Research Network. 2010.
7. Brody JG, Moysich KB, Humblet O, et al. Environmental pollutants and breast cancer: epidemiologic studies. Cancer 2007;109:2667-711.
8. Mistry M, Parkin DM, Ahmad AS, et al. Cancer incidence in the United Kingdom: projections to the year 2030. Br J Cancer 2011;105:1795-803.
9. Howlader N, Noone AM, Krapcho M, et al. eds. SEER Cancer Statistics Review, 1975-2009 (Vintage 2009 Populations), National Cancer Institute. Bethesda, MD, 2012. Retrieved September 7, 2012.
10. DeSantis C, Ma J, Bryan L, et al. Breast cancer statistics, 2013. CA Cancer J Clin 2014;64:52-62.
11. Tominaga S, Kuroishi T. Epidemiology of breast cancer in Japan. Cancer Lett 1995;90:75-9.
12. Peng LH, Ling C, Yew CK, et al. Singapore Cancer Registry Interim Annual Registry Report Trends in Cancer Incidence in Singapore 2008-2012. National Registry of Diseases Office (NRDO).
13. Tam CY, Martin LJ, Hislop G, et al. Risk factors for breast cancer in postmenopausal Caucasian and Chinese-Canadian women. Breast Cancer Res 2010;12:R2.
14. Cui X, Dai Q, Tseng M, et al. Dietary patterns and breast cancer risk in the shanghai breast cancer study. Cancer Epidemiol Biomarkers Prev 2007;16:1443-8.
15. Chen M, Rao Y, Zheng Y, et al. Association between soy isoflavone intake and breast cancer risk for pre- and post-menopausal women: a meta-analysis of epidemiological studies. PLoS One 2014;9:e89288.
16. Gomez SL, Quach T, Horn-Ross PL, et al. Hidden breast cancer disparities in Asian women: disaggregating incidence rates by ethnicity and migrant status. Am J Public Health 2010;100 Suppl 1:S125-31.
17. Hong Kong Cancer Registry 2011. Available online: www.pco.org.hk
18. Abdullah NA, Wan Mahiyuddin WR, Muhammad NA, et al. Survival rate of breast cancer patients in Malaysia: a population-based study. Asian Pac J Cancer Prev 2013;14:4591-4.
19. Chiang CJ, Chen YC, Chen CJ, et al. Cancer trends in Taiwan. Jpn J Clin Oncol 2010;40:897-904.

Cite this article as: Azim HA, Ibrahim AS. Breast cancer in Egypt, China and Chinese: statistics and beyond. J Thorac Dis 2014;6(7):864-866. doi: 10.3978/j.issn.2072-1439.2014.06.38

Editorial

Advantages and drawbacks of long-term macrolide use in the treatment of non-cystic fibrosis bronchiectasis

Li-Chao Fan, Jin-Fu Xu

Department of Respiratory Medicine, Shanghai Pulmonary Hospital, Tongji University School of Medicine, Shanghai 200433, China
Correspondence to: Jin-Fu Xu, MD, PhD. Shanghai Pulmonary Hospital, Tongji University School of Medicine, No. 507 Zhengmin Road, Shanghai 200433, China. Email: jfxucn@gmail.com.

Abstract: Non-cystic fibrosis (non-CF) bronchiectasis is a respiratory disease characterized by persistent airway inflammation and dilation of bronchial wall driven by various causes. Patients with bronchiectasis suffer from excessive sputum production, recurrent exacerbations, and progressive airway destruction. Major therapy for bronchiectasis is focused on breaking the "vicious cycle" of mucus stasis, infection, inflammation, and airway destruction. Growing evidences have been shown that macrolides possess immunoregulatory and anti-inflammatory functions beyond their antimicrobial effects. Macrolide antibiotics have been effectively used in the treatment of diffuse panbronchiolitis, CF and bronchiolitis obliterans syndrome. Currently a number of clinical trials were performed to assess macrolide treatment in the management of non-CF bronchiectasis. The purpose of this paper is to review the efficacy and potential risks of these recent studies on the use of macrolides in non-CF bronchiectasis.

Keywords: Macrolides; bronchiectasis; advantages; drawbacks

Submitted Apr 17, 2014. Accepted for publication Jul 08, 2014.
doi: 10.3978/j.issn.2072-1439.2014.07.24
View this article at: http://dx.doi.org/10.3978/j.issn.2072-1439.2014.07.24

Non-cystic fibrosis (non-CF) bronchiectasis is an inflammatory respiratory disease characterized by chronic bacterial infection, and irreversible dilation of the bronchial walls. Some patients with bronchiectasis often suffer from chronic cough, excessive sputum production, and recurrent exacerbations. Left untreated, non-CF bronchiectasis is always associated with a very poor prognosis (1).

In clinical practice, the prevalent access to high-resolution computed tomography (HRCT) has resulted in the increased diagnosis of non-CF bronchiectasis cases. Trends in bronchiectasis diagnoses in the United States indicated the detection of 1,106 cases per 100,000 individuals, with an annual percentage increase of 8.74% (2). Further, the average annual hospitalization rate was 9.4 per 100,000 residents in Germany during 2005-2011, with the highest rates, 39.4 hospitalizations per 100,000 individuals, apparent among men aged 75-84 years (3). Until now, no accurate prevalence data was available to quantify the incidence of bronchiectasis in developing countries. However, morbidity rates in developing countries are typically elevated due to the inherently high burden of infectious disease.

Interventions for the management of bronchiectasis include treatment of the underlying disease, management of infections, promotion the clearance of mucus stasis, and the bolstering of immunity to break the "vicious cycle" (4). Evidence has indicated that 14- and 15-membered ring macrolides possess immunomodulation and anti-inflammatory functions beyond their antimicrobial properties (5). The underlying mechanisms that account for the anti-inflammatory actions of macrolides have not yet to be elucidated, and the activities do not appear to be controlled by a single mechanism. Nevertheless, investigations have shown that macrolides down-regulate cytokine production by blocking the activation of nuclear factor kappa B (NF-kappaB), and the phosphorylation of extracellular signal-regulated kinase 1/2 (ERK1/2). Likewise, the ability of macrolides to mediate the innate and adaptive immune responses by inhibiting neutrophil activation has been demonstrated (6).

As early as 1984, the effectiveness of macrolides for the treatment of inflammatory disease was apparent, as the

administration of erythromycin to patients with diffuse panbronchiolitis (DPB) led to dramatic increases in 10-year survival rates from 10-20% to over 90% (7). Further, published reports have demonstrated that macrolides provide compelling benefits in the treatment of DPB, CF, COPD and bronchiolitis obliterans syndrome (8-11). Currently, a number of clinical trials have elucidated the effects of macrolides in the treatment of non-CF bronchiectasis. Findings from studies have shown that when used as chronic maintenance therapies, macrolides could reduce the frequency and duration of infectious exacerbations, as well as decrease the volume of sputum production, improve quality of life, and attenuate lung function deterioration. However, prior studies have also indicated that the number of side effects, as well as resistance to macrolides, increased among treatment groups.

Studies have reported that long-term treatment with macrolides can decrease the frequency of pulmonary exacerbations. A randomized, doubled-blind, placebo-controlled trial involving the administration of azithromycin (500 mg) 3 times a week for 6 months resulted in a 62% relative reduction in the rate of exacerbations, compared to rates apparent following treatment with a placebo. The improvements continued for a 12-month period, and corresponded to a 42% relative reduction in the annual rate of exacerbations following treatment with azithromycin (P<0.0001). Additionally, the median time to a first exacerbation was 239 days in the azithromycin treatment group and 85 days in the placebo group (RR =0.44; 95% CI, 0.29-0.65; P<0.0001) (12). Another randomized, doubled-blind, placebo-controlled study reported that the number of exacerbations was significantly diminished following the daily administration of azithromycin (250 mg) for 12 months. The percentage of patients who had at least one exacerbation was reduced 33.5% in the azithromycin-treated group compared to treatment with the placebo (13). The time to a first exacerbation was also prolonged in the azithromycin group. In the pivotal Bronchiectasis and Low-dose Erythromycin Study (BLESS) conducted by Serisier and colleagues (14), 117 patients (58 placebo, 59 erythromycin) were randomized into groups that received either erythromycin ethylsuccinate 400 mg (250 mg erythromycin base) twice daily, or a placebo for 48 weeks. The results of the study demonstrated a significant reduction in the incidence of protocol-defined pulmonary exacerbations (PDPEs) in the erythromycin-treated group (1.29 in the treatment group *vs.* 1.97 in the placebo group, P=0.003). A well designed multicenter study involving 99 children who had been diagnosed with either bronchiectasis or chronic suppurative lung disease, and received either azithromycin (30 mg/kg) or a placebo once a week for up to 24 months, found improvement in pulmonary exacerbations (15). A limited number of clinical studies involving a small number of samples also investigated macrolides in bronchiectasis. The results of a recent meta-analysis that assessed the long-term use of macrolides for the treatment of non-CF bronchiectasis revealed a decrease in the number of participants with exacerbations (RR =0.70; 95% CI, 0.60-0.82), as well as a reduction in the average number exacerbations per participant of –1.01 (16). Taken together, the evidence has suggested that long-term treatment of bronchiectasis with a macrolide may be associated with an attenuated frequency of exacerbations.

At present, whether prolonged macrolide therapy possess beneficial effects on the improvement of pulmonary function is ambiguous. Erythromycin significantly attenuated the decline in the post-bronchodilator forced expiratory volume at the end of the first second of forced expiration (FEV1) percent predicted value (change from baseline =–1.6 in the erythromycin group and –4.0 in the placebo group, P=0.04) (14). In the bronchiectasis and long-term azithromycin treatment (BAT) randomized controlled trial, the percent of predicted FEV1 increased 1.03 per 3 months in the azithromycin group, and decreased 0.10 per 3 months in patients receiving the placebo (P=0.047). Additionally, the changes in percent of predicted forced vital capacity (FVC) were directly correlated to changes apparent in FEV1 (13). The results of the EMBRACE study also suggested a trend in the attenuation of lung function deterioration associated with azithromycin treatment, despite the lack of statistical significance (12). Interestingly, Diego and colleagues (17) did not detect significant improvement in FEV1 or FVC in patients treated with azithromycin compared to controls. As well, a small open-label, crossover-design study involving eleven patients who received routine medications and azithromycin 500 mg twice weekly for 6 months, reported no significant difference in lung function during azithromycin therapy, or in the control phase (18). Differences in macrolide doses, duration of treatment, and sample size could explain the discrepancies apparent in previously published findings. Results of prior studies suggest the efficacy of macrolide therapy in the improvement of pulmonary function was modest. Future, well-designed, studies that involve a large number of participants are required to assess macrolide effectiveness to lung function. Additional considerations

include the potential stratification of patients with different exacerbations, as well as including individuals with persistent *Pseudomonas aeruginosa* infections.

The results of macrolide clinical trials also suggested an improvement in sputum characteristics. The mechanism by which macrolides inhibit mucus secretion is thought to be through the suppression of mucin synthesis by inhibition of MUC5AC and MUC2 genes (19). In associated studies, the administration of 250 mg of azithromycin 3 times per week for 3 months in 30 patients with stable non-CF bronchiectasis resulted in a significant decrease in sputum volume [mean (SD), –8.9 (1.8) *vs.* 2.1 (3.4) mL] (17). In the BLESS trial, erythromycin significantly reduced the 24 h sputum volume from baseline values, compared with volumes in the placebo group (median difference =–4.3 g, IQR =–7.8 to –1, P=0.01). Further, the results of a randomized, double-blind, placebo-controlled study involving 25 children (1:1 ratio) treated for 12 weeks with roxithromycin (4 mg/kg, twice a day), or a placebo, indicated treatment with roxithromycin significantly improved the sputum purulence and leucocyte scores after 6 weeks (20). Another randomized double-blind study involving 21 patients who received erythromycin (500 mg) or a placebo twice daily, reported improvement in 24 h sputum volume, but no change in sputum pathogens, leukocytes, interleukin-1α (IL-1α), IL-8, tumor necrosis factor-α (TNFα), or leukotriene B4 (21).

The clinical effects of macrolide treatment on quality of life assessments were varied. In the BAT randomized controlled trial, quality of life, when measured by the St. George Respiratory Questionnaire (SGRQ) and the lower respiratory tract infection visual analog scale (LRTI-VAS) score, was significantly improved in patients receiving azithromycin compared to those receiving only a placebo (13). Similarly, a meta-analysis suggested that the SGRQ total scores were significantly reduced in the macrolide treated group compared with controls (weighted mean difference =–5.39; 95% CI, –9.89 to –0.88; P=0.02) (16). Conversely, in the EMBRACE study, a significant reduction in SGRQ component scores of azithromycin group symptoms was observed at 6 months when compared with symptoms associated with placebo administration, but no significant differences were noted at 12 months (12). Finally, the administration of erythromycin did not significantly alter Leicester cough questionnaire scores, or SGRQ scores, in the BLESS study (14). Consequently, the need for further investigations to determine the optimal duration of macrolide therapy to achieve maximal anti-inflammatory properties is patently clear.

In addition to varied outcomes related to efficacy, there are existing safety concerns associated with the use of macrolides for maintenance therapy. The main adverse events reported include nausea, vomiting, diarrhea, and abdominal pain. In the EMBRACE trial, there was a significantly increased number of complaints regarding gastrointestinal symptoms in the azithromycin group compared to the placebo group (P=0.005). Similarly, in the BAT trial, patients receiving azithromycin exhibited a higher risk of developing diarrhea (relative risk =8.36; 95% CI, 1.10-63.15) and abdominal pain (RR =7.44; 95% CI, 0.97-56.88). Other adverse effects including rash, auditive complaints, itching, heart palpitations, hearing decrement and headaches were comparable between the treated and placebo groups.

Macrolide use also raises concerns over the associated induction of prolonged QTc intervals, which serve as an indicator of ventricular tachyarrhythmias, including Torsades de pointes (Tdp). In the BLESS trial, no differences existed between the placebo and erythromycin groups in terms of prolonged QTc intervals or induced cardiac arrhythmia over the course of the study. However, electrocardiograms (ECG) should be closely monitored, and the co-administration of other known QT-prolonging agents (such as ciprofloxacin, moxifloxacin) should be avoided during the use of macrolides, in order to prevent the development of potential cardiovascular events.

Another primary concern that limits the long-term use of macrolides is the introduction of potential selective pressures for the development of resistant strains of bacteria. In the BLESS trial, the percentage of macrolide resistant commensal oropharyngeal streptococcal species was significantly increased in patients receiving erythromycin treatment. Likewise, azithromycin exhibited a high associated risk of macrolide resistant pathogens in the BAT trial (88% *vs.* 26%, P<0.001). Although macrolide resistance was not routinely tested in the EMBRACE trial, 4% of participants still developed macrolide-resistant *Streptococcus pneumoniae* in the azithromycin treatment group. The proportion of azithromycin-resistant bacteria in Valery's trial (15) was of 46% compared 11% in the placebo group (P=0.002). Consequently, a potential apprehension related to the increased use of long-term macrolides therapy is the risk of the emergence of drug resistant pathogens in the surrounding community (22). Although macrolides are the most important regimens in the treatment of NTM, macrolides monotherapy was not recommended owing to the risk for developing macrolide resistance (23,24). Patients with bronchiectasis should excluded NTM infection

for the use of long-term macrolides treatment. Thus, attention should be directed to EM703 and CYS0073, the new class of macrolides currently in development that possess anti-inflammatory actions but lack anti-bacterial properties (25,26).

In conclusion, macrolide maintenance therapy could improve the frequency of exacerbations, sputum volume, and lung function in patients with inflammatory respiratory disease. Considering the published evidence, the potential for using long-term low-dose macrolides to treat non-CF bronchiectasis is patently clear. However, the introduction of selective pressures for microbial resistance, and the adverse effects associated with macrolide maintenance therapy, may ultimately limit the use of macrolide antibiotics in clinical practice. A balance between apparent clinical benefits, and the potential development of pathogen resistance to macrolides and associated adverse events should be weighed carefully. Regarding the long-term treatment of chronic inflammatory respiratory diseases, investigations are needed into the application of novel, synthetically derived macrolides that retain the anti-inflammatory function, but reduce the risk of microbial resistance. Additional randomized controlled trials involving larger patient populations are likewise warranted, to confirm the appropriate dosage and duration of macrolide therapy, and to benefit non-CF bronchiectasis patients.

Acknowledgements

Funding: This work was supported by the National Science Foundation of China (NSFC81170003, 81370109), Projects from STCSM (12PJD004, 134119a6400), and the Shanghai Elite Medical Talent Project (XYQ2011006).
Disclosure: The authors declare no conflict of interest.

References

1. Pasteur MC, Bilton D, Hill AT, et al. British Thoracic Society guideline for non-CF bronchiectasis. Thorax 2010;65 Suppl 1:i1-58.
2. Seitz AE, Olivier KN, Adjemian J, et al. Trends in bronchiectasis among medicare beneficiaries in the United States, 2000 to 2007. Chest 2012;142:432-9.
3. Ringshausen FC, de Roux A, Pletz MW, et al. Bronchiectasis-associated hospitalizations in Germany, 2005-2011: a population-based study of disease burden and trends. PLoS One 2013;8:e71109.
4. Cole PJ. Inflammation: a two-edged sword--the model of bronchiectasis. Eur J Respir Dis Suppl 1986;147:6-15.
5. Bartold PM, du Bois AH, Gannon S, et al. Antibacterial and immunomodulatory properties of azithromycin treatment implications for periodontitis. Inflammopharmacology 2013;21:321-38.
6. Kanoh S, Rubin BK. Mechanisms of action and clinical application of macrolides as immunomodulatory medications. Clin Microbiol Rev 2010;23:590-615.
7. Kudoh S, Azuma A, Yamamoto M, et al. Improvement of survival in patients with diffuse panbronchiolitis treated with low-dose erythromycin. Am J Respir Crit Care Med 1998;157:1829-32.
8. Koyama H, Geddes DM. Erythromycin and diffuse panbronchiolitis. Thorax 1997;52:915-8.
9. Clement A, Tamalet A, Leroux E, et al. Long term effects of azithromycin in patients with cystic fibrosis: A double blind, placebo controlled trial. Thorax 2006;61:895-902.
10. Ramos FL, Criner GJ. Use of long-term macrolide therapy in chronic obstructive pulmonary disease. Curr Opin Pulm Med 2014;20:153-8.
11. Vos R, Vanaudenaerde BM, Ottevaere A, et al. Long-term azithromycin therapy for bronchiolitis obliterans syndrome: divide and conquer? J Heart Lung Transplant 2010;29:1358-68.
12. Wong C, Jayaram L, Karalus N, et al. Azithromycin for prevention of exacerbations in non-cystic fibrosis bronchiectasis (EMBRACE): a randomised, double-blind, placebo-controlled trial. Lancet 2012;380:660-7.
13. Altenburg J, de Graaff CS, Stienstra Y, et al. Effect of azithromycin maintenance treatment on infectious exacerbations among patients with non-cystic fibrosis bronchiectasis: the BAT randomized controlled trial. JAMA 2013;309:1251-9.
14. Serisier DJ, Martin ML, McGuckin MA, et al. Effect of long-term, low-dose erythromycin on pulmonary exacerbations among patients with non-cystic fibrosis bronchiectasis: the BLESS randomized controlled trial. JAMA 2013;309:1260-7.
15. Valery PC, Morris PS, Byrnes CA, et al. Long-term azithromycin for Indigenous children with non-cystic-fibrosis bronchiectasis or chronic suppurative lung disease (Bronchiectasis Intervention Study): a multicentre, double-blind, randomised controlled trial. Lancet Respir Med 2013;1:610-20.
16. Wu Q, Shen W, Cheng H, et al. Long-term macrolides for non-cystic fibrosis bronchiectasis: a systematic review and meta-analysis. Respirology 2014;19:321-9.
17. Diego AD, Milara J, Martinez-Moragón E, et al. Effects of long-term azithromycin therapy on airway oxidative stress

markers in non-cystic fibrosis bronchiectasis. Respirology 2013;18:1056-62.
18. Cymbala AA, Edmonds LC, Bauer MA, et al. The disease-modifying effects of twice-weekly oral azithromycin in patients with bronchiectasis. Treat Respir Med 2005;4:117-22.
19. Poachanukoon O, Koontongkaew S, Monthanapisut P, et al. Macrolides attenuate phorbol ester-induced tumor necrosis factor-α and mucin production from human airway epithelial cells. Pharmacology 2014;93:92-9.
20. Koh YY, Lee MH, Sun YH, et al. Effect of roxithromycin on airway responsiveness in children with bronchiectasis: a double-blind, placebo-controlled study. Eur Respir J 1997;10:994-9.
21. Tsang KW, Ho PI, Chan KN, et al. A pilot study of low-dose erythromycin in bronchiectasis. Eur Respir J 1999;13:361-4.
22. Serisier DJ. Risks of population antimicrobial resistance associated with chronic macrolide use for inflammatory airway diseases. Lancet Respir Med 2013;1:262-74.
23. Griffith DE, Aksamit T, Brown-Elliott BA, et al. An official ATS/IDSA statement: diagnosis, treatment, and prevention of nontuberculous mycobacterial diseases. Am J Respir Crit Care Med 2007;175:367-416.
24. Griffith DE, Brown-Elliott BA, Langsjoen B, et al. Clinical and molecular analysis of macrolide resistance in Mycobacterium avium complex lung disease. Am J Respir Crit Care Med 2006;174:928-34.
25. Ikeda H, Sunazuka T, Suzuki H, et al. EM703, the new derivative of erythromycin, inhibits transcription of type I collagen in normal and scleroderma fibroblasts. J Dermatol Sci 2008;49:195-205.
26. Mencarelli A, Distrutti E, Renga B, et al. Development of non-antibiotic macrolide that corrects inflammation-driven immune dysfunction in models of inflammatory bowel diseases and arthritis. Eur J Pharmacol 2011;665:29-39.

Cite this article as: Fan LC, Xu JF. Advantages and drawbacks of long-term macrolide use in the treatment of non-cystic fibrosis bronchiectasis. J Thorac Dis 2014;6(7):867-871. doi: 10.3978/j.issn.2072-1439.2014.07.24

Editorial

Evidence based imaging strategies for solitary pulmonary nodule

Yi-Xiang J. Wang[1], Jing-Shan Gong[2], Kenji Suzuki[3], Sameh K. Morcos[4]

[1]Department of Imaging and Interventional Radiology, Faculty of Medicine, The Chinese University of Hong Kong, Prince of Wales Hospital, Shatin, New Territories, Hong Kong SAR, China; [2]Department of Radiology, Shenzhen People's Hospital, Jinan University Second Clinical Medicine College, Shenzhen 518020, China; [3]Department of Radiology, The University of Chicago, Chicago, IL 60637, USA; [4]Diagnostic Imaging, The University of Sheffield, Sheffield, UK

Correspondence to: Dr. Yi-Xiang J. Wang. Department of Imaging and Interventional Radiology, Faculty of Medicine, The Chinese University of Hong Kong, Prince of Wales Hospital, Shatin, New Territories, Hong Kong SAR, China. Email: yixiang_wang@cuhk.edu.hk.

Abstract: Solitary pulmonary nodule (SPN) is defined as a rounded opacity ≤3 cm in diameter surrounded by lung parenchyma. The majority of smokers who undergo thin-section CT have SPNs, most of which are smaller than 7 mm. In the past, multiple follow-up examinations over a two-year period, including CT follow-up at 3, 6, 12, 18, and 24 months, were recommended when such nodules are detected incidentally. This policy increases radiation burden for the affected population. Nodule features such as shape, edge characteristics, cavitation, and location have not yet been found to be accurate for distinguishing benign from malignant nodules. When SPN is considered to be indeterminate in the initial exam, the risk factor of the patients should be evaluated, which includes patients' age and smoking history. The 2005 Fleischner Society guideline stated that at least 99% of all nodules 4 mm or smaller are benign; when nodule is 5-9 mm in diameter, the best strategy is surveillance. The timing of these control examinations varies according to the nodule size (4-6, or 6-8 mm) and the type of patients, specifically at low or high risk of malignancy concerned. Noncalcified nodules larger than 8 mm diameter bear a substantial risk of malignancy, additional options such as contrast material-enhanced CT, positron emission tomography (PET), percutaneous needle biopsy, and thoracoscopic resection or videoassisted thoracoscopic resection should be considered.

Keywords: Pulmonary nodule; computerized tomography; follow-up; positron emission tomography (PET); magnetic resonance imaging; guideline; biopsy; lung cancer

Submitted Jun 25, 2014. Accepted for publication Jun 29, 2014.
doi: 10.3978/j.issn.2072-1439.2014.07.26
View this article at: http://dx.doi.org/10.3978/j.issn.2072-1439.2014.07.26

Introduction

Lung cancer is the leading cause of cancer related death throughout the world (1). Lung cancer screening programs are being investigated in the United States, Japan, and other countries with low-dose helical/multi-detector CT. Despite the controversy on its cost-effectiveness (2), evidences suggest that early detection of lung cancer allow more timely therapeutic intervention and thus a more favorable prognosis for the patient (3-5). Solitary pulmonary nodule (SPN) is defined as a rounded opacity 3 cm in diameter surrounded by lung parenchyma (6). Lesions larger than 3 cm are called masses and are often malignant (6). On CT, nodules can be solid, semisolid (mixed attenuation), or ground-glass attenuation. Traditionally, chest radiography provides basic information about SPN. Nowadays, patients with SPN detected on radiographs are likely to undergo early CT scan (7). The majority of smokers who undergo thin-section CT have been found to have small lung nodules, most of which are smaller than 7 mm in diameter (8,9). However, the clinical importance of these small nodules differs substantially from that of larger nodules detected on chest radiographs, in that the vast majority are benign. This has been highlighted in several recent publications on CT screening for lung cancer (10-15). In the past, multiple follow-up examinations over a 2-year period, including CT follow-up at 3, 6, 12, 18, and 24 months, were recommended when such nodules are detected

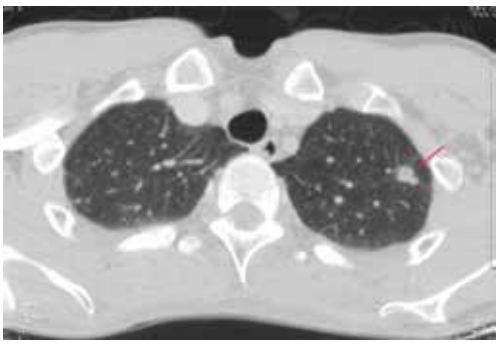

Figure 1 CT shows a case of a small hamartoma (arrow) appearing as a non-calcification solid nodule with lobulated margin, mimics a malignant nodule.

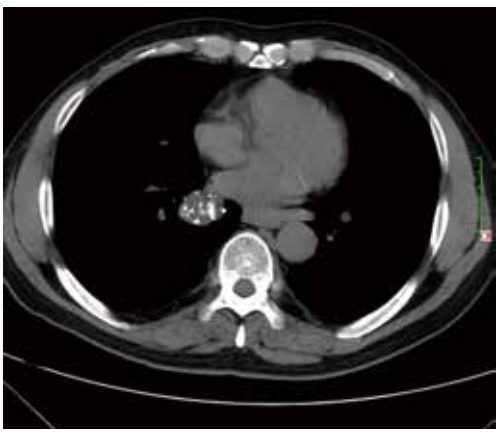

Figure 2 CT shows a case of hamartoma (size: 24 mm) with "popcorn" pattern calcification.

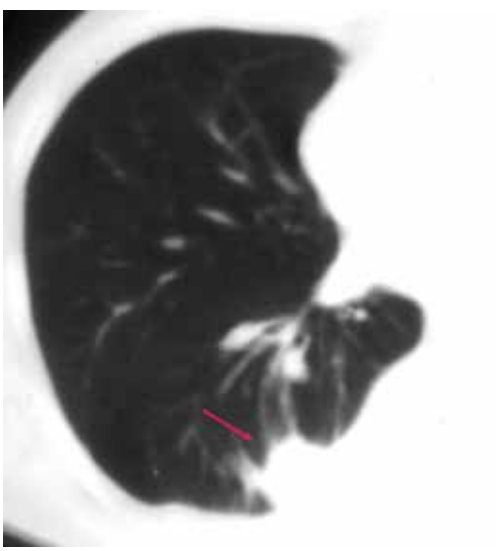

Figure 3 CT shows a case of rounded atelectasis (arrow) with morphological features of subpleural location, curved course of blood vessels into the opacity, and evidence of pleural disease.

incidentally (16,17). The policy increases radiation burden for the affected population (18-21). This editorial will present the current evidence based imaging strategies for SPN.

Morphologic assessment of solitary pulmonary nodule (SPN)

The most common intrapulmonary malignant lesions are metastases and primary bronchopulmonary carcinoma. All histological types of cancer may give rise to pulmonary nodules, but adenocarcinoma is the most frequent (22). Eighty percent of benign nodules are granulomas or intrapulmonary lymph nodes, 10% are hamartomas and 10% are other rarer benign lesions (23,24). Nodule features such as shape, edge characteristics, cavitation, and location have not yet been found to be accurate for distinguishing benign from malignant nodules (*Figure 1*) (25,26). Features favoring benignity include evidence of stability for two years or more, small nodule size, smooth demarcated margins, and certain pattern of calcifications (central dense, diffuse, laminated or popcorn). Clustering of multiple nodules in a single location in the lung tend to favor an infectious process, although a dominant nodule with adjacent small satellite nodules can be seen in primary lung cancer (27,28). A laminated or central pattern is typical of a granuloma, whereas a classic "popcorn" pattern is most often seen in hamartomas (*Figure 2*) (24). In approximately half the cases of hamartoma, high-resolution CT can show a definitive pattern of fat and cartilage (29). Fat content suggests a hamartoma or occasionally a lipoid granuloma or lipoma (30). Calcification patterns that are stippled or eccentric have been associated with cancer. Another benign entity is rounded atelectasis. Diagnosis for rounded atelectasis can be made as it has specific diagnostic morphological features including subpleural location, curved course of blood vessels into the opacity, and evidence of pleural disease (*Figure 3*) (31). When nodules considered as benign no further investigation is necessary.

SPNs with irregular, spiculated margins, or lobulated contours, are typically associated with malignancy. Two patterns of the margins of a nodule are relatively specific for cancer. One is the corona radiata sign, consisting of very fine linear strands extending 4 to 5 mm outward from the nodule; they have a spiculated appearance on plain radiographs (*Figures 4,5*). A scalloped border is associated with an intermediate probability of cancer. Although most SPNs with smooth, well-defined margins are benign, these

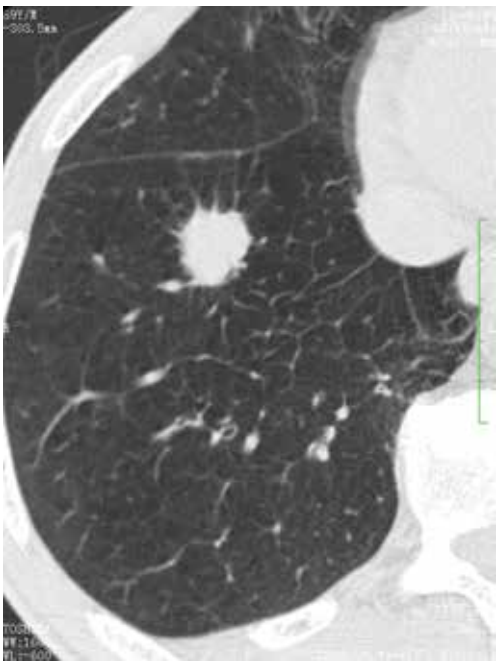

Figure 4 CT shows a pulmonary adenocarcinoma presenting as a SPN (size: 22 mm) with spiculated margins. SPN, solitary pulmonary nodule.

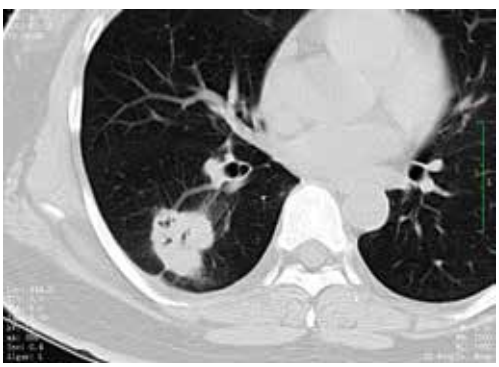

Figure 5 CT shows a pulmonary adenocarcinoma presenting as a SPN (size: 30 mm) with lobular contour, spiculated margin and plural indentation. SPN, solitary pulmonary nodule.

features are not diagnostic of benignity. A total of 21% of malignant nodules had well-defined margins (29).

For a single nodule, upper lobe location increases the likelihood of malignancy, because primary lung cancers are more common in the upper lobes (32). On the other hand, small, irregular, benign subpleural opacities, presumably due to scarring, are extremely common in the apical areas in older patients. Triangular or ovoid circumscribed nodules 3-9 mm in diameter adjacent to pleural fissures commonly represent intrapulmonary lymph nodes (33).

In general, purely linear or sheetlike lung opacities are unlikely to represent neoplasms and do not require follow-up (34).

Approaches to indeterminate solitary pulmonary nodule (SPN)

When SPN is considered to be indeterminate in the initial exam, the risk factor of the patients should be evaluated. Increasing patient age generally correlates with increasing likelihood of malignancy. On the other hand, lung cancer is uncommon in patients younger than 40 years and is rare in those younger than 35 years (<1% of all cases) (35). The relative risk for developing lung carcinoma in male smokers was about 10 times that in nonsmokers (36). For heavy smokers, the risk was 15-35 times greater (37). Also, the cancer risk for smokers increases in proportion to the degree and duration of exposure to cigarette smoke (38). Other established risk factors include exposure to asbestos, uranium, and radon (39-41). A history of lung cancer in first-degree relatives is also a risk factor, and strong evidence for a specific lung cancer susceptibility gene has been discovered recently (42,43). A history of cancer can greatly increase the likelihood of a nodule being malignant (44). Low-risk individuals are <50 years old and have <20 pack-year smoking history. Moderate-risk group is defined as age >50 and >20 pack-year smoking history or second hand exposure, and no additional risk factor (random exposure, occupational exposure, cancer history, family history, or lung cancer).

The positive relationship of lesion size to likelihood of malignancy has been clearly demonstrated (10-15). The standard size value used is an average of the largest and smallest cross-sectional diameters of the most representative area of the nodule. In a meta-analysis of eight large screening trials, the prevalence of malignancy depended on the size of the nodules, ranging from 0% to 1% for nodules 5 mm or smaller, 6% to 28% for those between 5 and 10 mm, and 64% to 82% for nodules 20 mm or larger. Even in smokers, the percentage of all nodules smaller than 4 mm that will eventually turn into lethal cancers is very low (<1%), whereas for those in the 8-mm range the percentage is approximately 10-20%. The 2005 Fleischner Society guideline (*Table 1*) stated that at least 99% of all nodules 4 mm or smaller are benign and because such small opacities are common on thin-section CT scans, follow-up CT in every such case is not recommended; in selected cases with

Table 1 The 2005 Fleischner Society guideline for solitary pulmonary nodule management [reproduced with permission from (45)]

Nodule size (mm)[a]	Low-risk patient[b]	High-risk patient[c]
≤4	No follow-up needed[d]	Follow-up CT at 12 mo; if unchanged, no further follow-up[e]
>4-6	Follow-up CT at 12 mo; if unchanged, no further follow-up[e]	Initial follow-up CT at 6-12 mo then at 18-24 mo if no change[e]
>6-8	Initial follow-up CT at 6-12 mo then at 18-24 mo if no change	Initial follow-up CT at 3-6 mo then at 9-12 and 24 mo if no change
>8	Follow-up CT at around 3, 9 and 24 mo, dynamic contrast-enhanced CT, PET and/or biopsy	Same as for low-risk patient

Note: newly detected in indeterminate nodule in persons 35 years of age or older. [a], average of length and width; [b], minimal or absent history of smoking and of other known risk factors; [c], history of smoking or of other known risk factors; [d], the risk of malignancy in this category (<1%) is substantially less than that in a baseline CT scan of an asymptomatic smoker; [e], nonsolid (ground-glass) or partly solid nodules may require longer follow-up to exclude indolent adenocarcinoma.

Figure 6 CT shows a case of adenocarcinoma in situ (arrow, size 6 mm) with pure ground glass opacity.

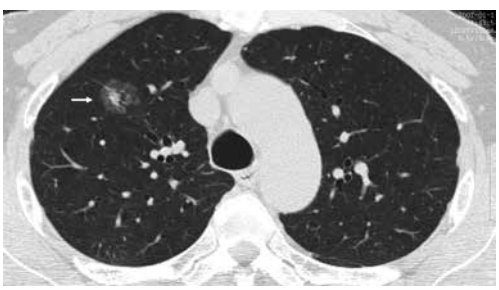

Figure 7 CT shows a case of minimally invasive adenocarcinoma, with a total size of 17 mm and solid component size of 7 mm.

suspicious morphology or in high-risk subjects, a single follow-up scan in 12 months should be considered (45). This protocol could result in a few indolent cancers being missed, the number of such instances would be extremely small relative to the reduction in the number of unnecessary studies (45).

The increased use of CT screening for lung cancer led to an increase in identification of early lesions such as adenocarcinoma in situ (AIS, histopathologically ≤30 mm, noninvasive lepidic growth, which at CT is usually nonsolid; *Figure 6*) and minimally invasive adenocarcinoma (MIA, histopathologically ≤30 mm and predominantly lepidic growth that has 5-mm or smaller invasion, which at CT is mainly nonsolid but may have a central solid component of up to approximately 5 mm; *Figure 7*) (22). These lesions should not be regarded as conventional invasive adenocarcinomas and can be observed rather than surgically resected (22).

When the nodule is 5-9 mm in diameter, approximately 6% of cases showed interval nodule growth detectable on 4-8 month follow-up scans (11). For these nodules the best strategy is surveillance. The timing of these control examinations is given in *Table 1*. This varies according to the nodule size (4-6, or 6-8 mm) and type of patients, specifically at low or high risk of malignancy concerned. Noncalcified nodules larger than 8 mm diameter can bear a substantial risk of malignancy (*Figure 8*) (46). In the case of nodules larger than 8 mm, additional options such as contrast material-enhanced CT, positron emission tomography (PET), percutaneous needle biopsy, and thoracoscopic resection or videoassisted thoracoscopic resection can be considered (13). A common aspect of invasive adenocarcinoma of the lung is metastasis to the brain (47,48). Its probability is a function of the size of the primary tumor, at least for tumors in the 20-60 mm size range. For node-negative invasive adenocarcinoma of the lung, a 20 mm primary lesion has been found to show a 14% probability of brain metastatic disease, progressing

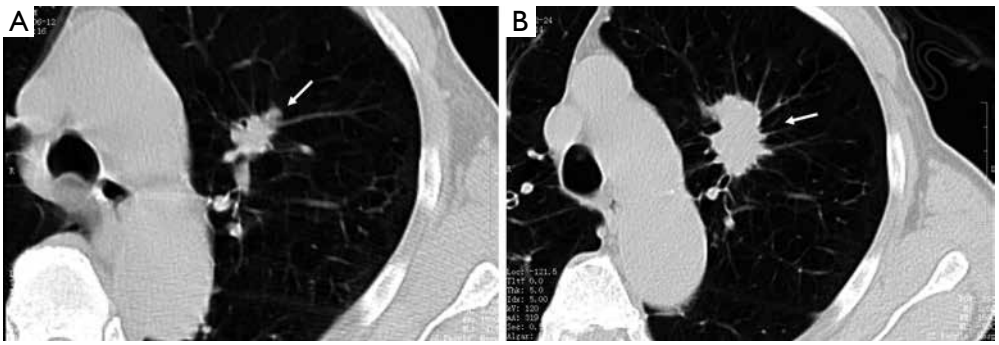

Figure 8 (A) CT shows a SPN (arrow, size =14 mm × 18 mm) in a 73 yrs male; (B) the same patient follow-up CT scan 20 month later. The size increased to 20 mm × 33 mm, with typical malignant the appearance of lobular contour and spiculated margin, and pathologically proved to be adenocarcinoma.

nearly linearly to a 60 mm primary node-negative lesion showing a 64% probability of brain metastatic disease (47).

In certain clinical settings, such as a patient presenting with neutropenic fever, the presence of a nodule may indicate active infection, and short-term imaging follow-up may be appropriate. Previous CT scans, chest radiographs, and other pertinent imaging studies should be obtained for comparison whenever possible, as they may serve to demonstrate either stability or interval growth of the nodule in question.

In a patient with known primary malignancy, lung nodules, regardless of being solitary or multiple, would be deemed suspicious for metastases. Pertinent factors will include the site, cell type, and stage of the primary tumor and whether early detection of lung metastases will affect care.

CT follow-up for solitary pulmonary nodule (SPN)

The volume doubling time (DT) for malignant bronchogenic tumors is rarely less than a month or more than a year. A nodule that was not present on a radiograph obtained less than two months before the current image is therefore not likely to be malignant. The "doubling time" (DT) of a nodule can be calculated using the following formula:

$$DT = (t.\ln 2)/\ln(Vf/Vi)$$

Where *Vi* is the initial volume of the nodule, *Vf* the final volume, *t* the time interval between observations and ln the logarithmic value. This formula is based on an exponential model of nodule growth (23). Note that a 5-mm nodule with a DT of 60 days will reach a diameter of 20.3 mm in 12 months, whereas a similar nodule with a DT of 240 days would reach a diameter of only 7.1 mm in the same period.

It has been considered that stability of nodule size for over 2 years for solid pulmonary nodules suggest benign nature. Recently, the radiologic-pathologic correlation of pure ground-glass attenuation nodules and mixed attenuation nodules with the histologic spectrum of pulmonary adenocarcinoma was described (49). Small purely ground-glass opacity (nonsolid) nodules that have malignant histopathologic features tend to grow very slowly, with a mean volume DT on the order of two years (50). Solid cancers, on the other hand, tend to grow more rapidly, with a mean volume DT on the order of 6 months. The growth rate of partly solid nodules tends to fall between these extremes, and this particular morphologic pattern is predictive of adenocarcinoma (46,51,52). Bronchoalveolar cell carcinomas and typical carcinoids occasionally appear to be stable for two or more years (53). Longer follow-up intervals are appropriate for nonsolid (ground-glass opacity) and very small opacities (50,51). Even if malignant, a nonsolid nodule that is smaller than 6 mm will probably not grow perceptibly in much less than 12 months (50,51). Currently, though the dictum that two-year stability on plain-film radiography indicates a benign process should be used with caution (54), it is still reasonable to use two-year stability on high-resolution CT as a practical guideline for predicting a benign process.

Hasegawa *et al.* (50) reported an analysis of the growth rates of small lung cancers detected during a 3-year mass screening program. They classified nodules as ground-glass opacity, as ground-glass opacity with a solid component, or as solid. Mean volume DTs were 813, 457, and 149 days, respectively. In addition, the mean volume DT for cancerous nodules in nonsmokers was significantly longer than that for cancerous

nodules in smokers. Authors of a number of other series have confirmed similar findings and have estimated the median tumor DTs, assuming a constant growth rate to be in the 160-180-day range (55,56). Authors of all of these reports, however, recognize wide variations, and in one study 22% of tumors had a volume DT of 465 days or more (56).

The use of stability as an indicator of a benign process is predicated on accurate measurement of growth and thus on the resolution of the imaging technique used. The accurate measurement of growth in subcentimeter nodules can be problematic. A doubling in volume of a sphere corresponds to an increase of only 26% of its diameter according to the formula $V=4/3\pi r^3$ where *r* is the radius. Therefore, it may be difficult to evaluate an increase or decrease in the axial diameter of a nodule between two successive CT examinations, or even of no value for small nodules less than or equal to 5 mm in size. In fact, a nodule of 5 mm which doubles in volume will only increase in diameter by 1.25 mm. Revel *et al.* determined that two-dimensional measurements obtained with electronic calipers were unreliable as a basis for distinguishing benign from malignant solid nodules in the 5-15-mm size range (57). Some authors compared diameter and cross-sectional area measurement with volume measurement in the assessment of lung tumour growth with serial CT. They demonstrated that growth assessment of lung tumours measuring less than 3 cm on CT serial CT scans with non-volumetric measurements frequently disagrees with growth assessment with volumetric measurements, and the three-dimensional measurements are more reliable (58-62). Volume measurement requires specific image analysis software, which allows segmentation and three-dimensional reconstruction of the nodule in order to appreciate the variations in morphology, and to automatically calculate the volume. Goodman *et al.* have raised additional caution in applying volumetric measurements, because the overall variability between scans in vivo is still substantial with wide confidence limits of 13.1%±26.6% (63). For this reason, it is recommended to act on variations in nodule volume of 20%. A variation of <20% should not be considered as significant as it could be due to the method of measurement. Factors that affect the reproducibility of nodule volume measurement on CT include nodule size at detection, examination technique, nodule relationship to adjacent structures, underlying lung disease, and patient factors such as phase of respiration and cardiac motion (58).

For optimal CT evaluation of subsolid pulmonary nodules, thin sections are advisable. Changes in nodule attenuation can also be assessed. For malignant subsolid nodules, measuring an increase in attenuation at serial CT examinations appears to be less subject to variability than measures of diameter or volume (64). Also, when subjective visual assessment of a nonsolid nodule at serial thin-section CT examinations suggests either possible but not definite enlargement of the nodule or possible but not definite development of a solid component, then increasing "mass" (mean volume multiplied by attenuation) may help identify early invasive growth, the increasing solid component corresponding to progression of local malignant invasion (64). For example, an increase of 100 HU in attenuation of a nonsolid nodule has been described as representing an approximately 10% increase in tumor volume (65). During surveillance of ground glass nodules, the appearance of a soft-tissue component is a highly suspicious sign of malignancy, even if the overall size of the nodule remains stable or diminishes (66).

An important aspect of adenocarcinomas of the lung is that, for small, solitary, early-stage tumors, the size of the invasive component-as measured histologically-is an independent predictor of survival (67). For part-solid lesions evaluated by using CT for tumor size, the size of the solid portion may be more predictive of prognosis than total size that includes the nonsolid dimension (67-69). A recent multicenter study in Japan has indicated that, for resected stage IA (T1N0M0) adenocarcinoma of the lung, disease-free survival correlated with solid tumor size but not with "whole tumor size" that included a nonsolid (ground-glass) component (70). For part-solid stage IA adenocarcinoma of the lung, an extensive nonsolid component is a favorable prognostic sign (22).

SPN can also appear as focal nodular areas of increased lung attenuation, including both well and poorly defined lesions, through which normal parenchymal structures, including airways and vessels, can be visualized. This appearance typically is referred to a ground-glass nodule. The term "subsolid" nodules are used to emphasize that both pure ground-glass nodules and part-solid ground-glass nodules. It is necessary to establish lesions as true ground-glass nodule by using contiguous thin CT sections (1 mm thickness) whenever possible to avoid the pitfall of interpreting lesions as subsolid on thick sections (typically 5 mm) when they are actually solid. The 2013 Fleischner Society recommendation for the management of Subsolid Pulmonary Nodules is shown in *Table 2* (71).

A low-dose, thin-section, unenhanced technique should

Table 2 The 2013 Fleischner Society recommendations for the management of subsolid pulmonary nodules detected at CT [reproduced with permission from reference (71)]

Nodule type	Management recommendations	Additional remarks
Solitary pure GGNs		
≤5 mm	No CT follow-up required	Obtain contiguous 1-mm-thick sections to confirm that nodule is truly a pure GGN
>5 mm	Initial follow-up CT at 3 months to confirm persistence then annual surveillance CT for a minimum of 3 years	FDG PET is of limited value, potentially misleading, and therefore not recommended
Solitary part-solid nodules	Initial follow-up CT at 3 months to confirm persistence. If persistent and solid component <5 mm, then yearly surveillance CT for a minimum of 3 years. If persistent and solid component ≥5 mm, then biopsy or surgical resection	Consider PET/CT for part-solid nodules >10 mm
Multiple subsolid nodules		
Pure GGNs ≤5 mm	Obtain follow-up CT at 2 and 4 years	Consider alternate causes for multiple GGNs ≤5 mm
Pure GGNs >5 mm without a dominant lesion(s)	Initial follow-up CT at 3 months to confirm persistence and then annual surveillance CT for a minimum of 3 years	FDG PET is of limited value, potentially misleading, and therefore not recommended
Dominant nodule(s) with part-solid or solid component	Initial follow-up CT at 3 months to confirm persistence. If persistent, biopsy or surgical resection is recommended, especially for lesions with >5 mm solid component	Consider lung-sparing surgery for patients with dominant lesion(s) suspicious for lung cancer

Note: these guidelines assume meticulous evaluation, optimally with contiguous thin sections (1 mm) reconstructed with narrow and/or mediastinal windows to evaluate the solid component and wide and/or lung windows to evaluate the nonsolid component of nodules, if indicated. When electronic calipers are used, bidimensional measurements of both the solid and ground-glass components of lesions should be obtained as necessary. The use of a consistent low-dose technique is recommended, especially in cases for which prolonged follow-up is recommended, particularly in younger patients. With serial scans, always compare with the original baseline study to detect subtle indolent growth.

be used, with limited longitudinal coverage, when follow-up of a lung nodule is the only indication for the CT examination. Malignant probability for nodules can be calculated using the software available on the website of Dr Gurney (http://www.chestx-ray.com).

Contrast-enhanced CT for solitary pulmonary nodule (SPN)

After administration of iodinated contrast material intravenously with power injection (300 mg/mL at 2 mL/sec), nodular enhancement of less than 15 HU is strongly predictive of benignity (*Figure 9*); whereas enhancement of more than 20 HU, reflecting presence of tumour neovascularisation, is indicative of malignancy (*Figure 10*). Results from a large multicenter study found that contrast-enhanced CT has a sensitivity of 98% and a specificity of 58% when using a cutoff of 15 Hounsfield units for enhancement (72). A recent meta-analysis of ten dynamic CT studies reported pooled sensitivity of 93%, specificity of 76%, positive predictive value (PPV) of 80% and negative predictive value (NPV) of 95% for SPN characterization (73). Higher accuracy is reported for dynamic enhancement evaluation on helical CT, by analyzing combined wash-in and washout characteristics. Malignant nodules show greater washout of contrast enhancement (74). Dual-energy CT imaging has also been used in several studies to evaluate nodules with similar diagnostic accuracy (75,76). Limitations of contrast-enhanced CT relate to its false positive results for malignancy caused by inflammatory lesions; and measurement error that can occur in evaluation of small nodules. Given that measurement of the density is

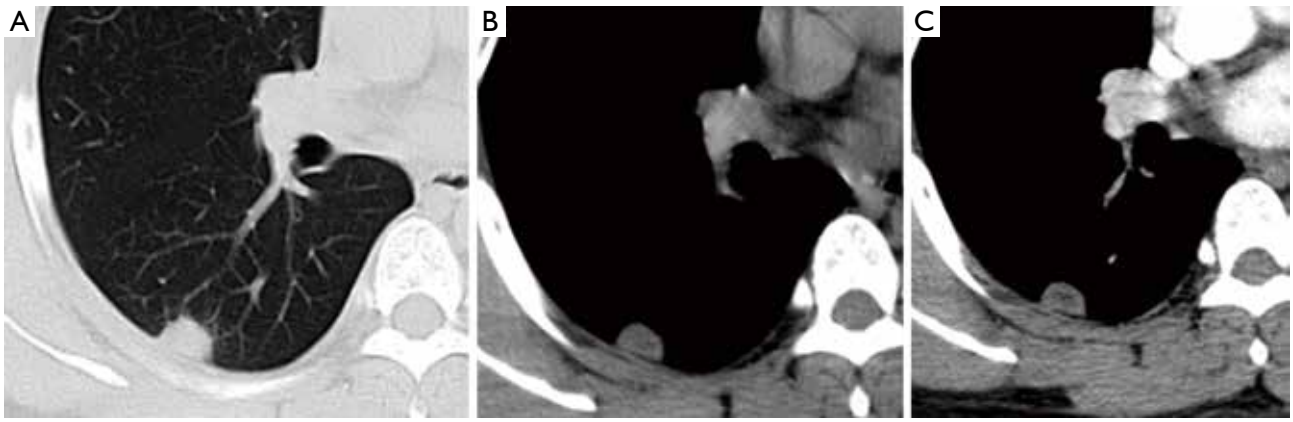

Figure 9 A small subpluera nodule (15 mm × 10 mm; arrow) with well-defined margin and enhancement of 16 Hounsfield units after CT contrast agent injection, pathologically proved to be a cryptococcal granuloma. (A,B): plain CT; contrast enhanced CT.

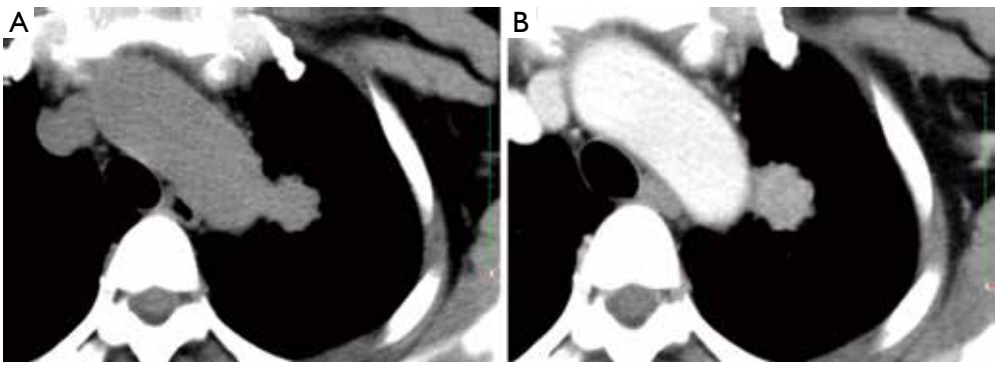

Figure 10 A pulmonary carcinoma (arrow) with enhancement of 37 Hounsfield units after CT contrast agent injection. (A) plain CT; (B) contrast enhanced CT.

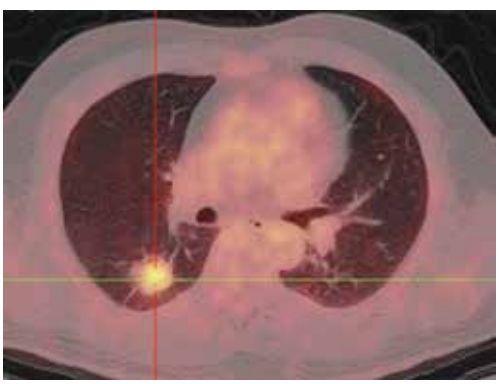

Figure 11 PET-CT shows a case of adenocarcinoma with a SUVmax of 4.14.

difficult for heterogeneous lesions and those less than 1 cm in diameter, in practice contrast-enhanced CT only yields reliable information for homogenous nodules equal to or above 8 mm in diameter.

Positron emission tomography (PET) and combined PET-CT

PET, using 18-fluorine fluoro-deoxyglucose (18F-FDG), a D-glucose analogue labeled with radio-isotope, can quantify the rate of glucose metabolism by cells, thereby detecting presence of metabolically active tissue. Malignant nodules consist of metabolically active cells that have higher uptake of glucose due to over-expression of glucose transporter protein (*Figure 11*). FDG is trapped and accumulates within these cells, as the radio-labeled glucose analogue is phosphorylated once but not metabolized further (77). A meta-analysis reported pooled sensitivity of 96.8% and specificity of 77.8% for malignant nodules for 8F-FDG PET technique alone (7). Integration of CT and PET results in an improved accuracy, with 97% sensitivity and 85% specificity, for differentiating malignant from benign SPNs (78). Kim *et al.* found that visual interpretation by experienced radiologist or nuclear medicine specialist is

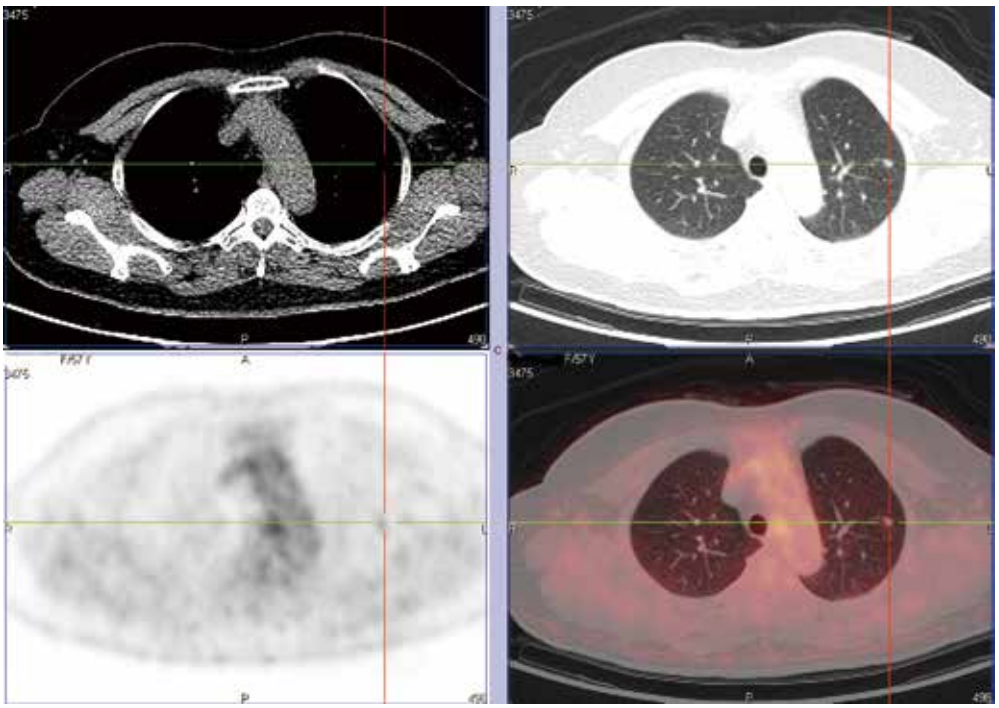

Figure 12 PET-CT shows a case of atypical adenomatous hyperplasia with a SUVmax of 1.42.

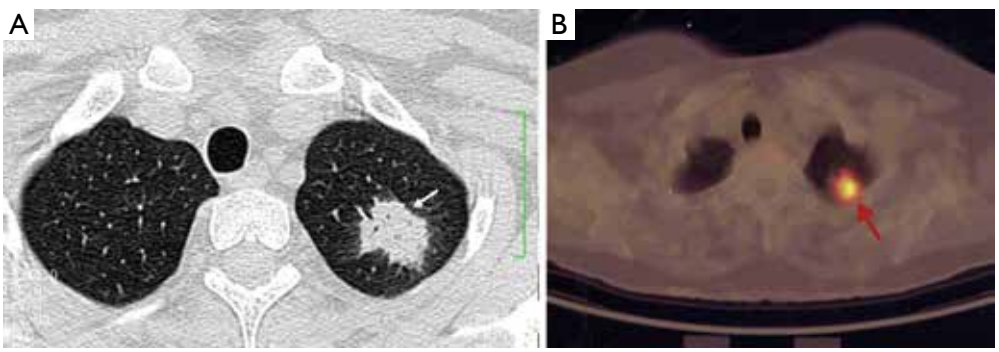

Figure 13 A case of cryptococcal granuloma (arrow) had a SUVmax of 4.5 on the FDG PET scan.

sufficient, if not superior, for characterizing SPN, and quantitative analysis (using 2.0 as cut-off SUVmax) did not improve accuracy (78). There is growing evidence that using threshold SUVmax to differentiate malignant from benign lesions is unrealistic, and SUVmax of 2.5 should not be embraced as a magic threshold.

Higher FDG uptake in lung cancer as measured by standardized uptake value (SUV) analysis is associated with aggressive cancers and shorter survival (79,80). On the other hand, lower levels of FDG uptake often correspond to histologically and clinically less aggressive tumour behavior (*Figure 12*) (81). An added value of PET-CT is the detection of other unexpected metabolically active lesion and/or lymphadenopathy to support probable diagnosis of SPN being a primary or secondary malignancy (82). Up to 14% of patients otherwise eligible for surgery have occult extrathoracic disease on whole body PET imaging (83). On the other hand, the sensitivity and specificity of CT scans for detecting mediastinal lymph-node involvement are 55% to 88% and 76% to 85%, respectively (84). The sensitivity and specificity of PET in the presence of abnormal lymph nodes on CT scanning are 94% and 82%, respectively. In one prospective study, the diagnostic accuracy of CT was 64%, that of PET 88%, and that of the combination of CT

and PET 96% (85).

In most studies, the sensitivity of 18F-FDG PET-CT tends to be higher than its specificity for assessment of SPN. Many benign conditions, such as granulomatous (for example histoplasmosis or tuberculosis) and inflammatory processes, can mimic malignant nodules and produce false-positive results (*Figure 13*) (86). On the other hand, false negative results for SPN characterization on PET-CT can occur in three main settings: small lesion size, low tumor metabolic activity, and hyperglycemia. Small lesions (<1 cm) are challenging due to limited spatial resolution of PET, which is approximately 7 mm for modern scanners (7). Some highly differentiated malignant tumors have relatively little metabolic activity and low rate of proliferation, resulting in false-negative PET-CT. FDG PET is falsely negative in around 50% of patients with bronchioloalveolar carcinoma (87), or adenocarcinoma in situ (88-90). In addition, metastasis from certain primary malignancy, such as renal cell carcinoma, testicular or prostate cancer, may show little FDG tracer accumulation and may even be undetectable on PET-CT (91). False negative FDG PET-CT scans may also occur in patients with hyperglycemia (77). Some authors have proposed dual time point FDG-PET imaging, using the change in SUVmax between early and delayed scans to help differentiate benign and malignant SPNs (92). However, the role of dual time point PET imaging (DTPI) has been disputed by some authors (93). A meta-analysis on diagnostic performance of dual time point FDG-PET imaging in assessing lung nodules reported similar sensitivity and specificity to single time point FDG-PET (94). Further studies are needed to clarify this point.

The major obstacles to widespread use of PET-CT are limited availability and high costs. In the United States, with increasing availability of PET scanners and the reimbursement for SPN evaluation and lung cancer staging with PET scans being supported by Medicare, PET-CT has become much more common. In the United Kingdom, the National Institute for Clinical Excellence (NICE) currently recommends 18F-FDG PET for investigation of SPNs in cases where a biopsy is not possible or has failed, depending on nodule size, position and CT characterization (95).

Magnetic resonance imaging (MRI)

Use of MRI in the evaluation of pulmonary nodules has so far been limited. Faster imaging sequences and techniques to mitigate artefacts have allowed for detection of smaller nodules (6 to 10 mm) with a sensitivity of almost 95% (96). For nodules >1 cm, contrast-enhanced dynamic MRI has been shown to be comparable to CT for distinguishing benign from malignant nodules (97-99). A meta-analysis of six dynamic contrast-enhanced MR studies reported pooled sensitivity of 94%, which is comparable to dynamic contrast enhanced CT, but with higher pooled specificity of 79% (73). Mori *et al.* found diffusion weighted imaging (DWI) was more specific for SPNs than FDG PET, due to fewer false positives for active inflammation, which does not affect diffusion of water molecules (100). An obvious advantage of MRI is this technique does not involve radiation. Further development in sequencing, scanners and coils, adaptation of parallel and sparse MR imaging will speed up the scan time (101,102), making MRI a realistic tool for the imaging of lung, particularly for lung cancer screen.

Computer-aided detection and diagnosis

Modern CT generates a large number of images that must be read by radiologists/physicians. This may lead to "information overload" for the radiologists/physicians. They may miss some cancers during their interpretation of CT images (52,103). Therefore, a computer-aided diagnosis (CAD) scheme for detection of lung nodules in CT images has been investigated as a tool for lung cancer detection. CAD is often categorized into two major groups: computer-aided detection (CADe) and computer-aided diagnosis (CADx). CADe focuses on a detection task, i.e., detection (or localization) of lesions in medical images. CADx focuses on a diagnosis (characterization) task, e.g., distinction between benign and malignant lesions, and classification among different lesion types (103,104). The use of CADe systems improves the performance of radiologists in the detection process of pulmonary nodules (105-107). It has been reported that CADe systems improved the sensitivity of radiologists in detecting small nodules on CT scans higher than that with conventional double reading (108). It has been also shown that observer's nodule detection remained imperfect, and that a maximum-intensity-projection processing technique reduced the number of overlooked small nodules, particularly in the central lung (109).

Various approaches have been proposed for CADe schemes for lung nodules in CT. Sensitivities for detection of lung nodules in CT range from 70% to 95%, with from a few to 70 false positives (FP) per case. *Figure 14* illustrates CADe outputs on a CT image of the lungs (110,111). Major sources of FPs are various-sized lung vessels. Major sources

of false negatives are ground glass nodules, nodules attached to vessels, and nodules attached to the lung wall (i.e., juxtapleural nodules). Ground glass nodules are difficult to detect, because they are subtle, of low-contrast, and have ill-defined boundaries.

A number of researchers developed CADx schemes distinguishing malignant nodules from benign nodules on CT images automatically and/or determining the likelihood of malignancy for the detected nodules. *Figure 15* illustrates CADx outputs on malignant and benign lung nodules on high-resolution CT images (112,113). The performance of CADx schemes ranges from area under the receiver-operating-characteristic curve (AUC) values of 0.85 to 0.95 (107). Overall, the sensitivities of CADe schemes are relatively high, but the number of FPs is high compared to radiologists' performance (107). Further improvement in specificity is necessary in future research.

Figure 14 CADe outputs (indicated by circles) on an axial CT slice of the lungs. A lung nodule (indicated by an arrow) was detected correctly by a CADe scheme with one false positive detection [branch of lung vessel; reproduced from (107) with permission].

Transthoracic fine-needle aspiration biopsy

Transthoracic fine-needle aspiration biopsy may be optimised by the presence of an onsite cytopathologist at the time of biopsy, allowing repeated sampling if insufficient cells are obtained. For those teams not have an onsite cytopathologist, coaxial cutting needles are recommended which yield more voluminous biopsy samples. This technique improves the accuracy of diagnosis without significant increase in the complication rate. CT may be useful in biopsy planning by specifying lesion depth and the point of the needle in order to aid the approach, and to avoid the needle path traversing a bulla or fissure. Although the minimum size varies according to the expertise of the radiologist, a diameter of at least 7 mm is usually required. For malignant lesions, transthoracic fine-needle aspiration biopsy offer the sensitivity of 80% to 95% and the specificity is 50% to 88%. For lesions that are less than 2 cm in diameter, transthoracic fine-needle aspiration biopsy has a sensitivity of more than 60 percent for detecting a malignant process (114). However, the false negative rate is 3% to 29% (115).

The Achilles heel of needle biopsy is negative biopsy result for malignancy without specific benign lesion diagnosis does not exclude malignancy. In addition, the technique has limited ability in producing specific diagnosis of benign lesions. SPN with high clinical suspicion of malignancy that is operable, the best approach is surgical

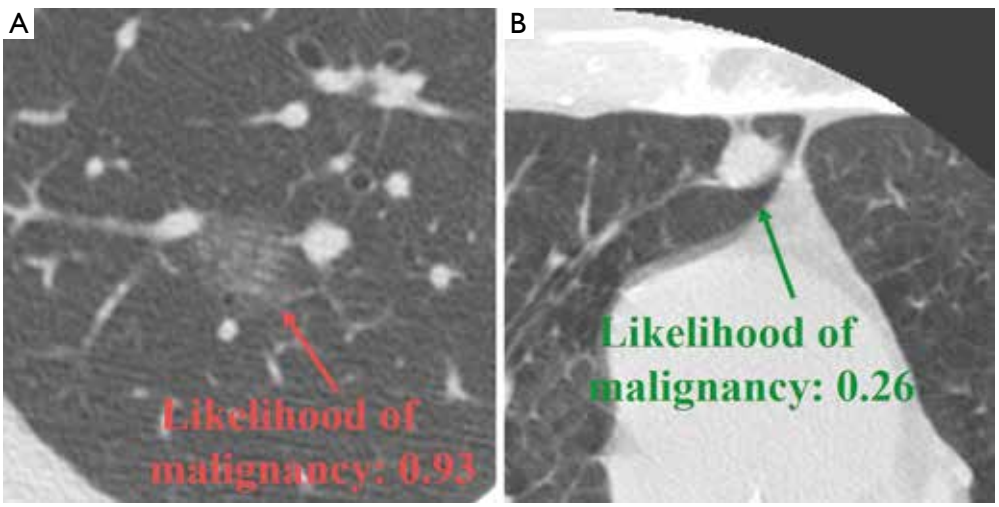

Figure 15 CADx scheme accurately determined the likelihood of malignancy for a malignant nodule (A) and a benign nodule (B).

resection as needle biopsy does not influence management (positive result confirms the high clinical suspicion and will be followed by resection, negative result does not exclude malignancy and the lesion has to be removed surgically because of the high clinical suspicion) so the result whether positive or negative does not alter the patient's management. For inoperable SPN, needle biopsy is justified to confirm the histology. Complication rates of needle biopsy are higher than those for bronchoscopy. Pneumothorax and haemorrhage are seen in 5-30% of cases, although in most cases, treatment is not required.

Bronchoscopy

If the nodule is linked to a narrowed or obstructed bronchus, a bronchus is visible within the nodule or an endobronchial lesion is detected on CT, then "bronchoscopy targeting" to the appropriate level is recommended. In such a case, the CT examination can optimize the approach to biopsy, and guide direct transbronchial biopsy. The sensitivity of bronchoscopy for detecting a malignant process in a SPN ranges from 20% to 80%, depending on the size of the nodule, its proximity to the bronchial tree, and the prevalence of cancer in the study population (116). For nodules that are less than 1.5 cm in diameter, the sensitivity is 10%, and for those that are 2.0 to 3.0 cm in diameter, it is 40% to 60% (116,117). When CT reveals a bronchus leading to the lesion, bronchoscopy may have a 70% sensitivity (118).

Conclusions

This paper highlights the importance of avoiding excessive patient irradiation caused by unnecessary follow-up CTs (45). The radiation dosage for a chest varies between 1-10 mSv, while that of whole body FDG-PET/CT is 10-30 mSv. More details on medical X-ray radiation risk can be found at http://www.xrayrisk.com/. After the publication of the Fleischner Society guideline in 2005, it was reported more frequent CT follow-ups than necessary are still being performed (119,120). The policy of low-dose, thin-section, with limited longitudinal coverage for follow-up CTs is not always carried out (119,120).

Information from the morphologic appearance of the nodule can be combined with clinical risk information to produce an overall probability for malignancy. If this probability can be set sufficiently low, strategies that include observing nodules for interval change can be advocated. The patient's age and the presence of comorbid conditions influence management recommendations. The patient's preference is also a very important factor, especially if the potential difference among strategies is small. It is also highly practical that management approaches differ from institution to institution because of the varying prevalence of lung disease in different parts of the world, varying skill levels of operators, and varying availability of equipments.

Acknowledgements

The authors thank Dr. Junqing Xu, Xijing Hospital, The Forth Military Medical University, Xi'an, China, for helpful discussion.

Disclosure: The authors declare no conflict of interest.

References

1. Ferlay J, Shin HR, Bray F, et al. Estimates of worldwide burden of cancer in 2008: GLOBOCAN 2008. Int J Cancer 2010;127:2893-917.
2. Goulart BH, Bensink ME, Mummy DG, et al. Lung cancer screening with low-dose computed tomography: costs, national expenditures, and cost-effectiveness. J Natl Compr Canc Netw 2012;10:267-75.
3. Sone S, Takashima S, Li F, et al. Mass screening for lung cancer with mobile spiral computed tomography scanner. Lancet 1998;351:1242-5
4. Heelan RT, Flehinger BJ, Melamed MR, et al. Non-small-cell lung cancer: results of the New York screening program. Radiology 1984;151:289-93.
5. National Lung Screening Trial Research Team, Aberle DR, Adams AM, et al. Reduced lung-cancer mortality with low-dose computed tomographic screening. N Engl J Med 2011;365:395-409.
6. Hansell DM, Bankier AA, MacMahon H, et al. Fleischner Society: glossary of terms for thoracic imaging. Radiology 2008;246:697-722.
7. Gould MK, Maclean CC, Kuschner WG, et al. Accuracy of positron emission tomography for diagnosis of pulmonary nodules and mass lesions: a meta-analysis. JAMA 2001;285:914-24.
8. Swensen SJ, Silverstein MD, Ilstrup DM, et al. The probability of malignancy in solitary pulmonary nodules. Application to small radiologically indeterminate nodules. Arch Intern Med 1997;157:849-55.
9. Swensen SJ. CT screening for lung cancer. AJR Am J Roentgenol 2002;179:833-6.
10. Wahidi MM, Govert JA, Goudar RK, et al. Evidence for

the treatment of patients with pulmonary nodules: when is it lung cancer? ACCP evidence-based clinical practice guidelines (2nd edition). Chest 2007;132:94S-107S.
11. Henschke CI, Yankelevitz DF, Naidich DP, et al. CT screening for lung cancer: suspiciousness of nodules according to size on baseline scans. Radiology 2004;231:164-8.
12. Swensen SJ, Jett JR, Hartman T, et al. Screening for lung cancer with CT: Mayo Clinic experience. Radiology 2003;226:756-61.
13. Henschke CI, McCauley DI, Yankelevitz DF, et al. Early Lung Cancer Action Project: overall design and findings from baseline screening. Lancet 1999;354:99-105.
14. Henschke CI, Naidich DP, Yankelevitz DF, et al. Early Lung Cancer Action Project: initial findings on repeat screening. Cancer 2001;92:153-9.
15. Diederich S, Wormanns D, Lenzen H, et al. Screening for asymptomatic early bronchogenic carcinoma with low dose CT of the chest. Cancer 2000;89:2483-4.
16. Ost D, Fein AM, Feinsilver SH. The solitary pulmonary nodule. N Engl J Med 2003;348:2535-42.
17. Tan BB, Flaherty KR, Kazerooni EA, et al. The solitary pulmonary nodule. Chest 2003;123:89S-96S.
18. Mayo JR, Alrich J, Muller NL. Radiation exposure at chest CT: a statement of the Fleischner Society. Radiology 2003;228:15-21.
19. Imhof H, Schibany N, Ba-Ssalamah A, et al. Spiral CT and radiation dose. Eur J Radiol 2003;47:29-37.
20. Kalra MK, Maher MM, Toth TL, et al. Strategies for CT radiation dose optimization. Radiology 2004;230:619-28.
21. Brenner DJ. Radiation risks potentially associated with low-dose CT screening of adult smokers for lung cancer. Radiology 2004;231:440-5.
22. Austin JH, Garg K, Aberle D, et al. Radiologic implications of the 2011 classification of adenocarcinoma of the lung. Radiology 2013;266:62-71.
23. Beigelman-Aubry C, Hill C, Grenier PA. Management of an incidentally discovered pulmonary nodule. Eur Radiol 2007;17:449-66.
24. Kradin RL, Spirn PW, Mark EJ. Intrapulmonary lymph nodes: clinical, radiologic, and pathologic features. Chest 1985;87:662-7.
25. Brandman S, Ko JP. Pulmonary nodule detection, characterization, and management with multidetector computed tomography. J Thorac Imaging 2011;26:90-105.
26. Zhao F, Yan SX, Wang GF, et al. CT features of focal organizing pneumonia: an analysis of consecutive histopathologically confirmed 45 cases. Eur J Radiol 2014;83:73-8.
27. Heitzman ER, Markarian B, Raasch BN, et al. Pathways of tumor spread through the lung: radiologic correlations with anatomy and pathology. Radiology 1982;144:3-14.
28. Yano M, Arai T, Inagaki K, et al. Intrapulmonary satellite nodule of lung cancer as a T factor. Chest 1998;114:1305-8.
29. Erasmus JJ, Connolly JE, McAdams HP, et al. Solitary pulmonary nodules. I. Morphologic evaluation for differentiation of benign and malignant lesions. Radiographics 2000;20:43-58.
30. Gaerte SC, Meyer CA, Winer-Muram HT, et al. Fat-containing lesions of the chest. Radiographics 2002;22:S61-78.
31. Batra P, Brown K, Hayashi K, et al. Rounded atelectasis. J Thorac Imaging 1996;11:187-97.
32. Byers TE, Vena JE, Rzepka TF. Predilection of lung cancer for the upper lobes: an epidemiologic inquiry. J Natl Cancer Inst 1984;72:1271-5.
33. Hyodo T, Kanazawa S, Dendo S, et al. Intrapulmonary lymph nodes: thin-section CT findings, pathological findings, and CT differential diagnosis from pulmonary metastatic nodules. Acta Med Okayama 2004;58:235-40.
34. Takashima S, Sone S, Li F, et al. Small solitary pulmonary nodules (≤1 cm) detected at population-based CT screening for lung cancer: reliable high-resolution CT features of benign lesions. AJR Am J Roentgenol 2003;180:955-64.
35. Gadgeel SM, Ramalingam S, Cummings G, et al. Lung cancer in patients < 50 years of age: the experience of an academic multidisciplinary program. Chest 1999;115:1232-6.
36. U.S. Department of Health and Human Services. The health consequences of smoking: a report of the surgeon general. Atlanta, Ga: U.S. Department of Health and Human Services, Centers for Disease Control and Prevention, National Center for Chronic Disease Prevention and Health Promotion, Office on Smoking and Health, 1982.
37. Guyatt GH, Newhouse MD. Are active and passive smoking harmful? determination of causation. Chest 1985;88:445-51.
38. Bach PB, Kattan M, Thornquist MD, et al. Variations in lung cancer risk among smokers. J Natl Cancer Inst 2003;95:470-8.
39. Lee PN. Relation between exposure to asbestos and smoking jointly and the risk of lung cancer. Occup Environ Med 2001;58:145-53.
40. Gottlieb LS, Husen LA. Lung cancer among Navajo uranium miners. Chest 1982;81:449-52.
41. Field RW, Steck DJ, Smith BJ, et al. Residential radon gas exposure and lung cancer: the Iowa Radon Lung Cancer Study. Am J Epidemiol 2000;151:1091-102.

42. Mayne ST, Buenconsejo J, Janerich D. Familial cancer history and lung cancer risk in United States nonsmoking men and women. Cancer Epidemiol Biomarkers Prev 1999;8:1065-9.
43. Bailey-Wilson JE, Amos CI, Pinney SM, et al. A major lung cancer susceptibility locus maps to chromosome 6q2325. Am J Hum Genet 2004;75:460-74.
44. Quint LE, Park CH, Iannettoni MD. Solitary pulmonary nodules in patients with extrapulmonary neoplasms. Radiology 2000;217:257-61.
45. MacMahon H, Austin JH, Gamsu G, et al. Guidelines for management of small pulmonary nodules detected on CT scans: a statement from the Fleischner Society. Radiology 2005;237:395-400.
46. Henschke CI, Yankelevitz DF, Mirtcheva R, et al. CT screening for lung cancer: frequency and significance of part-solid and nonsolid nodules. AJR Am J Roentgenol 2002;178:1053-7.
47. Mujoomdar A, Austin JH, Malhotra R, et al. Clinical predictors of metastatic disease to the brain from non-small cell lung carcinoma: primary tumor size, cell type, and lymph node metastases. Radiology 2007;242:882-8.
48. Komaki R, Cox JD, Stark R. Frequency of brain metastasis in adenocarcinoma and large cell carcinoma of the lung: correlation with survival. Int J Radiat Oncol Biol Phys 1983;9:1467-70.
49. Godoy MC, Naidich DP. Subsolid pulmonary nodules and the spectrum of peripheral adenocarcinomas of the lung: recommended interim guidelines for assessment and management. Radiology 2009;253:606-22.
50. Hasegawa M, Sone S, Takashima S, et al. Growth rate of small lung cancers detected on mass CT screening. Br J Radiol 2000;73:1252-9.
51. Aoki T, Nakata H, Watanabe H, et al. Evolution of peripheral lung adenocarcinomas: CT findings correlated with histology and tumor doubling time. AJR Am J Roentgenol 2000;174:763-8.
52. Li F, Sone S, Abe H, et al. Lung cancers missed at low-dose helical CT screening in a general population: comparison of clinical, histopathologic, and imaging findings. Radiology 2002;225:673-83.
53. Fein AM, Feinsilver SH, Ares CA. The solitary pulmonary nodule: a systemic approach. In: Fishman AP. eds. Pulmonary diseases and disorders. 3rd ed. New York: McGraw-Hill, 1998.
54. Yankelevitz DF, Henschke CI. Does 2-year stability imply that pulmonary nodules are benign? AJR Am J Roentgenol 1997;168:325-8.
55. Usuda K, Sato Y, Sagawa M, et al. Tumor doubling time and prognostic assessment of patients with primary lung cancer. Cancer 1994;74:2239-44.
56. Winer-Muram HT, Jennings SG, Tarver RD, et al. Volumetric growth rate of stage I lung cancer prior to treatment: serial CT scanning. Radiology 2002;223:798-805.
57. Revel MP, Bissery A, Bienvenu M, et al. Are two-dimensional CT measurements of small noncalcified pulmonary nodules reliable? Radiology 2004;231:453-8.
58. Kostis WJ, Yankelevitz DF, Reeves AP, et al. Small pulmonary nodules: reproducibility of three-dimensional volumetric measurement and estimation of time to follow-up CT. Radiology 2004;231:446-52.
59. Revel MP, Lefort C, Bissery A, et al. Pulmonary nodules: preliminary experience with three-dimensional evaluation. Radiology 2004;231:459-66.
60. Yankelevitz DF, Gupta R, Zhao B, et al. Small pulmonary nodules: evaluation with repeated CT - preliminary experience. Radiology 1999;212:561-6.
61. Yankelevitz DF, Reeves AP, Kostis WJ, et al. Small pulmonary nodules: volumetrically determined growth rates based on CT evaluation. Radiology 2000;217:251-6.
62. Wormanns D, Kohl G, Klotz E, et al. Volumetric measurements of pulmonary nodules at multi-row detector CT: in vivo reproducibility. Eur Radiol 2004;14:86-92.
63. Goodman LR, Gulsun M, Washington L, et al. Inherent variability of CT lung nodule measurements in vivo using semiautomated volumetric measurements. AJR Am J Roentgenol 2006;186:989-94.
64. de Hoop B, Gietema H, van de Vorst S, et al. Pulmonary ground-glass nodules: increase in mass as an early indicator of growth. Radiology 2010;255:199-206.
65. Zhang L, Yankelevitz DF, Carter D, et al. Internal growth of nonsolid lung nodules: radiologic-pathologic correlation. Radiology 2012;263:279-86.
66. Kakinuma R, Ohmatsu H, Kaneko M, et al. Progression of focal pure ground-glass opacity detected by low-dose helical computed tomography screening for lung cancer. J Comput Assist Tomogr 2004;28:17-23.
67. Borczuk AC, Qian F, Kazeros A, et al. Invasive size is an independent predictor of survival in pulmonary adenocarcinoma. Am J Surg Pathol 2009;33:462-9.
68. Sakao Y, Miyamoto H, Sakuraba M, et al. Prognostic significance of a histologic subtype in small adenocarcinoma of the lung: the impact of nonbronchioloalveolar carcinoma components. Ann Thorac Surg 2007;83:209-14.
69. Sakao Y, Nakazono T, Tomimitsu S, et al. Lung adenocarcinoma can be subtyped according to tumor dimension by computed tomography mediastinal-

window setting: additional size criteria for clinical T1 adenocarcinoma. Eur J Cardiothorac Surg 2004;26:1211-5.
70. Tsutani Y, Miyata Y, Nakayama H, et al. Prognostic significance of using solid versus whole tumor size on high-resolution computed tomography for predicting pathologic malignant grade of tumors in clinical stage IA lung adenocarcinoma: a multicenter study. J Thorac Cardiovasc Surg 2012;143:607-12.
71. Naidich DP, Bankier AA, MacMahon H, et al. Recommendations for the management of subsolid pulmonary nodules detected at CT: a statement from the Fleischner Society. Radiology 2013;266:304-17.
72. Swensen SJ, Viggiano RW, Midthun DE, et al. Lung nodule enhancement at CT: multicenter study. Radiology 2000;214:73-80.
73. Cronin P, Dwamena BA, Kelly AM, et al. Solitary pulmonary nodules: meta-analytic comparison of cross sectional imaging modalities for diagnosis of malignancy. Radiology 2008;246:772-82.
74. Jeong YJ, Lee KS, Jeong SY, et al. Solitary pulmonary nodule: characterization with combined wash-in and washout features at dynamic multi-detector row CT. Radiology 2005;237:675-83.
75. Chae EJ, Song JW, Seo JB, et al. Clinical utility of dual-energy CT in the evaluation of solitary pulmonary nodules: initial experience. Radiology 2008;249:671-81.
76. Kang MJ, Park CM, Lee CH, et al. Dual-energy CT: clinical applications in various pulmonary diseases. Radiographics 2010;30:685-98.
77. Sim YT, Poon FW. Imaging of solitary pulmonary nodule-a clinical review. Quant Imaging Med Surg 2013;3:316-26.
78. Kim SK, Allen-Auerbach M, Goldin J, et al. Accuracy of PET/CT in characterization of solitary pulmonary lesions. J Nucl Med 2007;48:214-20.
79. Bryant AS, Cerfolio RJ. The maximum standardized uptake values on integrated FDG-PET/CT is useful in differentiating benign from malignant pulmonary nodules. Ann Thorac Surg 2006;82:1016-20.
80. Grgic A, Yüksel Y, Gröschel A, et al. Risk stratification of solitary pulmonary nodules by means of PET using (18) F-fluorodeoxyglucose and SUV quantification. Eur J Nucl Med Mol Imaging 2010;37:1087-94.
81. Kwee TC, Basu S, Saboury B, et al. A new dimension of FDG-PET interpretation: assessment of tumor biology. Eur J Nucl Med Mol Imaging 2011;38:1158-70.
82. Sahiner I, Vural GU. Positron emission tomography/computerized tomography in lung cancer. Quant Imaging Med Surg 2014;4:195-206.
83. Schmid RA, Hillinger S, Bruchhaus H, et al. The value of positron emission tomography (FDG PET) in detecting extrathoracic metastases in non-small cell lung cancer. Am J Respir Crit Care Med 1998;157:A256.
84. Martini N, Flehinger BJ, Zaman MB, et al. Prospective study of 445 lung carcinomas with mediastinal lymph node metastases. J Thorac Cardiovasc Surg 1980;80:390-9.
85. Vansteenkiste JF, Stroobants SG, De Leyn PR, et al. Mediastinal lymph node staging with FDG-PET scan in patients with potentially operable non-small cell lung cancer: a prospective analysis of 50 cases. Chest 1997;112:1480-6.
86. Deppen S, Putnam JB Jr, Andrade G, et al. Accuracy of FDG-PET to diagnose lung Cancer in a region of endemic granulomatous disease. Ann Thorac Surg 2011;92:428-32.
87. Orlacchio A, Schillaci O, Antonelli L, et al. Solitary pulmonary nodules: morphological and metabolic characterisation by FDG-PET-MDCT. Radiol Med 2007;112:157-73.
88. Travis WD, Brambilla E, Noguchi M, et al. International association for the study of lung Cancer/American thoracic society/European respiratory society international multidisciplinary classification of lung adenocarcinoma. J Thorac Oncol 2011;6:244-85.
89. Higashi K, Ueda Y, Seki H, et al. Fluorine- 18-FDG PET imaging is negative in bronchioloalveolar lung carcinoma. J Nucl Med 1998;39:1016-20.
90. Erasmus JJ, McAdams HP, Patz EF Jr, et al. Evaluation of primary pulmonary carcinoid tumors using FDG-PET. AJR Am J Roentgenol 1998;170:1369-73.
91. Van Tassel D, Tassel LV, Gotway MB, et al. Imaging evaluation of the solitarypulmonary nodule. Clin Pulm Med 2011;18:274-99.
92. Yang P, Xu XY, Liu XJ, et al. The value of delayed (18) F FDG-PET imaging in diagnosis of solitary pulmonary nodules: A preliminary study on 28 patients. Quant Imaging Med Surg 2011;1:31-4.
93. Laffon E, de Clermont H, Begueret H, et al. Assessment of dual-time-point 18F-FDG-PET imaging for pulmonary lesions. Nucl Med Commun 2009;30:455-61.
94. Barger RL, Nandalur KR. Diagnostic performance of dual-time 18F-FDG PET in the diagnosis of pulmonary nodules: a meta-analysis. Acad Radiol 2012;19:153-8.
95. National Institute for Health and Clinical Excellence. The diagnosis and treatment of lung cancer (update of NICEclinical guideline 24). Available online: www.nice.org.uk/guidance/index.jsp?action=byID&o=13456
96. Schroeder T, Ruehm SG, Debatin JF, et al. Detection of pulmonary nodules using a 2D HASTE MR

sequence:comparison with MDCT. AJR Am J Roentgenol 2005;185:979-84.
97. Kim JH, Kim HJ, Lee KH, et al. Solitary pulmonary nodules: a comparative study evaluated with contrast-enhanced dynamic MR imaging and CT. J Comput Assist Tomogr 2004;28:766-75.
98. Schaefer JF, Vollmar J, Schick F, et al. Solitary pulmonary nodules: dynamic contrast-enhanced MR imaging–perfusion differences in malignant and benign lesions. Radiology 2004;232:544-53.
99. Kono R, Fujimoto K, Terasaki H, et al. Dynamic MRI of solitary pulmonary nodules: comparison of enhancement patterns of malignant and benign small peripheral lung lesions. AJR Am J Roentgenol 2007;188:26-36.
100. Mori T, Nomori H, Ikeda K, et al. Diffusion-weighted magnetic resonance imaging for diagnosing malignant pulmonary nodules/masses: comparison with positron emission tomography. J Thorac Oncol 2008;3:358-64.
101. Zhang X, Ji JX. Parallel and sparse MR imaging: methods and instruments-Part 1. Quant Imaging Med Surg 2014;4:1-3.
102. Ji JX, Zhang X. Parallel and sparse MR imaging: methods and instruments-Part 2. Quant Imaging Med Surg 2014;4:68-70.
103. Gurney JW. Missed lung cancer at CT: imaging findings in nine patients. Radiology 1996;199:117-22.
104. Jaeger S, Karargyris A, Candemir S, et al. Automatic screening for tuberculosis in chest radiographs: a survey. Quant Imaging Med Surg 2013;3:89-99.
105. Jeon KN, Goo JM, Lee CH, et al. Computer-aided nodule detection and volumetry to reduce variability between radiologists in the interpretation of lung nodules at low-dose screening computed tomography. Invest Radiol 2012;47:457-61.
106. Bogoni L, Ko JP, Alpert J, et al. Impact of a computer-aided detection (cad) system integrated into a picture archiving and communication system (pacs) on reader sensitivity and efficiency for the detection of lung nodules in thoracic ct exams. J Digit Imaging 2012;25:771-81.
107. Suzuki K. A review of computer-aided diagnosis in thoracic and colonic imaging. Quant Imaging Med Surg 2012;2:163-76.
108. Rubin GD, Lyo JK, Paik DS, et al. Pulmonary nodules on multi-detector row CT scans: performance comparison of radiologists and computer-aided detection. Radiology 2005;234:274-83.
109. Gruden JF, Ouanounou S, Tigges S, et al. Incremental benefit of maximum-intensityprojection images on observer detection of small pulmonary nodules revealed by multidetector CT. AJR Am J Roentgenol 2002;179:149-57.
110. Suzuki K, Armato III SG, Li F, et al. Massive training artificial neural network (MTANN) for reduction of false positives in computerized detection of lung nodules in low-dose CT. Medical Physics 2003;30:1602-17.
111. Li F, Arimura H, Suzuki K, et al. Computer-aided detection of peripheral lung cancers missed at CT: ROC analyses without and with localization. Radiology 2005;237:684-90.
112. Suzuki K, Li F, Sone S, et al. Computer-aided diagnostic scheme for distinction between benign and malignant nodules in thoracic low-dose CT by use of massive training artificial neural network. IEEE Transactions on Medical Imaging 2005;24:1138-50.
113. Li F, Aoyama M, Shiraishi J, et al. Radiologists' performance for differentiating small benign from malignant lung nodules on high-resolution CT by using computer-estimated likelihood of malignancy. AJR Am J Roentgenol 2004;183:1209-15.
114. Conces DJ Jr, Schwenk GR Jr, Doering PR, et al. Thoracic needle biopsy: improved results utilizing a team approach. Chest 1987; 91:813-6.
115. Berquist TH, Bailey PB, Cortese DA, et al. Transthoracic needle biopsy: accuracy and complications in relation to location and type of lesion. Mayo Clin Proc 1980;55:475-81.
116. Cortese DA, McDougall JC. Bronchoscopic biopsy and brushing with fluoroscopic guidance in nodular metastatic lung cancer. Chest 1981;79:610-1.
117. Swensen SJ, Jett JR, Payne WS, et al. An integrated approach to evaluation of the solitary pulmonary nodule. Mayo Clin Proc 1990;65:173-86.
118. Henschke CI, Davis SD, Auh Y, et al. Detection of bronchial abnormalities: comparison of CT and bronchoscopy. J Comput Assist Tomogr 1987;11:432-5.
119. Jeudy J, White CS, Munden RF, et al. Management of small (3-5-mm) pulmonary nodules at chest CT: global survey of thoracic radiologists. Radiology 2008;247:847-53.
120. Eisenberg RL, Bankier AA, Boiselle PM. Compliance with Fleischner Society guidelines for management of small lung nodules: a survey of 834 radiologists. Radiology 2010;255:218-24.

Cite this article as: Wang YX, Gong JS, Suzuki K, Morcos SK. Evidence based imaging strategies for solitary pulmonary nodule. J Thorac Dis 2014;6(7):872-887. doi: 10.3978/j.issn.2072-1439.2014.07.26

Original Article

VATS biopsy for undetermined interstitial lung disease under non-general anesthesia: comparison between uniportal approach under intercostal block *vs*. three-ports in epidural anesthesia

Vincenzo Ambrogi, Tommaso Claudio Mineo

Thoracic Surgery Division and Department of Thoracic Surgery, Policlinico Tor Vergata University, Rome, Italy

Correspondence to: Vincenzo Ambrogi, MD. Cattedra di Chirurgia Toracica, Policlinico Tor Vergata, Viale Oxford, 8100133 Rome, Italy. Email: ambrogi@med.uniroma2.it.

Objective: Video-assisted thoracoscopic (VATS) biopsy is the gold standard to achieve diagnosis in undetermined interstitial lung disease (ILD). VATS lung biopsy can be performed under thoracic epidural anesthesia (TEA), or more recently under simple intercostal block. Comparative merits of the two procedures were analyzed.

Methods: From January 2002 onwards, a total of 40 consecutive patients with undetermined ILD underwent VATS biopsy under non-general anesthesia. In the first 20 patients, the procedures were performed under TEA and in the last 20 with intercostal block through a unique access. Intraoperative and postoperative variables were retrospectively matched.

Results: Two patients, one from each group, required shift to general anesthesia. There was no 30-day postoperative mortality and two cases of major morbidity, one for each group. Global operative time was shorter for operations performed under intercostal block (P=0.041). End-operation parameters significantly diverged between groups with better values in intercostal block group: one-second forced expiratory flow (P=0.026), forced vital capacity (P=0.017), oxygenation (P=0.038), $PaCO_2$ (P=0.041) and central venous pressure (P=0.045). Intraoperative pain coverage was similar. Significant differences with better values in intercostal block group were also experienced in 24-hour postoperative quality of recovery-40 questionnaire (P=0.038), hospital stay (P=0.033) and economic expenses (P=0.038). Histology was concordant with radiologic diagnosis in 82.5% (33/40) of patients. Therapy was adjusted or modified in 21 patients (52.5%).

Conclusions: Uniportal VATS biopsies under intercostal block can provide better intraoperative and postoperative outcomes compared to TEA. They allow the indications for VATS biopsy in patients with undetermined ILD to be extended.

Keywords: Interstitial lung disease (ILD); lung biopsy; video-assisted thoracic surgery (VATS)

Submitted Nov 09, 2013. Accepted for publication Jun 13, 2014.
doi: 10.3978/j.issn.2072-1439.2014.07.06
View this article at: http://dx.doi.org/10.3978/j.issn.2072-1439.2014.07.06

Introduction

Despite the advent of high-resolution computed tomography (HRCT) or fine needle biopsy surgical lung biopsy is still considered the gold standard to achieve a definitive diagnosis in undetermined interstitial lung disease (ILD) in order to establish a correct therapy and to predict a reliable prognosis (1-3). These procedures have successfully been accomplished via video-assisted thoracic surgery (VATS) with a lower morbidity, less pain and a shorter hospital stay (4-7) in comparison with traditional open accesses. However, one of the major risks during surgical biopsy is still represented by the general anesthesia under one-lung ventilation, which may precipitate altered respiratory function, pulmonary hypertension and infections (8,9). Current guidelines by the American Thoracic Society/European Respiratory Society (10,11) recommend surgical biopsy only for those ILD

Table 1 Demographic variables and histologic findings of the study population

	TEA (n=20)	IB (n=20)	P value
Age [years]	61 [48-70]	61 [48-70]	0.911
Oxygen support (n, pts)	6 (30%)	7 (35%)	0.122
Oral steroids dependant (n, pts)	16 (80%)	15 (75%)	0.234
Azathioprine user (n, pts)	4 (20%)	3 (15%)	0.327
Body mass index [kg/m^2]	22 [18-25]	22 [18-25]	1
6-minute walking test [%, pred]	62 [54-69]	60 [53-71]	0.312
Forced expiratory volume one-second [%, pred]	65 [56-72]	61 [50-69]	0.653
Forced vital capacity [%, pred]	66 [54-76]	64 [56-75]	0.327
Diffusion lung carbon-monoxide [%, pred]	50 [41-59]	51 [42-62]	0.211
PaO_2 [mmHg]	82 [78-95]	84 [76-92]	0.645
$PaCO_2$ [mmHg]	43 [38-55]	42 [39-54]	0.783
American Society of Anesthesiology score [1-4]	2 [1-3]	2 [1-3]	1
Histology			
Idiopathic interstitial pneumonia			
Idiopathic pulmonary fibrosis	8 (40%)	9 (45%)	0.749
Nonspecific interstitial pneumonia	2 (10%)	1 (5%)	0.548
Cryptogenic organizing pneumonia	2 (10%)	2 (10%)	1
Acute interstitial pneumonia	1 (5%)	1 (5%)	1
Respiratory bronchiolitis-associated ILD	1 (5%)	–	0.311
Desquamative interstitial pneumonia	–	1 (5%)	0.311
ILD, not specified	2 (10%)	3 (15%)	0.633
Other diffuse diseases			
Granulomatous disease	1 (5%)	–	0.311
Hypersensitivity pneumonitis	–	1 (5%)	0.311
Other	2 (10%)	2 (10%)	1
Inadequate biopsy	1 (5%)	–	0.311

TEA, thoracic epidural anesthesia; IB, intercostal block. Data are expressed as median (interquartile range).

patients who are at acceptable risk to tolerate the procedure and this has severely limited the use of this precious diagnostic device.

To avoid potential complications we initially introduced awake VATS biopsy under thoracic epidural anesthesia (TEA), but more recently we established a new procedure through a unique access under a simple intercostal block in non-general anesthesia (12). Hereby we analyzed comparative merits of this procedure in comparison to VATS biopsy under TEA.

Methods

This investigation is a branch of the mainstay program started in 2001, previously referred to as "awake thoracic surgery" and now more widely defined as "thoracic surgery under monitored anesthesia care" (13).

Patients

From January 2002 onwards a total of 40 consecutive patients with an undetermined ILD underwent VATS biopsy under non-general anesthesia. In the first 20 patients the VATS biopsy was performed under TEA and in the last 20 with intercostal block through a unique access. Demographics variables and histologic findings are summarized in *Table 1*. Patients were selected according to clinical and radiologic findings by a multidisciplinary panel

formed by one pulmonologist, one thoracic surgeon, one anesthesiologist experienced in non-intubated procedures and one radiologist dedicated to ILD. Patients routinely underwent HRCT (General Electric Medical Systems, Milwaukee, WI, USA) and evaluation included the pattern of parenchymal abnormality (i.e., consolidation, ground-glass opacity, reticular pattern), anatomic distribution and presence of associated pathologies (i.e., mediastinal lymphadenopathy).

Imaging of diffuse honeycombing pattern was considered by itself a criteria for excluding lung biopsy. Other exclusion criteria were age >75 years, end-stage disease with need of mechanical ventilation, BMI >22 and <30, diffusing lung capacity for carbon monoxide (DLCO) <30% predicted, basal room air PaO_2 <50 mmHg, $PaCO_2$ >50 mmHg, American Society of Anesthesiology score <3 and presence of immunodeficiency status or active cancer. We considered tenacious pleura-pulmonary adhesions or patient's anxiety common contraindication for a non-general anesthesia procedure.

All patients gave their written informed consent. Local institutional review board approval was obtained for study (ref #CT0013-7268). Respiratory assessments included timed spirometry and plethysmography with single-breath DLCO (V_{max} 22; Sensor Medics, Yorba Linda, CA, USA) and arterial blood gas analysis. Exercise tolerance was assessed with the standard 6-minute walk test. Quality of life was assessed with the St. George Respiratory Questionnaire (SGRQ) general score (best =0, worst =100) (14,15). In addition all patients underwent preoperative fiberoptic bronchoscopy with bronchoalveolar lavage and cardiac evaluation including color Doppler echocardiography for pulmonary artery pressure non-invasive estimation. Right heart catheterism was performed in selected cases only. Laboratory tests entailed complete blood cell count with differential leukocyte counts, renal and liver function tests, and urinalysis.

Technique

Lung areas suitable for biopsy were chosen after panel discussion. We preferentially chose the middle lobe and the lingula, which are the lung areas most suited to surgical biopsy. The other most targeted areas were the apical segment of the lower lobe or the ventral of the right upper lobe. All these regions easily provided a large quantity of tissue, with a relatively short and straight suture line. The ultimate decision of the area targeted for biopsy was taken intraoperatively according to the most diagnostic site and the most reachable area in a breathing lung. Generally, target areas appeared as cobblestone road with subpleural nodularity, covered by thick and greyish visceral pleura with evidence of neoangiogenesis. These visible findings were usually coupled by the palpatory sensation of an anelastic parenchyma with increased resistance.

A resection volume greater than 1 mL (1 cm^3) was usually considered satisfactory and we routinely collected two or more biopsies without creating supplementary incisions.

Patients were continuously monitored by electrocardiogram, pulse oxymeter, systemic and central venous blood pressure, body temperature, arterial blood gases, and end-tidal CO_2 by insertion of one detector into a nostril. Forced expiratory volume in one second (FEV1) and forced vital capacity (FVC) were re-assessed immediately pre and postoperatively by a portable spirometer (V_{max} Encore 29, Sensor Medics, Yorba Linda, CA, USA).

Intraoperative monitoring included assessment of all these parameters at different standardized times: before incision, at pneumothorax induction, at chest closure and 1-hour postoperatively. Evaluation of acute pain was assessed using a visual analogue scale (VAS) (0= absent, to 10= most severe imaginable pain) (16). Procedures took place in a calm and cooperative setting with a low-volume classical or melodic music played in the background. During the procedure, a venturi mask was used to keep oxygen saturation greater than 90%. Hypercapnia was well tolerated and correction was performed only when PH decreased to less than 7.2.

A chest drain with an underwater seal or a simple endoscopic suction device system was always kept ready to rapidly contrast a discomfort secondary to iatrogenic pneumothorax. Mild sedation with midazolam or propofol was useful to control the discomfort induced by pneumothorax or panic attacks. Shift to general anesthesia was allowed only in the following conditions: irritation or intolerance of the patient before the accomplishment of the biopsy, elevated level of $PaCO_2$ (50 mmHg), operation technically difficult or hemorrhagic complications.

VATS biopsy under TEA

After insertion of venous and radial artery catheters, an epidural catheter was positioned at T4-T5 level through which a bolus of 5 mg ropivacaine plus 5 μg sufentanyl was injected. Continuous infusion of ropivacaine 2 mg/mL (5 mL/hour) was then started 20 minutes prior to operation with the patient lying on the side targeted for biopsy. After

achievement of satisfactory anesthesia the patient was turned on the other side ready for the operation.

The procedure was classically carried out through three ports. Usually the camera port was placed in the eighth intercostal space along the midaxillary line, the operating ports were usually placed in the fifth intercostal space, anterior and posterior axillary lines. In the case of biopsies located in the posterior segments of the lower lobes, theoperative port was set more caudally than the camera port and the monitor was positioned at the bottom of the patient to avoid mirror image effect. The biopsy was preferentially performed along a straight line an endostapler endopath® 30 or 45 with staples of 4.5 mm suturing with as less number of bites as possible in order to decrease the risk of bleeding. Blood and air leakage from the resection line were carefully controlled both at the time of suture completion and at chest closure. A 28 CH chest tube was inserted through the lowest incision. At end-procedure, lung re-expansion was achieved under thoracoscopic vision by asking the patient to breathe deeply and cough repeatedly. The epidural catheter was usually removed on postoperative day one.

Uniport VATS biopsy under intercostal block

After insertion of venous and radial artery catheters, an aerosolized 5 mL solution of 2% lidocaine was administered for 5 minutes in order to avoid cough reflex. The intercostal block was accomplished by local injection of 20-30 mL solution of 2% lidocaine and 7.5% ropivacaine, for achieving a rapid onset with a long duration of the analgesic effect. Site of inoculation was done along the space selected for uniportal VATS and included subcutaneous layers, intercostal nerves and parietal pleura. The grade of local anesthesia was always adequate. In a few cases benzodiazepine (midazolam 0.03-0.1 mg/kg) or opioids (remifentanil 15 μg/kg/min) were intravenously supplemented during lung manipulation or stapling manoeuvres.

All VATS biopsies were carried out from a single small 30-40 mm uniport skin incision carried out along the space judged the most suitable to reach the foreseen area. In the case of lingula or middle lobe biopsy incision was usually performed along the fourth intercostal space medially from the anterior axillary line, whereas posterior segments were biopsied through an eighth intercostal space posterior incisions. Rib spreading by retractor was always avoided. Through the incision we introduced the operative thoracoscope, the articulated stapler and incidentally a gauze pad mounted on a ring-forceps in order to contrast lung movements during breathing or coughing. In many instances we were able to exteriorize the most distal target area and accomplish the resection outside from the chest. At the end of the procedure one 28 CH chest tube was collocated through the posterior end of the incision. No trans-intercostal suture was necessary. Muscle sutures were tightened after asking the patient to breathe deeply or cough to achieve maximal lung re-expansion.

Postoperative care

Postoperative care was similar after both procedures. After a short stage in the weaning areas the patient was directly sent to the ward. Liquids infusion was stopped immediately and drinking, meal intake and ambulation were started on the same day of surgery. Chest X-ray was routinely performed at 24 hours from the procedure to confirm adequate lung expansion.

State of consciousness and postoperative recovery was evaluated by the quality of recovery (QoR-40), which is a 40-item self-administered questionnaire (17). Each item is linked to a 5-point Likert scale [1-5] with a minimum cumulative score of 5 (maximal impairment) and maximum of 200 (no impairment). Time of discharge was determined by chest tube removal, which generally took place in the absence of air leak and with a daily fluid leakage less than 150 mL.

The biopsy samples were sent fresh and reviewed by the institutional pathologist with a hub on ILD. A fragment was also sent for microorganism cultures.

Statistics

All data was statistically analyzed using the SPSS (SPSS® 9.05 for Windows, SPSS Inc., Chicago, 1998). Interdependence among factors and group comparisons were prudentially assessed by non-parametric tests. Data were expressed with median and interquartile range deviation. P values <0.05 were regarded as statistically significant in two tailed tests.

Results

Two patients, one from each group, required the shift to general anesthesia with intubation and single lung ventilation. No patient needed conversion to open thoracotomy.

A total of 95 biopsies were performed: 48 (2.4 per patient) in TEA group and 47 (2.35 per patient) in intercostal block

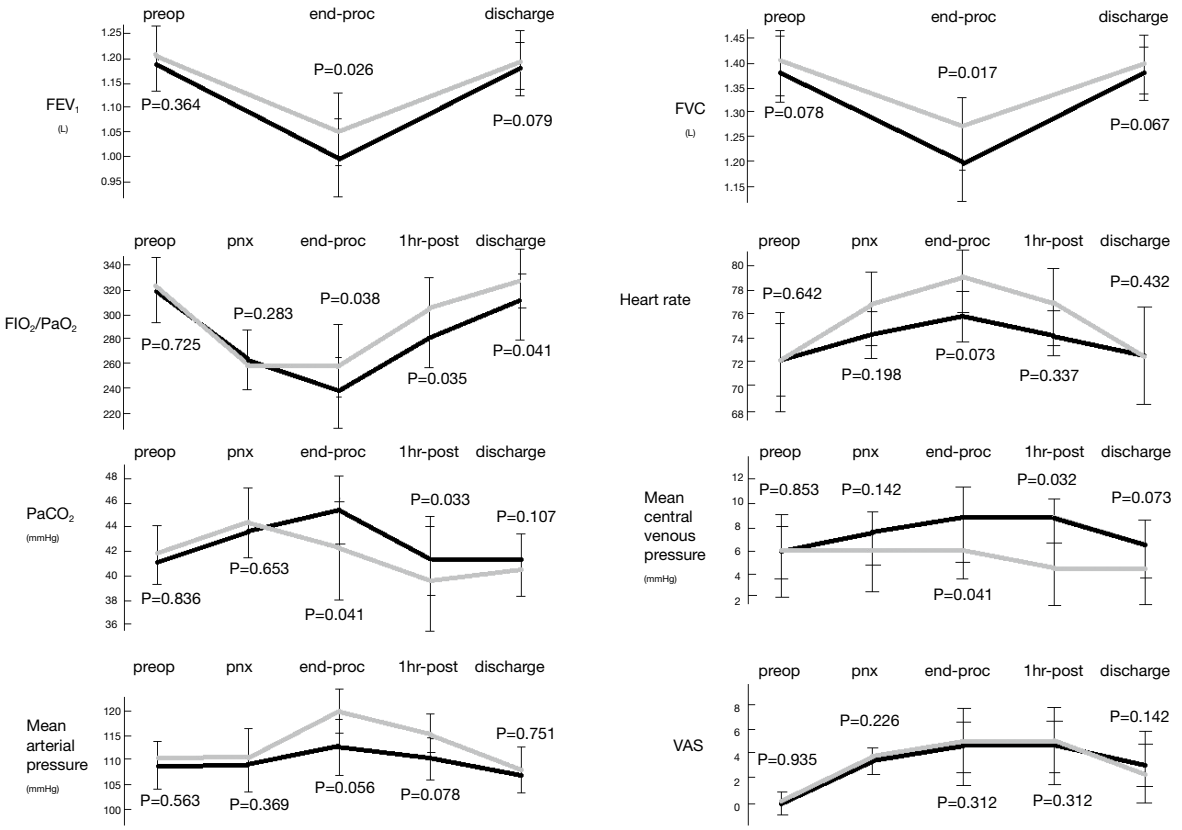

Figure 1 Intraoperative measurements of patients undergoing intercostal block (gray line) and thoracic epidural anesthesia (black line).

group, respectively. No 30-day postoperative mortality was experienced. We reported one case of acute respiratory insufficiency resolved by non-invasive ventilation in the TEA group and one acute pneumonia in the intercostal block group. We also recorded minor complications related to TEA: hypotension antagonized by noradrenalin infusion (n=2) and urinary block (n=3) requiring catheterization.

Global operative time was significantly shorter for operations performed under intercostal block {61 [53-68] *vs*. 70 [62-78]; P=0.041} and this was mainly due to the lack of epidural catheter introduction and time for the onset of anesthesia.

Intraoperative findings of main physiologic parameters are shown in *Figure 1*. FEV1 and FVC presented a significant decrement in both groups at end-operation, but the fall was lesser in the intercostal one, with a significant difference at intergroup analysis (FEV1, P=0.026 and FVC, P=0.017). As a result, oxygenation (FiO_2/PaO_2) and $PaCO_2$ were significantly different between groups at end-operation (P=0.038 and P=0.041, respectively) and at 1 hour postoperatively (P=0.035 and P=0.033, respectively). Interestingly, the values of central venous pressure were significantly less elevated during intercostal block at the end of the procedure (P=0.041) and after 1 hour from the procedure (P=0.032). Pain coverage was satisfactory throughout the procedure and without significant differences in both groups (*Figure 1*). Similarly, there was no difference in basal and under cough VAS at 24 and 48 hours, respectively. Postoperative QoR was significantly better in intercostal group after 24 (P=0.038) hours from the operation, whereas quality of life at 7 and 30 days was similar between groups. Hospital stay was significantly shorter in patients undergoing intercostal block (P=0.033) and this also impacted the economic expenses (P=0.038) (*Table 2*).

A reliable pathologic specimen was obtained by surgical biopsy 97.5% (39/40) of the patients, and in 94.7% (90/95) of biopsies. The biopsy specimens were concordant in 82.5% (33/40) of patients and in 68.4% (65/95) of the biopsies. No differences were found between groups (*Table 2*). On the basis of histopathology findings, therapy was adjusted or modified in 21 patients (52.5%).

Table 2 Comparison of outcomes between groups

Patients	TEA (n=20)	IB (n=20)	P value
Global in-operating room [min]	70 [62-78]	61 [53-68]	0.041
Operative time [min]	38 [32-48]	40 [31-49]	0.082
Biopsy number (n, pts)	2.3 (1.6-2.8)	2.1 (1.5-2.6)	0.623
Biopsy cumulative volume (cm^3)	6.4 (5.3-6.9)	6.1 (5.6-7.3)	0.831
HRCT/histology concordance per patient [%]	17/20 [85]	16/20 [80]	0.677
HRCT/histology concordance per lesion [%]	32/48 [67]	33/47 [70]	0.710
24-hour postop QoR40 [5-200]	114 [96-138]	126 [89-157]	0.038
24-hour postop basal VAS	4.4 [2-6]	4.3 [2-6]	0.621
24-hour postop cough VAS	5.9 [3-7]	5.2 [3-7]	0.041
48-hour postop QoR40 [5-200]	156 [122-194]	164 [131-183]	0.054
48-hour postop basal VAS	2.1 [1-4]	2.0 [1-3]	0.765
48-hour postop cough VAS	4.4 [2-6]	4.3 [2-6]	0.212
Hospital stay [day]	3.7 [1-6]	3.0 [2-4]	0.033
Major morbidity n [%]	1 [5]	1 [5]	1
7-day quality of life (SGRQ) [%]	38 [29-48]	35 [28-49]	0.342
30-day mortality rate [%]	0	0	1
30-day quality of life (SGRQ) [%]	21 [12-40]	23 [19-41]	0.547
Estimated costs [euro]	3,124 [2,334-4,190]	2,632 [2,088-3,253]	0.038

TEA, thoracic epidural anesthesia; IB, intercostal block. Data are expressed as median (interquartile range). HRCT, high resolution computed tomography; VAS, visual analogue scale; QoR, quality of recovery questionnaire; SGRQ, St.George respiratory questionnaire.

Discussion

The use of intercostal block associated with intravenous sedation during thoracoscopy for diagnostic and therapeutic purposes has already been described in different thoracic pathologies with satisfactory results (18-21). In this personal series we presented the additional advantages of intercostal block compared to TEA during VATS lung biopsy in patients with ILD undetermined lesions.

In our study we experienced that intercostal block may significantly attenuate intraoperative lung-volumes fall as well as hypoxia (FiO_2/PaO_2) and hypercapnia respect to same procedures under TEA.

It has been reported that TEA causes a significant decrement of inspiratory capacity (22) as a probable blockade of efferent or afferent pathways of the intercostal nerve roots resulting in a decreased contribution of the rib cage to tidal breathing (23). TEA may also produce a wide adrenergic tone fall with prevalence of bronchus-constriction as evidenced by FEV1 decrement (24). The documented increment of the central venous pressure in TEA could be a consequence of lung flow reduction as well as of the impairment of ventricle sympathetic outflow due to the adrenergic block (25-27).

These effects are absent or minimal under intercostal block, which leaves normal adrenergic tone without interfering on skeletal, bronchus and cardiac muscle motility (12) also avoiding the intrinsic risks and unpleasant side-effects related to TEA.

The risk of coughing is high when stapling the lung under intercostal block but it can be minimized by the use of aerosolized 2% lidocaine with transitory side effects. As far as the expected lesser duration of pain coverage is concerned, we found it more useful to have pain control with intravenous drugs rather than the prolonged and fastidious disturbances following TEA. Furthermore, the QoR-40 questionnaire clearly documented a significant greater and faster postoperative recovery after the intercostal block.

This study is retrospective and non-randomized and the results need to be interpreted as such. Another potential limitation is represented by the reliability of respiratory

functional tests performed during a surgical operation, which can be altered by patient fatigue, lack of cooperation and iatrogenic pneumothorax. However these potential artifacts were homogeneous between groups and do not appear to interfere with the global trend of the measurements.

Conclusions

We would suggest that uniportal VATS biopsies under intercostal block can provide better intraoperative and postoperative outcomes compared to TEA, thus increasing the safety as well as enlarging the indication of VATS biopsy in presently not-eligible patients. These results stimulate our interest in thoracic surgery under monitored anesthesia care (12), which permits a quicker postoperative recovery as well as lower morbidity, hospital stay and economical costs with satisfaction of patients, surgeons, pneumologists and administrators.

Acknowledgements

We express our sincere gratitude to all pneumologists, physicians and general practitioners for referring us their patients in order to achieve a definitive diagnosis. Both authors take responsibility for the content of the manuscript, including the data and analysis.

Both authors made substantial contributions to conception, design, acquisition or analysis and interpretation of data; Vincenzo Ambrogi has drafted the submitted article; Tommaso Claudio Mineo has provided final approval of the version to be published; each author has agreed for all aspects of the work in ensuring that any part of the work is appropriately investigated and resolved.

Disclosure: The authors declare no conflict of interest.

References

1. Raghu G, Mageto YN, Lockhart D, et al. The accuracy of the clinical diagnosis of new-onset idiopathic pulmonary fibrosis and other interstitial lung disease: a prospective study. Chest 1999;116:1168-74.
2. Flaherty KR, Travis WD, Colby TV, et al. Histopathologic variability in usual and nonspecific interstitial pneumonias. Am J Respir Crit Care Med 2001;164:1722-7.
3. Kayatta MO, Ahmed S, Hammel JA, et al. Surgical biopsy of suspected interstitial lung disease is superior to radiographic diagnosis. Ann Thorac Surg 2013;96:399-401.
4. Boutin C, Viallat JR, Cargnino P, et al. Thoracoscopic lung biopsy. Experimental and clinical preliminary study. Chest 1982;82:44-8.
5. Bensard DD, McIntyre RC Jr, Waring BJ, et al. Comparison of video thoracoscopic lung biopsy to open lung biopsy in interstitial lung disease. Chest 1993;103:765-70.
6. Ferson PF, Landreneau RJ, Dowling RD, et al. Comparison of open versus thoracoscopic lung biopsy for diffuse infiltrative pulmonary disease. J Thorac Cardiovasc Surg 1993;106:194-9.
7. Krasna MJ, White CS, Aisner SC, et al. The role of thoracoscopy in the diagnosis of interstitial lung disease. Ann Thorac Surg 1995;59:348-51.
8. Fishbein MC. Diagnosis: To biopsy or not to biopsy: assessing the role of surgical lung biopsy in the diagnosis of idiopathic pulmonary fibrosis. Chest 2005;128:520S-525S.
9. Lettieri CJ, Veerappan GR, Helman DL, et al. Outcomes and safety of surgical lung biopsy for interstitial lung disease. Chest 2005;127:1600-5.
10. American thoracic society. Idiopathic pulmonary fibrosis: diagnosis and treatment. International consensus statement. American Thoracic Society (ATS), and the European Respiratory Society (ERS). Am J Respir Crit Care Med 2000;161:646-64.
11. American Thoracic Society, European Respiratory Society. American Thoracic Society/European Respiratory Society International Multidisciplinary Consensus Classification of the Idiopathic Interstitial Pneumonias. This joint statement of the American Thoracic Society (ATS), and the European Respiratory Society (ERS) was adopted by the ATS board of directors, June 2001 and by the ERS Executive Committee, June 2001. Am J Respir Crit Care Med 2002;165:277-304.
12. Mineo TC, Ambrogi V. Efficacy of awake thoracic surgery. J Thorac Cardiovasc Surg 2012;143:249-50.
13. Mineo TC, Tacconi F. From "Awake" to "Monitored Anesthesia Care" Thoracic Surgery: a 15 Years Evolution. Thoracic Cancer 2014;5:1-13.
14. Jones PW, Quirk FH, Baveystock CM, et al. A self-complete measure of health status for chronic airflow limitation: The S.George's respiratory disease questionnaire. Am Rev Resp Dis 1992;145:1321-7.
15. Carone M, Bertolotti G, Anchisi F, et al. Il Saint George's Respiratory Questionnaire (SGRQ): la versione italiana. Rass Mal App Resp 1999;14:31-37.
16. Price DD, McGrath PA, Rafii A, et al. The validation of visual analogue scales as ratio scale measures for chronic and experimental pain. Pain 1983;17:45-56.

17. Myles PS, Weitkamp B, Jones K, et al. Validity and reliability of a postoperative quality of recovery score: the QoR-40. Br J Anaesth 2000;84:11-5.
18. Rusch VW, Mountain C. Thoracoscopy under regional anesthesia for the diagnosis and management of pleural disease. Am J Surg 1987;154:274-8.
19. Danby CA, Adebonojo SA, Moritz DM. Video-assisted talc pleurodesis for malignant pleural effusion utilizing local anesthesia and IV sedation. Chest 1998;113:739-42.
20. Nezu K, Kushibe K, Tojo T, et al. Thoracoscopic wedge resection of blebs under local anesthesia with sedation for treatment of a spontaneous pneumothorax. Chest 1997;111:230-5.
21. Migliore M, Giuliano R, Aziz T, et al. Four-step local anesthesia and sedation for thoracoscopic diagnosis and management of pleural diseases. Chest 2002;121:2032-5.
22. Warner DO, Warner MA, Ritman EL. Human chest wall function during epidural anesthesia. Anesthesiology 1996;85:761-73.
23. Kochi T, Sako S, Nishino T, et al. Effect of high thoracic extradural anaesthesia on ventilatory response to hypercapnia in normal volunteers. Br J Anaesth 1989;62:362-7.
24. Clemente A, Carli F. The physiological effects of thoracic epidural anesthesia and analgesia on the cardiovascular, respiratory and gastrointestinal systems. Minerva Anestesiol 2008;74:549-63.
25. Sundberg A, Wattwil M, Arvill A. Respiratory effects of high thoracic epidural anaesthesia. Acta Anaesthesiol Scand 1986;30:215-7.
26. Takasaki M, Takahashi T. Respiratory function during cervical and thoracic extradural analgesia in patients with normal lungs. Br J Anaesth 1980;52:1271-6.
27. Sakura S, Saito Y, Kosaka Y. The effects of epidural anesthesia on ventilatory response to hypercapnia and hypoxia in elderly patients. Anesth Analg 1996;82:306-11.

Cite this article as: Ambrogi V, Mineo TC. VATS biopsy for undetermined interstitial lung disease under non-general anesthesia: comparison between uniportal approach under intercostal block *vs.* three-ports in epidural anesthesia. J Thorac Dis 2014;6(7):888-895. doi: 10.3978/j.issn.2072-1439.2014.07.06

Original Article

Clinicopathological variables predicting *HER-2* gene status in immunohistochemistry-equivocal (2+) invasive breast cancer

Yongling Ji[1], Liming Sheng[1], Xianghui Du[1], Guoqin Qiu[1], Bo Chen[2], Xiaojia Wang[3]

[1]Department of Radiation Therapy, [2]Department of Pathology, [3]Department of Medical Oncology, Zhejiang Cancer Hospital, Hangzhou 310022, China
Correspondence to: Xianghui Du, MD. Department of Radiation Therapy, Zhejiang Cancer Hospital, 38 Guangji Road, Hangzhou 310022, China. Email: vip20132014@126.com.

Background and objective: Human epidermal growth factor receptor-2 (*HER-2*) gene status is crucial to guide treatment decisions regarding the use of HER-2-targeted therapies in breast cancer. An invasive breast cancer with *HER-2* 2+ score is regarded as *HER-2* status equivocal and should further determine by fluorescent in situ hybridization (FISH), which is considered the standard test for HER-2 status. Here, we aimed to establish a risk score to allow for prediction of the presence of *HER-2* gene status.

Methods: A total of 182 HER-2 2+ by immunohistochemistry (IHC) invasive breast cancer cases were enrolled in this study. The association between clinicopathological variables like age, sex, tumor grade, hormone receptor (HR) status, P53 and proliferation index (Ki67), and FISH result using US Food and Drug Administration (FDA) criteria was evaluated. Also, we compared the HER-2 FISH results using FDA criteria and 2013 American Society of Clinical Oncology/College of American Pathologists (ASCO/CAP) guideline.

Results: The study population had a median age of 48 years (range, 29-78 years). Estrogen receptor (ER) was expressed in 131 (72.0%) patients. 73.1% of patients (133/182) were progesterone receptor (PR) positive. The median Ki67 value was 20% (range, 3-90%). There was good agreement between the FDA and 2013 ASCO/CAP guideline. Sixty-three of all patients were *HER-2* FISH amplified (positive) based on FDA criteria. Tumors with *HER-2* amplified were more likely to harbor ER negative (58.8% *vs.* 25.2%, P<0.001) or PR negative (57.1% *vs.* 26.3%, P<0.001) or P53 negative (44.8% *vs.* 29.8%, P=0.048). A significant high level of Ki67 was detected in *HER-2* amplified groups (P=0.006). We created a risk score that comprised HR, P53 and Ki67. A significant association between risk score and *HER-2* FISH amplification was observed (χ^2=30.41, P<0.001).

Conclusions: This novel immunohistochemical risk score could be highly useful to predict the presence of *HER-2* gene status in invasive breast cancer.

Keywords: Invasive breast cancer; human epidermal growth factor receptor-2 (HER-2); immunohistochemistry (IHC); fluorescent in situ hybridization (FISH); prediction

Submitted Nov 21, 2013. Accepted for publication Jul 03, 2014.
doi: 10.3978/j.issn.2072-1439.2014.07.27
View this article at: http://dx.doi.org/10.3978/j.issn.2072-1439.2014.07.27

Background

Breast cancer is regarded as a heterogeneous group of tumors that are diverse in terms of underlying biology, pathological characteristics, response to therapy, and clinical outcome (1). Breast cancer is divided into at least five distinct molecular subtypes [luminal A, luminal B, human epidermal growth factor receptor-2 (*HER-2*), normal-like, and basal] by gene expression analysis (2). Breast cancer with *HER-2* overexpression currently comprises 15% to 20% of all cases in the world (3). *HER-2*/neu, located on chromosome 17q21, encodes for the 185 kD transmembrane glycoprotein *HER-2*, which is one of the most targeted proteins. Studies indicate that *HER-2* is involved in the activation of

intracellular signal transduction pathways that regulate cell growth, proliferation, adhesion, and motility (4). *HER-2* overexpression or amplification in breast cancer has been extensively studied worldwide (5-7). Overexpression or amplification of *HER-2* has been demonstrated to be an independent parameter for bad prognosis, and is shown to be associated with resistance to certain chemotherapeutic agents (8-11). *HER-2*-targeted therapies have significantly improved disease-free survival in women with *HER-2*-positive cancers both in early and metastatic breast cancer (12,13). Three *HER-2*-targeted agents, trastuzumab (Herceptin), lapatinib (Tykerb), and pertuzumab (Perjeta), have been made available in the past decade for the treatment of *HER-2*-positive metastatic breast cancer (14). Combinations of *HER-2*-directed agents may yield additive or synergistic effects that lead to better prognosis (15).

Overexpression of the *HER-2* protein has become a marker for eligibility for *HER-2*-directed treatments. False positive or false negative results in *HER-2* patients may lead to inappropriate treatment administration (16). Therefore, *HER-2* status is crucial in the guidance of treatment decisions for the use of trastuzumab and is becoming a standard recommendation in the pretreatment work-up of patients with invasive breast cancer. Two conventional methods are used for determining *HER-2* status, namely, immunohistochemistry (IHC) and fluorescent in situ hybridization (FISH). IHC is most frequently used in initial pathological tests for *HER-2* protein expression, and is convenient and inexpensive. *HER-2* IHC results are generally divided into four scale scores (range, 0-3+) on the basis of percentage of positive tumor cells and staining intensity. The US Food and Drug Administration (FDA) and American Society of Clinical Oncology/College of American Pathologists (ASCO/CAPs) recommends that *HER-2* IHC scores of 0 and 1+ should be regarded as *HER-2* negative and those with *HER-2 3*+ scores should be considered *HER-2* positive. An invasive breast cancer with *HER-2 2*+ score is regarded as *HER-2* equivocal and should be further assessed by FISH, which is considered the standard test for *HER-2* status. FISH is more accurate and reliable than IHC; however, its use for routine testing is hindered by drawbacks such as high cost, need for a skilled operator, long procedure, need for special equipment, and difficult preservation of slides for later review.

Invasive breast cancer with *HER-2 2*+ IHC status can be divided into two groups: those that have been possibly *HER-2* amplified and those that have not been *HER-2* amplified. Going *et al.* (17) interpreted 4,343 assessable HercepTests on successive breast cancer tissues and found that 35.7% (315/883) of patients with *HER-2 2*+ were *HER-2* amplified. A few studies have reported the possibility of predicting *HER-2* positivity from *HER-2 2*+ IHC samples (18,19). In our present study, we designed a retrospective clinical analysis to develop a multivariate logistic regression analysis that predicts the presence of *HER-2* amplification in *HER-2 2*+ invasive breast cancer patients.

Materials and methods

Patients

The present study enlisted 277 operable patients diagnosed with invasive breast cancer between October 2006 and December 2012 at Zhejiang Cancer Hospital, China. All patients were newly confirmed for invasive breast cancer status and have not received treatment. A total of 182 patients with *HER-2 2*+ IHC evaluation were included in this study. The extent of disease was determined by TNM staging according to the new staging system of the American Joint Committee on Cancer/International Union against Cancer (AJCC/UICC) (20). Patient clinical history and tumor characteristics were obtained from histopathology reports and medical records. Gathered data included patient age, tumor location, histological grade, tumor size, regional lymph node status, lympho-vascular invasion (LVI), estrogen receptor (ER), progesterone receptor (PR), HER-2 status, and Ki-67 index. This study was approved by the Institutional Review Board of the hospital. All patients provided informed consent prior to surgery.

Immunohistochemistry (IHC)

All surgical specimens were routinely fixed in 10% buffered formalin solution and embedded in paraffin. Each specimen was verified by two pathologists before inclusion in this study. *HER-2* IHC was performed on unstained sections from representative paraffin blocks using HercepTest. After deparaffinization and dehydration, tissue sections were placed in 0.1 M sodium citrate buffer (PH 6) for 40 min at 99 °C, after which the antigen was retrieved. The slides were cooled at room temperature, rinsed with distilled water, incubated with rabbit monoclonal anti-human *HER-2*/neu antibody for 1 h, then applied with biotinylated secondary antibody for 10 min. The signal was visualized using avidin-peroxidase. The slides were counterstained with Mayer's hematoxylin solution, dehydrated, and

mounted. *HER-2* positivity was defined by membranous staining.

HER-2 immunoreactivity was localized in the cell membrane. *HER-2* expression was scored using HercepTest according to manufacturer's recommendations. Guidelines for scoring were as follows: 0, no immunostaining; 1+, faint perceptible staining of the tumor cell membranes; 2+, weak to moderate complete membrane staining in more than 10% of the tumor cells; and 3+, strong circumferential staining of the entire tumor cell membrane.

All cases also underwent ER, PR, and proliferation index (Ki67) IHC testing. A cut-off level of 10% or greater was defined as positive for ER and PR expression. Positivity for Ki67 was defined by a cut-off level of 15% or greater.

Fluorescence in situ hybridization (FISH)

HER-2/neu FISH were assessed on all specimens with *HER-2* IHC 2+. The selected paraffin-embedded tissues sections (4 μm) containing representative invasive breast cancer cells were analyzed by dual-color FISH (a mixture of a spectrum orange DNA probe, covering a 218 kb region that includes the *HER-2* gene, and a spectrum green probe for the chromosome 17 centromere) using the PathVysion *HER-2* DNA Probe kit (Vysis, Inc., USA) according to the manufacturer's instructions. After 5 min denaturation at 82 ℃, the slides and probe mix were incubated overnight at 45 ℃ in a humidified hybridization chamber. The following morning, a fluorescence-mounting medium containing DAPI was applied after a series of stringent washes. The FISH specimens were analyzed on a Nikon Eclipse 80i fluorescence microscope with special filters.

The screening protocol included two independent observers. For each specimen, orange and green signals were counted from a minimum of 80 tumor cell nuclei in at least two distinct areas. *HER-2* gene status was evaluated based on the ratio of *HER-2* signals and chromosome 17 centromic signals. In our study, a case was regarded *HER-2* gene amplified if the ratio of *HER-2/CEP17* was equal to or more than 2.0 as FDA recommendation. Also, the result were classified following 2013 ASCO/CAP guideline: positive (*HER-2/CEP*7 ratio ≥2.0 with an average *HER-2* copy number ≥4.0 signals per cell; *HER-2/CEP*7 ratio ≥2.0 with an average *HER-2* copy number <4.0 signals per cell; *HER-2/CEP*7 ratio <2.0 with an average *HER-2* copy number ≥6.0 signals per cell.), equivocal (*HER-2/CEP*7 ratio <2.0 with an average *HER-2* copy number ≥4.0 and <6.0 signals per cell.) and negative (*HER-2/CEP*7 ratio <2.0 with an average *HER-2* copy number <4.0 signals per cell).

Statistical analysis

Pearson's chi-square test was performed to evaluate the association between clinicopathological variables and *HER-2* FISH positivity. Student's *t*-test was used to compare the Ki67 between the *HER-2* negative and positive group. Risk factors influencing *HER-2* FISH positivity were evaluated by unconditional logistic regression analysis. All statistical calculations were performed with SPSS 13.0 for Windows (Chicago, IL, USA). A P value <0.05 was considered statistically significant.

Results

This study included 182 invasive breast cancer patients with *HER-2* IHC score of 2+. The characteristics of these patients are summarized in *Table 1*. The study population had a median age of 48 years (range, 29-78 years). Tumor cell grade was available in 153 patients (84.1%), 105 being grade 1 or 2 (57.7%) and 48 being grade 3 (26.4%). Hormone receptor (HR) status was available in all patients. ER was expressed in 131 (72.0%) patients. PR positivity was shown in 73.1% of the patients (133/182). Median Ki67 value was 20% (range, 3-90%). A total of 121 patients had high and 61 had low Ki67 value, according to the Ki67 cut-off value of 15%. According to the new TNM staging system, 19 of all the cases (10.4%) were stage I, 132 (72.5%) were stage II, and 31 (17.0%) were stage III.

The distribution of *HER-2* FISH results according to both FDA and 2013 ASCO/CAP recommendation are shown in *Table 2*. *HER-2* FISH amplified (positive) was found in 34.6% (63/182) according to FDA criteria and 32.9% (60/182) with 2013 ASCO/CAP guideline. There was good agreement between the FDA and 2013 ASCO/CAP guideline. Some changes have been also observed. There were only three patients who had positive according to FDA criteria that changed to negative according to ASCO/CAP guideline, and five patients with positive based on ASCO/CAP cut-off changed to negative with FDA recommendation. The majority of *HER-2* equivocal (ASCO/CAP guideline) patients had *HER-2* negative (90.9%, 10/11).

Then, we take the *HER-2* test guideline of FDA as the major guideline. Sixty-three of all patients were *HER-2* FISH amplified (positive). Patients with *HER-2* FISH amplified tumors were more likely to have higher histological grades (χ^2=8.73, P=0.033) compared with

Table 1 Correlation of HER2 FISH results with clinicopathological features in 182 IHC score 2+ breast cancer

Factors	FDA			2013 ASCO/CAP			
	HER2 positive, n (%)	HER2 negative, n (%)	P	HER2 positive (%)	HER2 equivocal (%)	HER2 negative (%)	P
Patients, N	63	119		60	11	111	
Age (years)			0.182				0.130
<50	69 (69.7)	30 (30.3)		27 (27.3)	5 (5.1)	67 (67.7)	
≥50	50 (60.2)	33 (39.8)		33 (39.8)	6 (7.2)	44 (53.0)	
Location			0.280				0.573
Left	61 (69.3)	27 (30.7)		28 (31.8)	7 (8.0)	53 (60.2)	
Right	58 (61.7)	36 (38.3)		32 (34.0)	4 (4.3)	58 (61.7)	
Histological grade			0.033				0.405
Grade 1-2	73 (69.5)	32 (30.5)		30 (28.6)	5 (4.8)	70 (66.7)	
Grade 3	25 (52.1)	23 (47.9)		20 (41.7)	4 (8.3)	24 (50.0)	
Not evaluable	21 (72.4)	8 (27.6)		10 (34.5)	2 (6.9)	17 (58.6)	
LVI			0.299				0.115
Negative	70 (68.6)	32 (31.4)		28 (27.5)	5 (4.9)	69 (67.6)	
Positive	49 (61.3)	31 (38.7)		32 (40.0)	6 (7.5)	42 (52.5)	
T stage			0.541				0.001
T1	19 (73.1)	7 (26.9)		7 (26.9)	1 (3.8)	18 (69.2)	
T2	84 (64.6)	46 (35.4)		43 (33.1)	4 (3.1)	83 (63.8)	
T3	14 (66.7)	7 (33.3)		7 (33.3)	6 (28.6)	8 (38.1)	
T4	2 (40.0)	3 (60.0)		3 (60.0)	0 (0)	2 (40.0)	
N stage			0.498				0.698
N0	55 (71.4)	22 (28.6)		22 (28.2)	52 (66.7)	4 (5.1)	
N1	33 (61.1)	21 (38.9)		35 (37.2)	53 (56.4)	6 (6.4)	
N2	17 (63.0)	10 (37.0)		3 (30.0)	6 (60.0)	1 (10.0)	
N3	12 (57.1)	9 (42.9)					
Clinical stage			0.370				0.082
I	15 (78.9)	4 (21.1)		4 (21.0)	1 (5.3)	14 (73.7)	
II	83 (62.9)	49 (37.1)		46 (34.8)	5 (3.8)	81 (61.4)	
III	21 (67.7)	10 (32.3)		10 (32.2)	5 (16.1)	16 (51.6)	
ER status			<0.001				<0.001
Negative	31 (41.2)	30 (58.8)		30 (58.8)	1 (2.0)	20 (39.2)	
Positive	98 (74.8)	33 (25.2)		30 (22.9)	10 (7.6)	91 (69.5)	
PR status			<0.001				<0.001
Negative	21 (42.9)	28 (57.1)		27 (55.1)	3 (5.1)	19 (38.8)	
Positive	98 (73.7)	35 (26.3)		33 (24.8)	8 (6.0)	92 (69.2)	
P53 status			0.048				0.138
Negative	32 (55.2)	26 (44.8)		25 (43.1)	3 (5.2)	30 (51.7)	
Positive	87 (70.2)	37 (29.8)		35 (28.2)	8 (6.5)	81 (6.5)	
Ki-67			<0.001				0.003
0-15%	51 (83.6)	10 (16.4)		47 (77.0)	4 (6.6)	10 (16.4)	
≥15%	68 (56.2)	53 (43.8)		64 (52.9)	7 (5.8)	50 (41.3)	

IHC, immunohistochemistry; LVI, lympho-vascular invasion; ER, estrogen receptor; PR, progesterone receptor; HER2, human epidermal growth factor receptor-2; FDA, Food and Drug Administration; ASCO/CAP, American Society of Clinical Oncology/College of American Pathologists.

Table 2 Distribution of HER2 FISH results based on FDA guideline and 2013 ASCO/CAP guideline

2013 ASCO/CAP	FDA	
	Negative	Positive
Negative	106	5
Equivocal	10	1
Positive	3	57

HER2, human epidermal growth factor receptor-2; FISH, fluorescent in situ hybridization; FDA, Food and Drug Administration; ASCO/CAP, American Society of Clinical Oncology/College of American Pathologists.

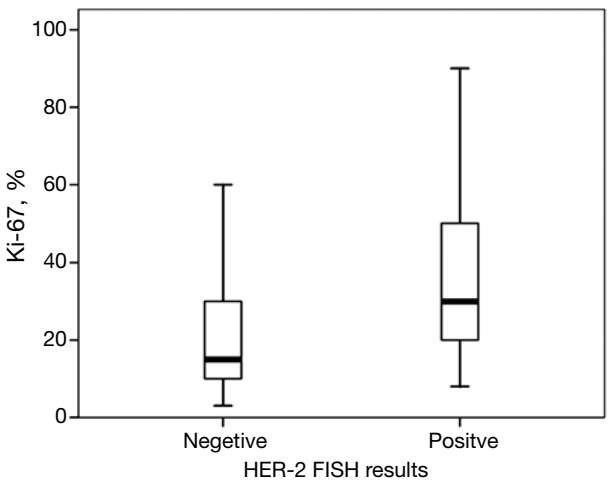

Figure 1 Box plots showing that higher Ki-67 in cancer with HER-2 FISH positive than in cancer with HER-2 FISH negative. HER-2, human epidermal growth factor receptor-2; FISH, fluorescent in situ hybridization.

patients with unamplified tumors. No significant difference between the groups were found with respect to age (<50 *vs.* ≥50 years, P=0.182), LVI (P=0.299), cancer location (P=0.280), or clinical stage (P=0.370). Tumors with *HER-2* amplification were more likely to be ER-negative (58.8% *vs.* 25.2%, P<0.001), PR-negative (57.1% *vs.* 26.3%, P<0.001), or P53-negative (44.8% *vs.* 29.8%, P=0.048). The median percentage of Ki67 was 15% in the non-*HER-2*-amplified group and 30% in the *HER-2*-amplified group. A significantly high level of Ki67 was detected in the *HER-2*-amplified groups (P=0.006, *Figure 1*). Based on the Ki67 cut-off value of 15%, patients were classified into either of two groups: relatively high Ki67 or low Ki67. A positive correlation was found between Ki67 and *HER-2* status (χ^2=13.46, P<0.001).

A logistic regression model was used to reveal risk factors for *HER-2* amplification. The association between clinicopathological variables and *HER-2* amplification is shown in *Table 3*. Cases with high Ki67 had significantly higher risk of *HER-2* amplification than those with low Ki67 (OR =3.975; 95% CI, 1.846-8.560; P<0.001). Subjects with ER positive expressions were less likely to exhibit *HER-2* amplification compared with those with ER negative expression (OR =0.236; 95% CI, 0.119-0.467; P<0.001). The risk was also much reduced in cases with PR positive expressions than those with PR negative expressions (OR =0.268; 95% CI, 0.135-0.531; P<0.001). Subjects with P53 positive expressions were less likely to develop *HER-2* amplification (OR =0.523; 95% CI, 0.275-0.997; P=0.049).

We created a risk score that comprised the following factors: ER (score 1 when IHC negative; 0 when positive), PR (score 1 when IHC negative; 0 when positive), P53 (score 1 when IHC negative; 0 when positive), and Ki67 (score 0 when IHC negative; 1 when positive). The sum of the above parameters allowed the establishment of a risk score for *HER-2* FISH amplification (*Table 4*). A significant association between risk score and *HER-2* FISH amplification was observed (χ^2=30.41, P<0.001, *Figure 2*). Receiver operator characteristic curves were constructed to compare the ability of the four tumor markers to differentiate between patients with or without *HER-2* FISH amplification. AUC was 0.64±0.04, 0.35±0.05, 0.37±0.05, and 0.43±0.05 for Ki67, ER, PR, and P53. AUC was 0.74±0.04 (95% CI, 0.66-0.81) for the sum of all four markers (*Figure 3*).

Discussion

Using trastuzumab supplement for neoadjuvant or adjuvant chemotherapy provides significant survival benefit in invasive breast cancer with *HER-2*-overexpressing tumor cells. However, for *HER-2*-negative cases, trastuzumab offers no benefit and only contributes cardiotoxicity and waste of money. Therefore, accurate determination of *HER-2* status in breast cancer patients is an important part of routine practice in pathological reporting. Cases with weak positive staining (2+) by *HER-2* IHC represent a subgroup of patients that requires additional assessment with FISH.

A variety of IHC antibodies and other methods have been developed to determine *HER-2* status in breast cancer patients. Ciftlik *et al.* (21) designed a glass/silicon micro-machined structure for applying microfluidic tissue

Table 3 Logistic regression analysis of risk factors for HER2 FISH positive (based on FDA guideline) in HER-2 IHC scores 2+ breast cancer patients

Factors	HR	95% CI	P
Age (years)			
<50	Ref		
≥50	1.518	0.822-2.805	0.183
Location			
Left	Ref		
Right	1.402	0.758-2.594	0.281
Histological grade			
Grade 1-2	Ref		
Grade 3	2.099	1.040-4.236	0.039
Not evaluable	0.869	0.348-2.168	0.763
LVI			
Negative	Ref		
Positive	1.384	0.749-2.558	0.300
T stage			
T1	Ref		
T2	1.486	0.582-3.798	0.408
T3	1.357	0.387-4.759	0.633
T4	4.071	0.558-29.725	0.166
N stage			
N0	Ref		
N1	1.591	0.761-3.326	0.217
N2	1.471	0.583-3.707	0.414
N3	1.875	0.693-5.075	0.216
Clinical stage			
I	Ref		
II	2.214	0.695-7.048	0.179
III	1.786	0.470-6.789	0.395
ER status			
Negative	Ref		
Positive	0.236	0.119-0.467	<0.001
PR status			
Negative	Ref		
Positive	0.268	0.135-0.531	<0.001
P53 status			
Negative	Ref		
Positive	0.523	0.275-0.997	0.049
Ki-67			
0-15%	Ref		
≥15%	3.975	1.846-8.560	<0.001

HER-2, human epidermal growth factor receptor-2; FISH, fluorescent in situ hybridization; FDA, Food and Drug Administration; IHC, immunohistochemistry; LVI, lympho-vascular invasion; ER, estrogen receptor; PR, progesterone receptor; HR, hormone receptor; Ref, Reference.

Table 4 Distribution of *HER2* gene amplification according to different risk score based on FDA guideline

Risk index	Patients, n (%)	Cases with HER-2 amplification
0	35 (19.2)	3
1	72 (40.0)	18
2	28 (15.4)	13
3	37 (20.3)	23
4	10 (5.5)	6

HER-2, human epidermal growth factor receptor-2; FDA, Food and Drug Administration.

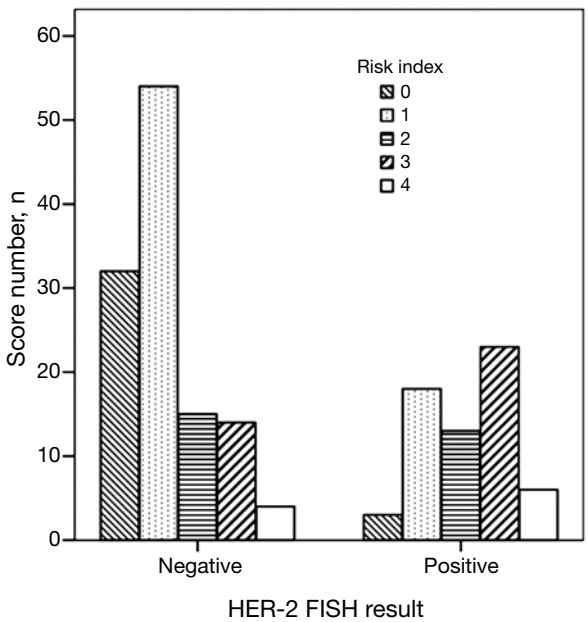

Figure 2 Distribution of HER2 gene status according to risk index. HER2, human epidermal growth factor receptor 2.

processing protocols, thus allowing rapid IHC processing of breast carcinomas and correct determination of *HER-2* status. The concordance rate between microfluidic processor results and subsequent in situ hybridization (ISH) of the same samples was 100%, although the number of cases included in this study was relatively small (score IHC 2+, n=27). SP3, a rabbit monoclonal antibody, was proven to have a high level of agreement with ISH methods (22). The concordance rates reported by D'Alfonso (23) from 100 breast cancer patients between SP3 and FISH in needle core biopsy and excisional biopsy specimens were 96% (95% CI, 91.9-99.7%) and 97% (95% CI, 90.3-99.3%), respectively. Despite the steps that have been made to

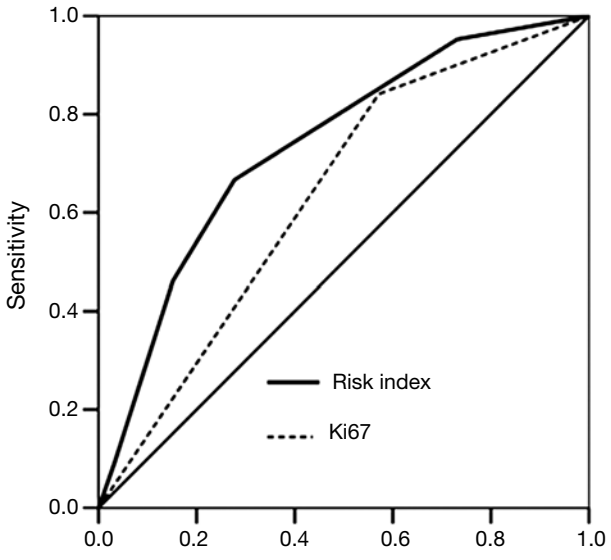

Figure 3 Receiver operator characteristic curves were constructed to compare the ability of risk index to differentiate between patients with or without HER2 FISH amplification. HER2, human epidermal growth factor receptor 2; FISH, fluorescent in situ hybridization.

standardize the process of IHC assessment, intra- and inter-observer variability in scoring is not uncommon (24). Computer-assisted analysis on *HER-2* IHC slides may be an effective supplement to conventional IHC analysis (25); however, this method requires special materials and could not be widely implemented for use within a short time.

Although numerous previous studies have reported that *HER-2* overexpression (IHC 3+) or *HER-2* amplification is associated with high tumor cell grade, absence of ER or PR expression, DNA aneuploidy, and high Ki67 (26-29), published evidence on the correlation between relevant prognostic factors and FISH-determined *HER-2* status in *HER-2* IHC 2+ cases is still lacking. A method with high discriminatory power will help clinical physicians obtain results faster without the performance of FISH. To date, only three publications have studied this relationship. Lee (30) recently characterized a relatively large series of 1735 invasive breast cancer tissues, among which 419 (24%) were scored *HER-2* 2+ by IHC. Additionally, 14% (57/413) were *HER-2* amplified according to FDA criteria (ratio of *HER-2* to chromosome 17≥2.0). *HER-2* amplification was related to the percentage of complete membrane staining. Chibon (31) selected 108 breast cancers with *HER-2* IHC score of 2+ to predict *HER-2* gene status. FISH amplification rate was determined to be 33%. Tumor grade and percentage of membrane staining were indicators of *HER-2* status. A study by Dieci *et al.* (32) analyzed 480 HER-2 2+ breast cancer samples, resulting in high tumor grade and high Ki67 being significantly associated with HER-2 FISH amplification. However, the ER and PR statuses were not determined in all cases. HR positivity is related with better prognosis in breast cancer patients. Furthermore, although the association between pathological variables (tumor grade and Ki67) and *HER-2* status has been well established, the power of these studies has been relatively low. To ensure that all women with *HER-2* amplified cancers receive adequate treatment, a powerful method for assessing *HER-2* amplification is imperative. In our study, we integrated clinical and pathological factors from 182 invasive breast cancer cases with IHC score of 2+ to develop a risk score that better predicts the occurrence of *HER-2* amplification. All samples were routinely submitted for FISH analysis to determine the *HER-2* gene status. We found that 34.6% (63/182) of all cases were *HER-2* amplified. A positive correlation was found between the HR, P53, and Ki67 and *HER-2* status. The risk score, derived by the sum of HR, P53, and Ki67, was a highly significant predictor of *HER-2* status (χ^2=30.41, P<0.001). Overall, compared with previous studies, this study examined cases that were all from surgical specimens, and incorporated multiple clinicopathological parameters for the development of a powerful predictive model for *HER-2* status. The additional variables allow for higher accuracy for validation of *HER-2* status.

Some limitations were observed in this study. First, our analysis focused on invasive breast cancer, thereby limiting our analysis from other histological classifications; second, this study was based on patients from one center, and results may not apply to other medical settings. Before clinical use, the evaluation of ER, PR, Ki67 should be standardized; third, any predictive model incorporates a certain degree of uncertainty, so predicting the status of an individual patient remains imperfect. More studies that address these issues are needed for confirmation. Despite the statistical accuracy for the prediction of *HER-2* amplification in invasive breast cancer, FISH analysis remains the gold standard for determining *HER-2* status.

Accurately evaluating the breast cancer *HER-2*/neu genotype has become an important task as emerging date showing that the benefit of using Herceptin in the treatment for *HER-2* positive patients. Subgroup of breast cancer patients achieves a pCR after the neoadjuvant chemotherapy. There is no residual tumor cell in the

surgical biopsy for examination. Tissue accessibility prohibits patients from obtaining *HER-2* status. Preoperation needle core biopsy tissue becomes the only available material in this group of patients. In such cases, our risk score can be used to prioritise the treatment of Herceptin. In a recently meta-analysis (33), *HER-2* IHC 0/1+ and 3+ cannot be absolutely considered as negative and positive. The discordance rates are 4% and 9% in 0/1+ and 3+ *HER-2* IHC score, respectively. In such instances, this IHC risk score would help physician to select those patients who will benefit from the target therapy.

Based on the results of our study, we present a novel IHC risk score that will help determine *HER-2* status accurately. In the future, we hope to validate this model by analyzing a larger series of invasive breast cancer tissues.

Acknowledgements

Disclosure: The authors declare no conflict of interest.

References

1. Ali AM, Provenzano E, Bartlett JM, et al. Prognosis of early breast cancer by immunohistochemistry defined intrinsic sub-types in patients treated with adjuvant chemotherapy in the NEAT/BR9601 trial. Int J Cancer 2013;133:1470-8.
2. Perou CM, Sørlie T, Eisen MB, et al. Molecular portraits of human breast tumours. Nature 2000;406:747-52.
3. López-Guerrero JA, Llombart-Cussac A, Noguera R, et al. HER2 amplification in recurrent breast cancer following breast-conserving therapy correlates with distant metastasis and poor survival. Int J Cancer 2006;118:1743-9.
4. Ithimakin S, Day KC, Malik F, et al. HER2 drives luminal breast cancer stem cells in the absence of HER2 amplification: implications for efficacy of adjuvant trastuzumab. Cancer Res 2013;73:1635-46.
5. Witton CJ, Reeves JR, Going JJ, et al. Expression of the HER1-4 family of receptor tyrosine kinases in breast cancer. J Pathol 2003;200:290-7.
6. Press MF, Sauter G, Bernstein L, et al. Diagnostic evaluation of HER-2 as a molecular target: an assessment of accuracy and reproducibility of laboratory testing in large, prospective, randomized clinical trials. Clin Cancer Res 2005;11:6598-607.
7. Persons DL, Borelli KA, Hsu PH. Quantitation of HER-2/neu and c-myc gene amplification in breast carcinoma using fluorescence in situ hybridization. Mod Pathol 1997;10:720-7.
8. Tandon AK, Clark GM, Chamness GC, et al. HER-2/neu oncogene protein and prognosis in breast cancer. J Clin Oncol 1989;7:1120-8.
9. Holmes P, Lloyd J, Chervoneva I, et al. Prognostic markers and long-term outcomes in ductal carcinoma in situ of the breast treated with excision alone. Cancer 2011;117:3650-7.
10. Di Leo A, Desmedt C, Bartlett JM, et al. HER2 and TOP2A as predictive markers for anthracycline-containing chemotherapy regimens as adjuvant treatment of breast cancer: a meta-analysis of individual patient data. Lancet Oncol 2011;12:1134-42.
11. Reis-Filho JS, Pusztai L. Gene expression profiling in breast cancer: classification, prognostication, and prediction. Lancet 2011;378:1812-23.
12. Nielsen DL, Kümler I, Palshof JA, et al. Efficacy of HER2-targeted therapy in metastatic breast cancer. Monoclonal antibodies and tyrosine kinase inhibitors. Breast 2013;22:1-12.
13. Davoli A, Hocevar BA, Brown TL. Progression and treatment of HER2-positive breast cancer. Cancer Chemother Pharmacol 2010;65:611-23.
14. Jelovac D, Emens LA. HER2-directed therapy for metastatic breast cancer. Oncology (Williston Park) 2013;27:166-75.
15. Esteva FJ, Franco SX, Hagan MK, et al. An open-label safety study of lapatinib plus trastuzumab plus paclitaxel in first-line HER2-positive metastatic breast cancer. Oncologist 2013;18:661-6.
16. Mendoza G, Portillo A, Olmos-Soto J. Accurate breast cancer diagnosis through real-time PCR her-2 gene quantification using immunohistochemically-identified biopsies. Oncol Lett 2013;5:295-8.
17. Going JJ. Observer prediction of HER2 amplification in HercepTest 2+ breast cancers as a potential audit instrument. Histopathology 2011;59:333-5.
18. Lee AH, Key HP, Bell JA, et al. Breast carcinomas with borderline (2+) HER2 immunohistochemistry: percentage of cells with complete membrane staining for HER2 and the frequency of HER2 amplification. J Clin Pathol 2011;64:490-2.
19. Chibon F, de Mascarel I, Sierankowski G, et al. Prediction of HER2 gene status in Her2 2+ invasive breast cancer: a study of 108 cases comparing ASCO/CAP and FDA recommendations. Mod Pathol 2009;22:403-9.
20. Rakha EA, Martin S, Lee AH, et al. The prognostic significance of lymphovascular invasion in invasive breast carcinoma. Cancer 2012;118:3670-80.

21. Ciftlik AT, Lehr HA, Gijs MA. Microfluidic processor allows rapid HER2 immunohistochemistry of breast carcinomas and significantly reduces ambiguous (2+) read-outs. Proc Natl Acad Sci U S A 2013;110:5363-8.
22. Nunes CB, Rocha RM, Reis-Filho JS, et al. Comparative analysis of six different antibodies against Her2 including the novel rabbit monoclonal antibody (SP3) and chromogenic in situ hybridisation in breast carcinomas. J Clin Pathol 2008;61:934-8.
23. D'Alfonso TM, Liu YF, Chen Z, et al. SP3, a reliable alternative to HercepTest in determining HER-2/neu status in breast cancer patients. J Clin Pathol 2013;66:409-14.
24. Press MF, Sauter G, Bernstein L, et al. Diagnostic evaluation of HER-2 as a molecular target: an assessment of accuracy and reproducibility of laboratory testing in large, prospective, randomized clinical trials. Clin Cancer Res 2005;11:6598-607.
25. Hall BH, Ianosi-Irimie M, Javidian P, et al. Computer-assisted assessment of the human epidermal growth factor receptor 2 immunohistochemical assay in imaged histologic sections using a membrane isolation algorithm and quantitative analysis of positive controls. BMC Med Imaging 2008;8:11.
26. Hussein MR, Abd-Elwahed SR, Abdulwahed AR. Alterations of estrogen receptors, progesterone receptors and c-erbB2 oncogene protein expression in ductal carcinomas of the breast. Cell Biol Int 2008;32:698-707.
27. Lal P, Tan LK, Chen B. Correlation of HER-2 status with estrogen and progesterone receptors and histologic features in 3,655 invasive breast carcinomas. Am J Clin Pathol 2005;123:541-6.
28. Liu C, Zhang H, Shuang C, et al. Alterations of ER, PR, HER-2/neu, and P53 protein expression in ductal breast carcinomas and clinical implications. Med Oncol 2010;27:747-52.
29. Hanley K, Wang J, Bourne P, et al. Lack of expression of androgen receptor may play a critical role in transformation from in situ to invasive basal subtype of high-grade ductal carcinoma of the breast. Hum Pathol 2008;39:386-92.
30. Lee AH, Key HP, Bell JA, et al. Breast carcinomas with borderline (2+) HER2 immunohistochemistry: percentage of cells with complete membrane staining for HER2 and the frequency of HER2 amplification. J Clin Pathol 2011;64:490-2.
31. Chibon F, de Mascarel I, Sierankowski G, et al. Prediction of HER2 gene status in Her2 2+ invasive breast cancer: a study of 108 cases comparing ASCO/CAP and FDA recommendations. Mod Pathol 2009;22:403-9.
32. Dieci MV, Barbieri E, Bettelli S, et al. Predictors of human epidermal growth factor receptor 2 fluorescence in-situ hybridisation amplification in immunohistochemistry score 2+ infiltrating breast cancer: a single institution analysis. J Clin Pathol 2012;65:503-6.
33. Bahreini F, Soltanian AR, Mehdipour P. A meta-analysis on concordance between immunohistochemistry (IHC) and fluorescence in situ hybridization (FISH) to detect HER2 gene overexpression in breast cancer. Breast Cancer 2014. [Epub ahead of print].

Cite this article as: Ji Y, Sheng L, Du X, Qiu G, Chen B, Wang X. Clinicopathological variables predicting *HER-2* gene status in immunohistochemistry-equivocal (2+) invasive breast cancer. J Thorac Dis 2014;6(7):896-904. doi: 10.3978/j.issn.2072-1439.2014.07.27

Original Article

The normative value of inflammatory cells in the nasal perfusate of Chinese adults: a pilot study

Yong Zhang[1], Qiuping Wang[1], Yanqing Xie[2], Zhiyi Wang[1], Derong Li[2], Li Ma[1], Xinju Pang[1], Weidong Yu[1], Nanshan Zhong[2]

[1]Department of ENT & Head & Neck Surgery, Jinling Hospital, Nanjing University School of Medicine, Nanjing 210002, China; [2]The First Affiliated Hospital of Guangzhou Medical School, Guangzhou Institute of Respiratory Diseases, Guangzhou 510120, China

Correspondence to: Qiuping Wang, MD. Department of ENT & Head & Neck Surgery, Jinling Hospital, Nanjing University School of Medicine, Nanjing 210002, China. Email: doczhang0107@163.com.

Objective: To establish stable, well-accepted nasal perfusion and a normative value of classifying cells in the nasal perfusate of Chinese adults.

Methods: A total of 500 healthy adults were divided into two groups of 250 people per group (group A, 16-30 years old and group B, 31-60 years old; male-to-female ratio, 1:1). All volunteers were non-smokers; they were irrigated with saline, and multiple inflammatory cells in the perfusate were analyzed.

Results: Irrigation was successfully performed in 479 cases, a success rate of 95.80%. The types of inflammatory cells showed a skewed distribution. The median number and interquartile range (IQR) of eosinophils were 0 and 0.2, respectively. These values were 0.4 and 2.2, respectively, for neutrophils and 0 and 0, respectively, for both lymphocytes and macrophages. There was no significant difference between males and females (P>0.05). There was a significant difference in the numbers of neutrophils and lymphocytes in the different age groups (P=0.000), but there was no significant difference in the numbers of eosinophils and macrophages (P>0.05). The 95% unilateral upper limited values (UULVs) of eosinophils and neutrophils in the nasal perfusates were 2.99 and 14.94, respectively, for group A and 1.41 and 17.08 for group B. As a result, the total 95% UULVs of eosinophils and neutrophils in the nasal perfusate were 2.00 and 16.80.

Conclusions: We established stable, well-accepted nasal perfusions and normal values for classifying the cells in the nasal perfusate of Chinese adults; the normative values of the inflammatory cells in nasal perfusate are 2.00 for the 95% UULV of eosinophils and 16.80 for neutrophils. Age might be one of the factors affecting the cells in rhinitis.

Keywords: Nasal perfusate; reference value; methodology; healthy Chinese adults

Submitted Nov 26, 2013. Accepted for publication Jun 09, 2014.
doi: 10.3978/j.issn.2072-1439.2014.06.45
View this article at: http://dx.doi.org/10.3978/j.issn.2072-1439.2014.06.45

Introduction

The nasal mucosa is the portion of the airway mucosa that might be the most convenient tissue for examining the effects of mucosal inflammation. Since Hansel first reported the examination method (1) in 1934, increasing numbers of researchers have performed studies on the effects of allergies, blood vessel activity and infection on rhinitis in nasal cells (2,3). The analysis of nasal cells can reveal alterations in the epithelial cells after exposure to physical and chemical inflammatory factors (4) and the progression of acute and chronic inflammation (5), which is of great interest in basic and clinical research. This type of examination can be easily repeated and used in patients of different ages due to its broad approach, simplicity and non-invasiveness (6). However, rhino cytology is only used in basic and subclinical research and is not effective in clinical applications (7). Although the examination is

simple and recommended by experts, there is no consensus on the standards for rhino cytology, especially for cell counting (8), which is usually applied to rhinitis patients (9) but not to healthy people (10). There are few reports on the normative values for the rhino cytology of nasal perfusates, but determining the classification for mucosal inflammation, categorizing the inflammatory status, updating the progression of inflammation and evaluating the treatment of inflammation are important (11). In addition, discussing the relevance of this analysis for lower airway inflammation has great clinical significance (12). The common rhino cytological examination consists of a smear of nasal secretion, nasal lavage, nasal brush and biopsy of the nasal mucosa. Inflammatory cells are highly relevant to various examinations (13). Although scraping samples are better than lavage samples, lavage is still the most stable and accurate examination for assessing the inflammatory status of the nose (3), and the repeatability of NAL is sufficient (14). Our research first focused on the nasal lavage of 500 healthy individuals and established a convenient, stable lavage and counting method for rhino cytology. We also determined the normal values for inflammatory cells in nasal lavage, which could provide clues for further research on the relevance between nasal and lower airway inflammatory diseases.

Subjects and methods

Subjects

A total of 500 healthy individuals treated at Nanjing Jinling Hospital and Guangzhou Respiratory Institute for Ordinary Physical Examination were enrolled in this study. The inclusion criteria were as follows: (I) negative result in the skin prick test; (II) all CBC values were normal; (III) non-smokers aged from 16-60 years old (250 cases from 16-30 years old and 250 cases from 31-60 years old with a male-to-female ratio of 1:1); (IV) no chronic respiratory diseases, no allergic constitution, no digestive difficulties and no history of other severe diseases; (V) no nasal spray, antihistamine, glucocorticoid or LTR treatment in the last week and (VI) no respiratory infection within the last four weeks. This study was approved by the Ethics Committee of Nanjing Jinling Hospital and Guangzhou Respiratory Institute. All of the participants were fully informed about the purpose of this study. All participants provided written informed consent before participation in the study.

Methods

Based on studies performed abroad (15,16), we performed the procedures as follows. First, we allowed the patients to sit with their heads anteverted at 45 degrees. Second, we told the patients to breathe through their mouths to close the nasopharynx and prevent the irrigation from flooding into the pharynx oralis. Third, we irrigated one of the nostrils with 5 mL of 37 ℃ saline usina syringe and closed the nostril with a plug to thoroughly irrigate the middle and lower nasal passages. The irrigation fluid was collected with a funnel (saline spilling from the other nostril is a sign of thorough irrigation). The irrigation was repeated three times, and the total time for the irrigation was approximately 5 minutes. Some of the fluid was removed by suction, and the remainder was collected with a funnel. Fourth, we performed the same procedure in the other nostril. Fifth, we recorded the volume and collection rate. Sixth, we stored the sample at 4 ℃ and ran the tests within 2 hours.

Apparatus and reagents

A centrifugal machine, microscope, oscillator, water bath, pipettor, electronic balance, hematoxylin-eosin dye solution (Nanjing Jiancheng Technology Company; Serial number: D006) and DTT (dispensed with Amresco, purity >99%) were utilized in this study.

Criterion of acceptability

A recollection rate of higher than 70% was acceptable.

Cellular test

The irrigated sample was collected and centrifuged. The supernatant was stored (used for other related data), and the sediment was used for cellular testing (*Figure 1*).

Cell counting

We observed the slice under a light microscope at 200 times magnification and counted the total number of various inflammatory cells, including eosinophils (Eos), neutrophils (N), macrophages (M) and lymphocytes (L), in five fields and identified every cell type at 200 HP. The total number of inflammatory cells indicated the severity of rhinitis.

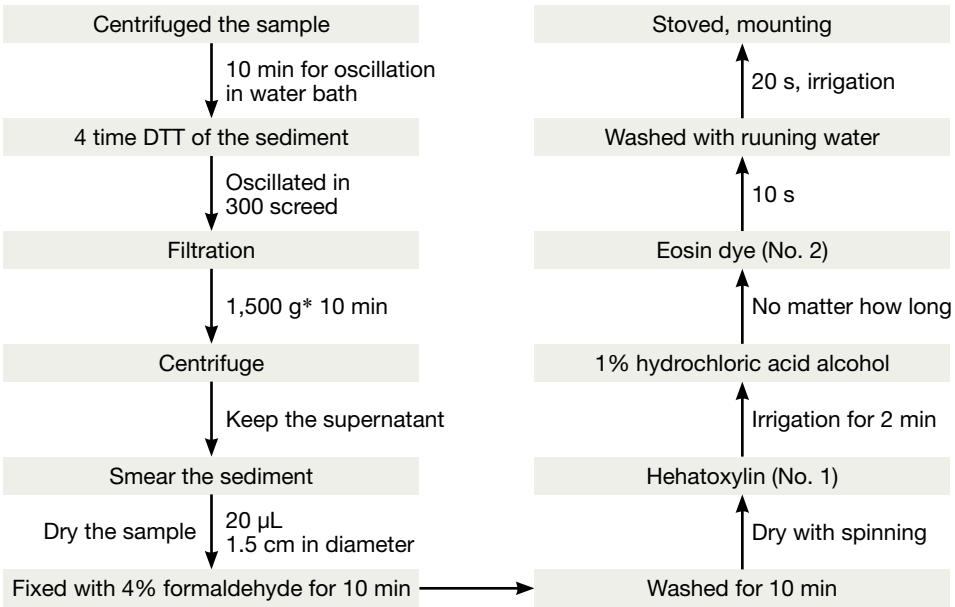

Figure 1 Process of nasal lavage cytology.

Statistic analysis

In this study, the data are all given as the $\bar{x}$ ± SD and were analyzed using SPSS (version 18.0). The Kolmogorov-Smirnoff test was used to test the normality of the distribution, and the reference range was shown to be 95%. The Mann-Whitney U non-parametric test was used for the analysis between the male and female participants and among the different age groups. A P value less than 0.05 indicated a significant difference.

Results

Consistency test

There were no significant differences in the age, sex or education level of the patients between the two hospitals (χ^2=2.33, P>0.05; χ^2=2.92, P>0.05; χ^2=3.01, P>0.05), indicating the consistency of the data.

Establishment of a method for nasal lavage

Nasal lavage samples were collected from 500 individuals. Cough occurred in 9 cases due to unconscious aspiration during irrigation (1.80%), and there was a collection rate of less than 70% in 12 cases (2.40%). Finally, we included a total of 479 cases (95.80%).

The normal range of cells in the nasal lavage

The numbers of all inflammatory cells showed a skewed distribution. The median number and interquartile range (IQR) of the Eos were 0 and 0.2, respectively. These values were 0.4 and 2.2, respectively, for N and 0 and 0, respectively, for both L and M. There was no significant difference between male and female patients (*Table 1*). There were significant differences for the N and L among the different age groups (P=0.000), but there were no differences for the Eos and M (P>0.05) (*Table 2*). The 95% UULVs of the Eos and N in the nasal perfusate were 2.99 and 14.94, respectively, for group A and 1.41 and 17.08, respectively, for group B. As a result, the total 95% UULVs of the Eos and N in the nasal perfusate were 2.00 and 16.80, respectively (*Tables 1-3* and *Figures 2-4*).

Discussion

Nasal lavage is a non-invasive method that is easily standardized and highly repeatable. Meanwhile, tests of the supernatant from the centrifuged lavage fluid could indicate various inflammatory conditions (17). Therefore, a standardized method and normal range of rhino cytology are important for research on the nasal passages and lower respiratory tract. We performed research on 500 individuals

Table 1 Statistical description of cell classification of nasal lavage of normal persons of different genders

Group	Number	Eosinophils	Neutrophils	Lymphocytes	Macrophages
Man	236	247.95	248.09	240.81	244.43
Women	243	232.28	232.14	239.21	235.70
Z		1.420	1.319	0.208	1.593
P		0.156	0.187	0.836	0.111

Table 2 Statistical description cell classification in nasal lavage of normal persons

Group	Number	Eosinophils	Neutrophils	Lymphocytes	Macrophages
16-30 years old	241	234.10	181.95	220.74	234.87
31-60 years old	238	245.97	298.78	259.51	245.19
Z		1.076	9.662	5.020	1.885
P		0.282	0.000	0.000	0.059

Table 3 95% percentile distribution of nasal cytology (/200 HP)

Group	Number	Eosinophils	Neutrophils	Lymphocytes	Macrophages
16-30 years old	241	2.99	14.94	0.20	0.00
31-60 years old	238	1.41	17.08	0.80	0.20
Total	479	2.00	16.80	0.60	0.20

and primarily confirmed the normal range of nasal cells in Chinese people.

We first established the cell counting method for the nasal lavage of healthy Chinese people and determined the normative range. Although there were some reports on noses with nasal lavage (18), they mainly focused on rhinitis and the normative range for Eos but not on the normal range of N, L, M and other nasal cells (3,19), and the methods differed among the reports (e.g., nasal brushing, scraping, smearing and lavage). The counting methods and normative ranges also differed. However, no research of this type has been performed in China. As a result, determining the normal range of each type of inflammatory cell in the nasal lavage was necessary. The counting range differed by researcher, and nearly all researchers in this study counted the Eos, N and L cells. They also advised that rhinitis should be studied based on all of the nasal cell types, such as goblet cells, M and epithelial cells (columnar and squamous) (19). With repeated studies, we finally confirmed that the nasal lavage could be evaluated using Eos, N, L and M and that other cells should be excluded. First, abnormally dyed cells (basophils and mast cells) were detected in only a few cases (15/1,620), and such findings had no significance for further data analysis (19) based on the smears of nasal secretions (relevance ratio: 0.93%). Second, a previous study found no abnormally dyed cells, most likely because the preparation of the sample from collection to processing was more complicated than a nasal smear, which might result in the destruction of the cells. Third, abnormally dyed cells were all immediate phase cells that could secrete inflammatory molecules, such as histamine and tachykinin, which could destroy the cells at an early stage (3). Fourth, rhinitis, especially AR, was represented by Eos, which are the core marker cell. The N cells are closely related to nasal infectious diseases, and the L cells are most likely associated with allergies. M are related to atmospheric contamination, such as glass fibers in the air and ozone (16,20). Fifth, epithelial cells are the basic structure of the nasal mucosa and do not reflect the severity of rhinitis. Sixth, Eos, N, L and M cells were commonly observed in the induced sputum (21), providing a foundation for the investigation of the relevance of upper and lower airway disease (22).

Some reports have indicated that the severity of rhinitis correlates with the percentage of each inflammatory cell type (8). There is a significant correlation between nasal Eos and nasal symptoms according to various data from

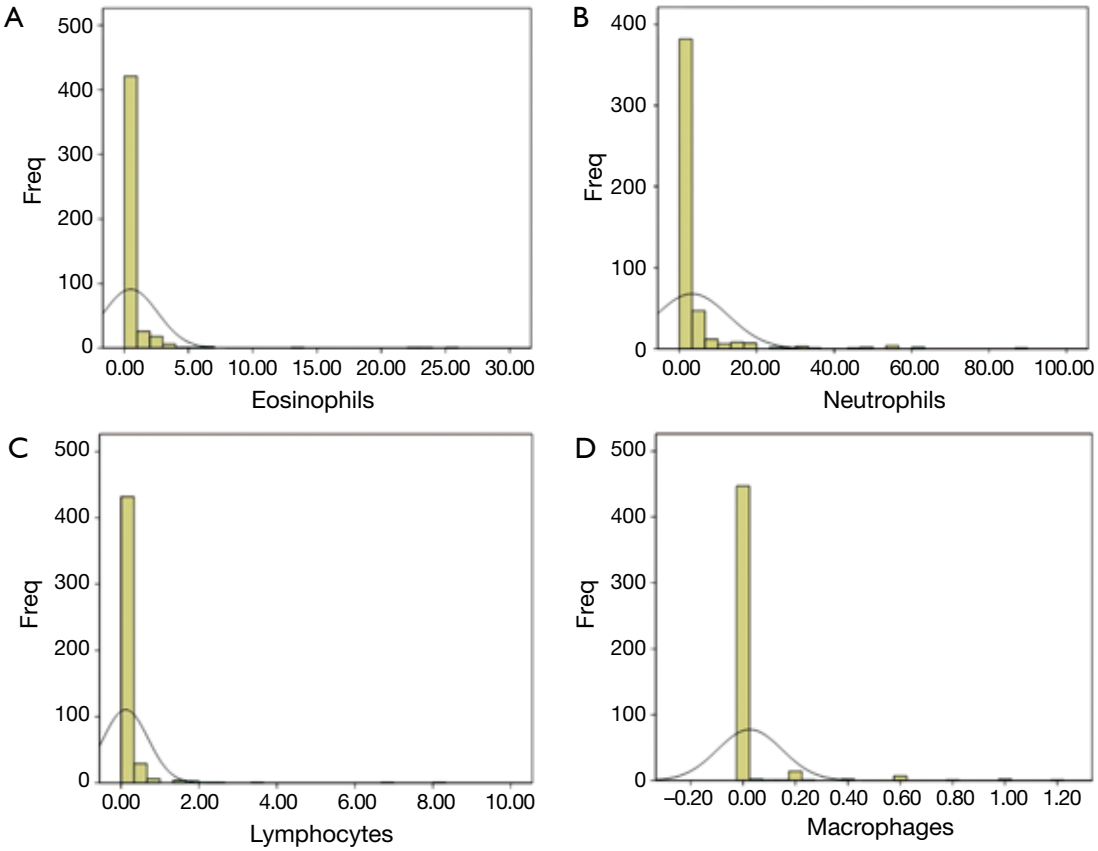

Figure 2 Distribution of actual numbers of eosinophils, neutrophils, lymphocytes and macrophages per 200 HP in nasal lavage in comparison with the normal distribution curve values for these cells.

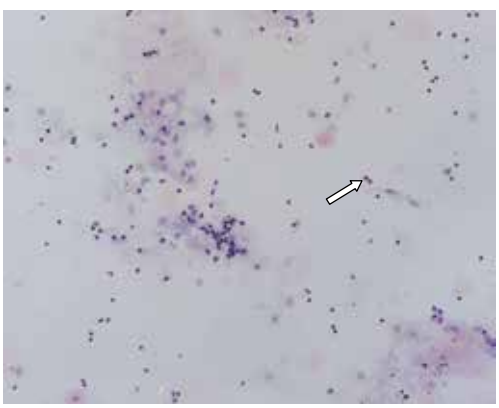

Figure 3 Normal person nasal lavage as shown by the white arrow is Eos; N, L and epithelial cell were also shown (HE, ×200).

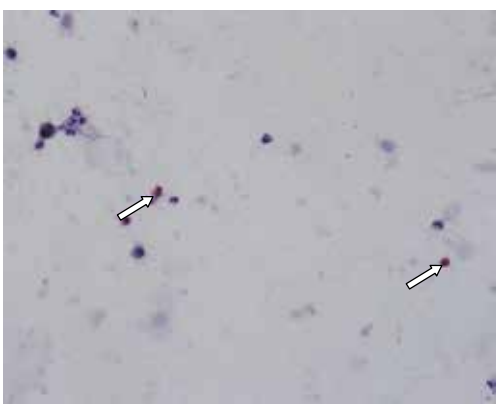

Figure 4 Normal person nasal lavage as shown by the white arrow is Eos; N and M were also shown (HE, ×400).

nasal lavages (IL-4, IL-5, IL-8 and IFN-γ), nasal resistance and pulmonary function. The correlation index is as high as 0.95, i.e., Eos play an important role in nasal cell tests (23). The sensitivity and specificity vary among the nasal tests that are performed abroad, mainly due to the differences in sampling, counting and scoring (8). For example, Mygind *et al.* (24) suggested that it should be 10%, whereas Jankowski *et al.* (25) indicated that it should be 20%;

however, Burrows *et al.* (26) reported that it should be 25%. A recent study showed that more than 8% of Eos could be the standard for allergic rhinitis (AR) in children under four years old (sensitivity: 80%; specificity: 95%) (19). However, these so-called standards were not based on research performed on healthy individuals.

The most popular field for research on rhinitis is AR. Basophils and mast cells are commonly the main course for the immediate phase of histamine release during the early stage of AR, and Eos and M can release the associated inflammatory molecules (18), which are related to the symptoms during the delayed phase. However, little is known about the effects of N and M in rhinitis. In 2004, Fransson *et al.* (27) reported on the role of N in intermittent AR and stated that N cells not only led to early-stage reactions but also are strongly associated with the symptoms of rhinitis, suggesting that N cells are the motor for the secretion of AR-related molecules in the early stage. However, this work has not been supported by further study. We found that the average number of N cells was 10 times higher than that of Eos (95% UULV of 16.80) and was far higher than the number of Eos in the nose, which might have occurred because CO_2 and ozone can elevate the N chemo attractive factor (28). Both the absolute numbers and 95% UULVs of L and M cells were low, especially for the M cells. There was only one cell in 25 slides. Research on L and M cells has been nearly absent. Recently, some studies have indicated that there are different nasal cells involved in the different types of rhinitis. L and M cells are much more common in patients with medium-severe, constant AR (29). A high concentration of ozone could decrease the number of M cells (20). Limited research has provided us clues for further studying and detailing the treatment of rhinitis.

Research from animal models and human subjects suggests that there are several important changes in the innate and adaptive immune responses with increasing age, a phenomenon termed "immunosenescence" (30). The function of immune-associated inflammatory cells, including the number, function and early-stage reaction, decreased in the older population, when activated (31). However, there are currently few reports on the age-associated changes in the inflammatory cell count and function. As a result, we divided the subjects into two groups, group A (16-30 years old) and group B (31-60 years old), and the average rank in group B was higher than that in group A. There were no significant differences in the Eos and M (*Table 2*), although the P value was close to 0.05 for the M. In contrast, there were significant differences in the N and L (P=0.000). A comparison of another *in vitro* Eos effect or function, leukotriene C4 production, revealed no difference between older and younger asthmatic subjects (32). Mathur *et al.* reported that there was also no significant difference between younger and older age groups in either the percentage or absolute number of Eos in the induced sputum of asthma patients. However, the degradation of Eos after stimulation with IL-5 was slower in the older group, and the production of ECP after stimulation was also slower. Therefore, age most likely affects the activity of Eos (21) but does not affect the absolute number of Eos. In addition to Eos, we also found that the N, Land M cells were all higher in the younger group, which is in agreement with the findings of other studies. As people age, their immune function declines, and they acquire infections more easily (21,33). Hence, we should pay more attention to age in our study.

Although we collected a large number of samples and studied the normal values in detail, there are still some disadvantages in this study. First, the concentration of inflammatory cells was not determined. There should be a primary result for the normal values of the concentrations of various inflammatory cells in the nasal lavage. Second, some of the study components used repeated nasal sprays and collected the condensed water from the anterior naris before analyzing the result. This method is more acceptable in children, which will be applied in a future study (27). Third, we did not collect samples from individuals with rhinitis. If there are data on AR, we can obtain the optimum value for diagnosing AR from the ROC (34) and determining the effect of AR on nasal cytology.

Conclusions

In conclusion, we developed a method for obtaining nasal lavages and determined the nasal cytology of healthy adults based on research conducted in two centers. We will further perform multi-center research to validate this study and prove the usefulness of these measures.

Acknowledgements

This work was supported by the grant of Open Research of State Key Laboratory of Respiratory Diseases (2007DA780154F0907) and National Science Fund Committee (NSFC81072366). We thank Zhihao Liu from

the Jiangsu Provincial Center for Disease Prevention and Control for support with the statistical analysis.
Disclosure: The authors declare no conflict of interest.

References

1. Matheson A, Rosenblum A, Glazer R, et al. Local tissue and blood eosinophils in newborn infants. J Pediatr 1957;51:502-9.
2. Ventura MT, Gelardi M, D'Amato A, et al. Clinical and cytologic characteristics of allergic rhinitis in elderly patients. Ann Allergy Asthma Immunol 2012;108:141-4.
3. Di Lorenzo G, Mansueto P, Pacor ML, et al. Clinical importance of eosinophil count in nasal fluid in patients with allergic and non-allergic rhinitis. Int J Immunopathol Pharmacol 2009;22:1077-87.
4. Glück U, Schütz R, Gebbers JO. Cytopathology of the nasal mucosa in chronic exposure to diesel engine emission: a five-year survey of Swiss customs officers. Environ Health Perspect 2003;111:925-9.
5. Gelardi M, Fiorella ML, Leo G, et al. Cytology in the diagnosis of rhinosinusitis. Pediatr Allergy Immunol 2007;18 Suppl 18:50-2.
6. Gelardi M. Atlas of nasal cytology. Torino: Centro Scientifico Editore, 2004.
7. Bousquet J, Khaltaev N, Cruz AA, et al. Allergic Rhinitis and its Impact on Asthma (ARIA) 2008 update (in collaboration with the World Health Organization, GA(2) LEN and AllerGen). Allergy 2008;63 Suppl 86:8-160.
8. Canakcioglu S, Tahamiler R, Saritzali G, et al. Evaluation of nasal cytology in subjects with chronic rhinitis: a 7-year study. Am J Otolaryngol 2009;30:312-7.
9. Garavello W, Somigliana E, Acaia B, et al. Nasal lavage in pregnant women with seasonal allergic rhinitis: a randomized study. Int Arch Allergy Immunol 2010;151:137-41.
10. Sanli A, Aydin S, Ateş G, et al. Comparison of nasal smear eosinophilia with skin prick test positivity in patients with allergic rhinitis. Kulak Burun Bogaz Ihtis Derg 2006;16:60-3.
11. Scadding GK, Durham SR, Mirakian R, et al. BSACI guidelines for the management of rhinosinusitis and nasal polyposis. Clin Exp Allergy 2008;38:260-75.
12. Gelardi M, Passalacqua G, Fiorella ML, et al. Nasal cytology: the "infectious spot", an expression of a morphological-chromatic biofilm. Eur J Clin Microbiol Infect Dis 2011;30:1105-9.
13. Piacentini GL, Kaulbach H, Scott T, et al. Evaluation of nasal cytology: a comparison between methods. Allergy 1998;53:326-8.
14. Castano R, Thériault G, Maghni K, et al. Reproducibility of nasal lavage in the context of the inhalation challenge investigation of occupational rhinitis. Am J Rhinol 2008;22:271-5.
15. Schiavino D, Nucera E, Milani A, et al. Nasal lavage cytometry in the diagnosis of nonallergic rhinitis with eosinophilia syndrome (NARES). Allergy Asthma Proc 1997;18:363-6.
16. Paananen H, Holopainen M, Kalliokoski P, et al. Evaluation of exposure to man-made vitreous fibers by nasal lavage. J Occup Environ Hyg 2004;1:82-7.
17. Watelet JB, Gevaert P, Holtappels G, et al. Collection of nasal secretions for immunological analysis. Eur Arch Otorhinolaryngol 2004;261:242-6.
18. Scavuzzo MC, Rocchi V, Fattori B, et al. Cytokine secretion in nasal mucus of normal subjects and patients with allergic rhinitis. Biomed Pharmacother 2003;57:366-71.
19. Nowacki Z, Neuberg J, Strzałka K, et al. Is prediction of the allergic march possible on the basis of nasal cytology? Pneumonol Alergol Pol 2010;78:263-70.
20. Liu L, Leech JA, Urch RB, et al. A comparison of biomarkers of ozone exposure in human plasma, nasal lavage, and sputum. Inhal Toxicol 1999;11:657-74.
21. Mathur SK, Schwantes EA, Jarjour NN, et al. Age-related changes in eosinophil function in human subjects. Chest 2008;133:412-9.
22. Trivedi SG, Lloyd CM. Eosinophils in the pathogenesis of allergic airways disease. Cell Mol Life Sci 2007;64:1269-89.
23. Ciprandi G, Vizzaccaro A, Cirillo I, et al. Nasal eosinophils display the best correlation with symptoms, pulmonary function and inflammation in allergic rhinitis. Int Arch Allergy Immunol 2005;136:266-72.
24. Mygind N, Nielsen LP, Hoffmann HJ, et al. Mode of action of intranasal corticosteroids. J Allergy Clin Immunol 2001;108:S16-25.
25. Jankowski R, Persoons M, Foliguet B, et al. Eosinophil count in nasal secretions of subjects with and without nasal symptoms. Rhinology 2000;38:23-32.
26. Burrows B, Hasan FM, Barbee RA, et al. Epidemiologic observations on eosinophilia and its relation to respiratory disorders. Am Rev Respir Dis 1980;122:709-19.
27. Fransson M, Benson M, Wennergren G, et al. A role for neutrophils in intermittent allergic rhinitis. Acta Otolaryngol 2004;124:616-20.

28. Holgate ST, Sandström T, Frew AJ, et al. Health effects of acute exposure to air pollution. Part I: Healthy and asthmatic subjects exposed to diesel exhaust. Res Rep Health Eff Inst 2003:1-30; discussion 51-67.
29. Gelardi M, Incorvaia C, Fiorella ML, et al. The clinical stage of allergic rhinitis is correlated to inflammation as detected by nasal cytology. Inflamm Allergy Drug Targets 2011;10:472-6.
30. Busse PJ, Mathur SK. Age-related changes in immune function: effect on airway inflammation. J Allergy Clin Immunol 2010;126:690-9; quiz 700-1.
31. Gomez CR, Nomellini V, Faunce DE, et al. Innate immunity and aging. Exp Gerontol 2008;43:718-28.
32. Nyenhuis SM, Schwantes EA, Mathur SK. Characterization of leukotrienes in a pilot study of older asthma subjects. Immun Ageing 2010;7:8.
33. Plackett TP, Boehmer ED, Faunce DE, et al. Aging and innate immune cells. J Leukoc Biol 2004;76:291-9.
34. Khianey R, Oppenheimer J. Is nasal saline irrigation all it is cracked up to be? Ann Allergy Asthma Immunol 2012;109:20-8.

Cite this article as: Zhang Y, Wang Q, Xie Y, Wang Z, Li D, Ma L, Pang X, Yu W, Zhong N. The normative value of inflammatory cells in the nasal perfusate of Chinese adults: a pilot study. J Thorac Dis 2014;6(7):905-912. doi: 10.3978/j.issn.2072-1439.2014.06.45

Original Article

The impact of hypertension on the electromechanical properties and outcome of catheter ablation in atrial fibrillation patients

Tao Wang[1], Yun-Long Xia[1], Shu-Long Zhang[1], Lian-Jun Gao[1], Ze-Zhou Xie[1], Yan-Zong Yang[1], Jie Zhao[2]

[1]First Affiliated Hospital of Dalian Medical University, Dalian 116011, China; [2]Department of Physiology, Dalian Medical University, Dalian 116000, China

Correspondence to: Yun-Long Xia. Department of Cardiology, First Affiliated Hospital of Dalian Medical University, Dalian 116011, China. Email: yunlong.xia@gmail.com; Professor Jie Zhao. Department of Physiology, Dalian Medical University, Dalian 116000, China. Email: dlzhaoj@163.com.

Background: Although hypertension is associated with atrial fibrillation (AF), the impact of hypertension on the electromechanical properties and outcome of catheter ablation in AF patients is unclear.

Methods: AF patients [n=213, 136 paroxysmal AF (PAF) patients and 77 persistent AF patients] undergoing circumferential pulmonary vein (PV) isolation guided by CARTO mapping were enrolled, and then were divided into normotension group and hypertension group. Several left atrial (LA) electroanatomical parameters determined by the CARTO system were compared between groups.

Results: The LA bipolar voltage was lower in PAF patients with than without hypertension (1.44±1.09 *vs.* 1.92±0.76 mV, P=0.048); a significant difference was also observed in persistent AF patients. Hypertension significantly increased the size of the LA scar and low-voltage zones (LVZs) in both PAF and persistent AF patients. However, hypertension did not significantly affect recurrence in either PAF or persistent AF patients. The LA bipolar voltage was higher in PAF patients without recurrence than in those with recurrence (1.77±1.01 *vs.* 1.29±0.93 mV, P=0.048); a significant difference was also observed in persistent AF patients. PAF and persistent AF patients with AF recurrence had significantly larger LA scar and LVZs than patients without recurrence.

Conclusions: Hypertension has a significant impact on the LA electromechanical properties in AF patients, and the LA substrate has an important influence on the outcome of catheter ablation.

Keywords: Hypertension; voltage; atrial fibrillation (AF); pulmonary vein (PV); catheter ablation; radiofrequency (RF) current

Submitted Feb 06, 2014. Accepted for publication May 13, 2014.
doi: 10.3978/j.issn.2072-1439.2014.06.31
View this article at: http://dx.doi.org/10.3978/j.issn.2072-1439.2014.06.31

Introduction

Atrial fibrillation (AF) is the most common tachyarrhythmia in clinical practice (1,2), and there is a significant increase in the prevalence of AF in patients with hypertension. Circumferential ablation of all four pulmonary veins (PVs) with conduction block between the PVs and left atrium has become the standard procedure to eliminate paroxysmal AF (PAF) (3). However, the patients in those studies always included younger subjects and often excluded very elderly subjects who have more underlying diseases such as hypertension. Hypertension plays an important role in AF genesis (1). Hypertension could lead to left atrial (LA) dilatation (4). An enlarged atrial size modulates the substrate for AF by increasing non-uniform anisotropy and conduction disturbances (5,6). A heterogeneous structure with different thicknesses of the cardiac chambers could play a crucial role in rotor dynamics, leading to wave splitting and stabilization of reentrant circuit (7). Hypertension could lead to fibrosis in the left atrium. Fibrosis plays an important role in the dynamics of AF, since local fibrotic areas could serve as anchors for reentrant circuits and alter wave-front propagation, causing fractionated

electrograms, wave breaks, and conduction delays (8). These mechanisms may be relevant in explaining the nature of the arrhythmogenic substrates present in patients with hypertension.

The aim of this study was to investigate the impact of hypertension on the properties of atrial substrate and the outcome of catheter ablation in patients with AF.

Methods

Study patients

A total of 213 consecutive patients (58.3±21.1 years old, 112 males and 101 females, 136 PAF patients and 77 persistent AF group patients) with drug-refractory AF were enrolled. All patients were undergoing circumferential PV isolation (CPVI) guided by the CARTO mapping system (CARTOTM XP, Biosense-Webster Inc, Diamond Bar, CA, USA). AF patients were divided into normotension group and hypertension group. According to the guidelines of JCN-7 (9), Hypertension was defined as blood pressure ≥140/90 mmHg and/or a history of treated hypertension. A total of 40 of these hypertension patients were prescribed with different ACEI or ARB or NDHP-CCBs to treat hypertension in our hospital. The other patients used no drugs to treat hypertension. All antiarrhythmic drugs were discontinued for at least five half-lives before the procedure. Patients who underwent a repeat ablation procedure were excluded from the study. Patients with diabetes or serious structural heart diseases (rheumatic heart disease, hypertrophic cardiomyopathy, dilated cardiomypathy, coronary heart disease or 3rd degree atrioventricular block) were also excluded. This retrospective protocol was approved by the Institutional Review Board of the Dalian Medical University.

Echocardiography was performed in all patients before the ablation procedure. The anteroposterior diameter of the left atrium at end-systole was measured by M mode echocardiography in the parasternal short axis view, and all measurements were performed by two independent observers.

Electrophysiological study and catheter ablation

The details of the electrophysiological study and 3-dimensional (3D) mapping were the same as described previously (3,10). After femoral venous access was obtained, a 7-French deflectable decapolar catheter was inserted into the coronary sinus. Dual transseptal puncture was performed under fluoroscopic guidance, with delivery of two 8 F long sheaths (SL1 and SR0, St. Jude Medical, St. Paul, MN, USA) into the LA. In PAF, the PV ostia were identified by enography and the drop-off site of the 3.5-mm tip ablation catheter (Navi-Star, Biosense-Webster), while dragging it out of the vein. Continuous circumferential lesions were created encircling the right and left PV ostia using the ablation catheter guided by the CARTO system. Radiofrequency (RF) current energy output was limited to a maximum of 70 W and 55 ℃. After completion of the circumferential lesion set, the ipsilateral superior and inferior PVs were mapped and ablated carefully. The end point of ablation was complete electrical disconnection of the PV antrum from the LA. After successful isolation of all four PVs, high current pulse duration stimulation from the proximal and distal CS was performed. If induced AF was sustained for >1 minute, an additional linear ablation was performed at the anterior roof and the mitral isthmus. In persistent AF, PV isolation plus linear ablation was performed as the first and second steps. If AF did not stop, sinus rhythm was restored by electric cardioversion.

Atrial substrate analysis using atrial activation maps and 3-dimensional (3D) electroanatomical maps

Sequential activation maps of LA were constructed in all 213 patients. Bipolar electrograms were recorded before catheter ablation from more than 80 sites in LA, and these sites were approximately equally distributed. The bipolar electrograms were filtered between 32 and 300 Hz and recorded digitally. The absolute peak of the waveform was selected as the point of local atrial activation. The ablation catheter was selected as the roving catheter. The roving catheter was moved to various points on the LA walls to determine local activation times (relative to a reference signal). The signals from the roving catheter were used to build a sequential activation map. The LA total activation time was defined as the time interval from the earliest to the latest activation point in the LA; the total activation time of both atria was defined as the time interval from the start of P wave of the most clear lead in the surface electrocardiogram (ECG) to the latest point of the LA.

After completion of the sequential activation maps, the LA bipolar electrograms were used to construct detailed electroanatomical maps using CARTO software. This analysis was performed offline, and the software determined the voltage contribution to the surface area of each point

Table 1 Clinical characteristics of AF patients with and without hypertension

Group	Case number (male/female)	Age	LA diameter (mm)	AF duration (years)	Systolic pressure (mmHg)
PAF					
Normotensive group	94 (53/41)	56.2±19.6	36.6±8.7	5	124.4±21.5
Hypertensive group	42 (24/18)	60.6±21.6	37.4±9.5	6	140.9±18.4*
Persistent AF					
Normotensive group	42 (22/20)	51.6±21.2	44.7±13.4	4	132.3±16.9
Hypertensive group	35 (18/17)	57.9±17.4	45.9±12.8	5	139.1±16.3*

*, P<0.05 normotensive group *vs*. hypertensive group. AF, atrial fibrillation; LA, left atrial; PAF paroxysmal AF.

using the distance to the nearest neighboring point, and presented the results as the weighted voltage (nearest distance × voltage)/mean overall nearest distance. There were 126±15 bipolar LA mapping sites used by the CARTO software to construct the electroanatomical maps. Scar was defined as the absence of any voltage or a bipolar voltage amplitude ≤0.05 mV that was indistinguishable from noise. The scar-zone index was defined as the scar surface area/total LA surface area. The low-voltage zone (LVZ) in the AF patients was defined as an amplitude ≤0.2 mV. The LVZ index was defined as the LVZ surface area/total LA surface area.

Clinical variables

The clinical variables that may influence the voltage were analyzed including gender, AF duration, LA enlargement (LA diameter ≥4 cm), hypertension and age.

AF recurrence during follow-up

After discharge, the patients underwent follow-up (1 day after catheter ablation, and then at 1, 3 and 6 months) at our cardiology clinic or with their referring physicians. Antiarrhythmic drugs were prescribed for 8 weeks to prevent the early recurrence of AF in patients with persistent AF. When patients experienced symptoms suggesting a tachycardia after ablation, 24-hour Holter monitoring was performed to define the cause of the clinical symptoms. If more than one episode of recurrent symptomatic AF was documented, the patients were encouraged to receive a second ablation procedure, or antiarrhythmic drugs were prescribed to control the recurrent AF. AF recurrence was defined as an episode confirmed by an ECG that lasted more than 1 minute and occurred 3 months or more after the ablation procedure. The successful AF ablation was defined as no AF recurrence was found during follow up after the AF catheter ablation.

Statistical analysis

All data for continuous variables are reported as the mean ± SD or the median. A chi-square test was used to compare categorical variables between groups. A student's test or a Wilcoxon rank-sum test was used to compare continuous variables between groups. The mean LA bipolar voltage was compared between the groups. A value of P<0.05 was considered to be statistically significant. All analyses were performed using SPSS software version 11.0 (SPSS, Chicago, Illinois, USA).

Results

Clinical characteristics of the patients with and without hypertension

The baseline characteristics of the patients with and without hypertension are presented in *Table 1*. The cohort in this study included 213 patients, 136 PAF patients and 77 persistent AF patients. In the 136 PAF patients, there were 94 in the normotensive group (53 males), and 42 patients in the hypertensive group (24 males); in the 77 persistent AF patients, there were 42 in normotensive group (22 males), and 35 in the hypertensive group (18 males). The gender, mean duration of AF and LA diameter were similar between the hypertensive and normotensive groups.

Effect of hypertension on the electroanatomical properties of the atrial substrate

The AF substrate variables determined by electranatomical mapping are shown in *Table 2*. The mean LA bipolar

Table 2 Atrial substrate characteristics in the normotensive and hypertensive groups

Group	Case number	LA bipolar voltage (mV)	Scar-zone index	LVZ index	LA single voltage (mV)	Atrial TAT [ms]	LA TAT [ms]
PAF							
Normotensive group	94	1.92±0.76	0 (0-0)	0.064 (0.03-0.106)	3.9±1.9	229 [171-264]	207 [136-244]
Hypertensive group	42	1.44±1.09*	0.0002* (0-0.018)	0.136* (0.063-0.176)	3.2±1.8	221 [164-266]	201 [130-240]
Persistent AF							
Normotensive group	42	0.74±0.59	0.007 (0-0.022)	0.195 (0.123-0.241)			
Hypertensive group	35	0.51±0.39*	0.013* (0-0.037)	0.265* (0.164-0.372)			

TAT, total activation time; LVZ, low voltage zone; AF, atrial fibrillation; LA, left atrial; PAF paroxysmal AF. *, P<0.05 normotensive group *vs*. hypertensive group.

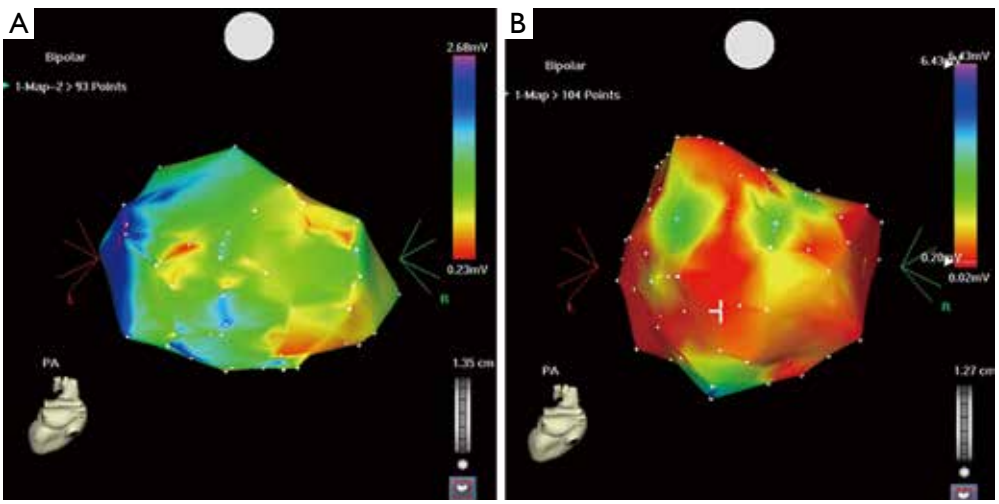

Figure 1 (A) is a CARTO map in a normotensive patient. The red color indicates the low-voltage zone (LVZ); (B) is a CARTO map in a hypertensive patient. Comparison of the two maps shows that there is a much larger LVZ in the patient with hypertension.

voltage was higher in the normotensive group than the hypertensive group in both PAF (1.92±0.76 *vs*. 1.44±1.09, respectively, P=0.048) and persistent AF patients (0.74±0.59 *vs*. B: 0.51±0.39, respectively, P=0.004) (*Table 2*, *Figure 1*). The total atrial activation time and LA activation time recorded during sinus rhythm were not significantly different between the normotensive and hypertensive PAF groups (activation time could not be assessed in persistent AF patients). The LA scar-zone index and LVZ index were significantly smaller in the normotensive group than in the hypertensive group in both PAF and persistent AF patients.

Several clinical factors that could affect the mean LA bipolar voltage were also analyzed (*Table 3*). Gender, mean duration of AF before ablation and LA diameter did not affect the mean LV bipolar voltage in either PAF or persistent AF patients. Hypertension significantly influenced the mean LA bipolar voltage in both PAF and persistent AF patients. Age significantly influenced the mean LA bipolar voltage only in patients with persistent AF.

The effect of hypertension on the outcome of AF ablation

The overall incidence of AF recurrence in our patients was 20.6% (44 patients). Although the success rate of ablation in hypertensive patients seemed to be smaller than that in normotensive patients (71.4% *vs*. 83.8%), the difference did not reach statistical significance (*Table 4*). A total of 14 of 44 AF recurrence patients receive a second ablation procedure, the others were prescribed with antiarrhythmic drugs (amiodarone or β-adrenoceptor blockers) to control the recurrent AF.

Table 3 Clinical variables affecting the atrial substrate properties in PAF and persistent AF

Group	PAF		Persistent AF	
	Mean LA bipolar voltage	P value	Mean LA bipolar voltage	P value
Gender		0.323		0.323
Male	1.78±1.16		0.78±0.46	
Female	1.58±1.13		0.68±0.67	
Age		0.096		0.011
≤65	1.71±1.05		0.73±0.6	
>65	1.64±1.07		0.51±0.36	
Hypertension		0.048		0.004
Yes	1.92±0.76		0.74±0.59	
No	1.44±1.09		0.51±0.39	
LA diameter		0.132		0.105
≤40 mm	1.71±1.1		0.75±0.6	
>40 mm	1.6±0.86		0.55±0.44	
AF duration		0.147		0.147
≤2 years	1.78±1.12		0.68±0.59	
>2 years	1.57±0.92		0.59±0.52	

AF, atrial fibrillation; LA, left atrial; PAF paroxysmal AF.

Table 4 The effect of hypertension on the outcome of AF ablation

Patients	Ablation success	Ablation recurrence	Success rate (%)	P value
PAF				0.067
Normotensive	78	16	82.9	
Hypertensive	29	13	69	
Persistent AF				0.207
Normotensive	36	6	85.7	
Hypertensive	26	9	74.2	
All patients				0.095
Normotensive	114	22	83.8	
Hypertensive	55	22	71.4	

AF, atrial fibrillation; PAF paroxysmal AF.

The clinical characteristics of patients and the outcome of AF ablation

The baseline characteristics of the patients with and without successful AF ablation are presented in *Table 5*. In the cohort of PAF patients, the ablation procedure was successful in 107 patients (66 males), whereas 29 patients (16 males) had AF recurrence. In the persistent AF patients, the ablation procedure was successful in 62 patients (32 males), whereas 15 patients (8 males) had AF recurrence. The gender, age, mean duration of AF, LA diameter and proportion of patients with hypertension were similar between the patients with and without AF recurrence (*Table 5*).

The atrial substrate characteristics and the outcome of AF ablation

The AF substrate properties determined by electroanatomical mapping in patients with and without successful AF ablation are shown in *Table 6*. The mean LA bipolar voltage was higher in the PAF patients with successful ablation than in those with AF recurrence (1.77±1.01 *vs*. 1.29±0.93, respectively, P=0.048). Likewise, the mean LA bipolar voltage was also higher in the persistent AF patients with successful ablation than those with AF recurrence (1.31±0.96 *vs*. 0.78±0.35, respectively, P=0.046) (*Table 6*). The total atrial activation time and total LA activation time recorded during sinus rhythm were not significantly different in the PAF patients with successful ablation from those had AF recurrence. The LA scar-zone index and LVZ index were smaller in both the PAF and persistent AF patients with

Table 5 Clinical characteristics of patients and the outcome of AF ablation

Group	Number of cases (male/female)	Age	LA diameter (mm)	AF duration (years)	Hypertension
PAF					
Success group	107 (66/41)	58.1±20.8	36.9±9.1	5	31
Recurrence group	29 (16/13)	59.3±23.0	37±9.3	6	11
Persistent AF					
Success group	62 (32/30)	54.5±19.6	45±13.4	4	28
Recurrence group	15 (8/7)	54.3±24.8	45.8±12	5	7

AF, atrial fibrillation; LA, left atrial; PAF paroxysmal AF.

Table 6 The atrial substrate characteristics and the outcome of AF ablation

Group	Case number	LA bipolar voltage (mV)	Scar-zone index	LVZ index	LA single voltage (mV)	Atrial TAT [ms]	LA TAT [ms]
PAF							
Success group	107	1.77±1.01	0 (0-0)	0.067 (0.07-0.116)	3.72±1.9	228 [174-265]	217 [137-245]
Recurrence group	29	1.29±0.93*	0.0004* (0-0.018)	0.139* (0.067-0.178)	2.79±1.4	222 [165-260]	201 [135-241]
Persistent AF							
Success group	62	1.31±0.96	0.005 (0-0.024)	0.147 (0.068-0.207)			
Recurrence group	15	0.78±0.35*	0.012* (0-0.036)	0.285* (0.165-0.378)			

TAT, total activation time; LVZ, low voltage zone; AF, atrial fibrillation; LA, left atrial; PAF paroxysmal AF. *, P<0.05 success group *vs*. recurrence group.

a successful ablation compared with those who had AF recurrence (*Table 6*, *Figure 2*).

Discussion

The mean LA bipolar voltage was significantly reduced, and the scar-zone index and LVZ index were significantly increased in AF patients with hypertension. However, hypertension did not appear to affect the incidence of AF recurrence after the first catheter ablation procedure. When patients with and without hypertension were combined, the mean LA bipolar voltage was significantly reduced, and the scar-zone index and LVZ index were significantly increased in the AF patients that had recurrence.

In contrast to the effect of hypertension on the mean LA bipolar voltage and size of the scar-index and LVZ index, we found that hypertension did not affect the LA activation time. Although the explanation for the lack of an effect of hypertension on LA activation time is not clear, it may be that both the magnitude and duration of hypertension may influence this activation time. Therefore, it is possible that the blood pressure was not high enough for a long enough period to alter LA activation time in the hypertensive patients in this study.

Effect of hypertension on the outcome of catheter ablation of AF

Our study has shown that the benefits of the PV isolation extend equally to all AF patients, and that the presence of hypertension does not significantly increase the risk of AF recurrence after catheter ablation. However, there was a non-significant trend towards a higher recurrence rate in the AF patients with hypertension (28.6% *vs*. 16.2%, *Table 4*). The possible explanation is that the process of electrical and structural remodeling in the atrium may differ between patients with and without hypertension. Increased automaticity and increased triggered activity might occur in human diseased atrial fibers. Furthermore, fibrillatory wavelets could be more easily induced and maintained in larger atria, which might increase the risk of AF recurrence event in the absence of PV discharge (11). It is possible that the blood pressure was not high enough for a long enough period to alter the ablation results significant in

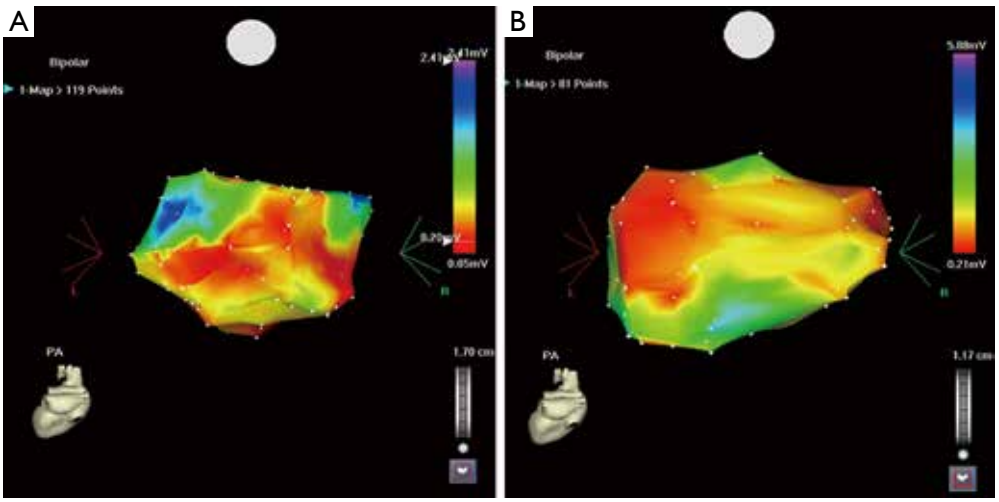

Figure 2 (A) is a CARTO map in a patient who did not have AF recurrence. The red color indicates the low-voltage zone (LVZ); (B) is a CARTP map in a patient who had AF recurrence. Comparison of the two maps shows that the LVZ is smaller in the patient without AF recurrence.

the hypertensive patients in this study and we had a relative small patient number.

Relationship between the LA substrate properties and recurrence

A decrease in the mean LA bipolar voltage, and increase in the LA scare-zone index and LVZ index were associated with recurrence after catheter ablation of AF in the present study. These findings can be explained by one of the following mechanisms: (I) the LVZ may aggravate intra-atrial conduction delay, resulting in the formation of reentrant circuits and thus promote AF perpetuation; and (II) the LVZ may serve as sites of ectopic beats that could trigger AF in the absence of PV discharge (12). In addition, LA scarring can be used as a strong predictor of procedural failure in patients undergoing catheter ablation of AF.

Study limitations

In this study, lack of detailed electoanatomical mapping of the right atrium was a limitation. Second, this was an observational study, and the associations that we observed do not prove the presence of cause and effect relationships. Third, atrial activation maps could not be obtained in the patients with persistent AF, and the detailed LA electroanatomical maps were constructed in these patients during AF rather than during sinus rhythm. Forth, the methods for detecting AF recurrence are suboptimal.

Conclusions

Hypertension has a significant impact on the properties of the LA substrate in AF, and AF patients with hypertension have a significantly lower mean LA bipolar voltage. The LA substrate has an important influence on the outcome of catheter ablation in AF patients.

Acknowledgements

Disclosure: The authors declare no conflict of interest.

References

1. Feinberg WM, Blackshear JL, Laupacis A, et al. Prevalence, age distribution, and gender of patients with atrial fibrillation. Analysis and implications. Arch Intern Med 1995;155:469-73.
2. Anyukhovsky EP, Sosunov EA, Chandra P, et al. Age-associated changes in electrophysiologic remodeling: a potential contributor to initiation of atrial fibrillation. Cardiovasc Res 2005;66:353-63.
3. Pappone C, Oreto G, Rosanio S, et al. Atrial electroanatomic remodeling after circumferential radiofrequency pulmonary vein ablation: efficacy of an anatomic approach in a large cohort of patients with atrial

fibrillation. Circulation 2001;104:2539-44.
4. Gottdiener JS, Reda DJ, Williams DW, et al. Left atrial size in hypertensive men: influence of obesity, race and age. Department of Veterans Affairs Cooperative Study Group on Antihypertensive Agents. J Am Coll Cardiol 1997;29:651-8.
5. Schotten U, Neuberger HR, Allessie MA. The role of atrial dilatation in the domestication of atrial fibrillation. Prog Biophys Mol Biol 2003;82:151-62.
6. Sanders P, Morton JB, Davidson NC, et al. Electrical remodeling of the atria in congestive heart failure: electrophysiological and electroanatomic mapping in humans. Circulation 2003;108:1461-8.
7. Chang SL, Tai CT, Lin YJ, et al. The role of left atrial muscular bundles in catheter ablation of atrial fibrillation. J Am Coll Cardiol 2007;50:964-73.
8. Tanaka K, Zlochiver S, Vikstrom KL, et al. Spatial distribution of fibrosis governs fibrillation wave dynamics in the posterior left atrium during heart failure. Circ Res 2007;101:839-47.
9. Chobanian AV, Bakris GL, Black HR, et al. The Seventh Report of the Joint National Committee on Prevention, Detection, Evaluation, and Treatment of High Blood Pressure: the JNC 7 report. JAMA 2003;289:2560-72.
10. Ouyang F, Bänsch D, Ernst S, et al. Complete isolation of left atrium surrounding the pulmonary veins: new insights from the double-Lasso technique in paroxysmal atrial fibrillation. Circulation 2004;110:2090-6.
11. Chang SL, Tai CT, Lin YJ, et al. Biatrial substrate properties in patients with atrial fibrillation. J Cardiovasc Electrophysiol 2007;18:1134-9.
12. Lo LW, Tai CT, Lin YJ, et al. Progressive remodeling of the atrial substrate--a novel finding from consecutive voltage mapping in patients with recurrence of atrial fibrillation after catheter ablation. J Cardiovasc Electrophysiol 2007;18:258-65.

Cite this article as: Wang T, Xia YL, Zhang SL, Gao LJ, Xie ZZ, Yang YZ, Zhao J. The impact of hypertension on the electromechanical properties and outcome of catheter ablation in atrial fibrillation patients. J Thorac Dis 2014;6(7):913-920. doi: 10.3978/j.issn.2072-1439.2014.06.31

Original Article

Performance evaluation of MR-proadrenomedullin and other scoring systems in severe sepsis with pneumonia

Serdar Akpinar[1], Kazım Rollas[1], Ali Alagöz[2], Fatih Seğmen[1], Tuğrul Sipit[1]

[1]Department of Respiratory Care Unit, [2]Department of Anesthesiology and Reanimation, Ataturk Chest Disease and Thoracic Surgery Education and Research Hospital, Ankara, Turkey

Correspondence to: Serdar Akpinar. Department of Respiratory Care Unit, Ataturk Chest Disease and Thoracic Surgery Education and Research Hospital, Sanatoryum Cad. Kecioren, Ankara, Turkey. Email: drserdarakpinar@yahoo.com.

Background: In sepsis, risk assessment is as crucial as early and accurate diagnosis. In this study, we aimed to evaluate the prognostic value of mid-regional proadrenomedullin (MR-proADM) with other scoring systems in severe sepsis and septic shock patients due to community acquired pneumonia (CAP).

Methods: Patients were divided into 2 groups as severe sepsis and septic shock due to CAP (group 1, n=31) and only CAP group (group 2, n=26). Serum MR-proADM, procalcitonin (PCT), C-reactive protein (CRP), and d-dimer level were analyzed. Acute Physiological and Chronic Health Evaluation (APACHE) II score, Sequential Organ Failure Assessment (SOFA) score, and Pneumonia Severity Index (PSI) were performed for all patients.

Results: There was no difference between groups in terms of serum MR-proADM levels (P=0.780). Serum MR-proADM was not found a significant value for the prediction of death within the 4 and 8 weeks in all patients. SOFA score was the most significant to predict mortality in 4 and 8 weeks (P<0.001). The combination of SOFA score and serum MR-proADM was a strong factor to predict death in 4 weeks (specifity 86.8% and sensitivity 66.7%). The combination of MR-proADM, SOFA score, and APACHE II score was found 75.0 % sensitive and 71.4% specific to predict mortality within 4 weeks in group 1.

Conclusions: The MR-proADM does not correlate with mortality or disease severity to predict mortality. The combination of SOFA, APACHE II scores, and MR-proADM was efficient to predict prognosis and mortality rate in severe sepsis or septic shock patients.

Keywords: Proadrenomedullin (proADM); sepsis; pneumonia; scoring systems; pneumonia severity index (PSI)

Submitted Jan 24, 2014. Accepted for publication Jun 15, 2014.
doi: 10.3978/j.issn.2072-1439.2014.06.42
View this article at: http://dx.doi.org/10.3978/j.issn.2072-1439.2014.06.42

Introduction

Sepsis is one of the leading causes of death in critically ill patients. Early and accurate diagnosis and risk evaluation are crucial for management of sepsis (1,2). Adrenomedullin (ADM) is a novel diagnostic instrument, and it may be helpful to manage the sepsis as well as predicting the prognosis in sepsis patients. ADM, a peptide with 52 amino acids, is one of the most potent vasodilating agents, and it has immune modulating activity and some metabolic properties (3,4). ADM also has a bactericidal activity that is further enhanced by modulation of complement activity and regulation. As a consequence of these activities, serum level of ADM increases in sepsis (5,6). The accurate measurement of ADM is a challenging procedure due to its rapid blood clearance. The stable mid-region part of proadrenomedullin (MR-proADM) directly shows level of the fast degraded active peptide of ADM, and it has been detected in plasma of patients (5,7). Because immediate and accurate diagnosis with appropriate risk assessment is vital for optimal care of critically ill patients, many studies, most of the these studies compared the sepsis and healthy control patients, have been worked to evaluate the importance of

MR-proADM as a sole diagnostic biomarker in sepsis and septic shock due to pneumonia (8,9).

In present study, we aimed to compare the effect of MR-proADM level, other diagnostic markers, and scoring systems between severe sepsis and CAP patients in terms of severity of disease and mortality rate.

Materials and methods

This observational, single-centre, and prospective randomised study was performed between September 2011 and September 2012. Study was approved by the local ethic committee for human studies, and written informed consent was obtained from all patients. Patients were divided into two groups. Thirty one patients were diagnosed as pneumonia according to their chest X-ray and Turkish Thorax Association Pneumonia Guideline, and they were also diagnosed as severe sepsis or septic shock according to 2001 International Sepsis Definitions Conference Report (10,11). Twenty six patients (control group) were admitted to emergency service due to CAP. Same treatment procedure was performed to all patients in ICU.

The CAP was defined by the presence of one or several newly acquired respiratory signs or symptoms which were included cough, sputum production, dyspnea, core body temperature >38.0 ℃, abnormal breath sounds and rales, leukocyte count >10 or <4×109 cells l-1 and an infiltration on chest X-ray (10).

Patients younger than 18, diagnosed with sepsis or septic shock with other reasons, and diagnosed with congestive heart failure were excluded from this study. Patients' age, sex, additional diseases, and body mass index (BMI) were recorded. Acute Physiology and Chronic Health Evaluation (APACHE) II, Sequential Organ Failure Assessment (SOFA) score, and pneumonia severity index (PSI) were calculated (12-14).

Measurement of serum biomarkers

C-reactive protein (CRP), d-dimer, white blood cell (WBC) counts, and serum procalcitonin (PCT) levels were measured. Blood sample was obtained from peripheral vein for each patient for MR-proADM analysis. The blood was separated into plasma immediately after sampling, and these samples were stored at –80 ℃ until analyzed. MR-proADM was measured using a new sandwich immunoassay method (MR-proADM; Brahms; Hennigsdorf, Germany).

Definitions

Intra-assay imprecision was under 10% over the entire measuring range, and the functional assay sensitivity [interassay coefficient of variation (CV) <20%] was 0.12 nmol/L. ProADM levels were considered normal when <4 nmol/L based in the median value of proADM observed in healthy adults (2). The time-resolved amplified cryptate emission technology assay was performed (Kryptorn PCT; Brahms, Hennigsdorf, Germany) to analyse serum PCT. Serum CRP concentrations were measured by immunoturbidimetric assay on modular analyser (Roche Diagnostics, Meylan, France).

Statistical analysis

All statistical analysis was performed using SPSS 11.5 (SPSS Inc) for Windows. Descriptive statistic was expressed as mean ± SD or median (min-max), and categorical variables were expressed as case number and percentage. Kolmogorov Smirnov test was carried out to analyze continuous variables. Student's *t*-test was performed to analyze the difference of mean in groups and Mann Whitney U test was used to analyze difference of median in groups. Categorical variables were analyzed to use Pearson's test or Fischer exact test. The effect of PSI, SOFA, and MR-proADR levels on 4- and 8-week mortality rate was analyzed to use multivariate linear regression analysis. Odds ratio and 95% confidence interval were calculated for all variables. Bonferroni correction was performed to control the type 1 error in all multivariate analysis.

Results

There was no statistically difference between the groups in terms of age, gender, BMI, d-dimer, WBC, and MR-proADM levels (*Table 1*). The PSI levels, SOFA scores and APACHE II scores were significantly higher in group 1 (P<0.001) (*Table 1*). Mean CRP levels were significantly higher in group 1 when compared the group 2 (P<0.010). Mean PCT levels were also higher in group 1 than the group 2 (P<0.001) (*Figure 1*). MR-proADM levels were 5.14 mg/mL in group 1 and 4.83 mg/mL in group 2. There was no significantly difference between the groups in terms of MR-proADM levels (P=0.780). The number of additional disease similar between the groups (P=1.000), whereas the number of patients who had acute respiratory distress syndrome were high in group 1 (P<0.012) (*Table 2*).

Table 1 Demographic and clinical characteristics of patients

Variables	Mean ± SD		P
	Group 1 (n: 31) [range]	Group 2 (n: 26) [range]	
Age (year)	61.8±17.2	56.6±18.2	0.274
Gender (F/M)	8/23	11/15	0.519
BMI (kg/m^2)	24.7±5.0	25.7±4.6	0.432
PSI	4 [2-5]	2 [1-4]	<0.001*
SOFA	8 [3-13]	2 [0-8]	<0.001*
APACHE II	21 [15-29]	12 [5-23]	<0.001*
CRP (mg/L)	14.0 [1.6-44.1]	7.9 [1.0-100.0]	0.010*
Sedimentation (mm/hr)	60 [6-120]	67 [12-120]	0.854
D-Dimer (ng/mL)	1,183 [229-6,861]	885 [398-2,300]	0.129
WBC	15 [6.2-33.0]	12.3 [3.6-37.9]	0.313
Procalcitonin (ng/mL)	2.8 [0.06-48.3]	0.2 [0.01-25]	<0.001
MR-proADM (ng/mL)	5.14 [1.9-14.4]	4.83 [1.6-10.7]	0.780
4th week mortality	16 (51.6%)	2 (7.7%)	<0.001

*, P<0.05: comparison between groups. Data are expressed as mean ± SD or median (min-max) and categorical variables are expressed as case number and percentage. PSI, pneumonia severity index; APACHE II, Acute Physiological and Chronic Health Evaluation; SOFA, Sequential Organ Failure Assessment scores; WBC, white blood cell; CRP, C-reactive protein; BMI, body mass index.

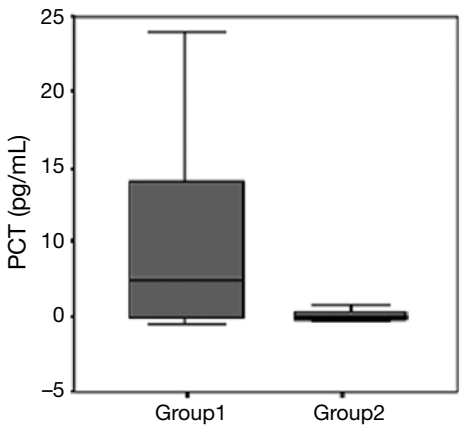

Figure 1 Distribution of procalcitonin (PCT) level in groups. Data are shown as means ± standard error of the mean.

We found correlation between the augmentation of MR-proADM levels and PSI scores, but there was no significantly different (P>0.05) (*Figure 2*). According to 4- and 8-week mortality rate, MR-proADM levels were higher in non-survivor group, but there was no significant different between the groups (P=0.90) (*Figure 3*).

SOFA scores were most significant predictors to determine the 4- and 8-week mortality when parameters evaluated separately in all patients (P<0.001). Each score increment in SOFA caused to 1.618 times (95% CI, 1.246-2.102) increasing the 4-week mortality rate (P<0.001) (*Figure 4*).

When patients were assessed separately in terms of 4- and 8-week mortality, SOFA score, PSI index, APACHE II scores were found significantly higher in patients who died in 4- and 8-week (P<0.001). Mean inotropic agents use, length of ICU stay, and d-dimer level were also higher in these patients (P<0.001, P<0.031, P<0.006, respectively). The ROC curves of all parameters that we compared for the prediction of 4- and 8-week mortality are shown in *Figure 5*. The values of area under the ROC curve for each parameter were also shown in *Table 3*.

Demographic and clinic characteristics of patients' survivor and non-survivor groups within are summarized in *Table 4*. The CRP level was significantly higher in patients who died in 8-week when compared the patients who died 4-week (P<0.020).

The MR-proADM was not a significant diagnostic tool to predict 4- and 8-week mortality in all patients (P=0.709, P=0.50, respectively). The PCT and CRP levels were not also valuable for the prediction of 4- and 8-week mortality (P>0.05).

When SOFA, APACHE II scores, and PSI levels

Table 2 Distribution of subjects according to additional diseases in group 1 and group 2

Variables	Group 1 (n: 31) (%)	Group 2 (n: 26) (%)	P
Additional diseases	28 (90.3)	23 (88.5)	1.000
COPD	17 (54.8)	12 (46.2)	0.514
Bronchiectasis	3 (9.7)	3 (11.5)	1.000
PTE	2 (6.5)	3 (11.5)	0.651
Other malignancy	2 (6.5)	2 (7.7)	1.000
Lung cancer	2 (6.5)	–	0.465
Heart failure[&]	3 (9.7)	1 (3.8)	0.617
Diabetes mellitus	6 (19.4)	8 (30.8)	0.319
Hypertension	4 (12.9)	4 (15.4)	1.000
Neuromuscular diseases	3 (9.7)	–	0.242
Becker muscular dystrophy	1	–	
Myestania gravis	2	–	

[&], P<0.05: comparison between groups. Data are expressed as case number and percentage. COPD, chronic obstructive pulmonary disease; PTE, pulmonary thromboembolism; ARDS, acute respiratory distress syndrome; CHF, congestive heart failure.

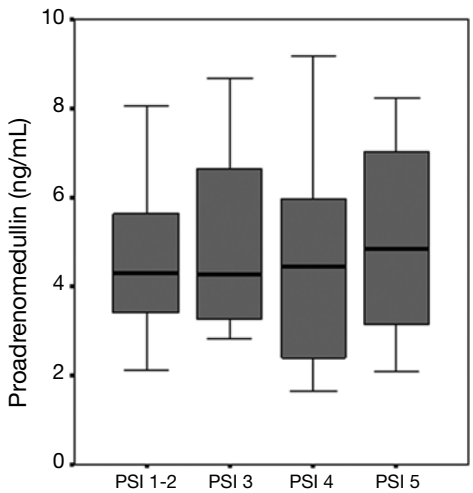

Figure 2 Distribution of MR-proADM levels According to PSI. PSI, pneumonia severity index.

compared to MR-proADM individually; all parameters were significantly superior to MR-proADM to predict 4-week mortality (P<0.001, P=0.003, and P<0.001, respectively).

The MR-proADM and SOFA scores combination was found 86.8% specific and 66.7% sensitive to predict 4-week mortality. Additionally, MR-ProADM and PSI combination had 92.1% specificity and 50.1% sensitivity to predict mortality in 4 weeks. When group 1 evaluated for 4-week mortality, MR-proADM and SOFA scores combination provided 78.6% specificity and 75.0% sensitivity, and MR-proADM, SOFA score, and APACHE II combination showed 71.4% specificity and 75% sensitivity.

The MR-proADM was found 90.3% specific and 24.0% sensitive to predict 8-week mortality. MR-proADM and PSI combination showed 71% specificity and 84% sensitivity to expect 8-week mortality. MR-proADM, SOFA scores, and APACHE II combination showed 80.6% specificity and 76.0% sensitivity, and it provided strong for the prediction 8-week mortality. In group 1, 77.8% specificity and 85.7% sensitivity were found when this combination used for the prediction of 8-week mortality.

Discussion

Present study has shown that MR-proADM was not enough to predict severity of disease and 4- and 8-week mortality rate by itself, but MR-proADM had high sensitivity and specifity when combined with SOFA and APACHE II scores. SOFA score was observed a most valuable determiner, when the PSI based evaluation was performed for all phases of the CAP patients.

Many markers and scoring systems have been studied to predict prognosis and mortality in sepsis, septic shock, and pneumonia. Evaluation of prognosis in CAP patients is very challenging procedure and it is required deep assessments.

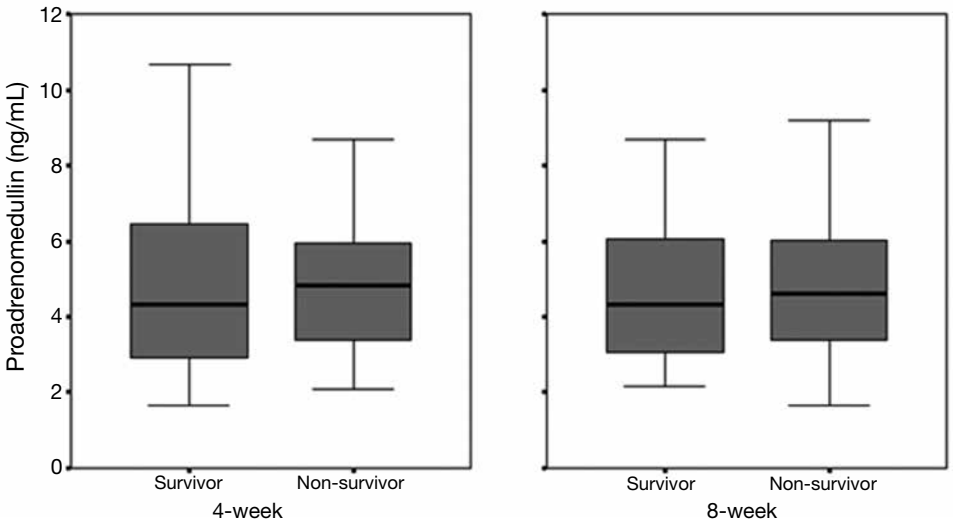

Figure 3 Distribution of MR-proADM levels according to survivor and non-survivor groups within 4- and 8-week.

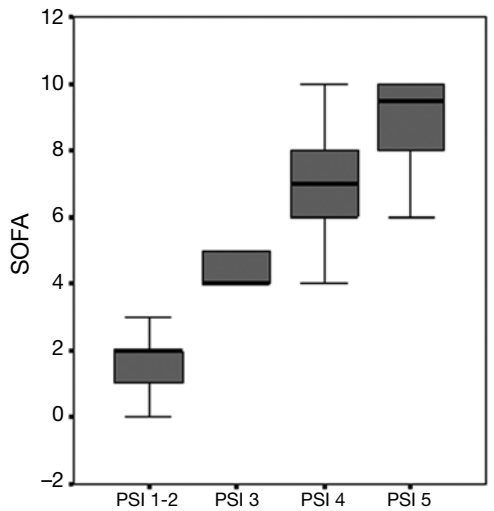

Figure 4 Distribution of SOFA Scores According to PSI level. PSI, pneumonia severity index; SOFA, sequential organ failure assessment scores.

Serum markers are as important as scoring systems to predict severity of disease and mortality rate (8,15). Some serum markers such as PCT and CRP are commonly being used by the researchers (16). Pierrakos and Vincent mentioned that neither PCT nor CRP was not solely enough to determine mortality rate, whereas PCT are superior to CRP in severe septic shock and sepsis patients (17-19). Pierrakos also stated that a single biomarker was not enough to determine prognosis, and combinations are needed for more accurate results (17). In our study, while PCT and CRP level were found high in severe sepsis and septic shock patients, these results were not enough to determine the mortality rate.

Recent studies have been mentioned that MR-proADM was superior to other markers to predict mortality rate, but characteristics of patients were different than our study in terms of severity of disease (2,8,20). Most of the participants in these studies had not a severe disease. Huang and co-workers performed a wide series study on 1,653 participants, and they found that MR-proADM was correlated with mortality and severity of disease but not a prognostic value in high risk CAP patients (9).

In present study, MR-proADM was high in all patients, but we didn't found any correlation between MR-proADM and severity of disease or mortality rate. These results are similar with Huang *et al.* (9) study, and our results suggest that MR-proADM is not a good prognostic value in patients who have a severe disease.

Many scoring systems have been used to determine prognosis in CAP patients. However PSI is one of the most important scoring systems to predict prognosis, 10% false classification might be found particularly patients who have high PSI level (21). Other disadvantage of PSI is an age dependent estimation failure. Overestimation might be occurring in elderly patients who have high comorbidity, whereas risk assessment can be underestimated in young patients who haven't any additional diseases. This estimation failure might cause an unnecessary hospital admission due to CAP with low mortality rate. Niederman *et al.* reported

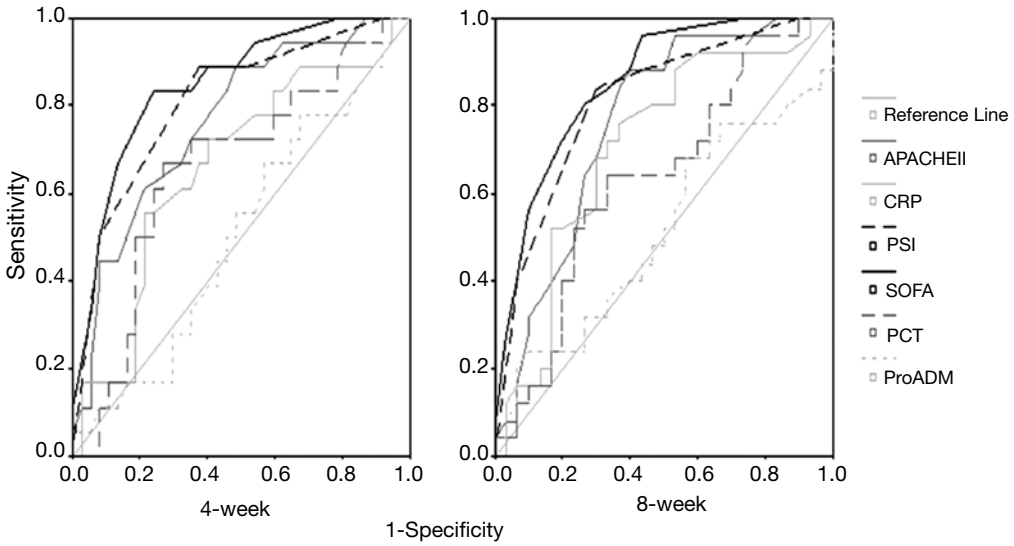

Figure 5 ROC curve for: sensitivity and specifity of all parameters and scoring systems for the prediction of mortality in 4-week and 8-week. APACHE II, acute physiological and chronic health evaluation; CRP, C-reactive protein; PSI, pneumonia severity index; SOFA, sequential organ failure assessment scores; PCT, Procalcitonin; proADM, proadrenomedullin.

Table 3 The values of area under the ROC curve for each parameter

	AUC	Standard error	P	95% CI for AUC
Prediction of 4-week mortality				
APACHE II	0.764	0.068	0.002	0.631-0.896
CRP	0.658	0.080	0.060	0.501-0.814
PSI	0.811	0.063	<0.001	0.687-0.934
SOFA	0.847	0.055	<0.001	0.739-0.955
Procalcitonin	0.655	0.080	0.063	0.499-0.812
MR-pro ADM	0.505	0.083	0.957	0.342-0.667
Prediction of 8-week mortality				
APACHE II	0.760	0.065	<0.001	0.632-0.888
CRP	0.706	0.072	0.009	0.565-0.847
PSI	0.811	0.059	<0.001	0.696-0.927
SOFA	0.851	0.050	<0.001	0.752-0.950
Procalcitonin	0.632	0.076	0.094	0.483-0.781
MR-proADM	0.513	0.081	0.866	0.355-0.671

AUC, area under the curve; CI, confidence Interval; APACHE II, acute physiological and chronic health evaluation; CRP, C-reactive protein; PSI, pneumonia severity index; SOFA, sequential organ failure assessment scores; PCT, procalcitonin; proADM, proadrenomedullin.

that at least 30-60% of low mortality risk patients admitted to hospital due to CAP (22-24). In present study, we found correlation between MR-proADM and PSI level in terms of augmentation, but this increment was not significantly different between patients who had PSI 4-5 and PSI 1-3. This result is considered that, PSI classification should reevaluate by the researchers.

Narvaez-Rivera *et al.* (25) performed a study on 33 CAP patients, and they compared SOFA, APACHE II, PSI, and CURB-65 scoring system with some serum markers.

Table 4 Demographic and clinical characteristics of survivor and non-survivor patients during 4 week

Variables	Survivor (n: 39) [range]	Non-survivor (n: 18) [range]	P
Age (year)	58.9±16.3	60.6±20.8	0.750
BMI (kg/m^2)	25.9±4.6	23.5±5.0	0.080
Additional disease	34 (87.2%)	17 (94.4%)	0.653
Inotropic agents	9 (23.1%)	14 (77.8%)	<0.001
ICU stay (day)	5 [0-110]	9 [1-24]	0.031
Hospital stay (day)	15 [2-135]	18.5 [2-73]	0.904
CRP (mg/L)	10 [0.99-100]	15.7 [1.8-42.0]	0.092
Sedimentation (mm/hr)	63 [6-120]	64.5 [13-120]	0.594
APACHE II	16 [5-28]	22 [10-29]	<0.001
PSI	3 [1-5]	4.5 [2-5]	<0.001
D-Dimer (ng/mL)	860 [229-4,075]	1,253 [481-6,861]	0.006
WBC (microliter)	12.9 [3.6-37.9]	16.6 [6.2-37.0]	0.589
Procalcitonin (ng/mL)	0.52 [0.01-48.3]	2.9 [0.06-18.5]	0.097
SOFA	3 [0-10]	8.5 [2-13]	<0.001
MR-proADM	4.3 [1.6-10.7]	4.8 [2.1-14.4]	0.902

*, P<0.05: comparison between groups, Data are expressed as mean ± SD or median (min-max) and categorical variables are expressed as case number and percentage. CRP, C-reactive protein; APACHE II, acute physiological and chronic health evaluation; PSI, pneumonia severity index; WBC, white blood cell; SOFA, sequential organ failure assessment scores.

They found that SOFA scores were most valuable factor in determining high risk patients. In present study, we found that SOFA score was superior to other serum markers and scoring systems. These results are corelated with Narvaez-Rivera *et al*. (25) results, and SOFA scores had a good correlation with severity of disease and mortality rate.

Travaglino *et al*. (26) compared MR-proADM, PCT, and APACHE II scores with suspicion for sepsis on 128 patients, and they found that MR-proADM and PCT were significantly higher according to healthy subjects. They also found that both markers correlated with APACHE II scores. They claim that combination of scores and serum markers is more helpful for the risk assessment (26).

Combination model of MR-proADM and various scoring system has been investigated in many studies. Crain and his co-workers compared MR-proADM with PSI score and PSI only, and they found a high accuracy rate in MR-proADM and PSI combination to predict treatment failure and prognosis (8,27). According to competence network or the study of community acquired pneumonia (CAPTNEZ) study, combination of MR-proADM and CURB65 had a better accuracy rate to predict prognosis in CAP patients (28).

In our study, when we assessed various scoring system with MR-proADM, SOFA score plus MR-proADM was a most remarkable combination in sepsis and septic shock subjects. MR-proADM, SOFA, and APACHE II scores were also successful to predict both 4- and 8-week mortality rates.

In our study we have some limitations. We analyzed only severe sepsis patients in study group; therefore number of patients in our study was limited. We tried to provide homogeneity in study group in terms of comorbidity, but it was not adequate due to study design.

Conclusions

In conclusion, MR-proADM was found higher in each step of the disease patients who have CAP. Increasing of MR-proADM level was not significant in high risk patients according to PSI risk assessment. SOFA score was a most important indicator for risk evaluation in severe sepsis and septic shock patients, and combination SOFA and MR-proADM provided a high sensitivity and specifity. When MR-proADM is used with scoring systems, physicians can get good results in terms of prediction of mortality and prognosis in CAP patients.

Acknowledgements

Disclosure: The authors declare no conflict of interest.

References

1. Angus DC, Linde-Zwirble WT, Lidicker J, et al. Epidemiology of severe sepsis in the United States: analysis of incidence, outcome, and associated costs of care. Crit Care Med 2001;29:1303-10.
2. Christ-Crain M, Morgenthaler NG, Struck J, et al. Mid-regional pro-adrenomedullin as a prognostic marker in sepsis: an observational study. Crit Care 2005;9:R816-24.
3. Linscheid P, Seboek D, Zulewski H, et al. Autocrine/paracrine role of inflammation-mediated calcitonin generelated peptide and adrenomedullin expression in human adipose tissue. Endocrinology 2005;146:2699-708.
4. Marutsuka K, Nawa Y, Asada Y, et al. Adrenomedullin and proadrenomudullin N-terminal 20 peptide (PAMP) are present in human colonic epithelia and exert an antimicrobial effect. Exp Physiol 2001;86:543-5.
5. Eto T. A review of the biological properties and clinical implications of adrenomedullin and proadrenomedullin N-terminal 20 peptide (PAMP), hypotensive and vasodilating peptides. Peptides 2001;22:1693-711.
6. Nishio K, Akai Y, Murao Y, et al. Increased plasma concentrations of adrenomedullin correlate with relaxation of vascular tone in patients with septic shock. Crit Care Med 1997;25:953-7.
7. Struck J, Tao C, Morgenthaler NG, et al. Identification of an adrenomedullin precursor fragment in plasma of sepsis patients. Peptides 2004;25:1369-72.
8. Christ-Crain M, Morgenthaler NG, Stolz D, et al. Pro-adrenomedullin to predict severity and outcome in community-acquired pneumonia [ISRCTN04176397]. Crit Care 2006;10:R96.
9. Huang DT, Angus DC, Kellum JA, et al. Midregional proadrenomedullin as a prognostic tool in community acquired pneumonia. Chest 2009;136:823-31.
10. Ozlu T, Bülbül Y, Alatas F, et al. Consensus report on diagnosis and treatment of community-acquired pneumonia in adults. Toraks 2009;10:1-24. Available online: http://toraks.dergisi.org/text.php3?id=639
11. Levy MM, Fink MP, Marshall JC, et al. 2001 SCCM/ESICM/ACCP/ATS/SIS International Sepsis Definitions Conference. Crit Care Med 2003;31:1250-6.
12. Knaus WA, Zimmerman JE, Wagner DP, et al. APACHE-acute physiology and chronic health evaluation: a physiologically based classification system. Crit Care Med 1981;9:591-7.
13. Vincent JL, de Mendonça A, Cantraine F, et al. Use of the SOFA score to assess the incidence of organ dysfunction/failure in intensive care units: results of a multicenter, prospective study. Working group on "sepsis-related problems" of the European Society of Intensive Care Medicine. Crit Care Med 1998;26:1793-800.
14. Lim WS, van der Eerden MM, Laing R, et al. Defining community acquired pneumonia severity on presentation to hospital: an international derivation and validation study. Thorax 2003;58:377-82.
15. Wipf JE, Lipsky BA, Hirschmann JV, et al. Diagnosing pneumonia by physical examination: relevant or relic? Arch Intern Med 1999;159:1082-7.
16. Kopterides P, Tsangaris I. Procalcitonin and sepsis: recent data on diagnostic utility prognostic potential and therapeutic implications in critically ill patients. Minerva Anestesiol 2012;78:823-35.
17. Pierrakos C, Vincent JL. Sepsis biomarkers: a review. Crit Care 2010;14:R15.
18. Suberviola B, Castellanos-Ortega A, Llorca J, et al. Prognostic value of proadrenomedullin in severe sepsis and septic shock patients with community acquired pneumonia. Swiss Med Wkly 2012;142:w13542.
19. Brunkhorst FM, Al-Nawas B, Krummenauer F, et al. Procalcitonin, C-reactive protein and APACHE II score for risk evaluation in patients with severe pneumonia. Clin Microbiol Infect 2002;8:93-100.
20. Potocki M, Breidthardt T, Reichlin T, et al. Midregional pro-Adrenomedullin in addition to b-type natriuretic peptides in the risk stratification of patients with acute dyspnea: an observational study. Crit Care 2009;13:R122.
21. Aronsky D, Haug PJ. Assessing the quality of clinical data in a computer-based record or calculating the pneumonia severity index. J Am Med Inform Assoc 2000;7:55-65.
22. Restrepo MI, Mortensen EM, Velez JA, et al. A comparative study of community-acquired pneumonia patients admitted to the Ward and the Intensive Care Unit. Chest 2008;133:610-7.
23. Valencia M, Badia JR, Cavalcanti M, et al. Pneumonia severity index class V patients with community-acquired pneumonia: characteristics, outcomes, and value of severity scores. Chest 2007;132:515-22.
24. Niederman MS. Making sense of scoring systems in community acquired pneumonia. Respirology 2009;14:327-35.
25. Narvaez-Rivera RM, Rendon A, Salinas-Carmona MC,

et al. Soluble RAGE as a severity marker in community acquired pneumonia associated sepsis. BMC Infect Dis 2012;12:15.
26. Travaglino F, De Berardinis B, Magrini L, et al. Utility of Procalcitonin (PCT) and Mid regional pro-Adrenomedullin (MR-proADM) in risk stratification of critically ill febrile patients in Emergency Department (ED). A comparison with APACHE II score. BMC Infect Dis 2012;12:184.
27. Courtais C, Kuster N, Dupuy AM, et al. Proadrenomedullin, a useful tool for risk stratification in high Pneumonia Severity Index score community acquired pneumonia. Am J Emerg Med 2013;31:215-21.
28. Krüger S, Ewig S, Giersdorf S, et al. Cardiovascular and inflammatory biomarkers to predict short- and longterm survival in community-acquired pneumonia: Results from the German Competence Network, CAPNETZ. Am J Respir Crit Care Med 2010;182:1426-34.

Cite this article as: Akpinar S, Rollas K, Alagöz A, Seğmen F, Sipit T. Performance evaluation of MR-proadrenomedullin and other scoring systems in severe sepsis with pneumonia. J Thorac Dis 2014;6(7):921-929. doi: 10.3978/j.issn.2072-1439.2014.06.42

Original Article

The potential role of extracellular regulatory kinase in the survival of patients with early stage adenocarcinoma

Simone de Leon Martini[1,2], Carolina Beatriz Müller[3], Rosalva Thereza Meurer[4], Marilda da Cruz Fernandes[4], Rodrigo Mariano[2], Mariel Barbachan e Silva[2], Fábio Klamt[3,5], Cristiano Feijó Andrade[1,2,6,7]

[1]Programa de Pós-graduação em Ciências Pneumológicas, Universidade Federal do Rio Grande do Sul (UFRGS), 90035-903 Porto Alegre (RS), Brazil; [2]Laboratório de Pulmão e Vias Aéreas, Hospital de Clínicas de Porto Alegre (HCPA), 90035-903, Porto Alegre (RS), Brazil; [3]Laboratório de Bioquímica Celular, Departamento de Bioquímica, ICBS/UFRGS, 90035-003 Porto Alegre (RS), Brazil; [4]Laboratório de Pesquisa em Patologia, Universidade Federal de Ciências da Saúde de Porto Alegre (UFCSPA), 90050-170 Porto Alegre (RS), Brazil; [5]Instituto Nacional de Ciência e Tecnologia-Translational em Medicina (INCT-TM), 90035-903 Porto Alegre (RS), Brazil; [6]Departamento de Cirurgia Torácica, Hospital de Clínicas de Porto Alegre (HCPA), 90035-903, Porto Alegre (RS), Brazil; [7]Hospital da Criança Santo Antônio, Santa Casa de Misericórdia de Porto Alegre, 90020-090 Porto Alegre (RS), Brazil

Correspondence to: Cristiano Feijó Andrade. Hospital de Clínicas de Porto Alegre-Thoracic Surgery Department. Ramiro Barcelos, 2.350, 90035-903 Porto Alegre (RS), Brazil. Email: cristianofa@gmail.com.

Background: Lung cancer is among the most common types of neoplasias, and adenocarcinoma is the most frequent histological type. There is currently an extensive search for prognostic biomarkers of nonsmall cell lung cancer (NSCLC).

Methods: We analyzed the correlation of clinical data and patient survival with the levels of activated extracellular regulatory kinase (ERK) in histological samples of surgically resected early stage lung adenocarcinoma. We randomly selected 36 patients with stage I or II lung adenocarcinoma who underwent pulmonary lobectomy between 1998 and 2004. Patients were divided into the following two groups according to immunohistochemical profile: a group with <15% ERK-positive tumor cells and a group with ≥15% ERK-positive tumor cells. For data comparison, an enrichment analysis of a microarray database was performed (GSE29016, n=72).

Results: Activated ERK levels were ≥15% and <15% in 21 (58%) and 15 (42%) patients, respectively. There were no statistically significant differences in age, sex, smoking history, and body mass index (BMI) among the groups stratified by ERK levels. The survival rate was lower in the ERK ≥15% group than in the ERK <15% group (P=0.045). Enrichment analyses showed no correlation between variations in gene expression of ERK in patients with adenocarcinoma and survival rates in patients with stage I and combined stage II + III disease.

Conclusions: Our findings suggest that high ERK positivity in cells from biological samples of lung adenocarcinoma is related with tumor aggressiveness and a poorer prognosis.

Keywords: Lung cancer; adenocarcinoma; extracellular regulatory kinase (ERK); survival

Submitted Feb 24, 2014. Accepted for publication Jun 10, 2014.
doi: 10.3978/j.issn.2072-1439.2014.07.10
View this article at: http://dx.doi.org/10.3978/j.issn.2072-1439.2014.07.10

Introduction

Lung cancer is among the most common types of neoplasms and is the leading cause of death in the United States and the second major cause of death in Brazil (1-3). Unfortunately, the disease is usually advanced at the time of diagnosis: thus, precluding surgical treatment and restricting patients to chemotherapy and/or radiation therapy with a minimal chance of cure (4). Due to this aggressive behavior of lung cancer, it is necessary to identify molecules, proteins, or signaling pathways related to tumor growth, which have an influence on the outcome. The study of these prognostic factors could stimulate the development of new potential

therapies targeting specific molecules (5).

A persistent search for prognostic biomarkers of nonsmall cell lung cancer (NSCLC) is currently ongoing (5). In this context, the epithelial growth factor receptor epidermal growth factor receptor (EGFR)-dependent RAS/RAF/MEK/ERK signaling cascade is under intensive investigation to identify new prognostic factors of lung cancer because they regulate signals for cell growth and survival and are involved in cell cycle regulation, angiogenesis, cell proliferation, and migration (6-8). A third of all forms of cancers are associated with enhanced activity of this cascade (9). For this reason, many EGFR (10,11), RAS, RAF, and MEK inhibitors have been developed as potential blockers of the activity or proliferation of different components of the extracellular signal-regulated kinase (ERK) signaling pathway (12-14). Therefore, the potential of overactive RAS, RAF, MEK, or ERK as prognostic factors for lung adenocarcinoma has become an interesting area of research.

Most of the studies searching for prognostic factors on NSCLC encompass all its types but do not discriminate in a specific cell type or samples from a particular stage, which makes it difficult to draw more detailed conclusions. Thus, it is essential to have a more specific population with minimal confusing factors to study potential prognostic factors in NSCLC. Based on these concerns, we selected only those patients who had been surgically treated for early lung adenocarcinoma to study the relationship of ERK and prognosis in this particular population.

We hypothesized that increased levels of activated ERK in patients with lung adenocarcinoma were associated with a poorer prognosis or decreased patient survival. Therefore, we conducted an immunohistochemical study using tumor samples from patients surgically treated for lung adenocarcinoma and performed a microarray analysis of experiments from different databases that included a population having a profile similar to that of our samples.

Materials and methods

We selected patients with lung adenocarcinoma who underwent pulmonary resection between 1998 and 2004 and were included in a previous study by Sánchez *et al*. (15). The present work was approved by the local Research Ethics Committee under protocol number 1852/08.

Surgical staging was determined according to the TNM classification system (16,17). All data related to preoperative evaluation, surgical techniques, and postoperative results are described in the article by Sánchez *et al*. (15). We randomly selected 36 patients with postoperative stage I or II disease and with available survival data and immunohistochemical samples.

Analysis of gene expression

Gene expression analyses were performed using microarray data from five different studies (18-22). However, we present data from a single study by Staaf *et al*., a database that included 39 adenocarcinoma patients with 72 available patients (GSE29016, Illumina HT-12 V3.0) (18). GSE29016 was retrieved from the gene expression database Gene Expression Omnibus (GEO) (http://www.ncbi.nlm.nih.gov/geo/), considering it was the only experiment that included all parameters analyzed in our study. To perform gene expression enrichment analysis, Gene Set Enrichment Analysis (GSEA) software, which requires a gene set, the parameters to be analyzed, and gene expression data for data processing was used. We used the Kyoto Encyclopedia of Genes and Genomes (KEGG) to obtain the gene set to be analyzed. Subsequently, we employed the online tool string to confirm interactions among the 261 genes of the group. The following parameters were analyzed: smoking status (8 nonsmokers and 21 smokers), TNM stage (30 with stage I and 9 with combined stage II + III disease, respectively), and sex (18 males and 21 females).

After the enrichment analysis was performed using GSEA as described by Mootha *et al*. (23), a survival curve for each of the parameters versus gene expression was plotted using GraphPad Prism 5.

Samples

Tissue samples for histopathological studies were obtained from surgical specimens of primary adenocarcinoma lesions from patients with surgical stage I or II. All samples were fixed in 10% buffered formalin and embedded in paraffin tissue blocks, which were then processed for immunohistochemical analyses. A tissue section was stained with hematoxylin and eosin (H&E) and analyzed by a pathologist to confirm the presence of adenocarcinoma in the sample.

Immunohistochemistry

Tissue sections measuring 4 cm in thickness were prepared on silanized slides. According to a previously standardized

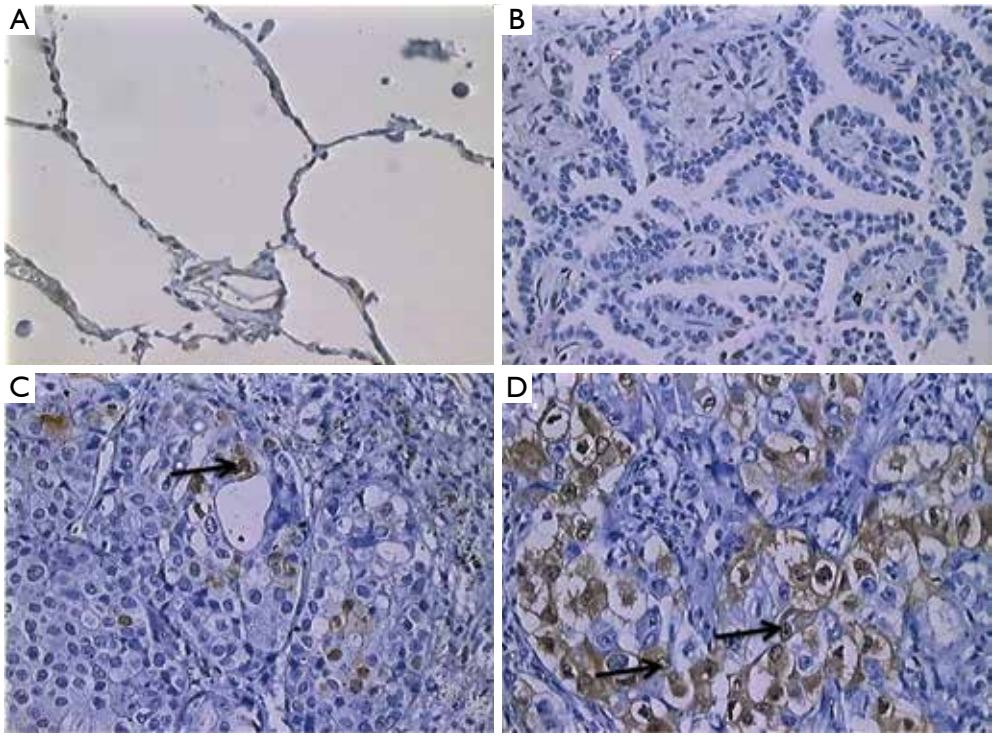

Figure 1 Immunohistochemical reaction for ERK, extracellular regulatory kinase detection in normal lung tissue. (A) Lung adenocarcinoma without ERK expression; (B) positive cases with low ERK expression; (C) high ERK expression; (D) nuclear and cytoplasmic staining is indicated by arrows. ERK, extracellular regulatory kinase.

protocol, the following procedures were performed after deparaffinization and rehydration: heat-mediated antigen retrieval with sodium citrate buffer, blocking of endogenous peroxidase in a 5% H_2O_2 solution in methanol, and blocking of nonspecific binding in 1% bovine serum albumin (BSA) solution. Subsequently, the slides were incubated overnight at 4 ℃ with rabbit polyclonal antibody specific for the double phosphorylated form of ERK1/2 (Thr202/Tyr204; Cell Signaling, Beverly, MA, USA) diluted in a 1:300 ratio in 1% BSA. Plate washing, incubation, and color reaction were performed using the HRP-labeled conjugated polymer kit (Invitrogen®). Sections were then counterstained with hematoxylin. Negative controls were obtained using the same protocol, but without the primary antibody.

Analysis of immunohistochemical reactions

Immunohistochemical analyses were performed by counting ERK-positive cells/1,000 cells in consecutive microscopic fields, taking into account only tumor cells. Cell count was performed by two independent observers. A maximum interobserver discrepancy of 30% was considered or a third observer was included. Cell counting was performed using a Zeiss® Imager microscope coupled to the Image Pro Plus® 6.1 software. For statistical analysis, patients were divided into the following two groups based on a previous study: a group with <15% ERK-positive tumor cells and a group with ≥15% ERK-positive tumor cells (24) (*Figure 1*).

Statistical analyses

Mean values were compared using Student's *t*-test, whereas categorical variables were compared using Fisher's exact test. In addition, for survival analyses, we used Kaplan-Meier curves and Cox regression analyses in univariate and multivariate survival platforms. Statistical data were processed and analyzed using SPSS software, version 18.0 (IBM, USA, Chicago, 2009).

Results

Activated ERK levels were ≥15% and <15% in 21 (58%)

Table 1 Characteristics of lung adenocarcinoma patients according to positivity for ERK, extracellular regulatory kinase in tumor cells

Characteristics	Cellular positivity for ERK [%]			
	Total n=36 [100]	<15 n=15 [42]	≥15 n=21 [58]	P
Age (in years)	64±8	63±8	65±9	0.37[a]
Males, number [%]	22 [61]	8 [53]	14 [67]	0.50[b]
Staging, number [%]				0.171[b]
I A	7 [19]	2 [13]	5 [24]	
I B	16 [44]	10 [67]	6 [29]	
II A	6 [17]	1 [7]	5 [24]	
II B	7 [19]	2 [13]	5 [24]	
Smokers, number [%]	26 [72]	9 [60]	17 [81]	0.26[b]
FEV1, %	82±22	77±24	87±19	0.174[a]
BMI, kg/m^2	25.5±5.5	25.3±5.5	25.6±5.6	0.84[a]

Data are presented as means ± standard deviation or cell count (percentage). FEV1%, forced expiratory volume in the first second; BMI, body mass index; P, statistical significance; [a], Student's *t*-test; [b], Fisher's exact test.

Table 2 Selected characteristics and their relation with survival in patients with lung adenocarcinoma

Characteristic	N	Event number [%]	Multivariate analysis	
			HR (95% CI)	P
ERK, per/1,000 cells				
≥15	21	11 [52]	4.2 (1.0-17.1)	0.045
<15	15	3 [20]	1.0	
Age (in years)	36	14 [39]	1.04 (0.97-1.12)	0.32
Sex				
Male	22	9 [41]	1.0	
Female	14	5 [36]	1.1 (0.3-3.9)	0.90
BMI, kg/m^2	36	14 [39]	0.91 (0.81-1.03)	0.139
FEV1%	36	14 [39]	0.99 (0.96-1.02)	0.324
Smoking history				
Present	26	10 [39]	0.4 (0.1-1.5)	0.40
Absent	10	4 [40]	1.0	

ERK, extracellular regulatory kinase.

and 15 (43%) patients, respectively (*Figure 1*). There were no statistically significant differences in age, sex, smoking history, and body mass index (BMI) between the groups stratified by ERK (*Table 1*). When survival was compared between the ERK ≥15% and ERK <15% groups, the former group showed lower survival than the latter during the study period (*Table 2*). We also performed statistical analyses using a cutoff threshold above and below 45% ERK positivity, and the results were very similar to those obtained when the cutoff threshold of above and below 15% were used.

By using the multivariate Cox model after adjusting for age, sex, BMI, forced expiratory volume, and smoking history, the difference in survival between the ERK ≥15% and <15% groups was not only maintained but also statistically significant (P=0.045). This difference is shown graphically in *Figure 2*.

Enrichment analysis showed no correlation of variations in ERK gene expression in the 39 adenocarcinoma patients with stage I and combined stage II + III disease. Likewise,

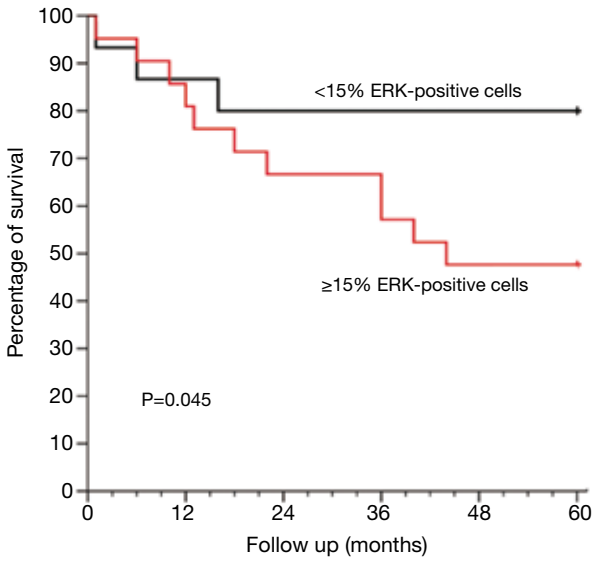

Figure 2 Kaplan-Meier mortality curves show that ERK, extracellular regulatory kinase quantification allows for discrimination between good and poor prognosis. The black line represents cases with <15% ERK-positive cells and the red line indicates cases with ≥15% ERK-positive cells. The gray line represents the cumulative survival for all patients throughout the 5-year evaluation period. ERK, extracellular regulatory kinase.

gender and smoking did not show a positive correlation with variations in ERK gene expression.

Discussion

Cancer is the result of the deregulation of multiple signaling pathways, and the inhibition of a single pathway may not be sufficient to trigger apoptosis or growth inhibition (6,25-27). ERK activation is involved in multiple cellular functions such as motility, proliferation, differentiation, and apoptosis (28,29). ERK activation influences the development and activation of normal cells as well as the abnormal proliferation of tumor cells (30,31). There is little evidence on the specific role of ERK activation in the development of NSCLC (24,32). By studying 111 patients with NSCLC, Vicent *et al.* demonstrated a positive correlation between ERK activation and later stages of the disease (24). Our study only examined patients with early stage adenocarcinoma who underwent surgical treatment: thus, constituting a population different from that described by Vicent *et al.* (24), which included patients with advanced stages and different histological types of lung carcinoma. Moreover, Vicent *et al.* separately analyzed ERK activation in the cytoplasm and nucleus and showed that there were no significant differences between these cell compartments (24). Therefore, we decided to collectively analyze these parameters in our study. However, Harding *et al.* suggested that receptor location, either in the plasma membrane or cytosol, may lead to different responses in the MAPK cascade activation (33). This finding is of great importance in the search for new therapies with ERK, and not MEK, as a target (34). It is believed that signal transduction is stronger in the plasma membrane and weaker in the cytosol (35). Therefore, activation of plasma membrane receptors would trigger a stronger cellular response, whereas ERK activation in the cytoplasm would affect only a subpopulation of cells, leading to an intermediate response (35). For this reason, future therapies would need to address differences in ERK cascade activation on the basis of receptor location. Furthermore, overexpression of this pathway may play an important role in the pathogenesis and progression of breast cancer and other cancers, making their components potential therapeutic targets (36-38).

We performed enrichment analysis using data from five different experiments (18-22), but because they yielded similar results, the dataset GSE29016 was selected because it was the only dataset containing all our study parameters. Our enrichment analysis had some limitations, in particular with regard to the number of patients diagnosed with adenocarcinoma. Only 39 patients were selected, and most of them were in stage I as verified in our dataset. Moreover, this experiment included few nonsmokers, which is expected in this disease group. Finally, our dataset contained more male patients, as opposed to the female predominance in the other datasets.

Our study demonstrated that high ERK levels are inversely correlated with survival. However, this was not revealed by the enrichment analysis, probably because of the sample type assayed (mRNA *vs.* protein) as well as the different patient profiles. In the literature, the presence of high ERK levels has been studied mainly in association with tumor aggressiveness and as potential therapeutic targets, and survival analyses have been restricted to only a few studies (39).

This study has several limitations that should be considered before interpreting the results. Our study included a small number of patients; however, they formed a specific group of individuals who did not show advanced stage disease and underwent surgical treatment. This

also explains the limited number of patients with stage II disease. However, this makes the study population more homogeneous and helps in avoiding bias associated with the inclusion of more patients with an advanced stages disease, which tend to show higher ERK expression.

Conclusions

Taken together, our results suggest that higher ERK positivity in cells from biological samples of patients with lung adenocarcinoma patients is associated with tumor aggressiveness and poorer prognosis. Despite its limitations, this study demonstrates the importance of the role of ERK in lung adenocarcinomas and reinforces the need for additional studies to confirm our findings.

Acknowledgements

Authors' contribution: S.L.M. conceived the study, collected the data, participated in the analysis of the samples and drafted the manuscript. C.B.M, R.T.M, M.C.F, R.M. collected the data, participated in the analysis of the samples and drafted the manuscript. M.B.S. participated in the microarray analysis. F.K, C.F.A. conceived the study, drafted and approved the manuscript final version.

This research was supported by grants from HCPA (Hospital de Clinicas de Porto Alegre Institutional Research Fund) and Universidade Federal do Rio Grande do Sul (UFRGS). We expressed our gratitude to Enago for proofreading this manuscript.

Disclosure: The authors declare no conflict of interest.

References

1. Jemal A, Siegel R, Xu J, et al. Cancer statistics, 2010. CA Cancer J Clin 2010;60:277-300.
2. Travis WD, Brambilla E, Noguchi M, et al. International association for the study of lung cancer/american thoracic society/european respiratory society international multidisciplinary classification of lung adenocarcinoma. J Thorac Oncol 2011;6:244-85.
3. Consonni D, De Matteis S, Lubin JH, et al. Lung cancer and occupation in a population-based case-control study. Am J Epidemiol 2010;171:323-33.
4. Nana-Sinkam SP, Powell CA. Molecular biology of lung cancer: Diagnosis and management of lung cancer, 3rd ed: American College of Chest Physicians evidence-based clinical practice guidelines. Chest 2013;143:e30S-9S.
5. Chanin TD, Merrick DT, Franklin WA, et al. Recent developments in biomarkers for the early detection of lung cancer: perspectives based on publications 2003 to present. Curr Opin Pulm Med 2004;10:242-7.
6. Kreeger PK, Lauffenburger DA. Cancer systems biology: a network modeling perspective. Carcinogenesis 2010;31:2-8.
7. Kolch W. Coordinating ERK/MAPK signalling through scaffolds and inhibitors. Nat Rev Mol Cell Biol 2005;6:827-37.
8. McKay MM, Morrison DK. Integrating signals from RTKs to ERK/MAPK. Oncogene 2007;26:3113-21.
9. Roskoski R Jr. ERK1/2 MAP kinases: structure, function, and regulation. Pharmacol Res 2012;66:105-43.
10. Ohashi K, Maruvka YE, Michor F, et al. Epidermal growth factor receptor tyrosine kinase inhibitor-resistant disease. J Clin Oncol 2013;31:1070-80.
11. Mok T, Yang JJ, Lam KC. Treating patients with EGFR-sensitizing mutations: first line or second line--is there a difference? J Clin Oncol 2013;31:1081-8.
12. Kulesza P, Ramchandran K, Patel JD. Emerging concepts in the pathology and molecular biology of advanced non-small cell lung cancer. Am J Clin Pathol 2011;136:228-38.
13. Avraham R, Yarden Y. Feedback regulation of EGFR signalling: decision making by early and delayed loops. Nat Rev Mol Cell Biol 2011;12:104-17.
14. Balko JM, Jones BR, Coakley VL, et al. MEK and EGFR inhibition demonstrate synergistic activity in EGFR-dependent NSCLC. Cancer Biol Ther 2009;8:522-30.
15. Sánchez PG, Vendrame GS, Madke GR, et al. Lobectomy for treating bronchial carcinoma: analysis of comorbidities and their impact on postoperative morbidity and mortality. J Bras Pneumol 2006;32:495-504.
16. Rami-Porta R, Bolejack V, Goldstraw P. The new tumor, node, and metastasis staging system. Semin Respir Crit Care Med 2011;32:44-51.
17. Pepek JM, Chino JP, Marks LB, et al. How well does the new lung cancer staging system predict for local/regional recurrence after surgery?: A comparison of the TNM 6 and 7 systems. J Thorac Oncol 2011;6:757-61.
18. Staaf J, Jönsson G, Jönsson M, et al. Relation between smoking history and gene expression profiles in lung adenocarcinomas. BMC Med Genomics 2012;5:22.
19. Govindan R, Ding L, Griffith M, et al. Genomic landscape of non-small cell lung cancer in smokers and never-smokers. Cell 2012;150:1121-34.
20. Landi MT, Dracheva T, Rotunno M, et al. Gene expression signature of cigarette smoking and its role in

lung adenocarcinoma development and survival. PloS One 2008;3:e1651.
21. Selamat SA, Chung BS, Girard L, et al. Genome-scale analysis of DNA methylation in lung adenocarcinoma and integration with mRNA expression. Genome Res 2012;22:1197-211.
22. Takeuchi T, Tomida S, Yatabe Y, et al. Expression profile-defined classification of lung adenocarcinoma shows close relationship with underlying major genetic changes and clinicopathologic behaviors. J Clin Oncol 2006;24:1679-88.
23. Mootha VK, Lindgren CM, Eriksson KF, et al. PGC-1alpha-responsive genes involved in oxidative phosphorylation are coordinately downregulated in human diabetes. Nat Genet 2003;34:267-73.
24. Vicent S, López-Picazo JM, Toledo G, et al. ERK1/2 is activated in non-small-cell lung cancer and associated with advanced tumours. Br J Cancer 2004;90:1047-52.
25. Ross JA, Rosen GD. The molecular biology of lung cancer. Curr Opin Pulm Med 2002;8:265-9.
26. Jeanmart M, Lantuejoul S, Fievet F, et al. Value of immunohistochemical markers in preinvasive bronchial lesions in risk assessment of lung cancer. Clin Cancer Res 2003;9:2195-203.
27. Greenberg AK, Lee MS. Biomarkers for lung cancer: clinical uses. Curr Opin Pulm Med 2007;13:249-55.
28. Schlessinger J. Cell signaling by receptor tyrosine kinases. Cell 2000;103:211-25.
29. Cuevas BD, Abell AN, Johnson GL. Role of mitogen-activated protein kinase kinase kinases in signal integration. Oncogene 2007;26:3159-71.
30. Yoon S, Seger R. The extracellular signal-regulated kinase: multiple substrates regulate diverse cellular functions. Growth Factors 2006;24:21-44.
31. Dhanasekaran DN, Johnson GL. MAPKs: function, regulation, role in cancer and therapeutic targeting. Oncogene 2007;26:3097-9.
32. Dhillon AS, Hagan S, Rath O, et al. MAP kinase signalling pathways in cancer. Oncogene 2007;26:3279-90.
33. Harding A, Tian T, Westbury E, et al. Subcellular localization determines MAP kinase signal output. Curr Biol 2005;15:869-73.
34. Roberts PJ, Der CJ. Targeting the Raf-MEK-ERK mitogen-activated protein kinase cascade for the treatment of cancer. Oncogene 2007;26:3291-310.
35. Raman M, Chen W, Cobb MH. Differential regulation and properties of MAPKs. Oncogene 2007;26:3100-12.
36. Sivaraman VS, Wang H, Nuovo GJ, et al. Hyperexpression of mitogen-activated protein kinase in human breast cancer. J Clin Invest 1997;99:1478-83
37. Mandell JW, Hussaini IM, Zecevic M, et al. In situ visualization of intratumor growth factor signaling: immunohistochemical localization of activated ERK/MAP kinase in glial neoplasms. Am J Pathol 1998;153:1411-23.
38. Adeyinka A, Nui Y, Cherlet T, et al. Activated mitogen-activated protein kinase expression during human breast tumorigenesis and breast cancer progression. Clin Cancer Res 2002;8:1747-53.
39. Friday BB, Adjei AA. Advances in targeting the Ras/Raf/MEK/Erk mitogen-activated protein kinase cascade with MEK inhibitors for cancer therapy. Clin Cancer Res 2008;14:342-6.

Cite this article as: de Leon Martini S, Müller CB, Meurer RT, Fernandes MC, Mariano R, Barbachan e Silva M, Klamt F, Andrade CF. The potential role of extracellular regulatory kinase in the survival of patients with early stage adenocarcinoma. J Thorac Dis 2014;6(7):930-936. doi: 10.3978/j.issn.2072-1439.2014.07.10

Original Article

Robotic lung segmentectomy for malignant and benign lesions

Alper Toker, Kemal Ayalp, Elena Uyumaz, Erkan Kaba, Özkan Demirhan, Suat Erus

Department of Thoracic Surgery, Istanbul Bilim University and Group Florence Nightingale, Istanbul, Turkey
Correspondence to: Suat Erus, MD. Naima sokak No: 4/7 Yeşilköy, 34149 Istanbul, Turkey. Email: suaterus@gmail.com.

Objective: Surgical use of robots has evolved over the last 10 years. However, the academic experience with robotic lung segmentectomy remains limited. We aimed to analyze our lung segmentectomy experience with robot-assisted thoracoscopic surgery.

Methods: Prospectively recorded clinical data of 21 patients who underwent robotic lung anatomic segmentectomy with robot-assisted thoracoscopic surgery were retrospectively reviewed. All cases were done using the da Vinci System. A three incision portal technique with a 3 cm utility incision in the posterior 10th to 11th intercostal space was performed. Individual dissection, ligation and division of the hilar structures were performed. Systematic mediastinal lymph node dissection or sampling was performed in 15 patients either with primary or secondary metastatic cancers.

Results: Fifteen patients (75%) were operated on for malignant lung diseases. Conversion to open surgery was not necessary. Postoperative complications occurred in four patients. Mean console robotic operating time was 84±26 (range, 40-150) minutes. Mean duration of chest tube drainage and mean postoperative hospital stay were 3±2.1 (range, 1-10) and 4±1.4 (range, 2-7) days respectively. The mean number of mediastinal stations and number of dissected lymph nodes were 4.2 and 14.3 (range, 2-21) from mediastinal and 8.1 (range, 2-19) nodes from hilar and interlobar stations respectively.

Conclusions: Robot-assisted thoracoscopic segmentectomy for malignant and benign lesions appears to be practical, safe, and associated with few complications and short postoperative hospitalization. Lymph node removal also appears oncologically acceptable for early lung cancer patients. Benefits in terms of postoperative pain, respiratory function, and quality of life needs a comparative, prospective series particularly with video-assisted thoracoscopic surgery.

Keywords: Lung resection; robotic surgery; segmentectomy; lung cancer

Submitted Feb 26, 2014. Accepted for publication Jun 06, 2014.
doi: 10.3978/j.issn.2072-1439.2014.06.40
View this article at: http://dx.doi.org/10.3978/j.issn.2072-1439.2014.06.40

Introduction

Anatomic segmentectomy of the lung is the removal of a segment of the lobe. For many decades pulmonary segmentectomy has been used for the treatment of bronchiectasis and tuberculosis via thoracotomy. Recently, with the developments in video instrumentation and refinements in surgical techniques, segmentectomy has been a popular approach with video-assisted thoracic surgery (VATS). It has been preferred for tumors smaller than 2 cm and negative lymph nodes (1,2) and for larger tumors in patients with poor pulmonary function who could not tolerate lobectomy, especially those who do not have visceral pleural invasion (2,3). Although VATS has been used for segmentectomy for the past 5 years, robotic anatomic lung segmentectomy has been reported to be feasible only in two articles in the pubmed search (4,5).

As an academic thoracic surgery center performing minimally invasive anatomical lung resections with VATS for 8 years, we have recently developed a robotic surgery program with the da Vinci Robotic System (Intuitive Surgical, Inc, Mountain View, California, USA) which started on October 2011. In this study we aimed to analyze the segmentectomy operations performed for various etiologies.

Figure 1 (A) The CT shows an 84-year-old male with squamous cell carcinoma who previously had colon carcinoma; (B) the CT shows a 37-year-old male admitted with hemoptysis, after bronchoscopy revealed no pathology. He underwent a left lower lobe common basal segmentectomy with the diagnosis of echinococcus alveolaris; (C) the CT shows a 67-year-old male with a history of undiagnosed cerebral mass of 1 cm. He underwent mediastinoscopy and resection of superior segment of right upper lobe. Pathology revealed adenocarcinoma.

Patients and methods

From the prospectively recorded database, anatomical segmentectomy patients' data was retrieved. The data was analyzed for age, gender, etiology, pulmonary function tests, complications, mortality, duration of chest tube and duration of postoperative hospital stay. The number of mediastinal lymph node stations dissected and the number of dissected lymph nodes in patients with either primary or secondary lung cancer were also analyzed. For metastasectomies only single lesions close to the segmentary bronchus and primary lung cancer smaller than 2 cm were candidates for robotic segmentectomy operations (*Figure 1*). Patients who had primary lung tumors larger than 2 cm but smaller than 4.5 cm (2 patients) with compromised pulmonary functions were also underwent robotic common basal segmentectomy operations. According to our protocol; all patients who had an indeterminate nodule, or proven lung cancer or a possible metastatic lung cancer, had a PET-CT. Mediastinoscopy was reserved only for the patient who had a possible brain metastases.

Robotic operations for indeterminate nodules were performed after localization of the nodule either with operative view (retraction of visceral pleura), after palpation with finger prior to the docking without access thoracotomy, or from 3 dimensional (3D) images of chest tomography.

All operations were performed by a single console surgeon (AT). All patients had anatomical segment resections as described below. Chest tubes were removed during the hospital stay if the length of stay was shorter than 5 days. If the drainage lasted longer and patients did not have any other problems (one patient), then the patients were discharged with chest tubes attached to the Heimlich valve.

Surgical technique

The patient was positioned on lateral decubitus position. The table was tilted either anteriorly or posteriorly depending on the type of segmentectomy operation to be performed. For superior segments of both lower lobes and posterior segment of the right upper lobe anterior tilt was preferred. For the resection of other segments a posterior tilt was preferred. Three ports were opened while trying to keep 10 cm between each port and 10 to 15 cm from the target which was hilum of the lobe containing the segment to be resected. The camera was placed in the middle port. The robot was docked from the posterior of the patient with 30 to 45 degrees between the vertebral column of the patient and transverse axis of the cart (*Figure 2*).

With the robotic camera in up position, ports and instruments were placed and pleural symphyses were divided. Service port was performed at 10^{th}-11^{th} intercostal space at the posterior part of the thoracic wall. The rest of the operation was done with the camera in down position. Maryland or curved bipolar forceps for right arm and prograsper for left arm were used as needed. Segmentectomies were performed by dissecting the fissure and removing the nodes around the segmentary artery and bronchus. Arteries and veins were clipped with Hem-o-Lok (Teleflex Medical, Research Triangle Park, NC) or stapled with a vascular stapler. Bronchus was always stapled (*Figures 3-5*). Imaginary intersegmental plane was stapled after ventilating

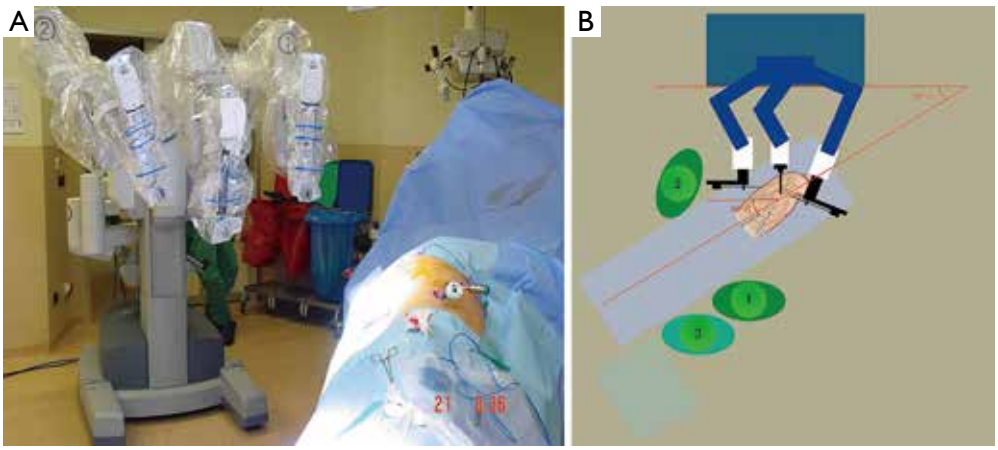

Figure 2 Docking of da Vinci. Arm numbers should be seen by the surgeon 1 at the table (arrows). The transverse axis of the da Vinci approaches from posterior of the patient with 30 to 45 degrees to vertebral column of the patient. 1, surgeon responsible from docking (may shift to console); 2, assistant surgeon is responsible for service, retraction, clipping and stapling; 3, nurse position.

Figure 3 Resection for a lingual sparing left upper lobectomy needs division of the superior segmentary vein, and proximal arteries to the left upper lobe and apicoposterior segment of the upper lobe bronchus.

Figure 4 Robotic right lower lobe superior segmentectomy (6).

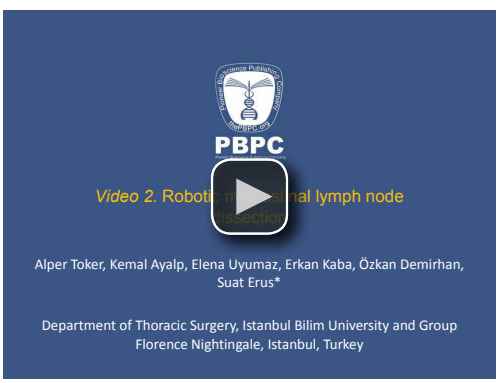

Figure 5 Robotic mediastinal lymph node dissection (7).

Table 1 Data of patients who underwent pulmonary segmentectomy operation

Items	RATS (n=21) [range]
Age	59±16 [28-84]
Gender	
Male	12 (57.1%)
Female	9 (42.8%)
Side	
Right	10 (47.6%)
Left	11 (52.3%)
Location	
Upper lobe	8
Apicoposterior right	4
Lingula sparing lobectomy	2
Lower lobe	13
Superior segmentectomy	5
Common basal segmentectomy	8
Mean duration of Console time (minutes)	84±26 [40-150]
Mean FEV_1 (mL)	2,278±662 [1,274-4,870]
Mean duration of drainage (days)	3±2.1 [1-10]
Mean duration of postoperative stay (days)	4±1.4 [2-7]
Morbidity rate	4 (19%)
Mortality rate	0
Pathology	
Malignant	15 (71.4%)
Benign	6 (28.5%)
Mean number of lymph nodes dissected from mediastinum (stations 2-9) (nodes)	14.3 [2-21]
Mean number of lymph nodes dissected from N1 stations (10-11-12) (nodes)	8.1 [2-19]
Mean number of mediastinal stations dissected	4.2 [2-6]
Pain scale	
Visual analog scale on postoperative day 2 and day 15	3.4-1.4
Histology of primary lung cancer	
Adenocarcinoma with lepidic pattern	5
Adenocarcinoma	3
Squamous cell carcinoma	2
Large cell neuroendocrine tumor	1
TNM staging of primary lung cancer patients	
T1aN0M0	6
T1bN0M0	2
T1aN1M0	1
T1bN1M0	1
T2aN0M1	1

and deflating the remnant lung. In none of the patients, glues or sealants were used. Chest was closed by placing a single 28 F chest tube from the camera port.

Pain management

Routine pain management was with intercostal blocks to two intercostal spaces upper and two intercostal spaces lower around the ports (not more than 20 mL Marcaine) (Astra Zeneca, Istanbul) and 1 gram perfalgan (Bristol-Myers Squibb, New York City) intravenous infusion every 6 hours, and voltaren SR 75 mg (Novartis, Basel) are given through intramuscular route twice a day until chest tube is removed. After the removal of the chest tube or discharge of the patient oral medication with paracetamol and non-steroid anti-inflammatory drugs were given. Visual Analog Scale (VAS) was recorded by the anesthesiologists at 48 hours after the operation and by surgical team on postoperative day 15 as a part of data collection for possible evaluation of our pain management approach.

Results

The mean age was 59 (range, 28-84) years. Twenty-one segmentectomies, 10 from the right lung and 11 from the left lung were performed. Eight patients had a segmentectomy from the upper lobes and 13 patients from the lower lobes. Common basal segmentectomy (eight patients) and superior segmentectomy of the lower lobes (five patients) were the most commonly employed segmentectomies. Mean duration of console time was 84±26 (range, 40-150) minutes. Mean force expiratory volume (FEV_1) in the first second was 2,278±662 (range, 1,274-4,870) mL. The mean duration of chest tube drainage and postoperative hospital stay were 3±2.1 (range, 1-10) and 4±1.4 (range, 2-7) days respectively. Conversion to open surgery was not necessary. Postoperative complications occurred in four patients (19%). The prolonged air leak (>5 days) was the cause of morbidity in all patients. None of the patients experienced a major cardiopulmonary complication. The mean number of mediastinal stations and number of dissected lymph nodes were 4.2 and 14.3 (range, 2-21) lymph nodes from mediastinal stations and 8.1 (range, 2-19) lymph nodes from hilar and interlobar stations, respectively. VAS was 3.4 and 1.4 on postoperative day 2 and day 15 (*Table 1*). The mean diameters of the malignant lesions were 1.9 (range, 1-4.3) cm. There were eight (72.7%) adenocarcinoma histology

including five patients with lepidic pattern as the most common primary lung cancer. Eight patients (72.7%) out of 11 primary lung cancer were recorded to be in stage 1A. Six patients were operated on for benign diseases (bronchiectasis one patient, granuloma four patients and echinococcus alveolaris one patient). Four patients had segmentectomy operation for single pulmonary metastases (three patients for colon carcinoma and one patient for uterus leiomyoma).

Discussion

VATS segmentectomy has been proved to be a safe procedure with fewer complications and a reduced hospital stay when compared with an open segmentectomy (8). The peri-operative outcome, including operative time, blood loss, duration of chest tube drainage and length of hospital stay, have been shown to be similar in another comparative study (9). This study also demonstrated that thoracoscopic segmentectomy is feasible with regard to peri-operative and oncological outcomes for Stage IA non-small cell lung cancer (NSCLC), especially T1a and carefully selected T1b descriptor (9). Thoracoscopic segmentectomy has been compared to thoracoscopic lobectomy when analyzing oncologic results in small (≤2 cm) peripheral stage IA NSCLC (10). Local recurrence rates with thoracoscopic segmentectomy (5.1%) have been reported to be similar to the thoracoscopic lobectomy (4.9%). No significant difference has been observed in 5-year overall or disease-free survival (10). Recent literature also demonstrated support for less invasive video thoracoscopic surgical techniques in pulmonary segmentectomy operations like uniportal and total thoracoscopic segmentectomies (11,12).

It is clear that, as lung screening programs increase around the world, the need for minimally invasive segmentectomies is also increasing. Certainly, robotic lung segmentectomies might be another minimally invasive lung segment resection technical option.

Growing knowledge of robotic lobectomies for lung cancer would provide additional experience for performing segmentectomy operations for lung cancer. Yet, there are only two articles published to assess the feasibility of robotic segmentectomy operation (4,5). In one of them Dylewski *et al.* (5) reported 35 segmentectomy patients and in the other Pardolesi *et al.* (4) reported 17 segmentectomy patients. Mean duration of surgery was reported to be 189 minutes with no major intraoperative complications and conversion to open procedure was reported as unnecessary (4). In this study postoperative morbidity rate was 17.6% with a median postoperative stay of 5 (range, 2-14) days, and postoperative mortality was 0% (4). The final pathology was reported to be NSCLC in eight patient, typical carcinoids in two, and lung metastases in seven. Because the other study (5) described a robotic series of almost 200 patients with mainly lobectomies, we do not have a detailed data regarding to segmentectomy operations.

Our indications and perioperative and postoperative outcomes are quite similar to those of Pardolesi and colleagues (4). In our experience, 15 out of 21 patients (75%) were operated on for malignant lung diseases. Conversion to open surgery was not necessary. Postoperative complications occurred in four patients (19%). Mean console robotic operating time was 84±26 (range, 40-150) minutes which was quite similar to that of Dylewski's experience (5). The duration of our console time was shorter than the reported experiences even with VATS. Mean duration of chest tube drainage and postoperative hospital stay were 3±2.1 (range, 1-10) and 4±1.4 (range, 2-7) days respectively, which was also quite similar to the above mentioned study (4). The mean number of mediastinal stations and number of dissected lymph nodes were 4.2 and 14.3 (range, 2-21) lymph nodes. From hilar and interlobar stations, a mean of 8.1 (range, 2-19) lymph nodes were dissected in patients primary or secondary lung cancer. We need to stress that, five of our patients were not good candidates for lung resection due to compromised pulmonary, renal and cardiac problems. But we did not experience any adverse event in those patients. Our surgical technique demonstrated similarities with those of Pardolesi's (4). However, our access port, similar in size to their experience (4), was located at posterior thoracic cavity at 10^{th}-11^{th} intercostal space. This port may not only have allowed the greater movement of the equipment within the cavity but also may have avoided the disturbance of the mammary gland in female patients. In our experience, we used only one Maryland forceps or curved bipolar forceps and one Prograsper forceps for each patient. Expenditures for these including the drapes cost a total of 600 USD, excluding the maintenance and initial costs of the robot.

The major difficulty in robotic segmentectomy operation is the resection without palpation. This could be overcome by palpating and tattooing the lesion prior to the implementation of the robotic arms. If this was not possible, 3D images could be used to identify the lesion, the vessels and the bronchus. Segmentectomy operation with robotic surgery requires a good knowledge of the anatomy of pulmonary vessels and bronchi in each patient (13).

The foreknowledge of the anatomy of each patient would contribute to the safety and accuracy of the operation (13). It has been reported that presurgical planning based on patient's actual 3D pulmonary model was useful for patients with stage IA NSCLC ≤2 cm in diameter and for selecting an appropriate VATS lung resection for an individual (14). Apparently, this may be a required preoperative technique in robotic segmentectomy as well. Although we only had three patients with this preoperative investigation, we discussed with experienced radiologists before each operation to delineate the borders of resection from axial, coronal and sagittal tomographies. Especially for metastasectomies, we believe that CT image evaluation on monitor with a qualified radiologist is essential to ensure that the lesion is solitary.

Robotic segmentectomy may provide better dissection capabilities around smaller vessels and the lymph nodes around lobar and segmentary bronchi. However, developing these techniques may require preparation and patience to overcome the difficulties of a correct docking, developing dissection techniques.

Yet, the provided data and results about performing robotic segmentectomies may not fully satisfy the thoracic surgical community. However, we have demonstrated that the robotic anatomic lung segmentectomy is a feasible and safe procedure with an acceptable operating time, adequate lymph node dissection, less pain and few complications.

Acknowledgements

Authors' Contribution: A.T. designed the overall study with contributions from K.A. K.A. designed and carried out experiments, collected data. E.U. designed and carried out experiments and collected and analyzed data with E.K. and Ö.D. S.E. carried out experiments, and analyzed data with A.T.
Disclosure: The authors declare no conflict of interest.

References

1. Keenan RJ, Landreneau RJ, Maley RH Jr, et al. Segmental resection spares pulmonary function in patients with stage I lung cancer. Ann Thorac Surg 2004;78:228-33; discussion 228-33.
2. Koike T, Yamato Y, Yoshiya K, et al. Intentional limited pulmonary resection for peripheral T1 N0 M0 small-sized lung cancer. J Thorac Cardiovasc Surg 2003;125:924-8.
3. Wolf AS, Richards WG, Jaklitsch MT, et al. Lobectomy versus sublobar resection for small (2 cm or less) non-small cell lung cancers. Ann Thorac Surg 2011;92:1819-23; discussion 1824-5.
4. Pardolesi A, Park B, Petrella F, et al. Robotic anatomic segmentectomy of the lung: technical aspects and initial results. Ann Thorac Surg 2012;94:929-34.
5. Dylewski MR, Ohaeto AC, Pereira JF. Pulmonary resection using a total endoscopic robotic video-assisted approach. Semin Thorac Cardiovasc Surg 2011;23:36-42.
6. Toker A, Ayalp K, Uyumaz E, et al. Robotic right lower lobe superior segmentectomy. Asvide 2014;1:245. Available online: http://www.asvide.com/articles/257
7. Toker A, Ayalp K, Uyumaz E, et al. Robotic mediastinal lymph node dissection. Asvide 2014;1:246. Available online: http://www.asvide.com/articles/258
8. Leshnower BG, Miller DL, Fernandez FG, et al. Video-assisted thoracoscopic surgery segmentectomy: a safe and effective procedure. Ann Thorac Surg 2010;89:1571-6.
9. Yamashita S, Tokuishi K, Anami K, et al. Thoracoscopic segmentectomy for T1 classification of non-small cell lung cancer: a single center experience. Eur J Cardiothorac Surg 2012;42:83-8.
10. Zhong C, Fang W, Mao T, et al. Comparison of thoracoscopic segmentectomy and thoracoscopic lobectomy for small-sized stage IA lung cancer. Ann Thorac Surg 2012;94:362-7.
11. Gonzalez-Rivas D, Fieira E, Mendez L, et al. Single-port video-assisted thoracoscopic anatomic segmentectomy and right upper lobectomy. Eur J Cardiothorac Surg 2012;42:e169-71.
12. Ramos R, Girard P, Masuet C, et al. Mediastinal lymph node dissection in early-stage non-small cell lung cancer: totally thoracoscopic vs thoracotomy. Eur J Cardiothorac Surg 2012;41:1342-8; discussion 1348.
13. Ikeda N, Yoshimura A, Hagiwara M, et al. Three dimensional computed tomography lung modeling is useful in simulation and navigation of lung cancer surgery. Ann Thorac Cardiovasc Surg 2013;19:1-5.
14. Kanzaki M, Kikkawa T, Shimizu T, et al. Presurgical planning using a three-dimensional pulmonary model of the actual anatomy of patient with primary lung cancer. Thorac Cardiovasc Surg 2013;61:144-50.

Cite this article as: Toker A, Ayalp K, Uyumaz E, Kaba E, Demirhan Ö, Erus S. Robotic lung segmentectomy for malignant and benign lesions. J Thorac Dis 2014;6(7):937-942. doi: 10.3978/j.issn.2072-1439.2014.06.40

Original Article

The SNPs (-1654C/T, -1641A/G and -1476A/T) of protein C promoter are associated with susceptibility to pulmonary thromboembolism in a Chinese population

Changtai Zhu[1,2*], Ting Jiang[3*], Yafang Miao[2*], Sugang Gong[2], Kebin Cheng[2], Jian Guo[2], Xiaoyue Tan[2], Jun Yue[4], Jinming Liu[2]

[1]Department of Transfusion Medicine, Shanghai Jiao Tong University Affiliated Sixth People's Hospital, Shanghai 200233, China; [2]Department of Respiratory Medicine, Shanghai Pulmonary Hospital, Tongji University School of Medicine, Shanghai 200433, China; [3]Department of Orthopedics, the Third Affiliated Hospital, Anhui Medical University, Hefei 230031, China; [4]Shanghai Key Laboratory of Tuberculosis, Shanghai Pulmonary Hospital, Medical School, Tongji University, Shanghai 200433, China

*These authors contributed equally to this work.

Correspondence to: Jinming Liu, PhD. Department of Respiratory Medicine, Shanghai Pulmonary Hospital, Tongji University School of Medicine, 507 Zheng Min Road, Shanghai 200433, China. Email: jinmingliu2013@163.com.

Background: Pulmonary thromboembolism (PTE) is a common and potentially lethal disease. It is significant to investigate the gene mutations of protein C for clarifying the etiology of PTE. In this present study, we investigated the promoter region polymorphism sites including -1654C/T, -1641A/G and -1476A/T of the protein C gene in a Chinese population.

Methods: A total of 110 cases of PTE and one hundred and ninety healthy controls in a Chinese population were genotyped for three polymorphisms (-1654C/T, -1641A/G and -1476A/T) of the protein C promoter. The statistical analysis was performed by Stata 11.0.

Results: The single nucleotide polymorphisms (SNPs) (-1654C/T, -1641A/G and -1476A/T) in protein C gene were associated with the susceptibility to PTE in Chinese population. According to the binary logistic regression analysis, the independently significant risk factors for PTE were the complications of deep vein thrombosis (DVT) or cancer, history of operation or injury, and the homozygous carriers of the TT genotype (protein C -1654C/T).

Conclusions: The SNPs (-1654C/T, -1641A/G and -1476A/T) of protein C promoter gene are associated with the susceptibility to PTE in a Chinese population. Especially, the homozygous carriers of genotype TT (-1654C/T) increase the risk of PTE in a Chinese population. Confirmation of our preliminary observations in a larger scale study is needed.

Keywords: Single nucleotide polymorphisms (SNPs); protein C; pulmonary thromboembolism (PTE); a Chinese population

Submitted Mar 01, 2014. Accepted for publication May 31, 2014.
doi: 10.3978/j.issn.2072-1439.2014.06.30
View this article at: http://dx.doi.org/10.3978/j.issn.2072-1439.2014.06.30

Introduction

Pulmonary thromboembolism (PTE) is a common and potentially lethal disease. There are the abnormal alterations in blood flow and the properties of the blood and the vessel wall associated with PTE. In recent years, the studies have revealed that thromboembolism was associated with single nucleotide polymorphism (SNP) and some gene mutations were attributable to PTE (1-12). Several distinct mutations in the 5'-promoter region of protein C gene have been identified (12). Theoretically, the gene mutations in the promoter may cause the express down-regulation of protein C and break the balance of the anticoagulation system and

increase the risk of PTE. Therefore, it is significant to investigate the gene mutations of protein C for clarifying the etiology of PTE. In this present study, we investigated the promoter region polymorphism sites including -1654C/T, -1641A/G and -1476A/T of the protein C gene to explore their relationship with PTE.

Materials and methods

Participants

PTE group included one hundred ten patients continuously recruited from Department of Respiratory Medicine Shanghai Pulmonary Hospital from June 2003 to June 2010. All the patients were definitely diagnosed as PTE by radionuclide pulmonary perfusion imaging and CTPA or pulmonary angiography. Pulmonary angiography was assessed according to the Guidelines on Diagnosis and Management of PTE by Respiratory Society of Chinese Medical Association [2001]. The diagnosis of deep vein thrombosis (DVT) of lower limb vessels were performed by radionuclide venography and (or) ultrasonic examination. In this study, 190 healthy subjects from a health care center were recruited as the controls. None of the controls had a history of arterial disease (stroke, myocardial infarction, angina, or peripheral vascular disease), venous thrombosis (PTE or DVT), or functional lesion of the liver and kidney. There was no difference in age and sex between two groups ($P<0.05$).

Ethics statement

All subjects were treated in accordance with the Declaration of Helsinki on the participation of human subjects in medical research. Written informed consent was obtained from each of participants and the study was approved by the Ethics Committee of Shanghai Pulmonary Hospital.

Blood sampling

Venous blood samples from the patients and the controls were collected in 0.129 M trisodium citrate (1:9) tubes. After centrifugation, plasma was aliquoted and stored at –20 ℃. A double-blind method was conducted to avoid the bias of tests.

PCR amplification and production purification

DNA was extracted by a commercial DNA extraction kit (Chaoshi Biotechnology, shanghai, China). Primer sequences were designed by the Oligo 6 software based on the DNA sequences of the protein C gene in GenBank (http://www.ncbi.nlm.nih.gov). The pair of primer sequences was listed as follows: 5'-ATTGGGATGGCATGTCATTG-3' and 5'-CCCTGGCTGGAGGATTCAG-3'. The expected PCR amplification included the three SNP sites (-1654C/T, -1641A/G and -1476A/T).

PCR amplifications were performed in a 50 μL reaction mixture containing 5 μL 10× PCR amplification buffer (100 mm of Tris-HCl, pH 8.3, 500 mm of KCl, 15 mm of $MgCl_2$), 4 μL dNTP (2.5 mm of each), 20 pM of each primers, 2.5 unit of Taq polymerase and 200 ng genomic DNA. The PCR protocol is as following: step 1, 95 ℃ for 5 m; step 2, (95 ℃ for 45 s, 58 ℃ for 45 s, and 72 ℃ for 60 s) 35 cycles; step 3, 72 ℃ for 7 m. The PCR products were verified by electrophoresis on a 1% agarose gel with ethidium bromide staining. Finally, PCR reaction products were purified by using QIA PCR purification kit (Qiagen, Hilden, Germay).

DNA sequencing

These samples were further analyzed by direct DNA sequencing to identify the polymorphisms. The sequencing reactions were done on double-strand DNA with the above primers used in the PCR. The sequencing reactions were performed by the ABI PRISM 3730 DNA analyzer (Applied Biosystems, Foster City, USA).

Statistical analysis

Categorical variables were presented using frequency counts. Chi-square test is given as 2-sided Pearson's Chi-Square and Fisher's exact test was used to distinguish the differences in the genotype/allele/haplotype frequencies of the SNPs. Hardy–Weinberg equilibrium was used to verify allele frequency and genotype distribution. Binary logistic regression analysis was performed to evaluate the odds ratios of PTE. The data analysis used Stata 11.0 software (Statacorp LP, Texas, USA).

Results

Characteristics of participants

General characteristics of the study are shown in *Table 1*. There was significantly difference in the indices involving

Table 1 Clinical characteristic in PTE group and in controls

Presence of potential risk factors	PTE group (n=110) (%)	Control group (n=190) (%)
Complications of DVT or cancer	50 (45.5)	0^
History of operation or injury	8 (7.3)	3 (1.6)*
Cigarette smoking	56 (50.9)	78 (41.1)
Alcohol drinking	40 (36.4)	67 (35.3)
Family history of cardiovascular diseases	5 (4.5)	6 (3.2)
Oral contraceptive	4 (3.6)	7 (3.9)
Family history of venous thromboembolism	0	0

PTE, pulmonary thromboembolism; DVT, deep venous thrombosis; ^, P<0.001; *, P<0.05.

history of operation or injury, and the complications from DVT or cancer between the PTE group and the controls (P<0.05). No significant difference was found in these indices including family history of venous thromboembolism and cardiovascular diseases, personal history of oral contraceptive, cigarette smoking and alcohol drinking between the two groups (P>0.05).

Genotype and allele frequencies of three SNPs of the protein C gene

The SNP site (-1654C/T) was divided into CC, CT and TT genotype, while there were AA, AG, and GG genotype in -1641A/G and AA, AT, TT genotype in -1476A/T. Frequencies of genotype/allele between the two groups are described in *Tables 2,3*. Both the genotype frequencies of the three SNP sites and the allele frequencies of the SNP site (-1654C/T) were significantly different between two groups (P<0.05).

Distribution of the poly-TAA/CAA/CGT genotypes and haplotype frequencies of three SNPs of the protein C gene

There are six kinds of genotypes (TAA-TAA, TAA-CAA, TAA-CGT, CGT-CGT, CAA-CGT, CAA-CAA) and three kinds of haplotypes (TAA, CGT, CAA), shown in *Table 4*. The frequency of haplotype TAA, especially the homozygous carriers with haplotype TAA (TAA-TAA) in the PTE group was significantly higher (P<0.05). On the contrary, the frequency of haplotype CAA in the PTE group was significantly lower than that in the controls (P<0.05).

Table 2 Genotype frequency of three SNPs of the protein C gene in PTE group and in controls

SNPs	Genotype	PTE group n (%)	Controls n (%)	P
-1654C/T	CC	16 (14.6)	36 (19.0)	0.021
	CT	48 (43.6)	104 (54.7)	
	TT	46 (41.8)	50 (26.3)	
-1641A/G	AA	81 (73.7)	128 (67.4)	0.034
	AG	25 (22.7)	61 (32.1)	
	GG	4 (3.6)	1 (0.5)	
-1476A/T	AA	81 (73.7)	128 (67.4)	0.034
	AT	25 (22.7)	61 (32.1)	
	TT	4 (3.6)	1 (0.5)	
Total numbers		110	190	

SNPs, single nucleotide polymorphisms; PTE, pulmonary thromboembolism. TT, homozygous carriers of the C-1654T mutation of the protein C gene; CT, heterozygous carriers of the C-1654T mutation of the protein C gene; CC, homozygous wild type. GG, homozygous carriers of the A-1641G mutation of the protein C gene; AG, heterozygous carriers of the A-1641G mutation of the protein C gene; AA, homozygous wild type. TT, homozygous carriers of the A-1476T mutation of the protein C gene; AT, heterozygous carriers of the A-1476T mutation of the protein C gene; AA, homozygous wild type.

There was no difference in haplotype CGT between the two groups (P>0.05).

Risk factors for PTE by logistic regression

Binary logistic regression analysis showed that the independently significant risk factors for PTE were the complications of DVT or cancer, history of operation or injury, and the homozygous carriers of the TT genotype in -1654C/T (P<0.05). However, the factors including oral contraceptive, cigarette smoking, and alcohol drinking weren't the significant risk factors for PTE (P>0.05).

Discussion

PTE is a common clinical problem which is associated with substantial morbidity and mortality (13). The incidence of PTE in the United States is estimated to be one case per 1,000 persons per year (13). The prospective investigation of pulmonary thromboembolism diagnosis (PIOPED) study

Table 3 Allele frequency of three SNPs of the protein C gene in PTE and in controls

SNPs	Allele	PTE group n (%)	Controls n (%)	Odds ratio (95% CI)	P
-1654C/T	C	80 (36.4)	176 (46.3)	0.662 (0.471-0.931)	0.018
	T	140 (63.6)	204 (53.7)	1.510 (1.074-2.123)	
-1641A/G	A	187 (85.0)	317 (83.4)	1.126 (0.712-1.781)	0.611
	G	33 (15.0)	63 (16.6)	0.888 (0.562-1.404)	
-1476A/T	A	187 (85.0)	317 (83.4)	1.126 (0.712-1.781)	0.611
	T	33 (15.0)	63 (16.6)	0.888 (0.562-1.404)	

SNPs, single nucleotide polymorphisms; PTE, pulmonary thromboembolism; CI, confidence interval.

Table 4 Distribution of the poly-TAA/CAA/CGT genotypes and haplotype frequencies in cases with PTE and controls

	All patients n (%)	Controls n (%)	Odds ratio (95% CI)	P
Protein C genotype distribution				
TAA-TAA	46 (41.8)	50 (26.3)*	2.012 (1.223-3.311)	0.006
TAA-CAA	30 (27.3)	58 (30.5)	0.853 (0.507-1.437)	0.551
TAA-CGT	18 (16.4)	46 (24.2)	0.612 (0.335-1.121)	0.110
CGT-CGT	4 (3.6)	1 (0.5)	7.132 (0.787-64.636)	0.062
CAA-CGT	7 (6.4)	15 (8.0)	0.793 (0.313-2.009)	0.624
CAA-CAA	5 (4.5)	20 (10.5)	0.405 (0.147-1.111)	0.071
Protein C haplotype				
TAA	140 (63.6)	204 (53.7)*	1.510 (1.074-2.123)	0.018
CGT	33 (15.0)	63 (16.6)	0.888 (0.562-1.404)	0.611
CAA	47 (21.4)	113 (29.7)*	0.642 (0.435-0.948)	0.025
Total numbers	110	190		

PTE, pulmonary thromboembolism; TAA/CAA/CGT, haplotype of three SNPs C-1654T/A-1641G/A-1476T of the protein C gene; SNPs, single nucleotide polymorphisms; CI, confidence interval; *, P<0.05.

showed that the 1-year mortality rate was 24% (14).

The risk factors of PTE are complex. However, accumulated evidences have shown that protein C plays an important role in PTE (9,11-25). Protein C is an important regulator of thrombin activity and the deficiency of protein C can result in the down-regulation of the coagulation system by inactivating factor Va and factor VIIIa. There are several transcriptional regulatory regions in the 5'-flanking sequence of the protein C gene, which regulates the expression of protein C. Some distinct mutations situated at the 5'-promoter region of human protein C gene have been identified (12). The polymorphic sites (-1654C/T, -1641A/G and -1476A/T) of the protein C gene have been shown to correlate with the incidence of DVT in Western countries (9,11).

In this study, we investigated the three SNPs in the protein C gene in PTE in a Chinese population. We found that both the genotype frequencies of three SNP sites (-1654C/T, -1641A/G and -1476A/T) and the C and T allele frequencies of -1654C/T were significantly different between PTE group and control group. The findings revealed that TT genotype of -1654C/T, GG genotype of -1641A/G and TT genotype of -1476A/T are significantly associated with the susceptibility to PTE in a Chinese population. The further sub-analysis showed that only TT genotype of -1654C/T was a significant risk factor for PTE (OR 2.245, 95% CI, 1.252 to 4.027), while neither GG genotype of -1641A/G nor TT genotype of -1476A/T was.

In this present study, we found that there were six kinds of genotype distribution (TAA-TAA, TAA-CAA, TAA-CGT, CGT-CGT, CAA-CGT, CAA-CAA) and three kinds of haplotype (TAA, CGT, CAA) in the included subjects. The frequency of TAA haplotype, particularly the homozygous carriers of TAA haplotype (TAA-TAA), was higher, while the frequency of CAA haplotype was lower in

PTE. We found that allele T of -1654C/T is a risk factor to PTE and that allele C of -1654C/T is a protective factor. Surprisingly, our finding is contrary to that of the study in Western country (11). However, the previous studies have demonstrated that the incidence and mortality rate of PTE appears to be significantly deferent in blacks than in whites (13,26,27). It suggested that ethnic background could play an important role in the genetics risk factors involving the development of PTE. The gene polymorphisms of factor V Leiden and coagulation factor II were considered as two main hereditary factors associated with venous thrombosis in Europe and America (28,29). But, their mutations were very rare in Asian populations (30). It showed that the molecular mechanism of PTE may be different in different populations. We postulated that the difference of the gene regulation and expression varies in different populations. However, we couldn't predict the exact mechanism of different effect of each allele on different populations due to its complexity based on currently available evidence.

According to the results by logistic regression analysis, "complications of DVT or cancer" and "history of operation or injury" were the major risk factors for the development of PTE in a Chinese population. While the factors including oral contraceptive, cigarette smoking, and alcohol drinking weren't the significant risks for PTE. However, TT genotype of -1654C/T were shown be another independent risk factor for PTE, especially the homozygous carriers of genotype TT of -1654C/T significantly increase the risk of PTE. It must be pointed out that the small number of subjects limited the reliability of the findings. Therefore, a large scale study to verify our preliminary observations in the future is needed.

Conclusions

The SNPs (-1654C/T, -1641A/G and -1476A/T) of protein C promoter gene are associated with susceptibility to PTE in a Chinese population. Especially, the homozygous carriers of genotype TT increase the risk of PTE in a Chinese population. This suggested that a Chinese population has distinct genetics features related to susceptibility to PTE. However, our results should be interpreted with caution. Confirmation of our preliminary observations in a larger scale study is needed.

Acknowledgements

This work was supported by the project of Shanghai Science Committee (No. 074119611, 11411951302 and 114119a3000).

Disclosure: The authors declare no conflict of interest.

References

1. Avdonin PV, Kirienko AI, Kozhevnikova LM, et al. C677T mutation in methylentetrahydrofolatereductase gene in patients with venous thromboses from the central region of Russia correlates with a high risk of pulmonary artery thromboembolism. Ter Arkh 2006;78:70-6.
2. Cho KH, Jeong MH, Sim DS, et al. Pulmonary thromboembolism due to severe hyperhomocysteinemia associated with a methyltetrahydrofolate reductase mutation. Korean J Intern Med 2013;28:112-5.
3. Dunn ST, Trong S. Evaluation of role of factor V Leiden mutation in fatal pulmonary thromboembolism. Thromb Res 1998;91:7-14.
4. Küpeli E, Cengiz C, Cila A, et al. Hyperhomocysteinemia due to pernicious anemia leading to pulmonary thromboembolism in a heterozygous mutation carrier. Clin Appl Thromb Hemost 2008;14:365-8.
5. Qin J, Dai J, Xu Z, et al. Genetic polymorphism of NOS3 with susceptibility to deep vein thrombosis after orthopedic surgery: a case-control study in Chinese Han population. PLoS One 2013;8:e70033.
6. Oguzulgen IK, Yilmaz E, Demirtas S, et al. The role of plasminogen activator inhibitor-1 polymorphism, factor-V-Leiden, and prothrombin-20210 mutations in pulmonary thromboembolism. Clin Appl Thromb Hemost 2009;15:73-7.
7. Ro A, Hara M, Takada A. The factor V Leiden mutation and the prothrombin G20210A mutation was not found in Japanese patients with pulmonary thromboembolism. Thromb Haemost 1999;82:1769.
8. Seki T, Okayama H, Kumagai T, et al. Arg506Gln mutation of the coagulation factor V gene not detected in Japanese pulmonary thromboembolism. Heart Vessels 1998;13:195-8.
9. Aiach M, Nicaud V, Alhenc-Gelas M, et al. Complex association of protein C gene promoter polymorphism with circulating protein C levels and thrombotic risk. Arterioscler Thromb Vasc Biol 1999;19:1573-6.
10. Ekim N, Oguzulgen IK, Demir N, et al. The role of angiotensin-converting enzyme gene polymorphism in pulmonary thromboembolism. Thromb Haemost 2004;92:432-3.
11. Spek CA, Koster T, Rosendaal FR, et al. Genotypic

variation in the promoter region of the protein C gene is associated with plasma protein C levels and thrombotic risk. Arterioscler Thromb Vasc Biol 1995;15:214-8.
12. Spek CA, Poort SR, Bertina RM, et al. Determination of the allelic and haplotype frequencies of three polymorphisms in the promoter region of the human protein C gene. Blood Coagul Fibrinolysis 1994;5:309-11.
13. Horlander KT, Mannino DM, Leeper KV. Pulmonary embolism mortality in the United States, 1979-1998: an analysis using multiple-cause mortality data. Arch Intern Med 2003;163:1711-7.
14. Worsley DF, Alavi A. Comprehensive analysis of the results of the PIOPED Study. Prospective Investigation of Pulmonary Embolism Diagnosis Study. J Nucl Med 1995;36:2380-7.
15. Ohwada A, Takahashi H, Uchida K, et al. Gene analysis of heterozygous protein C deficiency in a patient with pulmonary arterial thromboembolism. Am Rev Respir Dis 1992;145:1491-4.
16. Takeda K, Kumagai H, Hayashi S, et al. A case of congenital protein C deficiency with pulmonary thromboembolism. Nihon Kyobu Shikkan Gakkai Zasshi 1994;32:497-501.
17. Kogure S, Makita K, Saitoh Y, et al. Anesthetic management of a patient with protein C deficiency associated with pulmonary thromboembolism. Masui 1998;47:831-4.
18. Ribeiro A, Correia A, Fernandes F, et al. Pulmonary thromboembolism in a female with resistance to activated protein C. Rev Port Cardiol 1999;18:601-7.
19. Taniyasu N, Akiyama K, Takazawa A, et al. Surgical treatment for chronic pulmonary thromboembolism in a patient with protein C deficiency. Kyobu Geka 2001;54:237-40.
20. Yoshimura S, Nishimura Y, Funada Y, et al. Pulmonary thromboembolism associated with familial protein C deficiency type I. Nihon Kokyuki Gakkai Zasshi 2003;41:451-6.
21. Bhargava K, Chandra N, Omar AK, et al. Protein C deficiency leading to pulmonary thromboembolism in a patient with hereditary spherocytosis. Indian Heart J 2006;58:444-6.
22. Yoshida M, Mukohara N, Obo H, et al. Pulmonary thromboendarterectomy for chronic pulmonary thromboembolism in protein C deficiency. Jpn J Thorac Cardiovasc Surg 2006;54:70-4.
23. Takami H, Fukushima K, Takizawa M, et al. Protein C deficiency manifested as pulmonary aretery thromboembolism induced by oral contraceptive. Nihon Naika Gakkai Zasshi 2007;96:341-3.
24. Chun C, Yang W, Xueding C, et al. Resveratrol downregulates acute pulmonary thromboembolism-induced pulmonary artery hypertension via p38 mitogen-activated protein kinase and monocyte chemoattractant protein-1 signaling in rats. Life Sci 2012;90:721-7.
25. Isoda S, Kimura T, Nishimura K, et al. A Case Report of Pulmonary Thromboendarterectomy for Chronic Thromboembolism in a Patient with Protein C Deficiency. Ann Thorac Cardiovasc Surg 2013. [Epub ahead of print].
26. Schneider D, Lilienfeld DE, Im W. The epidemiology of pulmonary embolism: racial contrasts in incidence and in-hospital case fatality. J Natl Med Assoc 2006;98:1967-72.
27. Kabrhel C, Varraso R, Goldhaber SZ, et al. Physical inactivity and idiopathic pulmonary embolism in women: prospective study. BMJ 2011;343:d3867.
28. Rosendaal FR, Doggen CJ, Zivelin A, et al. Geographic distribution of the 20210 G to A prothrombin variant. Thromb Haemost 1998;79:706-8.
29. De Stefano V, Martinelli I, Mannucci PM, et al. The risk of recurrent deep venous thrombosis among heterozygous carriers of both factor V Leiden and the G20210A prothrombin mutation. N Engl J Med 1999;341:801-6.
30. Lu Y, Zhao Y, Liu G, et al. Factor V gene G1691A mutation, prothrombin gene G20210A mutation, and MTHFR gene C677T mutation are not risk factors for pulmonary thromboembolism in Chinese population. Thromb Res 2002;106:7-12.

Cite this article as: Zhu C, Jiang T, Miao Y, Gong S, Cheng K, Guo J, Tan X, Yue J, Liu J. The SNPs (-1654C/T, -1641A/G and -1476A/T) of protein C promoter are associated with susceptibility to pulmonary thromboembolism in a Chinese population. J Thorac Dis 2014;6(7):943-948. doi: 10.3978/j.issn.2072-1439.2014.06.30

Original Article

Prognostic factors in patients with recurrence after complete resection of esophageal squamous cell carcinoma

Xiao-Dong Su[1,2]*, Dong-Kun Zhang[3]*, Xu Zhang[1,2], Peng Lin[1,2], Hao Long[1,2], Tie-Hua Rong[1,2]

[1]Department of Thoracic Surgery, Cancer Center, Sun Yet Sen University, Guangzhou 510060, China; [2]State Key Laboratory of Oncology in Southern China, Guangzhou 510060, China; [3]Department of Thoracic Surgery, Guangdong Provincial Hospital, Guangzhou 510180, China

*These two authors contributed equally to this work.

Correspondence to: Dr. Tie-Hua Rong. Department of Thoracic Surgery, Cancer Center, Sun Yet Sen University, Guangzhou 510060, China. Email: rongth@hotmail.com.

Background: Recurrence following complete resection of esophageal squamous cell carcinoma (SCC) still remains common. The aim of this study was to investigate the prognostic factors in patients with recurrence after complete resection of esophageal SCC.

Methods: The medical records of 190 patients with recurrent disease after complete resection of esophageal SCC were retrospectively reviewed. Recurrence pattern was classified as loco-regional recurrence and distant metastases. The Kaplan-Meier method was used for the survival analysis. Cox proportional hazards model was used for multivariate analysis.

Results: Mediastinal nodal clearance area was the most common sites of loco-regional recurrence, whereas lung, liver and bone were the most common sites for distant metastases. The median survival after recurrence was 8 months. The 1, 3, 5-year post-recurrence survival rates were 45.9%, 10.6% and 6.4%, respectively. The overall 1, 3, 5-year survival rates were 76.6%, 27.3% and 12.3%, respectively. The independent prognostic factors included time of recurrence (≥12 months *vs.* <12 months, HR: 3.228, 95% CI: 2.233-4.668), pattern of recurrence (local-regional recurrence *vs.* distant metastases, HR: 1.690, 95% CI: 1.170-2.439), and treatment of recurrence [no treatment *vs.* treatment (radiotherapy or surgery or chemotherapy), HR: 0.642, 95% CI: 0.458-0.899].

Conclusions: Our retrospective study showed that time of recurrence, pattern of recurrence and treatment of recurrence were independent prognostic factors in patients with recurrence after complete resection of esophageal SCC.

Keywords: Esophageal carcinoma; esophagectomy; recurrence; prognostic factor

Submitted Mar 24, 2014. Accepted for publication Jun 15, 2014.
doi: 10.3978/j.issn.2072-1439.2014.07.14
View this article at: http://dx.doi.org/10.3978/j.issn.2072-1439.2014.07.14

Introduction

Esophageal cancer is one of the most common cancers worldwide, causing more than 400,000 deaths annually (1). Surgical resection is generally recommended for the treatment of esophageal carcinoma in early stage. Advances in anesthesia and surgical techniques and improvements in perioperative management have reduced the postoperative mortality to acceptable levels. However, the overall 5 years survival rate after esophagectomy remains about 25% (2). This dismal result is attributed to recurrences after resection of the primary tumor. Local-regional recurrences or/and distant organ metastases are found in approximately half of patients within 2-3 years of surgical treatment (3-5). The pattern of recurrence after esophagectomy has been well documented (3,5,6). Histologic tumor depth invasion (3,5), local-regional lymph node metastases (5) and intramural metastasis (6) have been reported to predict recurrence.

Recent advances in chemotherapy and radiation techniques may particularly benefit patients with recurrent

disease after esophagectomy. In fact, recurrent disease sometimes responds better to anticancer treatment, and those patients can achieve relatively long-term survival. Thus, the factors affecting this survival after recurrence in patients with esophageal SCC need to be further investigated. In this study, we sought to better understand factors affecting overall survival in patients with disease of recurrence following complete resection of esophageal SCC.

Methods

Patients

A total of 773 patients with esophageal cancer received surgical resection at the Department of Thoracic Surgery, Sun Yat-sen University Cancer Center, from January 2001 to December 2005. All tumors were pathologically confirmed as squamous cell carcinoma (SCC) by biopsy under endoscopy. Other preoperative examinations included plain chest radiography, barium swallow, chest and abdominal computed tomography (CT) scan and cervical ultrasonography. Bronchoscopy was also done in patients with tumor located in the upper third thoracic esophagus.

Clinical data regarding cancer recurrence after surgery were collected. Patients were excluded if: (I) there was no complete follow-up data or no pathologic or radiographic examination results to confirm recurrence; (II) surgery was non-curative resection (R1 or R2); (III) the patient received neoadjuvant radiotherapy or chemotherapy; or (IV) there was a second primary cancer. This study was officially approved by the Ethics Committee of our hospital.

A total of 190 patients were included in the study. There were 146 males and 44 females. The median patient age was 55 years (range, 32-76 years). Primary sites of 13 (6.8%) patients were in the upper thoracic esophagus, 129 (67.9%) in the middle thoracic esophagus and 48 (25.3%) in the lower thoracic esophagus.

Esophageal cancer patients with a primary tumor in the lower thoracic esophagus were treated using the left transthoracic procedure or Ivor-Lewis procedure (if there was evidence of mediastinal lymphadenopathy on chest CT) with intrathoracic anastomosis. Patients with a primary tumor in the upper thoracic esophagus underwent cervical-thoracoabdominal procedure with a left cervical anastomosis. Patients with tumor in the middle thoracic esophagus were treated using the left transthoracic procedure with intrathoracic anastomosis (if no evidence of mediastinal lymphadenopathy on chest CT) or the cervical-thoracoabdominal procedure with a left cervical anastomosis (if mediastinal lymphadenopathy was showed on chest CT). All patients underwent esophageal reconstruction using stomach to replace the esophagus. Lymph node dissection was performed including the left and right tracheobronchial, subcarinal, paraesophageal, diaphragmatic lymph nodes as well as the paracardial, lesser gastric curvature, left gastric artery and celiac nodes. The lymph nodes next to the left and right recurrent laryngeal nerves were removed when a right thoracotomy was used. Nine patients developed a post-operative anastomotic leakage, ten atelectasis and pneumonia, and one chylothorax. No postoperative adjuvant radiotherapy or chemotherapy was administered.

The pathologic staging was based on the UICC sixth edition [2002] for staging criteria of esophageal cancer (7). There was one stage I patient (one case of pT1N0M0), 68 stage IIA (30 pT2N0M0 and 38 pT3N0M0) patients, 28 stage IIB (28 pT2N1M0) patients, and 93 stage III (93 pT3N1M0) patients.

Recurrence identification

All patients were examined every 3 to 4 months during the first 2 years after surgery, followed by every 6 months for 3 to 5 years after surgery, and once a year thereafter. The patients were asked to visit the hospital for examination if any symptoms such as hoarseness or dysphagia occurred. Follow-up examinations included physical examination, chest X-Ray, barium swallow and abdominal and cervical ultrasonography. If any suspected recurrence or metastasis was found on X-ray or ultrasonography, or enlarge supraclavicular lymph nodes palpated, chest and abdominal CT scans and esophageal endoscopy were performed. Patients with bone pain had a bone scintigraphy scan.

Tumor diagnosed at least 6 months or more after surgery were considered a recurrence. Loco-regional recurrences was defined as anastomotic recurrence or/and occurring either in the mediastinum or upper abdomen at the site of previous esophageal resection and nodal clearance or in the cervical area where no lymphadenectomy had been performed. Distant metastasis was defined as occurring in distant organs, pleura and peritoneum. If both loco-regional recurrence and distant metastases occurred, the case was considered as distant metastases (3). Diagnosis of recurrence was made using cytological and histopathological results which were obtained by biopsy of suspected recurrence at anastomotic site or supraclavical lymph nodes and tumor

Table 1 Treatment of recurrent diseases

Modality	Cases	Dose or regimen
Radiotherapy	81 pts (74 pts with radiotherapy alone, 7 pts with chemoradiotherapy)	Median radiation dose: 60 Gy (range, 24-75 Gy)
Chemotherapy	19 pts	Cisplatin and 5-fluorouracil: 2-6 cycles
Surgery	7 pts {metastectomy of lung [3], brain [1] and skin [1], liver metastases treated with RFA [2]}	
No treatment	83 pts	

Abbreviations: pts, patients; RFA, radiofrequency ablation.

imaging studies. Criteria used to determine CT lymph node metastases were a lymph node diameter greater than 1 cm.

Treatment of recurrent disease

The modalities of treatment of recurrent disease are showed in *Table 1*. In the surgical group, a solitary metastasis to the lung or brain was confirmed by the imaging tests including chest and abdominal CT scan, brain magnetic resonance imaging (MRI). One patient with a solitary metastasis to the lung survived 71 months after pulmonary wedge resection. Among the non-treatment group, 83 patients received only symptomatic and supportive treatment due to age, poor general health status, financial considerations, or patient choice.

Follow-up

The follow-up department of our hospital was responsible for postoperative follow-up of all patients. Patients, follow-up data were obtained by reviewing records of clinical re-examination or by directly contacting the patient or their family by telephone. Follow up was stopped upon patient's death or on January 2012. Eight cases were lost to follow-up and defined as censored cases. The follow-up rate was 95.8%. The mean follow-up was 30.15±28.90 months (range, 2-131 months). Progression-free survival was defined as time from date of surgery to the first recurrence or last follow-up. Post-recurrence survival was calculated as time between the first recurrence and death or last follow-up. Overall survival time was calculated as the time between surgery and death or last follow-up.

Statistical analysis

SPSS16.0 (SPSS, Chicago, IL, USA) statistical software was used for statistical analysis. Quantitative data were expressed as mean ± standard deviation ($\bar{x} \pm s$), and a *t*-test was performed for comparison. Survival analysis was performed using the Kaplan-Meier method, and compared by means of the log-rank test. Hazard ratios were calculated using a Cox regression model. Multivariable analysis for prognostic factors was performed using a Cox proportional hazard model. A P value of less than 0.05 was considered statistically significant.

Results

Clinical and pathological features of the patients are shown in *Table 2*. A total of 106 (55.8%) patients recurred within 1 year, 154 (81.1%) within 2 years, and 169 (88.9%) within 3 years after surgery. The pattern of recurrence after esophagectomy is showed in *Table 3*. The overall median time to recurrence was 10 months (range, 6-94 months). The median time to recurrence in patients with loco-regional recurrence and distant metastases was 13 months (range, 6-94 months) and 8 months (range, 6-44 months), respectively. The mean time to recurrence in patients with loco-regional recurrence and distant metastases was 18.66±16.30 months and 11.05±7.77 months (P=0.001), respectively.

The 1, 3, 5-year progression-free survival rates were 52.2%, 14.9% and 4.2%, respectively (*Figure 1*). The overall median survival time after recurrence was 8 months. The 1, 3, 5-year post-recurrence survival rates were 45.9%, 10.6% and 6.4%, respectively (*Figure 2*). The median overall survival time was 21.5 months. The overall 1, 3, 5-year survival rates were 76.6%, 27.3% and 12.3%, respectively (*Figure 3*).

The median survival time after recurrence in the loco-regional recurrence group and the distant metastasis group was 10 months (range, 2-125 months) and 5 months (range, 1-162 months), respectively. The mean survival time after

Table 2 Clinical and histopathologic characteristic of 190 patients with disease of recurrence after esophagectomy

Characteristics	Local-regional recurrence (n=124)	Distant metastases (n=66)
Gender		
Male	96	50
Female	28	16
Tumor location		
Upper third	10	3
Middle third	83	46
Lower third	31	17
Anastomotic site		
Cervical	27	15
Intrathoracic	97	51
Differentiation		
Well	32	13
Moderately	61	34
Poorly	31	19
Depth of invasion		
pT1	0	1
PT2	41	17
PT3	83	48
Lymph node metastasis		
pN0	48	21
PN1	76	45
pTNM stage		
I	0	1
IIa	48	20
IIb	19	9
III	57	36

Table 3 Patterns of recurrence after esophagectomy[a]

Patterns of recurrence	Cases
Local-regional recurrence[b] (n=138)	
Cervical	43
Mediastinal	95
Abdominal	11
Anastomotic	13
Distant metastases[c] (n=66)	
Lung	21
Liver	18
Bone	15
Brain	4
Subcutaneous	4
Adrenal	3
Stomach	2
Pleura	3
Peritoneum	1

[a], Local-regional recurrence and distant metastasis were recognized simultaneously in 14 patients. These patients were classified into distant metastases group; [b], recurrence in multiple areas were recognized in 23 patients; [c], metastases in multiple distant organs were recognized in 5 patients.

recurrence in the loco-regional recurrence group and the distant metastasis group was 13.71±14.71 months and 7.18±7.21 months (P=0.001), respectively.

Univariate analysis showed that tumor location, depth of invasion, lymph node metastasis, pathological stage, time of tumor recurrence, type of recurrence and treatment after recurrence were significantly related to survival. Gender, age and tumor tissue differentiation were not related to survival (*Table 4*). Factors related to survival in the univariate analysis were evaluated with the Cox model. Time of tumor recurrence, type of recurrence and treatment after recurrence were found to be independent factors that affected prognosis (*Table 5*, *Figure 4*).

Discussion

Esophagectomy with radical lymph node dissection is the main treatment for esophageal cancer. However, the rich lymphatic capillary network in the esophageal mucosa and submucosa facilitate local recurrences or distant metastases after surgery. It has been reported that more than half of esophageal cancer patients have recurrence or metastases within 2-3 years after resection (3,4). Mariette *et al.* (5) have reported 90% of recurrence occurred within 38 months after surgery. 88.9% of our patients had recurrence or metastasis within 3 years after surgery. The fact that nearly half of patients [in both Mariette *et al.* (5) and our study] had stage III disease may have contributed to these high recurrent rates. Loco-regional recurrence of esophageal cancer, especially in lymph nodes located in the mediastinum and cervicothoracic junction, was common. Different methods have been used to try to reduce loco-regional recurrence. There is no standard lymph node dissection used in the treatment of esophageal cancer. In theory, a three-field lymphadenectomy is the most thorough method, and might reduce loco-regional recurrence. However, even with

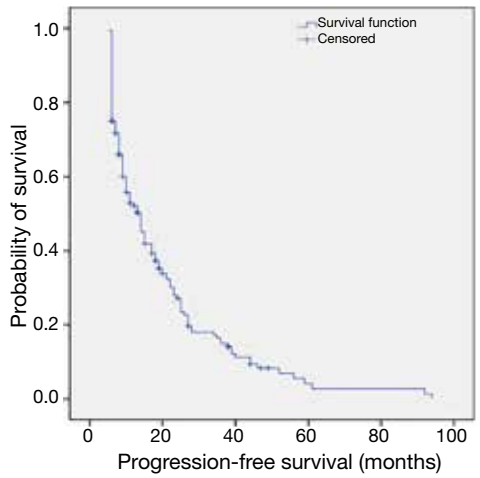

Figure 1 Kaplan-Meier estimating the probability of progression-free survival among 190 patients with disease of recurrence after esophagectomy.

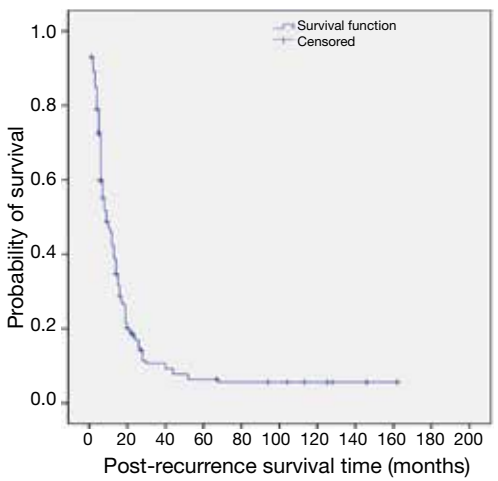

Figure 2 Kaplan-Meier estimating the probability of post-recurrence survival among 190 patients with disease of recurrence after esophagectomy.

three-field lymphadenectomy, loco-regional recurrence in esophageal cancer has been 14.2-20.4% (5,8). This is not significantly different from two-field lymphadenectomy (9). Neoadjuvant chemoradiotherapy is now widely used because it is believed to improve local-regional control and prolong survival in patients with local advanced esophageal cancer. Local-regional recurrence is still seen in 13-22% of patients who obtained a pathologically complete response after neoadjuvant therapy (10,11). Therefore, recurrences following complete resection of esophageal cancer still

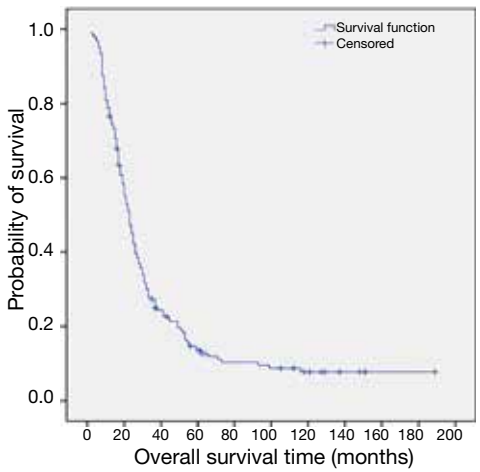

Figure 3 Kaplan-Meier estimating the probability of overall survival among 190 patients with disease of recurrence after esophagectomy.

remain common.

We found the presence of distant metastases to be a poor prognostic factor. Liver, lung and bone were the most common sites of reported hematogenous metastases (3-5,12). In a study by Smit *et al*. (13), 40.3% of distant recurrences were present in the skin or soft tissue, which were the most frequent sites for distant recurrence. In our study, the most common sites for distant recurrence were still the lung, liver and bone, accounting for 81.8% of all metastases. The median time to distant metastasis was significantly shorter than to loco-regional recurrence (8 *vs*. 13 months), similar to that reported by Mariette *et al*. (5) (11 *vs*. 13 months). This suggests that tumor micrometastases were present at the time of surgery (14). Loco-regional lymph node recurrences do not always occur before distant metastases. Hematogenous metastases and loco-regional recurrences are thought to occur independently (15,16). 27.5% of our patients had only distant metastases, that supporting this view. O'Sullivan *et al*. (17) found preoperative rib and iliac bone marrow micrometastases in respectively 88% and 15% of patients with esophageal cancer. Mariette *et al*. (5) reported that distant metastases occurred within one year after surgery among some stage I and stage IIA patients. These findings suggest that even at an early stage, esophageal cancer is already a systemic disease, and once distant metastases occur, prognosis becomes very poor (3,12). We found the 5-year survival rate of patients with distant metastasis to be only 2.3%.

Table 4 Univariate analysis of prognostic factors in 190 patients with disease of recurrence after esophagectomy

Variable	n	Median survival time (months)	5-year survival rate	P value	HR	95% CI for HR
Gender				0.737	1.057	0.696-1.605
Male	146	23	11.2			
Female	44	21	15.9			
Age (years)				0.837	0.976	0.593-1.606
<65	155	23	12.2			
≥65	35	22	11.9			
Tumor location				0.002	1.189	1.011-1.445
Upper third	13	10	0			
Middle third	129	25	15.0			
Lower third	48	18	6.8			
Differentiation				0.097	1.088	0.856-1.383
Well	43	22	11.9			
Moderately	95	23	10.1			
Poorly	52	24	8.7			
Depth of invasion				0.011	1.237	1.031-1.533
pT1	1	13	0			
pT2	58	23	19.8			
pT3	131	23	5.2			
Lymph node metastasis				0.000	1.487	1.071-2.065
N0	69	28	18.8			
N1	121	21	7.6			
pTNM stage				0.029	1.242	1.046-1.476
I	1	13	0			
IIa	68	28	19.7			
IIb	28	20	16.9			
III	93	21	8.4			
Time of recurrence				0.000	0.320	0.231-0.443
<12months	103	15	4.5			
≥12months	87	37	24.1			
Pattern of recurrence				0.000	1.832	1.320-2.543
Local-regional	124	26	17.3			
Distant metastases	66	17	2.3			
Treatment of recurrence				0.004	0.734	0.587-0.917
No treatment	83	19	10.5			
Chemotherapy	19	21	14.0			
Radiotherapy	81	30	14.8			
Surgery	7	71	16.7			

Abbreviations: HR, hazard Ratio; CI, confidential interval.

Table 5 Multivariate analysis of prognostic factors in 190 patients with disease of recurrence after esophagectomy

Variable	B	Wald	P	Exp.(ß)	95% CI for Exp.(ß)
Time of recurrence[a]	1.172	38.831	0.000	3.228	2.233-4.668
Pattern of recurrence[b]	0.524	7.836	0.000	1.690	1.170-2.439
Treatment[c]	–0.443	6.633	0.010	0.642	0.458-0.899

[a], ≥12 months *vs.* <12 months; [b], local-regional recurrence *vs*. distant metastases; [c], no treatment *vs*. treatment (radiotherapy or surgery or chemotherapy). Abbreviations: Exp., Experiences; CI, Confidence interval.

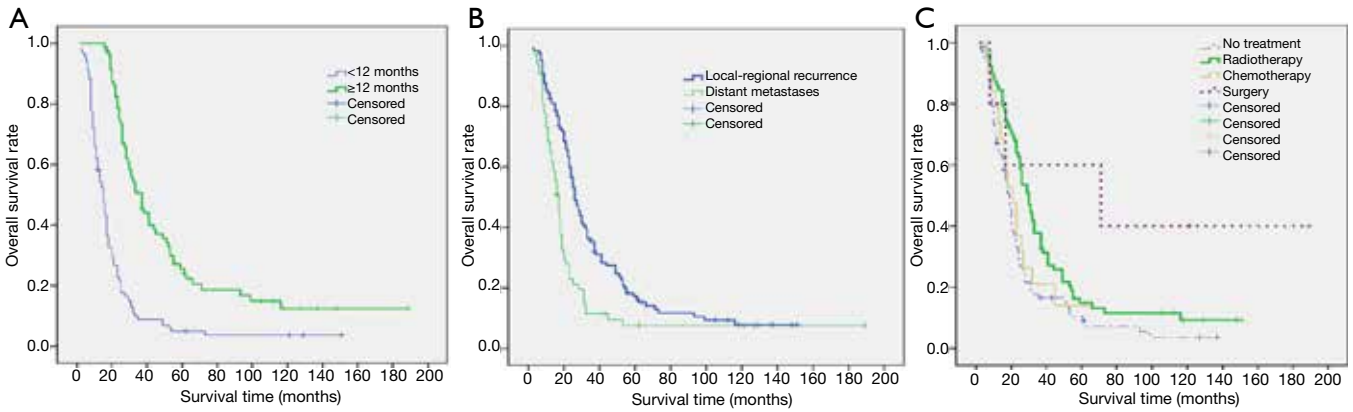

Figure 4 Kaplan-Meier estimating the overall survival among 190 patients with disease of recurrence after esophagectomy. A, survival according to time of recurrence; B, survival according to pattern of recurrence; C, survival according to treatment of recurrence disease.

The time interval between esophageal resection and recurrence was also a prognostic factor. Hsu *et al*. (12) reported that recurrence within 10 months after surgery was an independent factor for poor prognosis. Shimada *et al*. (18) reported that patients who recurred within one year after treatment had one year shorter subsequent survival than patients that recurred later. Osugi *et al*. (19) showed that the time to recurrence correlated with survival after recurrence in esophageal carcinoma patients who underwent esophagectomy and extended lymphadenectomy We found that the 5-year survival rate of patients who had recurrence within 12 months after surgery was significantly lower than those who had recurrence after 12 months (4.5% *vs*. 24.1%), consistent with previous reports. Distant metastases occurred sooner than loco-regional recurrence, hence recurrences that occurred within 1 year after surgery were mostly distant metastasis (3). This suggests that patients with distant metastases had highly malignant tumors and that effective treatments of distant metastases are still lacking.

While recurrent diseases may not be curative, multidisciplinary treatments can improve survival. Miyata *et al*. (20) found that radiotherapy, chemotherapy and surgery increased survival in 196 esophageal cancer patients with postoperative recurrence, and 26.2% of patients who received radiotherapy survived longer than 2 years after recurrence. Zhang *et al*. (21) and Maruyama *et al*. (22) reported that radiochemotherapy of recurrent mediastinal lymph nodes improved survival. The treatment result was found to be related to radiation dose (21,23). We also found that treatment was an independent prognostic factor for survival. Surgical resection was effective in some patients with solitary metastases. We treated one patient with a solitary lung metastasis that survived 71 months after surgery. In a retrospective study on the clinical outcome of patients who developed pulmonary metastasis after undergoing radical esophagectomy, Takemura *et al*. (24) showed that survival was significantly worse in patients who did not undergo resection than in those who did, and concluded that metastasectomy was an acceptable choice of treatment for solitary pulmonary metastasis. However, only few patients were included in the study (24) and in our series, they may be considered as cases of personalized therapy. Nakamura *et al*. (25) reported that surgical resection plus adjuvant chemotherapy for mediastinal lymph node recurrence achieved significantly better survival

than chemotherapy alone, but was not significantly different from concurrent chemoradiotherapy. Mediastinal lymph node recurrences are mostly multi-station recurrences and the patients are generally in poor health. As a consequence, most patients cannot tolerate surgery and radio-chemotherapy may become the main modality for patients with local-regional recurrences (20-23).

There are several limitations in this retrospective study. There may be bias regarding patient selection. Because of this, we did not analyze factors that may be associated with tumor recurrence. Secondly, nearly half of patients were in the disease of stage III. Since neoadjuvant chemoradiotherapy have shown survival benefit in the patients with esophageal carcinoma (26), it has become the main modality in the management of stage III disease in our institution. Finally, because different doses and schedules were used in the study, the optimum treatment regimen cannot be established for recurrence.

We found clinical and pathological features before recurrence did not correlate with prognosis after recurrence. Prognostic factors after recurrence included time of recurrence, type of recurrence and treatment after recurrence. Similar findings have been reported in the literature (12,18,19). These prognostic factors are useful in evaluating the prognosis of patients with postoperative recurrence of esophageal cancer in order to provide appropriate treatment.

Conclusions

Our retrospective study showed that time of recurrence, pattern of recurrence and treatment of recurrence were independent prognostic factors in patients with recurrence after complete resection of esophageal carcinoma. Postoperative recurrence of esophageal cancer is relatively common. Close follow-up should be performed for 2-3 years after surgery in order to timely detect tumor recurrence. For patients with local regional recurrence, chemo-radiotherapy should be given to improve survival.

Acknowledgements

Disclosure: The authors declare no conflict of interest.

References

1. Jemal A, Bray F, Center MM, et al. Global cancer statistics. CA Cancer J Clin 2011;61:69-90.
2. Mariette C, Piessen G, Triboulet JP. Therapeutic strategies in oesophageal carcinoma: role of surgery and other modalities. Lancet Oncol 2007;8:545-53.
3. Nakagawa S, Kanda T, Kosugi S, et al. Recurrence pattern of squamous cell carcinoma of the thoracic esophagus after extended radical esophagectomy with three-field lymphadenectomy. J Am Coll Surg 2004;198:205-11.
4. Chen G, Wang Z, Liu XY, et al. Recurrence pattern of squamous cell carcinoma in the middle thoracic esophagus after modified Ivor-Lewis esophagectomy. World J Surg 2007;31:1107-14.
5. Mariette C, Balon JM, Piessen G, et al. Pattern of recurrence following complete resection of esophageal carcinoma and factors predictive of recurrent disease. Cancer 2003;97:1616-23.
6. Kosugi S, Kanda T, Yajima K, et al. Risk factors that influence early death due to cancer recurrence after extended radical esophagectomy with three-field lymph node dissection. Ann Surg Oncol 2011;18:2961-7.
7. Sobin LH, Wittekind C. eds. TNM Classification of Malignant Tumours Sixth Edition. UICC International Union Against Cancer. New York: Wiley-Liss, 2002.
8. Lerut T, Nafteux P, Moons J, et al. Three-field lymphadenectomy for carcinoma of the esophagus and gastroesophageal junction in 174 R0 resections: impact on staging, disease-free survival, and outcome: a plea for adaptation of TNM classification in upper-half esophageal carcinoma. Ann Surg 2004;240:962-72; discussion 972-4.
9. Tachibana M, Kinugasa S, Yoshimura H, et al. Extended esophagectomy with 3-field lymph node dissection for esophageal cancer.Arch Surg 2003;138:1383-9; discussion 1390.
10. van Hagen P, Wijnhoven BP, Nafteux P, et al. Recurrence pattern in patients with a pathologically complete response after neoadjuvant chemoradiotherapy and surgery for oesophageal cancer. Br J Surg 2013;100:267-73.
11. Meguid RA, Hooker CM, Taylor JT, et al. Recurrence after neoadjuvant chemoradiation and surgery for esophageal cancer: does the pattern of recurrence differ for patients with complete response and those with partial or no response? J Thorac Cardiovasc Surg 2009;138:1309-17.
12. Hsu PK, Wang BY, Huang CS, et al. Prognostic factors for post-recurrence survival in esophageal squamous cell carcinoma patients with recurrence after resection. J Gastrointest Surg 2011;15:558-65.
13. Smit JK, Pultrum BB, van Dullemen HM, et al. Prognostic factors and patterns of recurrence in esophageal cancer assert arguments for extended two-field transthoracic

esophagectomy. Am J Surg 2010;200:446-53.
14. van Lanschot JJ, Tilanus HW, Voormolen MH, et al. Recurrence pattern of oesophageal carcinoma after limited resection does not support wide local excision with extensive lymph node dissection. Br J Surg 1994;81:1320-3.
15. Morita M, Kuwano H, Ohno S, et al. Characteristics and sequence of the recurrent patterns after curative esophagectomy for squamous cell carcinoma. Surgery 1994;116:1-7.
16. Matsubara T, Ueda M, Kaisaki S, et al. Localization of initial lymph node metastasis from carcinoma of the thoracic esophagus. Cancer 2000;89:1869-73.
17. O'sullivan GC, Sheehan D, Clarke A, et al. Micrometastases in esophagogastric cancer: high detection rate in resected rib segments. Gastroenterology 1999;116:543-8.
18. Shimada H, Kitabayashi H, Nabeya Y, et al. Treatment response and prognosis of patients after recurrence of esophageal cancer. Surgery 2003;133:24-31.
19. Osugi H, Takemura M, Higashino M, et al. Causes of death and pattern of recurrence after esophagectomy and extended lymphadenectomy for squamous cell carcinoma of the thoracic esophagus. Oncol Rep 2003;10:81-7.
20. Miyata H, Yamasaki M, Kurokawa Y, et al. Survival factors in patients with recurrence after curative resection of esophageal squamous cell carcinomas. Ann Surg Oncol 2011;18:3353-61.
21. Zhang J, Peng F, Li N, et al. Salvage concurrent radiochemotherapy for post-operative local recurrence of squamous-cell esophageal cancer. Radiat Oncol 2012;7:93.
22. Maruyama K, Motoyama S, Anbai A, et al. Therapeutic strategy for the treatment of postoperative recurrence of esophageal squamous cell carcinoma: clinical efficacy of radiotherapy. Dis Esophagus 2011;24:166-71.
23. Zhu YL, Li Q, Gao JM, et al. A retrospective evaluation of radiotherapy for the treatment of local esophageal squamous cell carcinoma recurrence after initial complete surgical resection. J Investig Med 2013;61:34-9.
24. Takemura M, Sakurai K, Takii M, et al. Metachronous pulmonary metastasis after radical esophagectomy for esophageal cancer: prognosis and outcome. J Cardiothorac Surg 2012;7:103.
25. Nakamura T, Ota M, Narumiya K, et al. Multimodal treatment for lymph node recurrence of esophageal carcinoma after curative resection. Ann Surg Oncol 2008;15:2451-7.
26. Sjoquist KM, Burmeister BH, Smithers BM, et al. Survival after neoadjuvant chemotherapy or chemoradiotherapy for resectable oesophageal carcinoma: an updated meta-analysis. Lancet Oncol 2011;12:681-92.

Cite this article as: Su XD, Zhang DK, Zhang X, Lin P, Long H, Rong TH. Prognostic factors in patients with recurrence after complete resection of esophageal squamous cell carcinoma. J Thorac Dis 2014;6(7):949-957. doi: 10.3978/j.issn.2072-1439.2014.07.14

Original Article

Sequential treatment of icotinib after first-line pemetrexed in advanced lung adenocarcinoma with unknown EGFR gene status

Yulong Zheng[1], Weijia Fang[1], Jing Deng[1], Peng Zhao[1], Nong Xu[1]*, Jianying Zhou[2]*

[1]Department of Medical Oncology, [2]Department of Respiratory Diseases, The First Affiliated Hospital of Zhejiang University, Hangzhou 310003, China
*These authors contributed equally to this work.

Correspondence to: Dr. Jianying Zhou. Department of Respiratory Diseases, the First Affiliated Hospital of Zhejiang University, 79 Qingchun Road, Hangzhou 310003, China. Email: zjyhz@zju.edu.cn; Nong Xu. Department of Medical Oncology, The First Affiliated Hospital of Zhejiang University, 79 Qingchun Road, Hangzhou 310003, China. Email: xunonghz@163.com.

Background: In non-small cell lung cancer (NSCLC), the well-developed epidermal growth factor receptor (EGFR) is an important therapeutic target. EGFR activating gene mutations have been proved strongly predictive of response to EGFR-tyrosine kinase inhibitors (TKI) in NSCLC. However, both in daily clinical practice and clinical trials, patients with unknown EGFR gene status (UN-EGFR-GS) are very common. In this study, we assessed efficacy and tolerability of sequential treatment of first-line pemetrexed followed by icotinib in Chinese advanced lung adenocarcinoma with UN-EGFR-GS.

Patients and methods: We analyzed 38 patients with advanced lung adenocarcinoma with UN-EGFR-GS treated with first-line pemetrexed-based chemotherapy followed by icotinib as maintenance or second-line therapy.

Results: The response rates to pemetrexed and icotinib were 21.1% and 42.1%, respectively. The median overall survival was 27.0 months (95% CI, 19.7-34.2 months). The 12-month overall survival probability was 68.4%. The most common toxicities observed in icotinib phase were rashes, diarrheas, and elevated aminotransferase. Subgroup analysis indicated that the overall survival is correlated with response to icotinib.

Conclusions: The sequence of first-line pemetrexed-based chemotherapy followed by icotinib treatment is a promising option for advanced lung adenocarcinoma with UN-EGFR-GS in China.

Keywords: Non-small cell lung cancer (NSCLC); epidermal growth factor receptor (EGFR); tyrosine kinase inhibitor (TKI); chemotherapy

Submitted Apr 12, 2014. Accepted for publication Jun 16, 2014.
doi: 10.3978/j.issn.2072-1439.2014.07.18
View this article at: http://dx.doi.org/10.3978/j.issn.2072-1439.2014.07.18

Introduction

Non-small cell lung cancer (NSCLC) accounts for 85% of all lung cancers, which are the leading cause of cancer-related death worldwide (1). The most common histological subtype of NSCLC is adenocarcinoma. Most lung cancers are diagnosed at late stage, conferring a bad prognosis. Less than 5% of stage IV patients live longer than five years. Platinum plus a third-generation agents is the standard regimen for patients with advanced NSCLC (2). One of the third-generation agents, pemetrexed, has been demonstrated efficacy in advanced non-squamous NSCLC as first-line, second-line or maintenance therapy (3-6). A meta-analysis, including four randomized trials, compared the efficacy and toxicities of the doublets of pemetrexed and platinum versus other platinum regimen in advanced NSCLC in the first-line setting (7). The analysis concluded that pemetrexed/platinum combination appear to offer significant survival advantage and acceptable toxicities, especially for NSCLC of non-squamous histology (7).

However, in advanced NSCLC the therapeutic plateau has been reached with conventional chemotherapy (8). The treatment paradigm for NSCLC patients is changing with the improved understanding of the molecular signaling

pathways. Some biomarkers of associated target therapies are established. Epidermal growth factor receptor (EGFR) tyrosine kinase inhibitor (TKI) was an important progress made towards treating NSCLC in last decade. Two individual studies have reported that EGFR gene activating mutation is strongly predictive of response to EGFR-TKIs in NSCLC (9,10). EGFR-TKIs are recommended for all lines of treating advanced NSCLC with EGFR activating mutations, but the role of EGFR-TKIs in EGFR wild-type NSCLC is still on debating (11).

In western countries, two reversible EGFR-TKIs are commercially available: gefitinib and erlotinib. A China company (Betta Pharmaceuticals Co., Ltd.) developed the third orally EGFR-TKI named icotinib hydrochloride (Conmana®) (12). The large, randomized, head-to-head, phase III clinical trial (ICOGEN) demonstrated that icotinib has comparable efficacy to gefitinib in Chinese pre-treated NSCLC (13). The most commonly observed side effects of icotinib were rash (41.0%) and diarrhea (22%), which was significantly less than gefitinib (13). The recommended dose for clinical treatment is 125 mg three times per day orally. Icotinib is becoming more widely used in clinical practice in China.

Either in daily clinical practice, or in clinical trials, patients with unknown EGFR gene status (UN-EGFR-GS) are very common to see (13-15). The optimal treatment for advanced NSCLC with UN-EGFR-GS is not established yet. In East Asian patients with lung adenocarcinoma, the incidence of EGFR activating mutations, about 40%, is much higher than in western population (14,16,17). Sequential first-line pemetrexed followed by icotinib seems to be a reasonable option for Chinese patients with UN-EGFR-GS advanced lung adenocarcinoma. Thus we conducted this retrospective study, aiming to assess the efficacy and tolerability of the treatment modality in selected patients.

Methods

Study design and treatment

The institutional ethics committee of the First Affiliated Hospital of Zhejiang University approved this study. Informed consent was obtained from each patient. We retrospectively analyzed the data of 38 patients with advanced lung adenocarcinoma and with UN-EGFR-GS between 2010 and 2012, who were treated with first-line pemetrexed-based chemotherapy, and subsequently treated with icotinib as second-line or maintenance therapy. All cases were histologically confirmed. The inclusion criteria were as follows: patients diagnosed with advanced lung adenocarcinoma; the EGFR mutation status was unknown; receive at least one cycle of pemetrexed-based chemotherapy; no more than six cycles of chemotherapy; switch to icotinib for the purpose of second-line or maintenance therapy; at least one measurable lesion according to RECIST criteria (18). Patients with known EGFR gene status (mutant or wild type) were excluded. We defined UN-EGFR-GS as: (I) no tumor sample was sent for detection of EGFR gene mutations; (II) tumor samples were sent for EGFR gene mutation test, but the results were not clear whether mutant or wild type.

The primary objective of this study is to assess overall survival (OS) and tolerability of treating advanced lung adenocarcinoma with the sequence. The OS was defined as the time of starting pemetrexed treatment to death or lost follow-up. The clinical characteristics, toxicity and survival status were collected through reviewing medical records, electronic preserved data, interviewing with patients or their family members. Pemetrexed was administered intravenously at the standard dose of 500 mg/m^2 on day 1 of 21-day cycle. The treatment was scheduled up to six cycles unless intolerable toxicity or progressive disease (PD). Switching to icotinib treatment when progression documented, or investigators consider icotinib maintenance therapy for patients not progressing after at least four cycles of pemetrexed-based chemotherapy. Icotinib was administered orally at the standard dose of 125 mg thrice per day until PD or intolerable treatment-related toxicity. Dose reduction or interruption/delay was permitted in the two-phase treatment.

Clinical assessments

The clinical course of included patients and treatment were prospectively monitored. Side effects were graded according to Common Terminology Criteria for Adverse Events, Version 3.0. Tumor response was assessed with RECIST criteria (version 1.1) (18). Clinical follow-up including physical examination, complete blood count, chemistry were performed every 2-3 weeks. Computed tomography (CT) or magnetic resonance imaging (MRI) was performed every 2-3 cycles of pemetrexed, and four weeks after initiating icotinib therapy, then every two months.

Statistical analysis

Statistical analyses were conducted through IBM SPSS 20

Table 1 Patients' characteristics (n=38)

Variables	Median (range)/frequency (%)
Age [years]	58.6 [40-75]
Sex	
Male	15 (39.5)
Female	23 (60.5)
Smoking status	
Smoker	11 (28.9)
Never-smoker	27 (71.1)
Performance status	
0-1	32 (84.2)
2	6 (15.8)
First-line chemotherapy	
Pemetrexed plus cisplatin	22 (57.9)
Pemetrexed plus carboplatin	10 (26.3)
Pemetrexed single use	6 (15.8)
Icotinib treatment	
Second line	27 (71.1)
Maintenance	11 (28.9)
Post-study treatment	
Paclitaxel	12 (31.5)
Platinum	10 (26.3)
Docetaxel	9 (23.6)
Gemcitabine	8 (21.0)
None	6 (15.7)
Other EGFR-TKIs	6 (15.7)

EGFR-TKIs, epidermal growth factor receptor tyrosine kinase inhibitors.

Table 2 Objective responses (n=38)

	Pemetrexed n (%)	Icotinib n (%)
CR	0 (0)	0 (0)
PR	8 (21.1)	16 (42.2)
SD	13 (34.2)	11 (28.9)
PD	17 (44.7)	11 (28.9)
ORR (CR + PR)	8 (21.1)	16 (42.2)
DCR (CR + PR + SD)	21 (55.3)	27 (71.1)

CR, complete response; PR, partial response; SD, stable disease; PD, progressive disease; ORR, overall response rate; DCR, disease control rate.

for Mac OSX. The median OS were calculated by Kaplan-Meier method, accompanying by 95% CI. Differences among subgroups were tested using the log-rank test. $P<0.05$ was considered statistically significant.

Results

Patient characteristics

During 2010 and 2012, about 350 cases with advanced lung adenocarcinoma in our electronic medical record were registered. Seventy patients were clear with EGFR gene status. Thirty-eight patients were included in this study according to the inclusion criteria. The patient characteristics are listed in *Table 1*. The whole cohort patients included 23 females and 15 males. The median age was 58.6 years old (range, 40-75 y). Among the 38 patients, 27 were non-smokers and 11 were smokers. All the patients at least received one cycle of pemetrexed chemotherapy, and then were treated with icotinib. Ten cases were received pemetrexed combined with carboplatin, 22 combined with cisplatin, and 6 as single use. The icotinib use of 11 patients was for the purpose of maintenance therapy, 27 for second line. The average time of patients taking icotinib was 38.7 weeks (range, 3.7-130 weeks).

Of the 38 patients, EGFR mutations failed to detect in 9 patients without enough specimens. Tumor sample were not available in 29 patients, who refused to repeat biopsy or send tumor specimen to screen EGFR mutations.

Objective response and toxicities

The mean cycles of pemetrexed given to patients were 3.8 (1-6 cycles). The response rate (RR) to pemetrexed was 21.1% (8/38), stable disease (SD) 34.2% (13/38), PD 44.7% (17/38). One patient stopped pemetrexed plus cisplatin chemotherapy because of grade 3 vomiting. The RR to icotinib was 42.1% (16/38), SD 28.9% (11/38), PD 28.9% (11/38). *Table 2* shows the objective response to pemetrexed and icotinib. All grades of side effects observed in the pemetrexed phase included neutropenia (57.8%; 22/38), vomiting (50%; 19/38), nausea (50%; 19/38), anemia (44.7%; 17/38), thrombocytopenia (31.6%; 12/38), and rashes (7.8%; 3/38). Totally, we observed grade 3-4 toxicities in 32 of 146 cycles during the pemetrexed treatment phase. There was no grade 3-4 toxicities observed during the icotinib treatment phase. The most common grade 1-2 toxicities were rashes (36.8%; 14/38), diarrheas (31.5%; 12/38), elevated amino-transferase (13.1%; 5/38) and elevated BUN (7.8%; 3/38). There

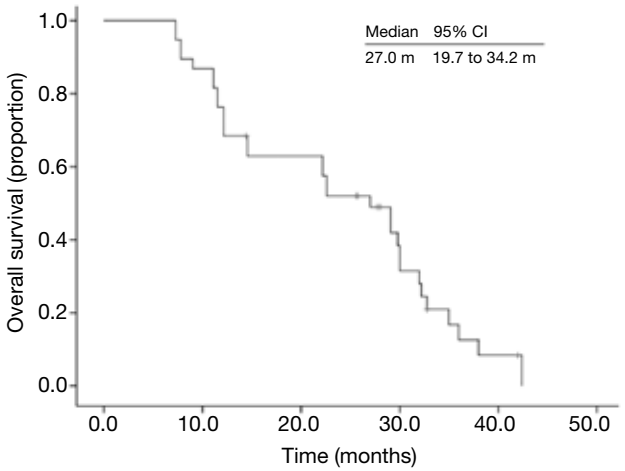

Figure 1 Kaplan-Meier overall survival curve of 38 advanced lung adenocarcinoma patients with unknown EGFR gene status. EGFR, epidermal growth factor receptor.

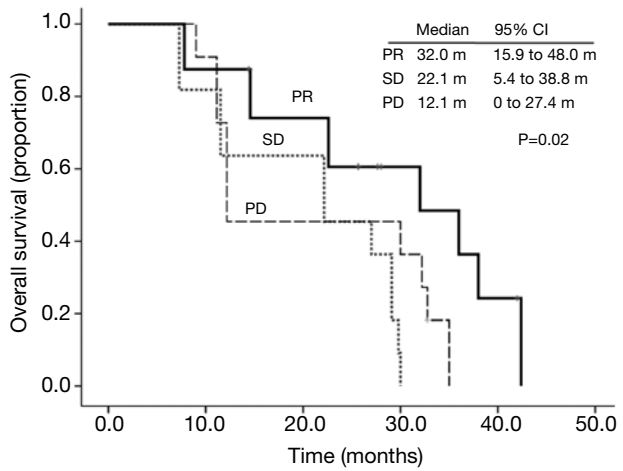

Figure 2 Kaplan-Meier overall survival curve stratified by response to icotinib.

was no dose reduction or interruption caused by icotinib therapy. No interstitial lung diseases were observed in this study.

Overall survival

The median follow-up time was 28.0 months (7.3-42.4 months). At the end of follow-up, 31 patients died, and 7 patients were still alive. Six patients were still on icotinib treatment. The median OS was 27.0 months (95% CI, 19.7-34.2 months) (*Figure 1*). The 12-month OS probability was 68.4%. The OS was correlated with response to icotinib. The median OS in patients obtained PR was 32.0 months (95% CI, 15.9-48.0 months), however the median OS in patients with SD and PD, was 22.1 months (95% CI, 5.4-38.8 months) and 12.1 months (95% CI, 0-27.0 months), respectively, (P=0.02) (*Figure 2*). The median OS was numerically longer in the maintenance group than the second-line group, which was 38.0 months (95% CI, 15.5-60.4 months) and 27.0 months (95% CI, 20.1-33.8 months), respectively. However, the difference was not statistically significant (P=0.35). According to the combined drugs, the patients were divided into cisplatin group or non-cisplatin group. The median OS in cisplatin group was 14.5 months (95% CI, 2.5-26.5 months) and the non-cisplatin group was 29.1 months (95% CI, 25.6-32.5 months). The difference was not statistically significant (P=0.98). There was also no significant OS difference between subgroups stratified by sex, performance score, smoking status, and response to pemetrexed.

Post-study treatment

Thirty-two patients documented PD from icotinib treatment. On disease progression, 6 patients received other EGFR-TKIs. Twelve patients received paclitaxel chemotherapy; 10 received platinum; 9 docetaxel; and 8 gemcitabine (see *Table 1*). Six patients received no further anti-cancer treatment.

Discussion

In the present study, we assessed the efficacy and tolerability of first-line pemetrexed followed by icotinib treatment in Chinese advanced lung adenocarcinoma with UN-EGFR-GS. To our best knowledge, this is the first study to discuss sequential pemetrexed and icotinib for selected NSCLC patients. The results showed that the sequential model is a promising treatment choice for advanced lung adenocarcinoma of Chinese patients.

According to EGFR gene status, NSCLC could be divided into three sub-categories: EGFR wild type, EGFR mutant type, and UN-EGFR-GS. Many randomized trials have compared EGFR-TKIs with chemotherapy for NSCLC with EGFR-sensitizing mutations in the first-line setting (14,19-22). EGFR-TKIs yield durable responses, prolonged progression free survival (PFS) and improved quality of life when compared to first-line chemotherapy. Additionally, the toxicities are much less than conventional

chemotherapy. All the trials did not produce significant OS improvement, probably due to crossover. In patients with EGFR wild type, the first-line EGFR-TKI treatment seems to be unsuitable (11,14,23). Beyond first-line setting, the role of EGFR-TKIs in treating NSCLC with wild-type EGFR is still a controversy (11,15,24-26).

Therefore performing EGFR gene testing may help managing NSCLC patients. However, either in daily clinical practice, or in clinical trials, NSCLC patients with UN-EGFR-GS are not rare (13-15). For example, in a recent published study tumor samples were available for EGFR testing from only 67% of patients and could be analyzed from 63%; UN-EGFR-GS for 47% of patients (27,28). In TAILOR and IPASS study, 23% and 64.1% patients were ineligible for EGFR gene testing, respectively (14,15). In ICOGEN study, tissue samples were available for only 38% (152/395) patients; 134 samples were eligible for EGFR gene testing; 66% (261/395) patients were with UN-EGFR-GS (13). In clinical trials, UN-EGFR-GS was mainly due to lack of sufficient tissue. In addition, more other reasons might cause UN-EGFR-GS in real world practice including: high cost of testing; re-biopsy not acceptable for some patients; limited testing technology. Especially in developing countries, the prevalence of NSCLC with UN-EGFR-GS would be probably much higher. In our institute, during 2010 to 2012 the EGFR gene status was tested in only about 20% of advanced NSCLC patients.

Treatment for advanced NSCLC is no longer a one-size-fits-all model. However, the demand is still there for one-size-fits-all approach currently because of high prevalence of UN-EGFR-GS. Based on our study, it is feasible to develop one size to fit Chinese advanced lung adenocarcinoma with UN-EGFR-GS. Pemetrexed-based chemotherapy is an appropriate first-line treatment option for advanced lung adenocarcinoma. In this study, the RR to the first-line pemetrexed-based chemotherapy is comparable to that of other studies (4,7,29). Gefitinb has been proved efficacy for East Asian patients with advanced NSCLC either in the second-line setting or maintenance therapy (30,31). So it is reasonable to choose icotinib as second line treatment or maintenance therapy for Chinese advanced lung adenocarcinoma in our study. In present study, the disease control rate was up to 71.0%, and the toxicity was mild, which both are similar to ICOGEN trial (13). In East Asian, EGFR activating mutations present in about 40% of lung adenocarcinoma, which strong drive the benefit of EGFR-TKIs (16,17). In selected patients (east Asian, never-smoker or light smoker, adenocarcinoma), the EGFR mutation rate is up to 60% (14,32). Such sub-group would possibly benefit from EGFR-TKIs without detecting the EGFR gene status.

We observed no significant survival difference between subgroups of sex, age, performance status, smoking status, platinum, maintenance or second-line therapy of icotinib and response to pemetrexed. We consider two reasons might be included to interpret our result. First, our study included relative small number of cases. Second, the overall survival was confounded by subsequent treatment of icotinib. Interestingly, we did find a relationship between overall survival and response to icotinib. The PR group lived longer than SD and PD group. Tsujino and colleagues (33) found that response rate is associated with median survival in clinical trials with EGFR-TKIs, which is consistent with our findings.

Sequential treatment strategies have been attracted more interests in recent lung cancer research. Fiala and colleagues (25) assessed the efficacy of second-line pemetrexed followed by third-line erlotinib to treatment with the reverse sequence in advanced lung adenocarcinoma with wild-type EGFR gene. The result demonstrated about 2-fold longer PFS (3.6 *vs*. 7.8 months; P=0.029) and 3-fold longer OS (7.9 *vs*. 26.3 months; P=0.006) for patients treated with erlotinib followed by pemetrexed than the reverse sequence. Another similar designed study showed significantly longer OS for patients managed with second-line erlotinib followed by third-line pemetrexed (23.6 *vs*. 16.3 months; P=0.042) in Chinese advanced lung adenocarcinoma (34). These studies support the use of EGFR-TKIs in the second-line setting in advanced NSCLC with adenocarcinoma histology. In our study, sequential therapy with first-line pemetrexed followed by icotinib yielded 27.0 months of median OS, which is comparable to second-line erlotinib followed by third-line pemetrexed.

In the first-line treatment, we included pemetrexed or combined with cisplatin or carboplatin. The cisplatin group lived no longer than non-cisplatin group. However meta-analysis demonstrated a significant survival improvement when cisplatin was used for patients with non-squamous histology. We speculate that this result was mainly interfered by the subsequent icotinib treatment.

In our study, we included patients treated with icotinib as either second-line or maintenance therapy. We suggest a sequential treatment is to treat patients with one therapy after another, whatever it is with or without interruption. Clinical trials have confirmed that erlotinib or gefitnib

may prolong PFS or OS regardless of the response to prior chemotherapy (30,35,36). The present study shows that the median OS is numerically longer in the maintenance group than the second-line group. Sequential icotinib maintenance therapy after pemetrexed in advanced lung adenocarcinoma probably is better than the second-line model, which need more investigations.

PFS is increasingly used as an important endpoint in clinical trials. However, we didn't discuss PFS in this study because the frequency of evaluation was different between patients. We think the major limitations of this study are its retrospective nature and relative small number of patients included. Selection bias might present in this study.

Conclusions

In conclusion, sequential therapy of first-line pemetrexed followed by icotinib for patients with advanced lung adenocarcinoma with UN-EGFR-GS seems to be an appealing treatment option. The sequence yielded promising results with acceptable toxicity. The sequential model for selected patients deserves further investigation in the future.

Acknowledgements

Zhejiang Provincial Natural Science Fund (LY13H160007), and Zhejiang Medicines & Health Science and Technology Project (201348801) supported this research. The authors thank the patients and family members for their participation in this study.
Disclosure: The authors declare no conflicts of interest.

References

1. Jemal A, Bray F, Center MM, et al. Global cancer statistics. CA Cancer J Clin 2011;61:69-90.
2. Fisher MD, D'Orazio A. Phase II and III trials: comparison of four chemotherapy regimens in advanced non small-cell lung cancer (ECOG 1594). Clin Lung Cancer 2000;2:21-2.
3. Hanna N, Shepherd FA, Fossella FV, et al. Randomized phase III trial of pemetrexed versus docetaxel in patients with non-small-cell lung cancer previously treated with chemotherapy. J Clin Oncol 2004;22:1589-97.
4. Scagliotti GV, Parikh P, von Pawel J, et al. Phase III study comparing cisplatin plus gemcitabine with cisplatin plus pemetrexed in chemotherapy-naive patients with advanced-stage non-small-cell lung cancer. J Clin Oncol 2008;26:3543-51.
5. Ciuleanu T, Brodowicz T, Zielinski C, et al. Maintenance pemetrexed plus best supportive care versus placebo plus best supportive care for non-small-cell lung cancer: a randomised, double-blind, phase 3 study. Lancet 2009;374:1432-40.
6. Paz-Ares L, de Marinis F, Dediu M, et al. Maintenance therapy with pemetrexed plus best supportive care versus placebo plus best supportive care after induction therapy with pemetrexed plus cisplatin for advanced non-squamous non-small-cell lung cancer (PARAMOUNT): a double-blind, phase 3, randomised controlled trial. Lancet Oncol 2012;13:247-55.
7. Li M, Zhang Q, Fu P, et al. Pemetrexed plus platinum as the first-line treatment option for advanced non-small cell lung cancer: a meta-analysis of randomized controlled trials. PLoS One 2012;7:e37229.
8. Gridelli C, Rossi A, Maione P. Treatment of non-small-cell lung cancer: state of the art and development of new biologic agents. Oncogene 2003;22:6629-38.
9. Paez JG, Jänne PA, Lee JC, et al. EGFR mutations in lung cancer: correlation with clinical response to gefitinib therapy. Science 2004;304:1497-500.
10. Lynch TJ, Bell DW, Sordella R, et al. Activating mutations in the epidermal growth factor receptor underlying responsiveness of non-small-cell lung cancer to gefitinib. N Engl J Med 2004;350:2129-39.
11. Laurie SA, Goss GD. Role of epidermal growth factor receptor inhibitors in epidermal growth factor receptor wild-type non-small-cell lung cancer. J Clin Oncol 2013;31:1061-9.
12. Zheng Y, Fang W, Liu X, et al. New EGFR-TKI: a case report of recurrent lung adenocarcinoma successfully treated with icotinib. Tumori 2012;98:e102-4.
13. Shi Y, Zhang L, Liu X, et al. Icotinib versus gefitinib in previously treated advanced non-small-cell lung cancer (ICOGEN): a randomised, double-blind phase 3 non-inferiority trial. Lancet Oncol 2013;14:953-61.
14. Mok TS, Wu YL, Thongprasert S, et al. Gefitinib or carboplatin-paclitaxel in pulmonary adenocarcinoma. N Engl J Med 2009;361:947-57.
15. Garassino MC, Martelli O, Broggini M, et al. Erlotinib versus docetaxel as second-line treatment of patients with advanced non-small-cell lung cancer and wild-type EGFR tumours (TAILOR): a randomised controlled trial. Lancet Oncol 2013;14:981-8.
16. Liam CK, Wahid MI, Rajadurai P, et al. Epidermal growth factor receptor mutations in lung adenocarcinoma in

Malaysian patients. J Thorac Oncol 2013;8:766-72.
17. Choi YL, Sun JM, Cho J, et al. EGFR mutation testing in patients with advanced non-small cell lung cancer: a comprehensive evaluation of real-world practice in an East Asian tertiary hospital. PLoS One 2013;8:e56011.
18. Eisenhauer EA, Therasse P, Bogaerts J, et al. New response evaluation criteria in solid tumours: revised RECIST guideline (version 1.1). Eur J Cancer 2009;45:228-47.
19. Mitsudomi T, Morita S, Yatabe Y, et al. Gefitinib versus cisplatin plus docetaxel in patients with non-small-cell lung cancer harbouring mutations of the epidermal growth factor receptor (WJTOG3405): an open label, randomised phase 3 trial. Lancet Oncol 2010;11:121-8.
20. Maemondo M, Inoue A, Kobayashi K, et al. Gefitinib or chemotherapy for non-small-cell lung cancer with mutated EGFR. N Engl J Med 2010;362:2380-8.
21. Zhou C, Wu YL, Chen G, et al. Erlotinib versus chemotherapy as first-line treatment for patients with advanced EGFR mutation-positive non-small-cell lung cancer (OPTIMAL, CTONG-0802): a multicentre, open-label, randomised, phase 3 study. Lancet Oncol 2011;12:735-42.
22. Rosell R, Carcereny E, Gervais R, et al. Erlotinib versus standard chemotherapy as first-line treatment for European patients with advanced EGFR mutation-positive non-small-cell lung cancer (EURTAC): a multicentre, open-label, randomised phase 3 trial. Lancet Oncol 2012;13:239-46.
23. Gridelli C, Ciardiello F, Gallo C, et al. First-line erlotinib followed by second-line cisplatin-gemcitabine chemotherapy in advanced non-small-cell lung cancer: the TORCH randomized trial. J Clin Oncol 2012;30:3002-11.
24. Shepherd FA, Rodrigues Pereira J, Ciuleanu T, et al. Erlotinib in previously treated non-small-cell lung cancer. N Engl J Med 2005;353:123-32.
25. Fiala O, Pesek M, Finek J, et al. Sequential Treatment of Advanced-stage Lung Adenocarcinoma Harboring Wild-type EGFR Gene: Second-line Pemetrexed Followed by Third-line Erlotinib versus the Reverse Sequence. Anticancer Res 2013;33:3397-402.
26. Okano Y, Ando M, Asami K, et al. Randomized phase III trial of erlotinib (E) versus docetaxel (D) as second- or third-line therapy in patients with advanced non-small cell lung cancer (NSCLC) who have wild-type or mutant epidermal growth factor receptor (EGFR): Docetaxel and Erlotinib Lung Cancer Trial (DELTA). J Clin Oncol 2013;31:abstr 8006.
27. Wu YL, Lee JS, Thongprasert S, et al. Intercalated combination of chemotherapy and erlotinib for patients with advanced stage non-small-cell lung cancer (FASTACT-2): a randomised, double-blind trial. Lancet Oncol 2013;14:777-86.
28. Hirsch FR, Gandara DR. FASTACT-2: but don't act too fast. Lancet Oncol 2013;14:684-5.
29. Rodrigues-Pereira J, Kim JH, Magallanes M, et al. A randomized phase 3 trial comparing pemetrexed/carboplatin and docetaxel/carboplatin as first-line treatment for advanced, nonsquamous non-small cell lung cancer. J Thorac Oncol 2011;6:1907-14.
30. Zhang L, Ma S, Song X, et al. Gefitinib versus placebo as maintenance therapy in patients with locally advanced or metastatic non-small-cell lung cancer (INFORM; C-TONG 0804): a multicentre, double-blind randomised phase 3 trial. Lancet Oncol 2012;13:466-75.
31. Sun JM, Lee KH, Kim SW, et al. Gefitinib versus pemetrexed as second-line treatment in patients with nonsmall cell lung cancer previously treated with platinum-based chemotherapy (KCSG-LU08-01): an open-label, phase 3 trial. Cancer 2012;118:6234-42.
32. Sun Y, Ren Y, Fang Z, et al. Lung adenocarcinoma from East Asian never-smokers is a disease largely defined by targetable oncogenic mutant kinases. J Clin Oncol 2010;28:4616-20.
33. Tsujino K, Kawaguchi T, Kubo A, et al. Response rate is associated with prolonged survival in patients with advanced non-small cell lung cancer treated with gefitinib or erlotinib. J Thorac Oncol 2009;4:994-1001.
34. Hong T, Zhang R, Cai D, et al. Second-line epidermal growth factor receptor inhibitors followed by third-line pemetrexed or the reverse sequence: a retrospective analysis of 83 Chinese patients with advanced lung adenocarcinoma. J Cancer Res Clin Oncol 2012;138:285-91.
35. Wu YL, Kim JH, Park K, et al. Efficacy and safety of maintenance erlotinib in Asian patients with advanced non-small-cell lung cancer: a subanalysis of the phase III, randomized SATURN study. Lung Cancer 2012;77:339-45.
36. Chen X, Liu Y, Røe OD, et al. Gefitinib or erlotinib as maintenance therapy in patients with advanced stage non-small cell lung cancer: a systematic review. PLoS One 2013;8:e59314.

Cite this article as: Zheng Y, Fang W, Deng J, Zhao P, Xu N, Zhou J. Sequential treatment of icotinib after first-line pemetrexed in advanced lung adenocarcinoma with unknown EGFR gene status. J Thorac Dis 2014;6(7):958-964. doi: 10.3978/j.issn.2072-1439.2014.07.18

Original Article

Regional differences of nontuberculous mycobacteria species in Ulsan, Korea

Mu Yeol Lee[1*], Taehoon Lee[1*], Min Ho Kim[2], Sung Soo Byun[1], Myung Kwan Ko[1], Jung Min Hong[1], Kyung Hoon Kim[1], Seung Won Ra[1], Kwang Won Seo[1], Yangjin Jegal[1], Joseph Jeong[3], Jong Joon Ahn[1]

[1]Department of Internal Medicine, [2]Biomedical Research Center, [3]Department of Laboratory Medicine, Ulsan University Hospital, University of Ulsan College of Medicine, Ulsan, Republic of Korea

*These authors contributed equally to this article.

Correspondence to: Jong Joon Ahn, M.D., Ph.D. Associate Professor, Department of Internal Medicine, Ulsan University Hospital, University of Ulsan College of Medicine, 877 Bangeojinsunhwan-doro, Dong-gu, Ulsan, 682-714, Republic of Korea. Email: drahnjj@gmail.com.

Background: In Korea recently, nontuberculous mycobacteria (NTM) have been more frequently isolated in respiratory specimens, while *Mycobacterium tuberculosis* (MTB) isolations have decreased. The major NTM lung disease species in Korea are *M. intracellulare*, *M. avium*, and *M. abscessus*, whereas *M. kansasii* is a rare species. This retrospective study was performed to determine if there are region-specific characteristics of lung disease-causing NTM species in Ulsan, a highly industrialized city in Korea.

Methods: Between January 2010 and July 2013, the results of all acid-fast bacilli (AFB) cultures of respiratory specimens performed at Ulsan University Hospital (Ulsan, Korea) were collected. NTM were identified and regional differences of NTM species were compared.

Results: AFB cultures were performed on 33,567 respiratory specimens, obtained from 10,208 patients, during the study period. Further, 10% of the specimens (3,287/33,567) were AFB culture-positive [MTB, 2,288/3,287 (70%); NTM 999/3,287 (30%)]. The proportion of NTM isolations gradually increased between 2010 and 2013, at 25% and 38%, respectively. The most common NTM species was *M. intracellulare* (356/999, 36%), followed by *M. kansasii* (295/999, 30%), *M. avium* (161/999, 16%), *M. abscessus* (117/999, 12%) and *M. fortuitum* (39/999, 4%). This trend was maintained throughout the study period.

Conclusions: In Ulsan, NTM isolation from respiratory specimens is increasing, consistent with previous studies performed in Korea. The distribution of respiratory NTM species, however, differed from previous studies that were performed in other regions of Korea: *M. kansasii* was the second most common NTM species in Ulsan. In Ulsan, there is a regional difference in the NTM species isolated.

Keywords: Nontuberculous mycobacteria (NTM); *M. kansasii*; Ulsan

Submitted Apr 12, 2014. Accepted for publication Jun 10, 2014.
doi: 10.3978/j.issn.2072-1439.2014.07.11
View this article at: http://dx.doi.org/10.3978/j.issn.2072-1439.2014.07.11

Background

In Korea, nontuberculous mycobacteria (NTM) are frequently identified in acid-fast bacilli (AFB) respiratory cultures. Indeed, NTM isolation rates have been reported to be equal to or exceed those of *Mycobacterium tuberculosis* (MTB) (1-5). With the increasing prevalence of NTM isolations in respiratory specimens, the occurrence of NTM lung disease, which is the most common disease caused by NTM, is increasing in Korea (5).

The NTM species that cause lung disease vary between countries and regions (6-8). In the United States and Japan, *M. avium* complex (*M. intracellular* and *M. avium*) and *M. kansasii* are the major causes of NTM lung disease. In the United Kingdom, *M. kansasii* is the most prevalent species in England and Wales. By contrast, *M. malmoense* is most common in Scotland, and *M. xenopi* in southeast England. In Korea, *M. intracellulare*, *M. avium*, and

*M. abscessu*s have been reported to be the major causative species of NTM lung disease (2-4,9). In contrast, *M. kansasii* is thought to be a rare cause of NTM lung disease in Korea.

This retrospective study was performed to determine if there are region-specific characteristics of lung disease-causing NTM species in Ulsan, a highly industrialized city in Korea.

Methods

Study population

At Ulsan University Hospital, a 1,000-bed referral hospital in Ulsan South Korea, the results of AFB cultures of respiratory specimens, collected between January 2010 and July 2013, were retrospectively analyzed. Respiratory specimens included sputa and bronchoscopic specimens, which included bronchial washing fluids and bronchoalveolar lavage fluids. This study was approved by the Institutional Review Board and Ethics Committee of Ulsan University Hospital.

Acid fast bacilli culture and identification

Respiratory specimens were cultured in both solid and liquid media: 3% Ogawa solid egg-based medium (Asan Pharmaceutical, Seoul, Korea) and Mycobacteria Growth Indicator Tube liquid medium (Becton Dickinson, Sparks, MD, USA). If an AFB culture was positive in either liquid or solid medium, high performance liquid chromatography was performed to identify the mycobacterial species (10).

Diagnostic criteria for NTM lung disease

The diagnosis of NTM lung disease was performed according to the 2007 American Thoracic Society (ATS)/Infectious Diseases Society Of America (IDSA) guidelines (11).

Comparison of the major NTM species in regions of Korea

To date, there have been four detailed surveys of respiratory NTM species in Korea (2,4,9); surveys were performed at the university hospital in Seoul [Seoul Samsung Medical Center (Seoul-SMC) and Seoul National University Hospital (Seoul-SNU)] (5,9), 1 was performed at the university hospital in Jeju (4), and 1 was performed at the referral hospital in Masan (2). To determine the regional differences in NTM species in Korea, the data from the previously published papers were compared to the data obtained in this study. The raw data from the study at Seoul National University (Seoul-SNU) (5) were obtained directly from the corresponding author, as there was insufficient data in the published paper. The number of patients with respiratory NTM and the number patients with NTM lung disease were compared separately. There were data limitations: data from the Jeju study was only available for patients with respiratory NTM and date from the Seoul-SNU study was only available for patients with NTM lung disease.

Statistical analysis

Statistical analyses were performed using the software R (a language and environment for statistical computing, R Foundation for Statistical Computing, Vienna, Austria; Version 3.0.2). Independent *t*-test and Kruskal-Wallis test were used to compare means. And, Fisher's exact test and Cochran-Armitage trend test were used to compare frequencies. A P value of less than 0.05 was considered to be significant.

Results

Numbers of patients and respiratory specimens

A total 33,567 respiratory specimens from 10,208 patients were collected for AFB culture during the study period.

Mycobacterial isolations from respiratory specimens

Over the 4-year collection period, 3,287 (10%) AFB culture-positive mycobacteria were isolated from 33,567 specimens. Of the samples in which mycobacteria were isolated, 70% were positive for MTB (2,288/3,287), while the remaining 30% were positive for NTM (999/3,287).

Change in proportions of NTM and MTB isolations from respiratory specimens

The proportion of NTM isolations increased, from 25% to 38% in 2010 and 2013, respectively. Over the same time period, the proportion of MTB isolations significantly decreased (*Figure 1*; P<0.001, Cochran-Armitage trend test).

Identification of NTM species isolated from respiratory specimens

In Ulsan, the most common NTM species was *M. intracellulare* (356/999, 36%), followed by *M. kansasii* (295/999, 30%), *M. avium* (161/999, 16%), *M. abscessus* (117/999, 12%), *M. fortuitum* (39/999, 4%), *M. szulgai* (23/999, 2%),

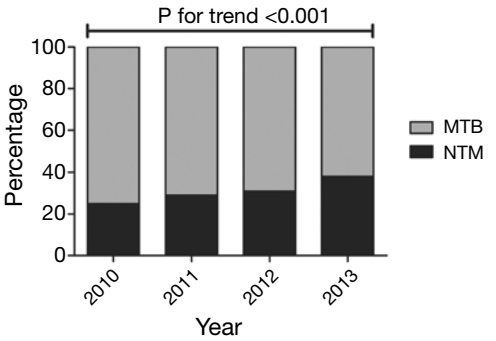

Figure 1 The proportion of nontuberculous mycobacteria (NTM) and *Mycobacterium tuberculosis* (MTB) isolations in Ulsan, Korea between January 2010 and July 2013.

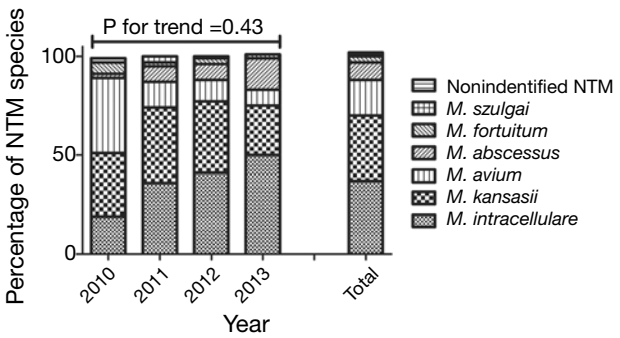

Figure 2 The proportion of nontuberculous mycobacteria (NTM) species in Ulsan, Korea between January 2010 and July 2013.

M. chelonae (3/999, 0.3%), *M. simiae* (1/999, 0.1%), and unidentified NTM (4/999, 0.4%). During the study period, *M. kansasii* was consistently the second most common NTM species (*Figure 2*; P=0.43, Cochran-Armitage trend test).

Pulmonary tuberculosis, respiratory NTM, and NTM lung disease frequency in patients

A total of 12% of patients (1,171/10,208 patients) were identified to be AFB culture-positive with mycobacteria isolated from the specimens. Of the mycobacteria infected patients, 65% (765/1,171) were diagnosed with pulmonary tuberculosis and 35% (410/1,171) were diagnosed with respiratory NTM. A total of 245 of the 410 patients diagnosed with respiratory NTM [21% (245/1,171) of all AFB culture-positive patients] were diagnosed with NTM lung disease.

In the patients diagnosed with respiratory NTM (N=410), the causative mycobacterial species were *M. intracellulare* (169/410, 41%), *M. kansasii* (102/410, 25%), *M. avium* (61/410, 15%), *M. abscessus* (33/410, 8%), *M. fortuitum* (24/410, 6%), *M. szulgai* (15/410, 4%), *M. chelonae* (3/410, 0.7%), *M. simiae* (1/410, 0.2%), and unidentified NTM (2/410, 0.5%). In the patients diagnosed with NTM lung disease (N=245), the causative mycobacterial species were *M. intracellulare* (93/245, 38%), *M. kansasii* (80/245, 33%), *M. avium* (39/245, 16%), *M. abscessus* (22/245, 9%), *M. fortuitum* (7/245, 3%), *M. szulgai* (3/245, 1%), and unidentified NTM (1/245, 0.4%).

Patients with NTM lung disease were older than those with pulmonary tuberculosis (mean age 62 and 55 years, respectively; P<0.001). There was a predominance of men in both the pulmonary tuberculosis and NTM lung disease patient populations. However, there were sex differences in the causative mycobacterial species isolated from the NTM lung disease patients. Patients with lung disease caused by *M. kansasii* were predominantly male, while patients with lung disease caused by the other NTM species were predominantly female (P<0.001; *Table 1*).

Regional differences in NTM species in patients with respiratory NTM and NTM lung disease

When the results of previous Korean NTM distribution studies were compared with the results obtained in this study, we found that in patients with respiratory NTM, the major causative species differed (*Figure 3A*). In the Masan study (2), the causative mycobacterial species were *M. intracellulare* (28/57, 49%), *M. abscessus* (12/57, 21%), *M. fortuitum* (7/57, 12%), *M. chelonae* (4/57, 7%), and *M. avium* (3/57, 5%). In the Jeju study (4), the causative mycobacterial species were *M. intracellulare* (27/62, 44%), *M. avium* (14/62, 23%), *M. abscessus* (8/62, 13%), *M. kansasii* (5/62, 8%), and *M. fortuitum* (4/62, 7%). In the Seoul-SMC study (9), the causative mycobacterial species were *M. fortuitum* (217/794, 27%), *M. abscessus* (141/794, 18%), *M. avium* (111/794, 14%), *M. intracellulare* (108/794, 14%), M. gordonae (84/794, 11%), *M. terrae* (48/794, 6%), *M. szulgai* (32/794, 4%), *M. chelonae* (25/794, 3%), and *M. kansasii* (14/794, 2%). In contrast, in Ulsan the proportion of respiratory NTM patients infected with *M. kansasii* was significantly higher (P<0.001; *Figure 3B*).

Similarly, when the distributions of NTM lung disease causative mycobacterial species were compared, the major causative species differed between the Korean regions

Table 1 Patients with pulmonary tuberculosis (*Mycobacterium tuberculosis*) and NTM lung disease in Ulsan, Korea between January 2010 and July 2013

	Patients (number)	Male (%)	P value	Age, years (mean)	P value
M. tuberculosis	765.0	56	0.825	55.2±19.6	<0.001
NTM lung disease	245.0	55		61.6±14.3	
NTM lung disease by species			<0.001		0.001
M. intracellulare	93.0	41		66.6±13.1	
M. avium	39.0	41		58.1±13.6	
M. kansasii	80.0	85		59.4±13.9	
M. abscessus	22.0	32		59.1±16.8	
M. fortuitum	7.0	29		58.9±16.2	
M. szulgai	3.0	100		62.7±15.4	
Unidentified NTM	1.0	0		38.0	

NTM, nontuberculous mycobacteria.

examined previously (*Figure 4A*). In the Masan study (2), the NTM lung disease causative mycobacterial species were *M. intracellulare* (19/26, 73%), *M. abscessus* (5/26, 19%), *M. fortuitum* (1/26, 4%), and M. chelonae (1/26, 4%). In the Seoul-SMC study (9), the NTM lung disease causative mycobacterial species were *M. abscessus* (64/195, 33%), *M. intracellulare* (56/195, 29%), *M. avium* (38/195, 19%), *M. fortuitum* (21/195, 11%), *M. kansasii* (7/195, 4%), *M. chelonae* (6/195, 3%), and *M. szulgai* (2/195, 1%). In the Seoul-SNU study (5), the major causative mycobacterial species were *M. avium* (212/585, 36%), *M. abscessus* (163/585, 28%), *M. intracellulare* (156/585, 27%), *M. kansasii* (18/585, 3%), *M. gordonae* (7/585, 1%), and *M. terrae* (4/585, 0.7%). In our study of Ulsan patients, the proportion of cases in which *M. kansasii* was the NTM lung disease causative species was significantly higher (P<0.001; *Figure 4B*).

Discussion

Similar to what has been observed previously in other regions of Korea, we showed that NTM isolation is increasing in Ulsan. However, the distribution of NTM species was different from previous studies: *M. kansasii* was the second most common NTM species in Ulsan; whereas in other regions of Korea, *M. kansasii* is rarely reported. Thus, we concluded that there is a regional difference in the NTM species isolated in Ulsan, Korea.

Consistent with previous studies, we found that in Ulsan, the proportion of NTM isolations has been increasing. Specifically, between 2010 and 2013, the proportion of NTM isolations increased from 25% to 38%. Over the same time period, the proportion of MTB isolations significantly decreased. In a previous study in Seoul, it was found that the proportion of NTM isolations increased from 22.2% in 2002 to 45.9% in 2008 (5); in a previous study in Jeju, the proportion of NTM isolations increased from 7% in 2003 to 19% in 2011 (4). The increase in NTM isolation appears to be happening throughout Korea, and the rate of NTM isolations seems to be proportionally correlated with the degree of urbanization, as Seoul is the most populated city in Korea and Jeju is a rural resort town in Korea.

Worldwide, NTM isolations have been increasing, a phenomenon that can be partially explained (3). First, improved laboratory diagnostic methods have enhanced recovery of mycobacteria (12). Second, exposure to NTM via aerosolized water is considered to be a cause of increased NTM infection in modern people (8). Finally, host factors including old age and chronic obstructive pulmonary disease are risk factors for the development of NTM disease (13). Further studies are required to fully elucidate the reason for the worldwide rapid increase in NTM isolations.

Depending on countries and/or regions, the distributions of lung disease-causing NTM species are different (6-8). In Korea, according to previous studies, *M. intracellulare*, *M. avium*, and *M. abscessus* are the major NTM lung disease species (2-4,9), in contrast, *M. kansasii* is a rare NTM lung disease species (3). In the current study, we showed that in Ulsan the distribution of NTM species differed when compared with other regions of Korea. *M. kansasii* was identified in 25% of patients with respiratory NTM and in

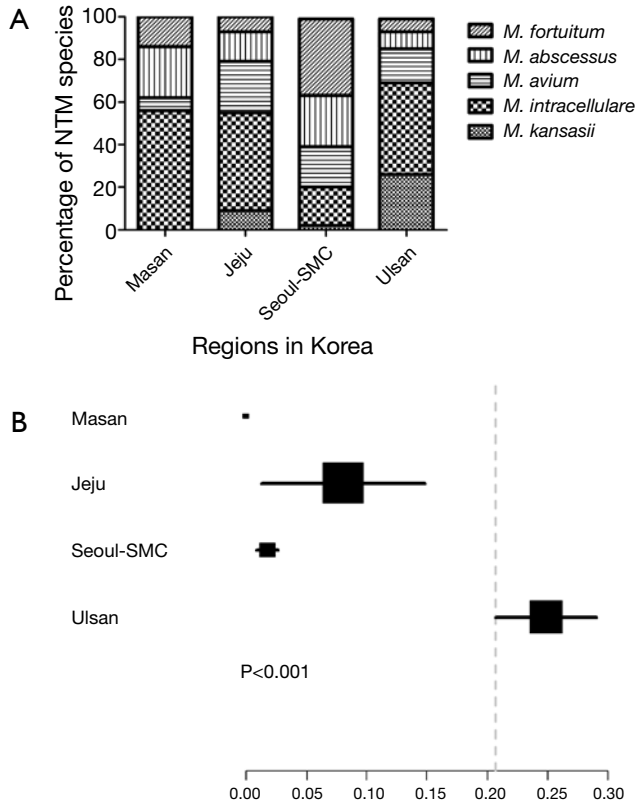

Figure 3 Nontuberculous mycobacteria (NTM) species in patients with respiratory NTM: (A) the distribution of NTM species in regions of Korea; (B) the ratios of *Mycobacterium kansasii* isolation by region of Korea. Seoul-SMC, Seoul Samsung Medical Center.

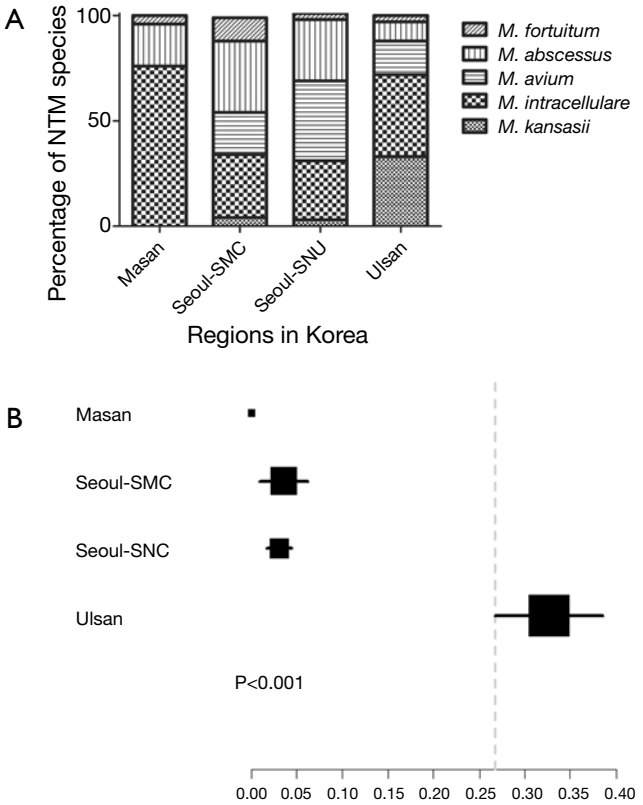

Figure 4 Nontuberculous mycobacteria (NTM) species in patients with NTM lung disease: (A) the distribution of NTM species in regions of Korea; (B) the ratios of *Mycobacterium kansasii* isolation by region of Korea. Seoul-SMC, Seoul Samsung Medical Center; Seoul-SNU, Seoul National University Hospital.

33% of patients with NTM lung disease. Thus, there is a significant regional difference in the distribution of NTM species within Korea.

The high proportion of *M. kansasii* isolations in Ulsan is not well understood. Unlike other NTM, *M. kansasii* is not found in soil or natural water supplies, but it has been recovered from tap water in cities where *M. kansasii* is endemic (11,14). In addition, *M. kansasii* is more likely to be isolated in urban or industrialized regions (14,15). However, urbanization and/or industrialization are not critical factors for M. kansasii infection, as there have been reports of rare *M. kansasii*—distribution in highly urbanized or industrialized cities (2,5,9). It is possible that there are environmental and occupational risk factors that are associated with *M. kansasii* infection. Thus, further studies to elucidate factors that are associated with *M. kansasii* infection are required.

There are limitations to this study. First, this study was a retrospective, single-center study. There may sources of bias that have not been identified or controlled for in this study. As our hospital is the only referral medical center in Ulsan, the results are likely indicative of the extent of respiratory NTM isolations in Ulsan. Second, our research identified the high proportion of *M. kansasii* species isolations in Ulsan, although we were unable to explain this observation. Therefore, further research is required.

Conclusions

In conclusion, we showed that in Ulsan respiratory NTM infection and NTM lung disease is increasing, similar to what has been observed worldwide and in other regions of Korea. However, the distribution of NTM species differed from previous studies in Korea: *M. kansasii*, a rarely

reported organism in other areas of Korea, was extremely common and was the second most commonly observed NTM species following *M. intracellulare*. Therefore, there is a regional difference in the distribution of NTM species in Ulsan, Korea.

Acknowledgements

Funding: This work was funded by Ulsan University Hospital (Biomedical Research Center Promotion Fund, UUH-2014-2).
Disclosure: The authors declare no conflict of interest.

References

1. Yoo JW, Jo KW, Kim MN, et al. Increasing trend of isolation of non-tuberculous mycobacteria in a tertiary university hospital in South Korea. Tuberc Respir Dis (Seoul) 2012;72:409-15.
2. Choi SP, Lee BK, Min JH, et al. Pathogenic Classification and Clinical Characteristics of Nontuberculous Mycobacterial Pulmonary Disease in a National Tuberculosis Hospital. Tuberc Respir Dis 2005;59:606-12.
3. Koh WJ, Chang B, Jeong BH, et al. Increasing Recovery of Nontuberculous Mycobacteria from Respiratory Specimens over a 10-Year Period in a Tertiary Referral Hospital in South Korea. Tuberc Respir Dis 2013;75:199-204.
4. Oh MS, Lee J. The Increase of Nontuberculous Mycobacterial Isolation in the Specimens from Respiratory System in Jeju. Ann Clin Microbiol 2013;16:13-8.
5. Park YS, Lee CH, Lee SM, et al. Rapid increase of non-tuberculous mycobacterial lung diseases at a tertiary referral hospital in South Korea. Int J Tuberc Lung Dis 2010;14:1069-71.
6. Koh WJ, Kwon OJ, Lee KS. Diagnosis and treatment of nontuberculous mycobacterial pulmonary diseases: a Korean perspective. J Korean Med Sci 2005;20:913-25.
7. Hoefsloot W, van Ingen J, Andrejak C, et al. The geographic diversity of nontuberculous mycobacteria isolated from pulmonary samples: an NTM-NET collaborative study. Eur Respir J 2013;42:1604-13.
8. Kendall BA, Winthrop KL. Update on the epidemiology of pulmonary nontuberculous mycobacterial infections. Semin Respir Crit Care Med 2013;34:87-94.
9. Koh WJ, Kwon OJ, Jeon K, et al. Clinical significance of nontuberculous mycobacteria isolated from respiratory specimens in Korea. Chest 2006;129:341-8.
10. Jeong J, Kim SR, Lee SH, et al. The Use of High Performance Liquid Chromatography to Speciate and Characterize the Epidemiology of Mycobacteria. Lab Med 2011;42:612-7.
11. Griffith DE, Aksamit T, Brown-Elliott BA, et al. An official ATS/IDSA statement: diagnosis, treatment, and prevention of nontuberculous mycobacterial diseases. Am J Respir Crit Care Med 2007;175:367-416.
12. Chihota VN, Grant AD, Fielding K, et al. Liquid vs. solid culture for tuberculosis: performance and cost in a resource-constrained setting. Int J Tuberc Lung Dis 2010;14:1024-31.
13. Andréjak C, Nielsen R, Thomsen VØ, et al. Chronic respiratory disease, inhaled corticosteroids and risk of non-tuberculous mycobacteriosis. Thorax 2013;68:256-62.
14. Steadham JE. High-catalase strains of Mycobacterium kansasii isolated from water in Texas. J Clin Microbiol 1980;11:496-8.
15. Rapid increase of the incidence of lung disease due to Mycobacterium kansasii in Japan. Chest 1983;83:890-2.

Cite this article as: Lee MY, Lee T, Kim MH, Byun SS, Ko MK, Hong JM, Kim KH, Ra SW, Seo KW, Jegal Y, Jeong J, Ahn JJ. Regional differences of nontuberculous mycobacteria species in Ulsan, Korea. J Thorac Dis 2014;6(7):965-970. doi: 10.3978/j.issn.2072-1439.2014.07.11

Original Article

Inhaled corticosteroids (ICS) and risk of mycobacterium in patients with chronic respiratory diseases: a meta-analysis

Songshi Ni*, Zhenxue Fu*, Jing Zhao, Hua Liu

Department of Respiratory Medicine, Affiliated Hospital of Nantong University, Nantong 226001, China

*These authors contributed equally to this paper.

Correspondence to: Hua Liu. Department of Respiratory Medicine, Affiliated Hospital of Nantong University, Nantong 226001, China. Email: ntuliuhua@126.com or ntuniversity2013@126.com.

Background: Studies have indicated that therapy with inhaled corticosteroids (ICS) can be associated with a higher risk of pneumonia. However, it is not known whether ICS increases the risk of mycobacterium. Most of these published studies were small, and the conclusions were inconsistent.

Methods: A meta-analysis was conducted into whether ICS increases the risk of mycobacterium in patients with chronic respiratory diseases. PubMed, OVID, EMBASE and Cochrane Library databases were searched.

Results: Five studies involving 4,851 cases and 28,477 controls were considered in the meta-analysis. From the pooled analyses, there was significant association between ICS and risk of mycobacterium in all patients with chronic respiratory diseases [risk ratio (RR) =1.81; 95% confidence interval (CI), 1.23-2.68; P=0.003]. Among patients with chronic respiratory diseases, the relationship between ICS and risk of tuberculosis (TB) was also significant (RR =1.34; 95% CI, 1.15-1.55; P=0.0001). And meta-analysis of four studies in patients with chronic obstructive pulmonary disease (COPD) (RR =1.42; 95% CI, 1.18-1.72; P=0.0003) or two studies in patients who have prior pulmonary TB (RR =1.61; 95% CI, 1.35-1.92; P<0.00001) or three studies in patients with high-dose ICS (RR =1.60; 95% CI, 1.28-1.99; P<0.0001) showed a relationship between ICS and risk of mycobacterium.

Conclusions: Significant relationship has been shown between ICS use and risk of mycobacterium in all patients with chronic respiratory diseases. ICS use also increases the risk of TB among the patients with chronic respiratory diseases. Use of ICS increases the risk of mycobacterium in patients with COPD or patients with prior pulmonary TB or patients inhaling high-dose corticosteroids. Further research is required to establish the potential adverse effect of ICS as a therapy for chronic respiratory diseases.

Keywords: Inhaled corticosteroids (ICS); mycobacterium; risk; meta-analysis

Submitted Dec 07, 2013. Accepted for publication Jun 10, 2014.

doi: 10.3978/j.issn.2072-1439.2014.07.03

View this article at: http://dx.doi.org/10.3978/j.issn.2072-1439.2014.07.03

Introduction

Inhaled corticosteroids (ICS) play an important role in the treatment of patients with chronic respiratory diseases, especially in the case of asthma, for which they are the most effective anti-inflammatory drugs. ICS control airway inflammation by reducing synthesis of inflammatory mediators, thus controlling the airway hypersensitivity to viral infection, allergens and irritants.

The systemic side effects of long-term treatment with ICS include easy bruising (1), adrenal suppression (2), and decreased bone mineral density (3). ICS have also been associated with cataracts (4) and glaucoma (5) in cross-sectional studies. Several recent studies of patients with chronic obstructive pulmonary disease (COPD) have reported an increased risk of pneumonia among patients treated with ICS, mainly fluticasone propionate (6-9). A recent meta-analysis (10) indicated that ICS have important

immunomodulatory effects on airways with COPD that may explain both their beneficial effects and the enhanced risk of pneumonia. Bahçeciler's study (11) suggested that inhaled corticosteroid therapy is safe in tuberculin-positive asthmatic children. Although systemic administration of corticosteroids is a known risk factor for tuberculosis (TB) (12), there is no obvious evidence that use of ICS is associated with the risk of mycobacterium. Sporadic reports (13,14) and several studies (15-21) have evaluated whether ICS increase the risk of mycobacterium. However, the sample sizes were relatively modest, and the results were inconclusive. In order to investigate the precise relationship between ICS and mycobacterium, we carried out this meta-analysis.

Methods

Search strategy

We conducted an exhaustive search for studies that examined the association of ICS with mycobacterium. We searched PubMed, EMBASE, OVID, and the Cochrane library to identify available articles published before August 2013 concerning the relationship between ICS and the risk of mycobacterium. The Medical Subject Heading (MeSH) terms and/or free words that were entered were 'ICS' or 'inhaled corticosteroid' in combination with 'TB' or 'mycobacterium'. Reviews and reference lists of relevant articles were also screened for additional articles of interest. There were no restrictions placed on language, race, ethnicity or geographic area.

Inclusion and exclusion criteria

Studies fulfilling the following selection criteria were included in this meta-analysis: (I) evaluation of the ICS and mycobacterium risk or TB; (II) using a case-control or cohort design; (III) exposure to ICS in both cases and controls should be available for estimating risk ratio (RR) and 95% confidence interval (CI); (IV) patients with chronic respiratory diseases. The exclusion criteria included: (I) reviews and abstracts; (II) the number exposure to ICS in both teams was not reported.

Quality score assessment

The quality of studies was independently assessed by two reviewers who used the quality assessment scores of the Newcastle-Ottawa Scale (NOS). The NOS assesses cohort and case-control studies in terms of selection of participants (sources and selection of cases and controls), and comparability of cases and controls and exposure (ascertainment of exposure and non-response rates) (22). Total scores ranged from 0 to 9, with a higher score meaning that the quality of the study was higher. There are only five included studies, so we cannot conduct a funnel plot.

Data term

Two investigators independently extracted data and appraised them. The data were compared and any discrepancies were resolved by discussion or a third author. From each study, we extracted the following information: first author, year of publication, study design, the number of cases and controls, and the study population (*Table 1*).

Statistical analyses

We performed a meta-analysis to assess whether exposure to ICS was associated with a risk of mycobacterium. Subgroup analyses were performed for different populations. All statistical tests were performed using Revman Software (version 5.1, Cochrane Collaboration, United Kingdom London), using RR and 95% CI for dichotomous outcomes. Cochran's Q test (23), based on the χ^2 test, was used to assess the heterogeneity between the studies. If the result of the heterogeneity test had a P value >0.10, RR was pooled according to the fixed effect model. Otherwise, the random effect model was used. A P value <0.05 was considered statistically significant.

Results

Studies included in the meta-analysis

Figure 1 outlines our study selection process. A total of 125 articles were identified after an initial search. After removing duplications, 30 articles were excluded. After reading the titles and abstracts, 76 articles were excluded because they were abstracts or reviews, or irrelevant to ICS, TB or mycobacterium. After review of the full-text articles, 14 articles were excluded from the meta-analysis, and five remained. There were two article (17,20) were excluded, for although they were well designed case-control study and the exposed factor was ICS, we could not conduct an

Table 1 Characteristic of included studies

Author	Study design	No. of subjects: all (cases/controls)	Population	NOS	Follow-up (months)	Cases
Brassard *et al.* 2011 (16)	A population-based cohort design with a nested case-control	6,204 (564/5,640)	Respiratory diseases	6	12	TB
Andrejak *et al.* 2013 (18)	Case-control	1,232 (112/1,120)	Chronic respiratory diseases	8	6	NTM
Shu *et al.* 2010 (15)	A case-control	554 (16/538)	COPD	5	46	Pulmonary TB
Lee *et al.* 2013 (20)	A nested case-control study	24,722 (4,139/20,583)	Chronic airway diseases	7	12	TB
Kim *et al.* 2013 (19)	Retrospective cohort study	616 (20/596)	COPD	6	37	Pulmonary TB

NO, number; NOS, Newcastle-Ottawa Scale; TB, tuberculosis; COPD, chronic obstructive pulmonary disease; NTM, non-tuberculosis mycobacteria.

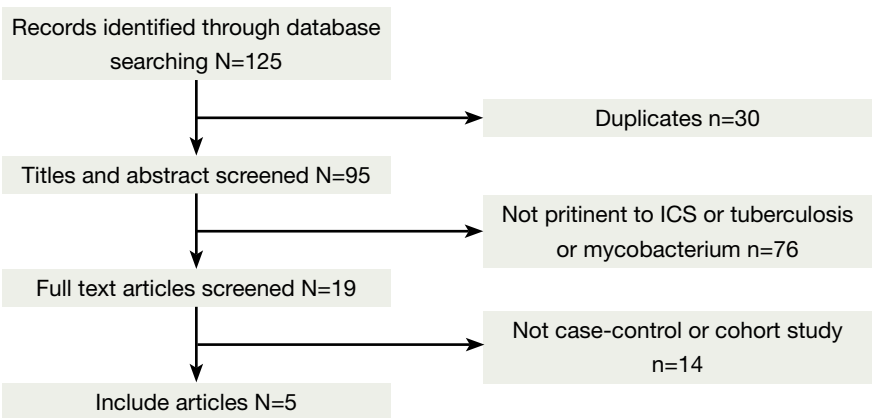

Figure 1 Study flow chart. ICS, inhaled corticosteroids.

effective fourfold table according to the data provided. Consequently, a total of five eligible studies were included in this meta-analysis, with a total sample size of 4,851 cases and 28,477 controls. One was performed in European populations, one in North American populations, and three in Asian populations. Four involved TB, and one involved non-tuberculous mycobacterium (NTM). Details of the studies are summarized in *Table 1*.

ICS and mycobacterium in chronic respiratory disease patients

A summary of the findings of the meta-analysis regarding an association between ICS and the risk of mycobacterium is provided in *Figure 2*. Meta-analysis of the five studies (4,851 cases and 28,477 control subjects) indicated significant association between ICS and the risk of mycobacterium (RR =1.81; 95% CI, 1.23-2.68; P=0.003). In addition, the outcomes of subgroup analyses are shown in *Figures 3*-7 and *Table 2*. Association was similarly found between ICS and risk of TB (*Figure 3*: RR =1.34; 95% CI, 1.15-1.55; P=0.0001). Compared with the control group, the patients who have prior pulmonary TB (*Figure 4*: RR =1.61; 95% CI, 1.35-1.92; P<0.00001) or patients with COPD (*Figure 5*: RR =1.42; 95% CI, 1.18-1.72; P=0.0003) after using ICS show an increased mycobacterium risk. There was also significant relationship between mycobacterium and ICS in patients who inhaling high-dose corticosteroids (fluticasone >500 μg/day) (*Figure 6*: RR =1.60; 95% CI, 1.28-1.99; P<0.0001). Accordingly, the equivalent doses for ICS were 100 mg beclomethasone, 50 mg beclomethasone HFA, 80 mg budesonide, 200 mg triamcinolone, 32 mg

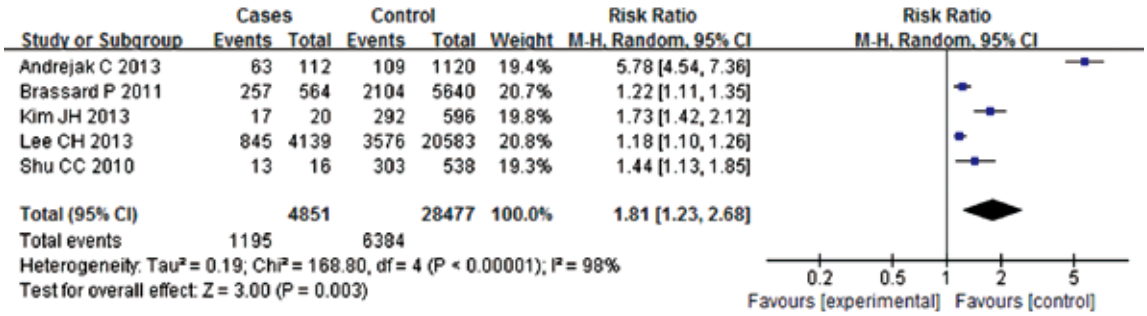

Figure 2 The relationship between ICS and mycobacterium in chronic respiratory diseases. ICS, inhaled corticosteroids.

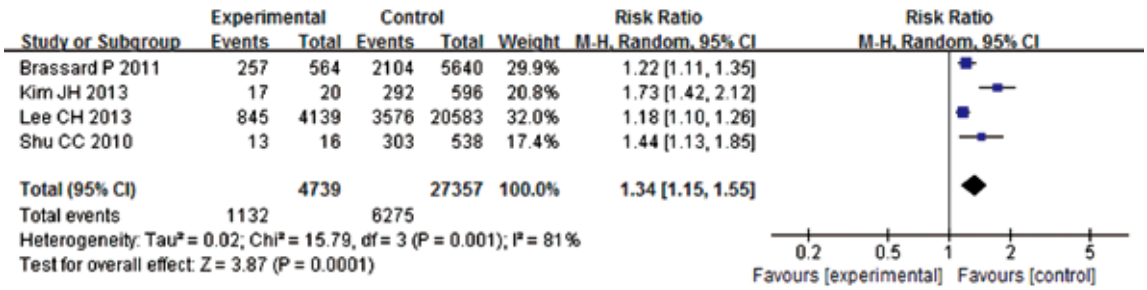

Figure 3 The relationship between ICS and tuberculosis risk. ICS, inhaled corticosteroids.

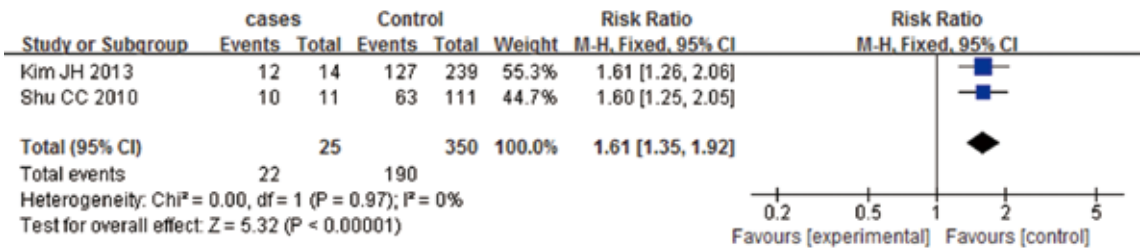

Figure 4 The relationship between ICS and mycobacterium in the patients prior to pulmonary TB. ICS, inhaled corticosteroids; TB, tuberculosis.

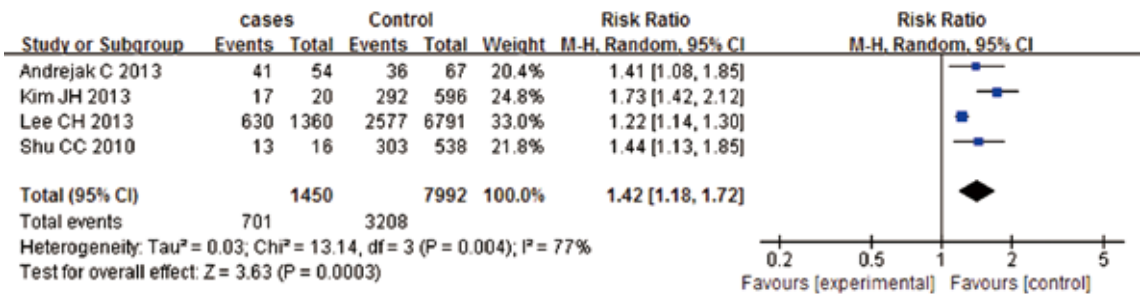

Figure 5 The relationship between ICS and mycobacterium in the patients with COPD. ICS, inhaled corticosteroids; COPD, chronic obstructive pulmonary disease.

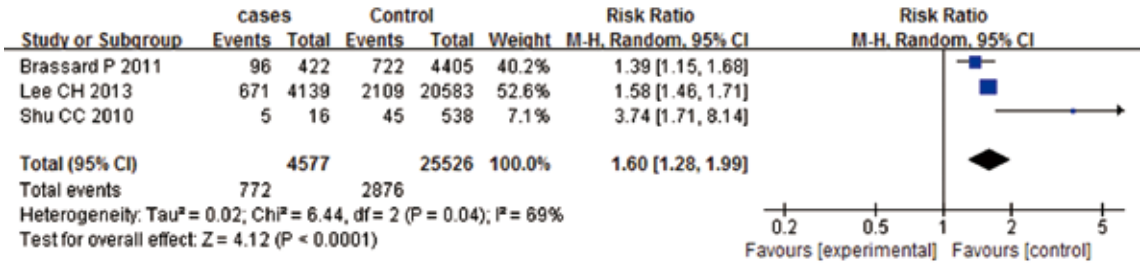

Figure 6 Relationship between mycobacterium and high-dose ICS. ICS, inhaled corticosteroids.

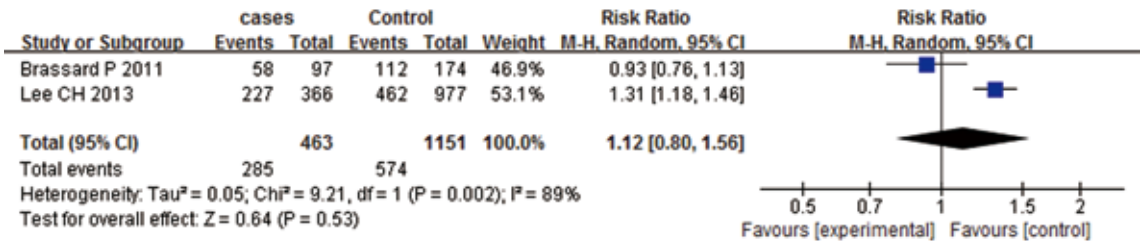

Figure 7 Relationship between mycobacterium and ICS in patients who using OCS. ICS, inhaled corticosteroids; OCS, oral corticosteroids.

Table 2 Subgroup analyses by populations between ICS and mycobacterium

Population	NO. of study	RR (95% CI)	P1	P2
Overall	5	1.81 (1.23-2.68)	0.003	<0.00001
Subgroup by population				
TB	4	1.34 (1.15-1.55)	0.0001	0.001
Prior TB	2	1.61 (1.35-1.92)	<0.00001	0.97
High doses	3	1.60 (1.28-1.99)	<0.0001	0.04
COPD	4	1.42 (1.18-1.72)	0.0003	0.004
OCS	2	1.12 (0.80-1.56)	0.53	0.002

NO, number; RR, risk ratio; CI, confidential interval; P1, P value of pooled effect; P2, P value of heterogeneity test; TB, tuberculosis; COPD, chronic obstructive pulmonary disease; OCS, oral corticosteroids; ICS, inhaled corticosteroids.

ciclesonide, 50 mg fluticasone and 200 mg flunisolide. All doses were converted to fluticasone equivalents. But we found that exposure to ICS does not increase the risk of mycobacterium in the presence of oral corticosteroids (OCS) (*Figure* 7: RR =1.12; 95% CI, 0.80-1.56; P=0.53).

Discussion

The sorts of mycobacterium are more, can be divided into mycobacterium TB, NTM and mycobacterium laprae. Mycobacterium TB is the cause of TB. Among infectious diseases, TB is one of the leading causes of mortality and morbidity worldwide, with over 95% of TB deaths occurring in low- and middle-income countries (24). Mycobacterium TB has developed strategies involving proteins and other compounds called virulence factors to subvert human host defences and damage and invade the human host. Therefore, it is an important task for us to prevent mycobacterium infection. ICS is frequently used to treat patients with chronic airway diseases, including asthma and COPD, as this is the most efficient anti-inflammatory treatment. ICS has become the first choice for long-

term treatment of persistent asthma. ICS are metabolized via the cytochrome P450 system, which is involved in biotransformation of the majority of all drugs current available. Of the various ICS available, ciclesonide has less systemic activity, and therefore is likely to be associated with fewer adverse effects of the upper airway (25). ICS do have various systemic side effects, although less than OCS, which are a recognized risk factor for the development of active TB (26). This meta-analysis was therefore performed under the hypothesis that ICS increase the risk of mycobacterium in respiratory diseases.

Overall, we can find that ICS could increase a risk of mycobacterium or TB in all patients with chronic respiratory diseases. The mechanism behind any association between ICS use and increased mycobacterium risk remains unclear. ICS could reduce local defences in peripheral airway and may exert systemic effects through partial but consistent systemic absorption. The structural abnormalities of poorly controlled chronic airway disease with remodeling may be a risk factor for mycobacterium infection. Clinicians should realize this association and do their best to confirm or exclude definitive mycobacterium infection.

Our meta-analysis reveals that patients with prior pulmonary TB have a higher risk of mycobacterium on ICS treatment. The result could provide a warming for the patients with prior pulmonary TB. The main immune protection mechanism of TB is cellular immunity and ICS could decrease local immunity of lung (27). Therefore, ICS could easily make the latent infection of mycobacterium TB to reproduction for the patients with prior pulmonary TB. For these patients, we can use less ICS or prevent it earlier. In our study, we also find that patients with COPD using ICS are at high risk for mycobacterium. While ICS have a smaller therapeutic role in COPD than asthma, patients are more at risk from side effects (28). This could be due to several reasons: firstly, patients with COPD usually use higher doses of ICS, and many side-effects are dose-related; Secondly, patients with COPD are often older and therefore may have several co-morbid conditions, making them more susceptible to the potential side effects of ICS, such as steroid bursts for COPD exacerbation; Lastly, immune suppression may be involved in the link between steroid use and increased risk of mycobacterium among COPD patients (12). Furthermore even though the guidelines points out those COPD patients of group C and D with frequent COPD exacerbations are candidates for ICS, many patients of group A and B were treated with ICS. Evidence-based guidelines have been released that support a limited role for ICS in COPD treatment (29). There are few studies examining this, and so further interventional and/or observational studies are required to investigate the relationship between ICS and mycobacterium risk in patients with COPD.

There were two prior studies (15-16) showing high dose ICS could increase the risk of TB. And our study also shows a significant relationship between high dose ICS treatment (>500 μg/day fluticasone) and the risk of mycobacterium. Glucocorticoids can interfere with the division and proliferation of lymphoid tissue under the action of antigen, and blockade the accumulation of monocytes and macrophages induced by sensitized T lymphocyte, and then suppress the immunization. ICS can attenuate the local and systemic immunity, as adverse effect is dose dependent , therefore high dose can enlarge the effect which makes it easily for the patients with high dose ICS to infect mycobacterium. Adverse effects caused by higher doses can be avoided by using combinations of different therapeutic classes. If some patients cannot avoid to use long-term high dose ICS, they should be considered to using an ICS with less systemic activity such as ciclesonide.

Some limitations of this meta-analysis should be taken into account. Firstly, this meta-analysis is limited to five studies with 33,328 subjects. This sample size is not large enough to provide decisional clinical evidence and is not well balanced. Secondly, the studies were conducted in Asian, North American and European populations only, therefore our conclusions may only be applicable to these ethnic groups. Finally, some relevant published and unpublished studies with insufficient information or with null results were excluded, which may have biased our results.

Conclusions

In conclusion, based on this meta-analysis, it can be concluded that there was significant association between ICS and mycobacterium susceptibility or TB when all patients with chronic respiratory diseases were included. Patients with COPD or prior pulmonary TB treated with ICS or patients inhaling high dose corticosteriods are at a highly increased risk of mycobacterium. More large-scale, well designed, high quality studies are required to validate our findings. More ethnicities and different types of respiratory diseases should also be considered in future studies.

Acknowledgements

Authors' contributions: Conceived and designed the experiments: NSS FZX. Performed the experiments: NSS LH. Analyzed the data: NSS ZJ. Contributed analysis tools: NSS LH. Wrote the paper: NSS FZX.

Funding: This study was supported by grants from: National Natural Science Foundation of China [No.30971306]; Nantong Social Development Project [No. S2009023]; Subject of Six Peek Talent of Jiangsu province [batch 7. No.033]; and the Project of the Fourth "226" High Level Talent of Nantong.

Disclosure: The authors declare no conflict of interest.

References

1. Mak VH, Melchor R, Spiro SG. Easy bruising as a side-effect of inhaled corticosteroids. Eur Respir J 1992;5:1068-74.
2. Lipworth BJ. Systemic adverse effects of inhaled corticosteroid therapy: A systematic review and meta-analysis. Arch Intern Med 1999;159:941-55.
3. Lung Health Study Research Group. Effect of inhaled triamcinolone on the decline in pulmonary function in chronic obstructive pulmonary disease. N Engl J Med 2000;343:1902-9.
4. Ernst P, Baltzan M, Deschênes J, et al. Low-dose inhaled and nasal corticosteroid use and the risk of cataracts. Eur Respir J 2006;27:1168-74.
5. Cumming RG, Mitchell P, Leeder SR. Use of inhaled corticosteroids and the risk of cataracts. N Engl J Med 1997;337:8-14.
6. Calverley PM, Anderson JA, Celli B, et al. Salmeterol and fluticasone propionate and survival in chronic obstructive pulmonary disease. N Engl J Med 2007;356:775-89.
7. Kardos P, Wencker M, Glaab T, et al. Impact of salmeterol/fluticasone propionate versus salmeterol on exacerbations in severe chronic obstructive pulmonary disease. Am J Respir Crit Care Med 2007;175:144-9.
8. Wedzicha JA, Calverley PM, Seemungal TA, et al. The prevention of chronic obstructive pulmonary disease exacerbations by salmeterol/fluticasone propionate or tiotropium bromide. Am J Respir Crit Care Med 2008;177:19-26.
9. Ernst P, Gonzalez AV, Brassard P, et al. Inhaled corticosteroid use in chronic obstructive pulmonary disease and the risk of hospitalization for pneumonia. Am J Respir Crit Care Med 2007;176:162-6.
10. Jen R, Rennard SI, Sin DD. Effects of inhaled corticosteroids on airway inflammation in chronic obstructive pulmonary disease: a systematic review and meta-analysis. Int J Chron Obstruct Pulmon Dis 2012;7:587-95.
11. Bahçeciler NN, Nuhoglu Y, Nursoy MA, et al. Inhaled corticosteroid therapy is safe in tuberculin-positive asthmatic children. Pediatr Infect Dis J 2000;19:215-8.
12. Jick SS, Lieberman ES, Rahman MU, et al. Glucocorticoid use, other associated factors, and the risk of tuberculosis. Arthritis Rheum 2006;55:19-26.
13. Shaikh WA. Pulmonary tuberculosis in patients treated with inhaled beclomethasone. Allergy 1992;47:327-30.
14. Smeenk FW, Klinkhamer PJ, Breed W, et al. Opportunistic lung infections in patients with chronic obstructive lung disease; a side effect of inhalation corticosteroids? Ned Tijdschr Geneeskd 1996;140:94-8.
15. Shu CC, Wu HD, Yu MC, et al. Use of high-dose inhaled corticosteroids is associated with pulmonary tuberculosis in patients with chronic obstructive pulmonary disease. Medicine (Baltimore) 2010;89:53-61.
16. Brassard P, Suissa S, Kezouh A, et al. Inhaled corticosteroids and risk of tuberculosis in patients with respiratory diseases. Am J Respir Crit Care Med 2011;183:675-8.
17. Hojo M, Iikura M, Hirano S, et al. Increased risk of nontuberculous mycobacterial infection in asthmatic patients using long-term inhaled corticosteroid therapy. Respirology 2012;17:185-90.
18. Andréjak C, Nielsen R, Thomsen VØ, et al. Chronic respiratory disease, inhaled corticosteroids and risk of non-tuberculous mycobacteriosis. Thorax 2013;68:256-62.
19. Kim JH, Park JS, Kim KH, et al. Inhaled corticosteroid is associated with an increased risk of TB in patients with COPD. Chest 2013;143:1018-24.
20. Lee CH, Lee MC, Shu CC, et al. Risk factors for pulmonary tuberculosis in patients with chronic obstructive airway disease in Taiwan: a nationwide cohort study. BMC Infect Dis 2013;13:194.
21. Lee CH, Kim K, Hyun MK, et al. Use of inhaled corticosteroids and the risk of tuberculosis. Thorax 2013;68:1105-13.
22. Cota GF, de Sousa MR, Fereguetti TO, et al. Efficacy of anti-leishmania therapy in visceral leishmaniasis among HIV infected patients: a systematic review with indirect comparison. PLoS Negl Trop Dis 2013;7:e2195.
23. Vangel MG, Rukhin AL. Maximum likelihood analysis for heteroscedastic one-way random effects ANOVA in

interlaboratory studies. Biometrics 1999;55:129-36.
24. Assam Assam JP, Penlap Beng V, Cho-Ngwa F, et al. Mycobacterium tuberculosis is the causative agent of tuberculosis in the southern ecological zones of Cameroon, as shown by genetic analysis. BMC Infect Dis 2013;13:431.
25. Boulet LP, Bateman ED, Voves R, et al. A randomized study comparing ciclesonide and fluticasone propionate in patients with moderate persistent asthma. Respir Med 2007;101:1677-86.
26. Brassard P, Lowe AM, Bernatsky S, et al. Rheumatoid arthritis, its treatments, and the risk of tuberculosis in Quebec, Canada. Arthritis Rheum 2009;61:300-4.
27. Suissa S, McGhan R, Niewoehner D, et al. Inhaled corticosteroids in chronic obstructive pulmonary disease. Proc Am Thorac Soc 2007;4:535-42.
28. Barnes PJ, Adcock IM. Glucocorticoid resistance in inflammatory diseases. Lancet 2009;373:1905-17.
29. Qaseem A, Wilt TJ, Weinberger SE, et al. Diagnosis and management of stable chronic obstructive pulmonary disease: a clinical practice guideline update from the American College of Physicians, American College of Chest Physicians, American Thoracic Society, and European Respiratory Society. Ann Intern Med 2011;155:179-91.

Cite this article as: Ni S, Fu Z, Zhao J, Liu H. Inhaled corticosteroids (ICS) and risk of mycobacterium in patients with chronic respiratory diseases: a meta-analysis. J Thorac Dis 2014;6(7):971-978. doi: 10.3978/j.issn.2072-1439.2014.07.03

Original Article

The upregulated expression of OX40/OX40L and their promotion of T cells proliferation in the murine model of asthma

Wei Lei[1*], Da-Xiong Zeng[1*], Can-Hong Zhu[2], Gao-Qin Liu[3], Xiu-Qin Zhang[1], Chang-Guo Wang[1], Qin Wang[3], Jian-An Huang[1]

[1]Department of Respiratory Medicine, The First Affiliated Hospital of Soochow University, Suzhou 215006, China; [2]Department of Respiratory Medicine, Children's Hospital of Soochow University, Suzhou 215003, China; [3]Institute of Medical Biotechnology of Soochow University, Suzhou 215007, China

*These authors contributed equally to this work.

Correspondence to: Jian-An Huang, PhD. The First Affiliated Hospital of Soochow University, No 188, Shizi Road, Gusu District, Suzhou 215006, China. Email: huang_jian_an@163.com; Qin Wang. Institute of Medical Biotechnology of Soochow University, Suzhou 215007, China. Email: qinwang96@sohu.com.

Objective: To investigate whether the expression of OX40/OX40 ligand (OX40L) was upregulated in a murine model of asthma and their significance in the pathogenesis of asthma.

Methods: After an ovalbumin-sensitized/challenged murine model of asthma was established, the expressions of OX40, OX40L in peripheral blood mononuclear cells (PBMCs) and bronchoalveolar lavage fluid (BALF) cell pellets were measured. Then T cell proliferation was analyzed by cell counting kit-8 (CCK8), and the protein levels of OX40 and OX40L in the lungs were determined by immunohistochemistry. The concentrations of IL-4 and IFN-γ in BALF and T cell culture supernatant were evaluated by ELISA.

Results: The percentages of $CD4^+OX40^+$, $CD19^+OX40L^+$, $F4/80^+OX40L^+$ in PBMCs and BALF cell pellets were higher in asthma group than in control group (all $P<0.01$). The proliferation capacity of T cells in asthma group was higher than that in control group ($P<0.05$). In asthma group, stimulation of OX40 by anti-OX40 mAb obviously promoted T cell proliferation and secretion of IL-4 and IFN-γ. Immunohistochemistry assay showed that OX40 and OX40L protein levels were higher in asthma group than those in control group (all $P<0.05$).

Conclusions: The expressions of OX40 and OX40L were upregulated in the murine asthmatic model. The upregulation of OX40/OX40L signals could induce the proliferation and cytokines secretion of T cells in asthmatic mice, indicating that OX40/OX40L signal was involved in the pathogenesis of asthma.

Keywords: Asthma; animal models; OX40; OX40 ligand (OX40L); T cell proliferation

Submitted Dec 07, 2013. Accepted for publication Jun 03, 2014.
doi: 10.3978/j.issn.2072-1439.2014.06.34
View this article at: http://dx.doi.org/10.3978/j.issn.2072-1439.2014.06.34

Introduction

Bronchial asthma (asthma) is a chronic airway inflammatory disease which is concerned with inflammatory cells including T lymphocytes, eosinophils (EOS), and the release of several inflammatory mediators (1,2). T lymphocytes play a central role in asthma. The activation of T cells requires two essential signals, while the OX40/OX40 ligand (OX40L) is a pair of important co-stimulatory signal molecules in the second-signal system (3,4).

The interactions between OX40 and OX40L regulated cytokine production from T cells and promoted antigen-specific T-cell expansion, survival and differentiation. In line with these important modulatory roles, OX40/OX40L interactions had been found to play a vital role in the pathogenesis of multiple inflammatory and autoimmune diseases, making them a research hot spot recently (5,6). In many animal models of diseases, the intervention on

OX40/OX40L pathway had achieved certain encouraging effects (7-9). Studies in the murine model of asthma showed that the use of blocking anti-OX40L mAb on intervening OX40/OX40L pathway could decrease airway hyper-responsiveness, lessen the generation of Th2 cytokines, and reduce the production of mucus (10).

OX40 is mainly expressed on activated $CD4^+$ T cells, OX40L is mainly expressed on B lymphocytes, DCs, and macrophage cells (11,12). Siddiqui S *et al.* (13) found that the expressions of OX40 and OX40L were increased in the lamina propria of asthma patients. The upexpressed OX40/OX40L promoted the polarization of naive T cells, and these polarized T cells produced Th2 cytokines such as IL-4, IL-5, and IL-13, which played an important role in asthma (14). Whether the expression of OX40/OX40L was upregulated in the asthmatic murine model, or the cells upexpressed of OX40/OX40L had some biological functions, thus contributing to the therapeutic effects of blocking anti-OX40L mAb. There are few relevant studies on this area. So our experiment was to provide insights as to the role of OX40/OX40L in the pathogenesis of asthma from the above two aspects.

Materials and methods

Establishment of asthmatic murine model

Specific pathogen free female BALB/c mice, aged 6-8 weeks and weighed 18-22 g, were randomly divided into two groups: control group and asthma group (n=8). The asthma group was sensitized with 200 μL sensitization liquid [20 μg ovalbumin (OVA) in 20 mg of aluminum hydroxide gel] on days 0, 7, 14, and challenged with 5% aerosolized OVA (Sigma, USA) for 45 min in a chamber using a nebulizer (PARI, Germany) on days 24-26. The control group was sensitized and challenged with 0.9% NaCl instead of OVA. The specific methods had slight changes on the basis of Justice JP, Mehta AK *et al.* (15,16). This study was carried out in strict accordance with the Helsinki Declaration, and was approved by the Medical Ethical Committee of Soochow University.

Measurement of airway hyper-responsiveness

The airway hyper-responsiveness was determined 24 h after the last challenge in the mice. Lung function was recorded as the index of lung resistance (RL) and dynamic compliance (Cdyn), the specific procedures referred to the methods of Pichavant M *et al.* (17).

Analysis of IL-4 and IFN-γ concentrations in bronchoalveolar lavage fluid (BALF), and OX40, OX40L expressions on BALF cell pellets

The lungs were lavaged three times with 1 mL pre-cooled (4 ℃) PBS to collect BALF, which was centrifuged at 2,000 rpm for 5 min to separate liquid from cells. The concentrations of IL-4 and IFN-γ of BALF were measured according to the instruction of the ELISA kits (eBioscience, USA). Total and differential cell counts were determined in the BALF cell pellets. Then, to detect the expressions of OX40 and OX40L, BALF cell pellets were double stained with PE-labeled anti-OX40 mAb (Biolegend, USA)/FITC-labeled anti-CD4 mAb (Immunotech, France), PE-labeled anti-OX40 mAb (Biolegend, USA)/FITC-labeled anti-CD8 mAb (Immunotech, France), PE-labeled anti-OX40L mAb/FITC-labeled anti-CD19 mAb (Immunotech, France) or PE-labeled anti-OX40L mAb/FITC-labeled anti-F4/80 mAb (Biolegend, USA) for 20 min at room temperature. After being washed, the stained cells were analyzed by flow cytometry (Beckman Coulter, USA). PE-anti-mouse IgG (mIgG) (Biolegend, USA) and FITC-anti-mIgG (Immunotech, France) were used as the controls in the experiment.

Collection of blood samples and detection the expressions of OX40, OX40L in peripheral blood mononuclear cell (PBMC)

The blood of the mice was collected in heparin tube. The blood was double stained with PE-labeled anti-OX40 mAb/FITC-labeled anti-CD4 mAb, PE-labeled anti-OX40 mAb/FITC-labeled anti-CD8 mAb, PE-labeled anti-OX40L mAb/FITC-labeled anti-CD19 mAb or PE-labeled anti-OX40L mAb/FITC-labeled anti-F4/80 mAb for 20 min at room temperature. Then the lysing reagent (Beckman Coulter, Brea, CA, USA) was added to the cell suspensions and incubated for another 10 min at 37 ℃. After being washed, the stained cells were analyzed by flow cytometry. PE-anti-mIgG and FITC-anti-mIgG were used as the controls.

Characterization of lung histology

Lung sections of 4 μm were cut and stained with hematoxylin-eosin (HE) for the evaluation of pathological changes. In addition, paraffin sections were used to test the protein levels of OX40 (eBioscience, USA), OX40L (R&D, USA) by immunohistochemistry assay. The OX40 and OX40L protein staining intensity was analyzed by Image Pro Plus

6.0 image analysis software at a magnification ×200. And integrated optical density (IOD) was used as relative amount of positive staining described as before (18).

T cell proliferation assay

Spleens were extracted and homogenized by pressing through a 40 μm nylon filter. After lymphocytes from homogenized spleens were isolated by centrifugation over Ficoll, T cells were collected by negatively selecting magnetic beads kit (Miltenyi Biotec, Germany). Then, purified $CD3^+$ T cells (1×10^5/well) from mice of control group or asthma group were cultured in anti-CD3 mAb (Abcam, USA, 2 μg/mL)-coated 96-well flat-bottom culture plates plus anti-OX40 mAb (Biolegend, USA, 5 μg/mL) or mIgG (Biolegend, USA, 5 μg/mL) as control, the intervention groups were setted as following: control (no anti-CD3 mAb intervention) wells (Con), anti-CD3 mAb intervention wells (CD3), anti-CD3 mAb + IgG (isotype control of anti-OX40 mAb) intervention wells (CD3 + IgG), anti-CD3 mAb + anti-OX40 mAb intervention wells (CD3 + OX40). CCK8 (Dojindo, Japan, 10 μL/well) was added at 68 h and optical density (OD) was measured at 450 nm by a microplate reader (Bio-rad, USA) at 72 h.

Statistical analysis

We analyzed all acquired data by SPSS 17.0 software. The differences among multiple groups were analyzed by one-way ANOVA. The difference between two groups was conducted by independent samples *t*-test. The difference was judged as statistically significant if $P<0.05$.

Results

Establishment and evaluation a murine model of asthma

Acute exacerbation of asthma symptoms

During the OVA-sensitized/challenged murine model of asthma was established, all mice in asthma group during nebulization process showed different symptoms of acute exacerbation of asthma: such as piloerection, nodding breathing, rubbing nose, forelimb contraction and raise, etc. While the mice in the control group moved about freely without the above performance.

The increase of airway hyper-responsiveness

The basal values of RL and Cdyn between the control and the asthma groups were similar. When we challenged the mice with saline and 0.025 mg/kg of methacoline, there was no significant difference of RL and Cdyn between the control and asthma group (t=1.86, 1.15; 1.68, 1.28, respectively; $P>0.05$). When we increased the dose of methacoline and challenged the mice with 0.05, 0.1, 0.2 mg/kg of methacoline, the RL in asthma group was significantly elevated compared with that in control group, while the Cdyn in asthma group was significantly decreased compared with that in control group (t=7.68, 17.10, 18.05; 3.22, 9.97, 13.08, respectively; $P<0.05$) (*Figure 1A,B*).

The increase of total and differential cell counts in the BALF cell pellets

After counting and classification of the BALF cell pellets, we found that the total number of cells, EOS, macrophages, lymphocytes, and neutrophils in asthma group were significantly higher than those in control group (t=26.22, 9.65, 9.65, 9.23, 7.35, respectively; $P<0.01$) (*Figure 1C*).

Pathological and morphological features of the lung tissues

The histopathology of the lung showed that the organization structure of the peripheral vessels, bronchioles in control group mice were clear. However, in mice of asthma group, there were lots of inflammatory cells around the airways, blood vessels, and lung tissues. The broaden alveolar septa and thickened bronchial wall were also obvious in mice of asthma group (*Figure 1D,E*).

The concentrations of IL-4 and IFN-γ in BALF of murine model of asthma

In order to validate the murine asthma model we established was successful, we determined the concentrations of IL-4 and IFN-γ in BALF. The result showed that the concentration of IL-4 in BALF of asthmatic mice was significantly higher than that in the control mice (t=14.31, $P<0.05$); instead, the concentration of IFN-γ in the BALF of asthmatic mice was significantly lower than that in the control group (t=15.28, $P<0.01$) (*Figure 1F*).

The upregulated OX40 expression on $CD4^+$ T cells and OX40L expression on B lymphocytes, mononuclear macrophages in PBMC and BALF cell pellets from murine model of asthma

In order to study the expression of OX40 and OX40L on B lymphocytes, mononuclear macrophages, and if

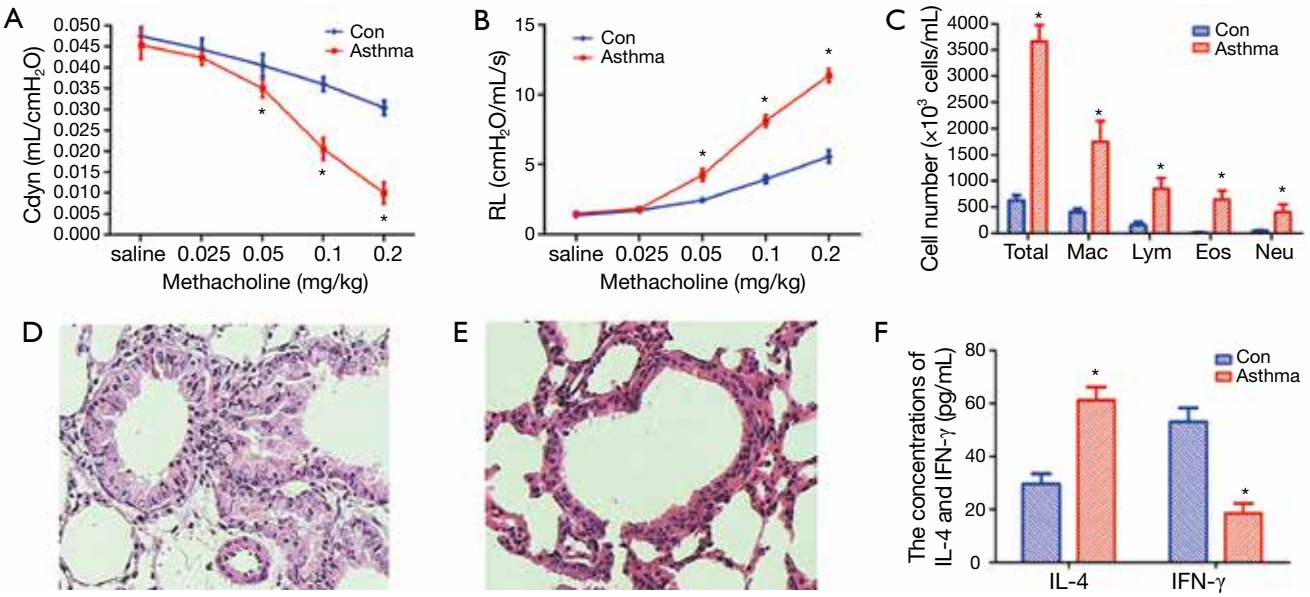

Figure 1 Establishment and evaluation of a murine model of asthma. After the OVA-sensitized/challenged murine model of asthma was established, the airway hyper-responsiveness, cell classification in BALF, the concentrations of IL-4 and IFN-γ in BALF, pulmonary histopathological examination were evaluated. (A) Cdyn to methacholine in different groups (n=8); (B) RL to methacholine in different groups (n=8); (C) Total cell counts and cell classification in BALF of different groups (×10^3/mL); (D) Pulmonary histopathological examination by HE stain in asthma group (×200); (E) Pulmonary histopathological examination by HE stain in control group (×200); (F) The concentrations of IL-4 and IFN-γ in BALF of different groups (n=8). OVA, ovalbumin; BALF, bronchoalveolar lavage fluid; Cdyn, dynamic compliance; RL, lung resistance; HE, hematoxylin-eosin; Con, control group; Asthma, asthma group; Mac, macrophages; Lym, lymphocytes; Eos, eosinophils; Neu, neutrophils; *, *vs.* control group P<0.05; bars indicated standard error.

Table 1 The expressions of OX40 and OX40L in PBMC in a murine model of asthma (%; mean ± SD, n=8)

Group	Con	Asthma	*t*	P
$CD4^+OX40^+$	1.17±0.31	4.50±0.80	11.00	<0.010
$CD8^+OX40^+$	1.48±0.68	1.58±0.74	0.28	0.783
$CD19^+OX40L^+$	4.64±0.80	8.03±1.18	6.71	<0.010
$F4/80^+OX40L^+$	11.64±1.94	23.89±6.04	5.46	<0.010

OX40L, OX40 ligand; PBMC, peripheral blood mononuclear cell; Con, control group; Asthma, asthma group.

Table 2 The expressions of OX40 and OX40L on BALF cell pellets in a murine model of asthma (%; mean ± SD, n=8)

Group	Con	Asthma	*t*	P
$CD4^+OX40^+$	2.06±0.91	8.41±1.93	8.44	<0.010
$CD8^+OX40^+$	2.09±0.92	2.14±0.97	0.11	0.917
$CD19^+OX40L^+$	15.91±4.58	29.94±7.47	4.53	<0.010
$F4/80^+OX40L^+$	8.56±2.20	28.18±4.86	10.40	<0.010

OX40L, OX40 ligand; BALF, bronchoalveolar lavage fluid; Con, control group; Asthma, asthma group.

there was a difference of OX40 and OX40L expression in different microenvironment. In PBMC, the percentages of $CD4^+OX40^+$, $CD19^+OX40L^+$ and $F4/80^+OX40L^+$ were significantly higher in asthma group than those in control group (*t*=11.00, 6.71, 5.46; P<0.01), while there was no significant difference between the percentage of $CD8^+OX40^+$ in the two groups (*t*=0.28, P=0.783) (*Table 1*). In BALF cell pellets, the percentages of $CD4^+OX40^+$, $CD19^+OX40L^+$ and $F4/80^+OX40L^+$ were also obviously higher in asthma compared with those in control group (*t*=8.44, 4.53, 10.40; P<0.01), while the percentage of $CD8^+OX40^+$ showed no significant difference between the two groups (*t*=0.11, P=0.917) (*Table 2*).

In asthma group, the percentages of $CD4^+OX40^+$ and $CD19^+OX40L^+$ in BALF cell pellets were higher than those in PBMC (*t*=5.33, 8.20; P<0.05). The percentages of $F4/80^+OX40L^+$ and $CD8^+OX40^+$ showed no significant difference between the two tissues (*t*=1.56, 1.30; P>0.05). The results indicated that the cells upregulated OX40/OX40L signal accumulated in the lungs.

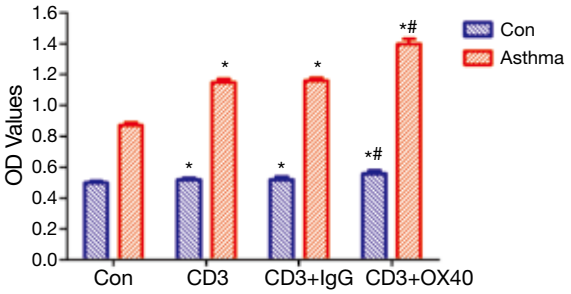

Figure 2 Effect of anti-OX40 mAb on T cell proliferation. T cells were collected by negatively selecting magnetic beads kit from homogenized spleens of control group or asthma group, purified $CD3^+$ T cells (1×10^5/mL per well) were cultured in the 37 ℃ CO_2 incubator in the 96-well plate. The intervention groups were setted as Con, CD3, CD3 + IgG and CD3 + OX40. The growth of T cells in the intervention groups was determined by Cell Counting Kit-8 assay and was showed as OD values (n=8). Con, coated without CD3; CD3, coated with CD3; CD3 + IgG, coated with CD3 and intervened with IgG (isotype of anti-OX40 mAb); CD3 + OX40, coated with CD3 and intervened with anti-OX40 mAb. OD, optical density; Con, control group; Asthma, asthma group; *, *vs.* con, P<0.05; #, *vs.* CD3 + IgG, P<0.05; bars indicated standard error.

OX40/OX40L signal promoted T cell proliferation and secretion of IL-4 and IFN-γ

In order to investigate the mechanism of OX40/OX40L signal in T cell proliferation, we conducted T cell proliferation. T cell proliferation assay showed that the OD values of Con, CD3, CD3+IgG, and CD3+OX40 in asthma group were significantly higher than those in control group (t=34.79, 52.14, 48.25, 42.93; P<0.05), indicating that the proliferative capacity of T cells in asthma group was stronger than that in control group. In both control group and asthma group, administration of agnostic anti-OX40 mAb obviously promoted T cell proliferation (P<0.05) (*Figure 2*).

In addition, we detected the concentrations of IL-4 and IFN-γ in supernatant of T cells. The results showed that the concentrations of IL-4 and IFN-γ which were secreted by T cells in all groups of asthmatic mice were significantly higher than those of the control mice (t=10.55, 20.13, 19.14, 25.46; P<0.01). In both control mice and asthmatic mice, the concentrations of IL-4 and IFN-γ in anti-OX40 mAb intervention group were higher than the other groups (P<0.05) (*Figure 3*), suggesting that OX40 could help T cells to secrete cytokines.

Upregulated OX40 and OX40L protein expressions in lung tissues

By immunohistochemistry, it was found that OX40 was mainly expressed in the cytoplasm and nucleus of lymphocytes and epithelial cells, while OX40L was mainly expressed in cytoplasm and nucleus of lymphocytes, epithelial cells and macrophages. IOD value of OX40 and OX40L in asthma group were significantly higher than those in control group (t=8.86, 15.46; P<0.01) (*Figure 4*).

Discussion

The etiology and pathogenesis of asthma are very complex. In view of the limitations of direct human experiments, the animal experiments are very important in the research of etiology, exploration of pathogenesis, and treatment evaluation. The murine asthma model has an irreplaceable role in the study of asthma (19).

Our experiment showed that the symptoms of the mice in asthma group during nebulization process were similar to the symptoms of human acute asthma attack. Compared with the mice of control group, in mice of asthma group the numbers of total cells and EOS of BALF significantly increased and the airway hyper-responsiveness was also obviously upregulated. The concentration of IL-4 in BALF was significantly higher in asthma group than that in control group. All these features showed that the murine asthma model which we established was successful (20).

OX40/OX40L was a pair of very important co-stimulatory molecules in tumor necrosis factor receptor (TNFR) family, and was one of the current research focuses (21). Studies found that in murine asthma model, the use of anti-OX40L mAb to block the OX40/OX40L signaling pathway could relieve the infiltration of EOS, decrease airway hyper-responsiveness, and lessen the generation of Th2 cytokines, which also indicated that OX40/OX40L signal played an important role in the pathogenesis of asthma (10). Whether the above effects of blocking anti-OX40L mAb indicated that there were upregulated of OX40/OX40L signal in the asthmatic murine model, there was little relevant research on this area.

OX40 is mainly expressed on activated $CD4^+$ T cells and also mildly expressed on activation of regulatory T cells, natural killer T cells, and neutrophils (22-27). There is little research on OX40 expression in the murine model of asthma. Our study found that there was low expression of OX40 on $CD4^+$ T cells in PBMC and BALF cell pellets of

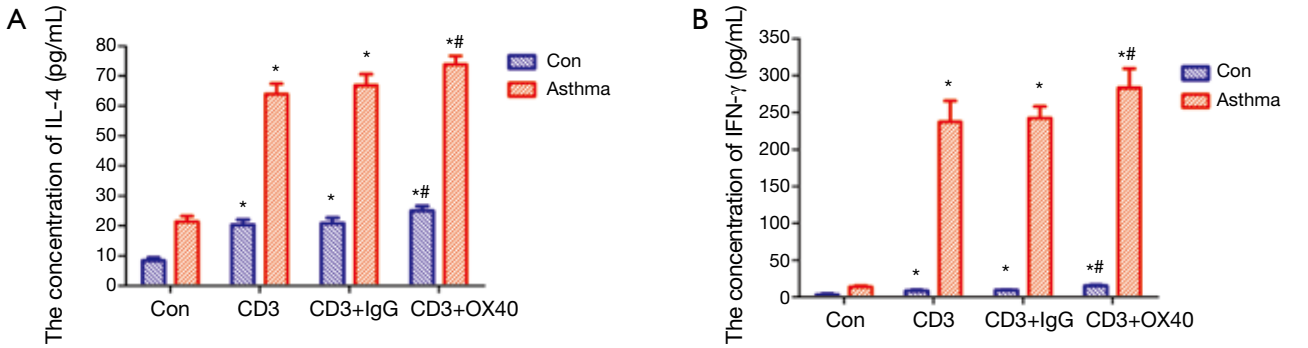

Figure 3 The concentrations of IL-4 and IFN-γ in the T cells culture supernatant. T cells were collected by negatively selecting magnetic beads kit from homogenized spleens of control group or asthma group, purified $CD3^+$ T cells (1×10^5/mL per well) were cultured in the 37 ℃ CO_2 incubator in the 96-well plate. The intervention groups were setted as Con, CD3, CD3 + IgG and CD3 + OX40. The concentrations of IL-4 and IFN-γ in the T cells culture supernatant were determined by ELISA kits (n=8). (A) The concentrations of IL-4 in the T cells culture supernatant; (B) The concentrations of IFN-γ in the T cells culture supernatant. Con, coated without CD3; CD3, coated with CD3; CD3 + IgG, coated with CD3 and intervened with IgG (isotype of anti-OX40 mAb); CD3 + OX40, coated with CD3 and intervened with anti-OX40 mAb. Con, control group; Asthma, asthma group; *, *vs.* con, P<0.05; #, *vs.* CD3 + IgG, P<0.05; bars indicated standard error.

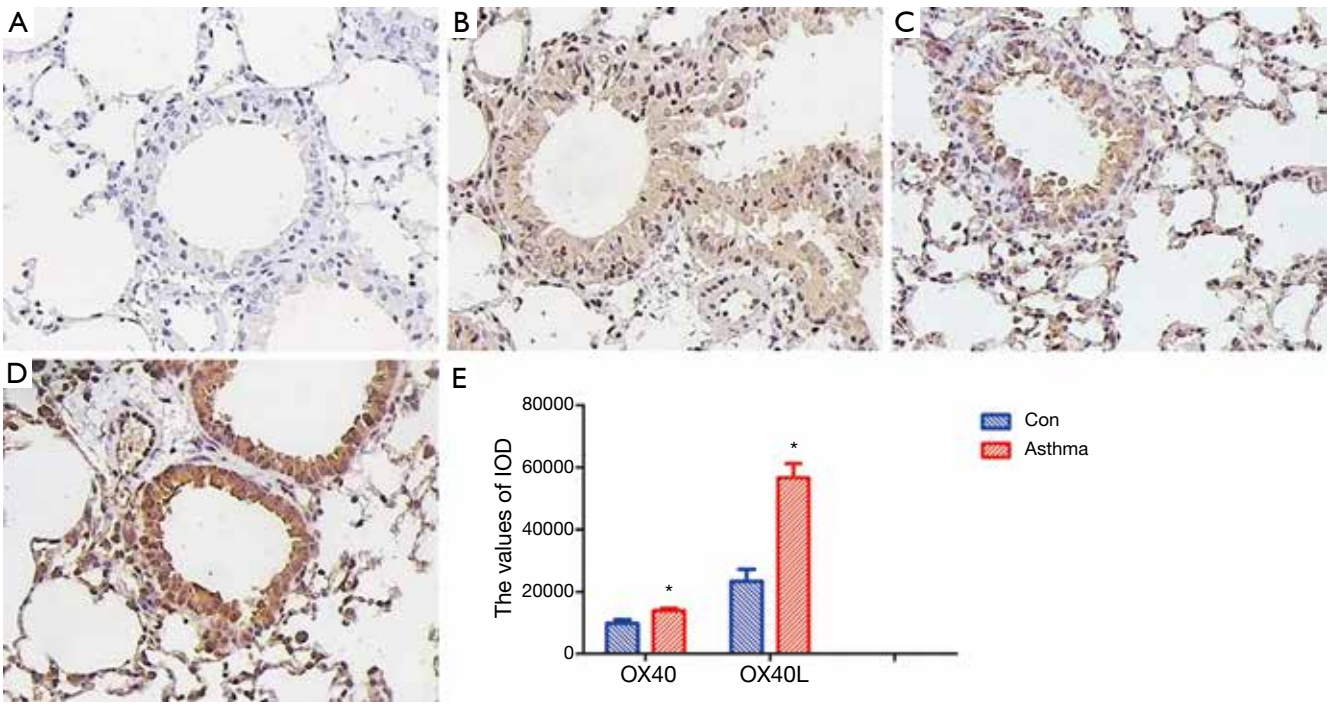

Figure 4 OX40 and OX40L protein expressions in lung tissues. (A,B) Immunohistochemistry assay for OX40 expression in lung tissues of control group mice (A) and asthma group mice (B) (×200); (C,D) Immunohistochemistry assay for OX40L expression in lung tissues of control group mice (C) and asthma group mice (D) (×200). (E) The OX40 and OX40L protein staining intensity was analyzed by Image Pro Plus 6.0 image analysis software at a magnification ×200. The expressions of OX40 and OX40L protein were showed as IOD values (n=8). OX40L, OX40 ligand; IOD, integrated optical density; Con, control group; Asthma, asthma group; *, *vs.* control group, P<0.05; bars indicated standard error.

control group. In the murine asthma model, the expression of OX40 on $CD4^+$ T cells was significantly elevated. There was low expression of OX40 on $CD8^+$ T cells in PBMC and BALF cell pellets of both control and asthma group, and there was no significant difference between the two groups. The phenomenon might also reveal the different status of $CD4^+$ and $CD8^+$ T cells in the pathogenesis of asthma.

OX40L is mainly expressed on B lymphocytes, DCs, and macrophage cells (11,12). In addition, OX40L is also expressed on the surface of Langerhans cells, smooth muscle cells, mast cells, vascular endothelial cells, and $CD4^+$ $CD3^-$ secondary cells (27-31). There is also few research on OX40L expression in the murine model of asthma. Our study showed that B lymphocytes and monocyte-macrophage cells upregulated OX40L in the PBMC and BALF cell pellets of asthma mice.

Our study also showed that the percentages of $CD4^+$ $OX40^+$, $CD19^+$ $OX40L^+$ were higher in BALF cell pellets than those in PBMC, which indicated that the cells upregulated OX40/OX40L signal accumulated in the lungs might play an important role in the pathogenesis of asthma.

Except measurement of OX40 and OX40L expressions on some cell populations by flow cytometry in the murine model of asthma, we also analyzed the OX40, OX40L protein expressions in the lung tissues by immunohistochemistry assay. The results showed that compared with the control mice, OX40 and OX40L protein expression levels were increased in the lung tissues of asthmatic mice, which was consistent with the findings of Siddiqui *et al.* (13). Our results indicated that the membrane forms of OX40 and OX40L were increased in the asthmatic mice. Previously, soluble forms of OX40L were also reported upregulated in asthmatic patients (32,33). These results suggested that there were upregulated OX40/OX40L signaling system in the murine model of asthma.

In order to know whether up-regulation of OX40 on T cells was involved in the pathogenesis of asthma, T cell proliferation assay in vitro was performed. It was found that proliferation and cytokines secretion capacity of T cells in asthmatic mice was stronger than that in control mice. In asthmatic mice, T cells stimulated by OX40 mAb *in vitro*, have significantly higher capacity of the proliferation and cytokines secretion capacity than other intervention groups, suggesting that upregulated expression of OX40/OX40L signaling pathway could promote T cell proliferation and secretion of cytokines, which contributed to the development of asthma. Whether there were other links, such as the interaction of upregulated membrane form of OX40 and soluble form of OX40L (32,33), it was worth further study.

Conclusions

In conclusion, we successfully established the murine model of asthma, and we found that there were upregulated OX40 expression on $CD4^+$ T lymphocytes, OX40L expression on B lymphocytes, and monocyte-macrophage cells in the asthmatic mice, and increased proteins of OX40, OX40L in lung tissues. We revealed the expressions of OX40 and OX40L more comprehensively in the murine asthmatic model. T cell proliferation assay in vitro showed that OX40/OX40L signaling pathway could promote the proliferation and cytokines secretion capacity of T cells. All these showed that OX40/OX40L signal pathway played an important role in the pathogenesis of asthma.

Acknowledgements

We thanked Hua Liu and Yin-Zi Zhang (Affiliated Hospital of Nantong University, Department of Respiratory Medicine) for measuring the lung function of asthmatic murine model. We thanked Taraka Venkata Pavan for editing this manuscript.

Funding: This work was supported by the social development program of Suzhou City (No: SS0706), youth science and technology project of Suzhou City (No: KJXW2012001), Clinical Key Speciality Project of China, and National Natural Science Foundation of China (No: 81300026, 81100038, 81072451).

Disclosure: The authors declare no conflict of interest.

References

1. Adcock IM, Caramori G, Chung KF. New targets for drug development in asthma. Lancet 2008;372:1073-87.
2. Asthma Workgroup; Chinese Thoracic Society; Chinese Societ of General Practitioners. Chinese guideline for the prevention and management of bronchial asthma (Primary Health Care Version). J Thorac Dis 2013;5:667-77.
3. Beier KC, Kallinich T, Hamelmann E. Master switches of T-cell activation and differentiation. Eur Respir J 2007;29:804-12.
4. Cavanagh MM, Hussell T. Is it wise to target the late costimulatory molecule OX40 as a therapeutic target?

Arch Immunol Ther Exp (Warsz) 2008;56:291-7.
5. Croft M, So T, Duan W, et al. The significance of OX40 and OX40L to T-cell biology and immune disease. Immunol Rev 2009;229:173-91.
6. Lombardi V, Singh AK, Akbari O. The role of costimulatory molecules in allergic disease and asthma. Int Arch Allergy Immunol 2010;151:179-89.
7. Yokouchi H, Yamazaki K, Chamoto K, et al. Anti-OX40 monoclonal antibody therapy in combination with radiotherapy results in therapeutic antitumor immunity to murine lung cancer. Cancer Sci 2008;99:361-7.
8. Chen M, Xiao X, Demirci G, et al. OX40 controls islet allograft tolerance in CD154 deficient mice by regulating FOXP3+ Tregs. Transplantation 2008;85:1659-62.
9. van Wanrooij EJ, van Puijvelde GH, de Vos P, et al. Interruption of the Tnfrsf4/Tnfsf4 (OX40/OX40L) pathway attenuates atherogenesis in low-density lipoprotein receptor-deficient mice. Arterioscler Thromb Vasc Biol 2007;27:204-10.
10. Salek-Ardakani S, Song J, Halteman BS, et al. OX40 (CD134) controls memory T helper 2 cells that drive lung inflammation. J Exp Med 2003;198:315-24.
11. Ito T, Amakawa R, Inaba M, et al. Plasmacytoid dendritic cells regulate Th cell responses through OX40 ligand and type I IFNs. J Immunol 2004;172:4253-9.
12. Karulf M, Kelly A, Weinberg AD, et al. OX40 ligand regulates inflammation and mortality in the innate immune response to sepsis. J Immunol 2010;185:4856-62.
13. Siddiqui S, Mistry V, Doe C, et al. Airway wall expression of OX40/OX40L and interleukin-4 in asthma. Chest 2010;137:797-804.
14. Linton PJ, Bautista B, Biederman E, et al. Costimulation via OX40L expressed by B cells is sufficient to determine the extent of primary CD4 cell expansion and Th2 cytokine secretion in vivo. J Exp Med 2003;197:875-83.
15. Justice JP, Borchers MT, Crosby JR, et al. Ablation of eosinophils leads to a reduction of allergen-induced pulmonary pathology. Am J Physiol Lung Cell Mol Physiol 2003;284:L169-78.
16. Mehta AK, Gaur SN, Arora N, et al. Effect of choline chloride in allergen-induced mouse model of airway inflammation. Eur Respir J 2007;30:662-71.
17. Pichavant M, Goya S, Hamelmann E, et al. Animal models of airway sensitization. Curr Protoc Immunol 2007;Chapter 15:Unit 15.18.
18. Liang W, Chen C, Shi J, et al. Disparate effects of eplerenone, amlodipine and telmisartan on podocyte injury in aldosterone-infused rats. Nephrol Dial Transplant 2011;26:789-99.
19. Al Heialy S, McGovern TK, Martin JG. Insights into asthmatic airway remodelling through murine models. Respirology 2011;16:589-97.
20. Lee MY, Yuk JE, Kwon OK, et al. Anti-inflammatory and anti-asthmatic effects of Viola mandshurica W. Becker (VM) ethanolic (EtOH) extract on airway inflammation in a mouse model of allergic asthma. J Ethnopharmacol 2010;127:159-64.
21. Beier KC, Kallinich T, Hamelmann E. Master switches of T-cell activation and differentiation. Eur Respir J 2007;29:804-12.
22. Mallett S, Fossum S, Barclay AN. Characterization of the MRC OX40 antigen of activated CD4 positive T lymphocytes--a molecule related to nerve growth factor receptor. EMBO J 1990;9:1063-8.
23. So T, Lee SW, Croft M. Immune regulation and control of regulatory T cells by OX40 and 4-1BB. Cytokine Growth Factor Rev 2008;19:253-62.
24. Marschner A, Rothenfusser S, Hornung V, et al. CpG ODN enhance antigen-specific NKT cell activation via plasmacytoid dendritic cells. Eur J Immunol 2005;35:2347-57.
25. Zaini J, Andarini S, Tahara M, et al. OX40 ligand expressed by DCs costimulates NKT and CD4+ Th cell antitumor immunity in mice. J Clin Invest 2007;117:3330-8.
26. Liu C, Lou Y, Lizée G, et al. Plasmacytoid dendritic cells induce NK cell-dependent, tumor antigen-specific T cell cross-priming and tumor regression in mice. J Clin Invest 2008;118:1165-75.
27. Zingoni A, Sornasse T, Cocks BG, et al. Cross-talk between activated human NK cells and CD4+ T cells via OX40-OX40 ligand interactions. J Immunol 2004;173:3716-24.
28. Burgess JK, Carlin S, Pack RA, et al. Detection and characterization of OX40 ligand expression in human airway smooth muscle cells: a possible role in asthma? J Allergy Clin Immunol 2004;113:683-9.
29. Nakae S, Suto H, Iikura M, et al. Mast cells enhance T cell activation: importance of mast cell costimulatory molecules and secreted TNF. J Immunol 2006;176:2238-48.
30. Kashiwakura J, Yokoi H, Saito H, et al. T cell proliferation by direct cross-talk between OX40 ligand on human mast cells and OX40 on human T cells: comparison of gene expression profiles between human tonsillar and lung-cultured mast cells. J Immunol 2004;173:5247-57.

31. Gaspal FM, Kim MY, McConnell FM, et al. Mice deficient in OX40 and CD30 signals lack memory antibody responses because of deficient CD4 T cell memory. J Immunol 2005;174:3891-6.
32. Ezzat MH, Imam SS, Shaheen KY, et al. Serum OX40 ligand levels in asthmatic children: a potential biomarker of severity and persistence. Allergy Asthma Proc 2011;32:313-8.
33. Lei W, Zhu CH, Zeng da X, et al. SOX40L: an important inflammatory mediator in adult bronchial asthma. Ann Acad Med Singapore 2012;41:200-4.

Cite this article as: Lei W, Zeng DX, Zhu CH, Liu GQ, Zhang XQ, Wang CG, Wang Q, Huang JA. The upregulated expression of OX40/OX40L and their promotion of T cells proliferation in the murine model of asthma. J Thorac Dis 2014;6(7):979-987. doi: 10.3978/j.issn.2072-1439.2014.06.34

Original Article

Relation of late gadolinium enhancement in cardiac magnetic resonance on the diastolic volume recovery of left ventricle with hypertrophic cardiomyopathy

Xiaorong Chen[1,2], Hongjie Hu[2], Yue Qian[2], Jiner Shu[1]

[1]Department of Radiology, Sir Run Run Shaw Hospital, Zhejiang University, Hangzhou 310016, China; [2]Department of Radiology, Jinhua Municipal Central Hospital, Jinhua Hospital of Zhejiang University, Jinhua 321000, China

Correspondence to: Hongjie Hu. Department of Radiology, Sir Run Run Shaw Hospital, Zhejiang University, Hangzhou 310016, China. Email: hongjiehu@zju.edu.cn.

Objective: The purpose of the study was to investigate the influence of late gadolinium enhancement (LGE) on the diastolic volume recovery of left ventricle in patients with hypertrophic cardiomyopathy (HCM).

Methods: Twenty-four HCM patients were studied through report-card 4.0. The presence or absence of late gadolinium enhancement was recorded according to a standardized methodology with a threshold value of six standard deviations above background. The LGE positive and negative groups were correlated to left ventricular end diastolic volume index (EDVI), left ventricular mass, left ventricular ejection fraction (EF), peak filling rate (PFR), peak ejecting rate (PER), normalized peak filling or ejecting rate (NPFR or NPER), time to peak filling or ejecting rate (TPFR or TPER), and diastolic volume recovery (DVR).

Results: PFR, NPFR, SV, SVI, EF, CO, CI, FS in LGE positive group were lower than LGE negative group, DVR_{10-40}, DVR_{100}, end systolic volume (ESV), end systolic volume index (ESVI), ESD were higher in LGE positive group, and the differences were statistically significant. The average LGE mass (ROI, region of interest) was 20.78 g, about 13.67% of left ventricle mass in LGE positive HCM group. Pearson correlation was noted between the LGE percent (ROI%) and ESV (0.692, $P<0.05$), ROI% and EF (–0.718, $P<0.05$), ROI% and PFR (–0.534, $P<0.05$), DVR_{20-40} (0.547, 0.544, 0.906, $P<0.05$) etc. The correlation between ROI% and DVR_{40} was best (0.906, $P<0.05$), and the correlation between ROI% and ESVI, ROI% and EF were both bigger than 0.7, showed the correlation was good.

Conclusions: In addition to common quotas used to assess the structure and function of left ventricle in HCM, volume-time curve parameters may have potential to evaluate cardiac function in HCM. The correlation between DVR generated from volume-time curve with LGE was good, and may be a marker of effect of enhancement/scar tissue on diastolic function.

Keywords: Hypertrophic cardiomyopathy (HCM); volume-time curve; magnetic resonance imaging; late gadolinium enhancement (LGE)

Submitted Apr 21, 2014. Accepted for publication May 19, 2014.
doi: 10.3978/j.issn.2072-1439.2014.06.37
View this article at: http://dx.doi.org/10.3978/j.issn.2072-1439.2014.06.37

Introduction

Cardiac magnetic resonance (CMR) plays an important role in the diagnosis of hypertrophic cardiomyopathy (HCM). Besides routine evaluation of cardiac structure and function, late gadolinium enhancement (LGE) of myocardium has the potential to demonstrate replacement fibrosis, a potential marker of poor outcome LGE was considered replacement of fibrosis (1). Pathologically, fibrotic myocardium is believed to be the basis of re-entrant ventricular arrhythmia as well as myocardial dysfunction. Quite a few studies (2-5) had demonstrated prognostic value of LGE in HCM recently. Presence and extent of LGE have been shown to

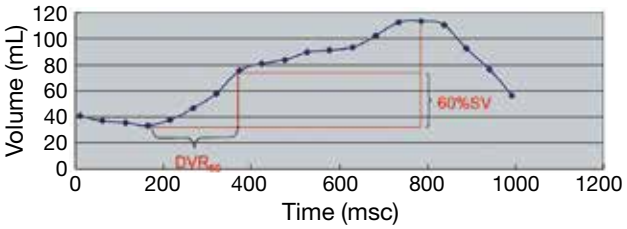

Figure 1 DVR60: the proportion of diastole required to recover 60% left ventricular stroke volume.

correlate with the incidence of major adverse cardiac events (MACE), and has prognostic value which is additive to standard clinical markers.

LGE affects the prognosis of HCM patients, but the changes on cardiac structure and function associated with LGE from the fibrosis (6) may affect prognosis because of altered diastolic function. Diastolic dysfunction usually appears before systolic function in HCM (7), but is generally not assessed on clinical CMR. Left ventricular volume filling curve or volume time curve is a potential method to evaluate diastolic function, but little clinical date is available in patients with HCM. Early data from Kawaji *et al.* (8) and Motoyasu *et al.* (7) found the reduced diastolic function in HCM patients compared with normal volunteers, but the relationship of these findings to factors that have been shown related with prognosis, such as LGE, are unclear. Our study was to assess correlation between diastolic function and presence or absence of LGE.

Materials and methods

Patients population

It was a retrospective study. A total of 34 consecutive patients with HCM undergoing CMR were studied from January 2010 to November 2012. The clinical diagnosis of HCM was established with echocardiography, CMR, electrocardiogram, laboratory examination, family history and other clinical data. The patients with atrial fibrillation and claustrophobia were excluded before examination. Ten patients were excluded because of former alcohol ablation (six patients) or no contrast scan (four patients). The rest 24 patients were composed of 13 obstructive HCM patients and 11 non-obstructive HCM (three apical obstructive HCM patients). These 24 patients were divided into two groups, LGE positive group and LGE negative group. The study was approved by the institutional ethics committees, and every patient was gave informed consent before examination.

CMR protocol

CMR images were obtained on a 1.5-T system (Signa CV/i, GE Healthcare, Milwaukee, USA), using an eight channel phased array coil and electrocardiographic triggering. All patients underwent an standard examination, which included a short axis bright-blood cine sequence (Fiesta) covering the entire left ventricule with a slice thickness of 8 mm, gap of 2 mm, TR/TE =35/1.5 ms, FLIP angle =45°, FOV =360 mm × 280 mm, VPS (views per segment) =14, slice reconstructed cardiac phases =20. Myocardial delay enhancement (MDE) images were acquired about ten minutes after the injection of 0.2 mmol/kg of GD-DTPA (Magnevist, Schering, Berlin, Germany), TR =6.5 ms, TE =3.0 ms, FLIP angle =20°, FOV =360 mm × 270 mm, VPS =24, slice thickness =8 mm, gap =2 mm, TI = 170-280 ms, including two-chamber view, four-chamber view and axial images (about 6-9 slices from the apex to base).

Images analysis

Automated segmentation of left ventricle

Automated segmentation of left ventricle was performed using report-card 4.0 (GE Health Care, USA). Indices obtained included end systole volume (ESV), end diastole volume (EDV), left ventricular ejection fraction (EF), peak ejecting rate (PER), normalized peak ejecting rate (NPER), time to peak ejecting rate (TPER), peak filling rate (PFR), normalized peak filling rate (NPFR), time to peak filling rate (TPFR) and diastolic volume recovery (DVR) (9) (*Figure 1*). Left ventricular volume was defined as the range from the apex to annulus of mitral valve, the papillary muscle was excluded from the volume and included in the left ventricular mass (10). At the base, slices were deemed to be within the left ventricle when the volume was encircled by 50% or more of ventricular myocardium (11), otherwise, they were considered to be within the left atrium and excluded. The function of LV analysis was part of report-card 4.0, it was used for analyzing the left ventricular filling curve. The endomyocardium was segmented automatically in all axial images that were defined as left ventricular volume, and the curve of left ventricular filling was generated, along with the indexes of cardiac function.

The algorithm of EDV, ESV was on the basis of the Simpson algorithm.EF=[(EDV–ESV)/EDV]×100%.

PFR=ΔV/ΔT, PFR is the peak rate of left ventricular filling, calculated from the difference between two continuous cardiac phases, then divided by the time between

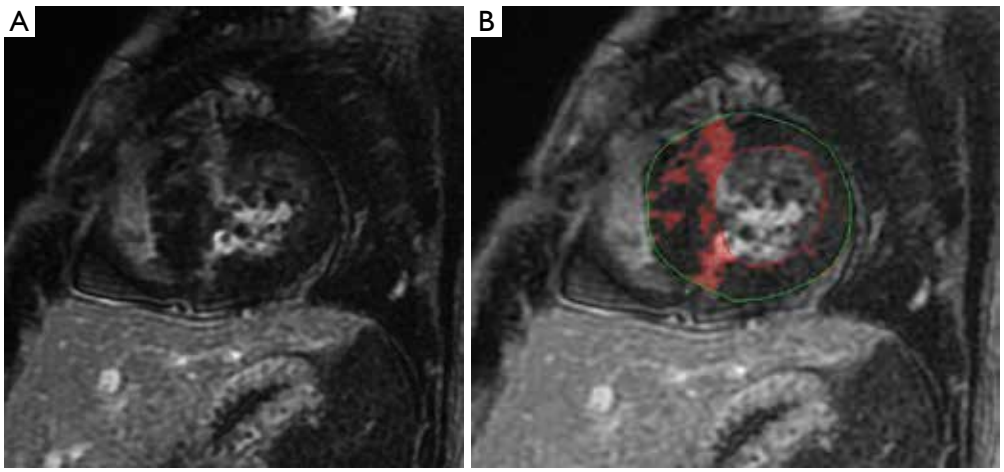

Figure 2 (A) The axial MDE image; (B) the red area shows the extent of LGE (calculated automatically through report-card 4.0).

two cardiac phases.

PER=ΔV/ΔT, PER is the peak rate of left ventricular ejecting, calculated from the difference between two continuous cardiac phases, then divided by the time between two cardiac phases.

NPFR=PFR/EDV, normalized PFR.

NPER=PER/EDV, normalized PER.

TPFR is the time between end systole and PFR. TPER meant the time between end diastole and PER, DVR was defined as the percent of the time of diastolic volume recovery that occupying the diastolic time.

DVR_{60} is the proportion of diastole required to recover 60% left ventricular stroke volume (*Figure 1*).

DVR_{10}-DVR_{100} was calculated through Matlab R2011a (Mathworks, USA).

The wall thickening of left ventricle (WT%) = (wall thickness at end systole-wall thickness at end diastole)/wall thickness at end systole. Fractional shortening (FS) of left ventricle = (end diastole diameter-end systole diameter)/end diastole diameter ×100%, left ventricular remodeling index (LVRI) = left ventricular mass/EDV (12), left ventricular mass was the mass calculated at diastole. The ratio of wall thickness (RWT) = the thickness of hypertrophied wall/the thickness of normal wall.

LGE analysis

Quantitative evaluation of LGE was performed with myocardial evaluation (ME), part of report-card 4.0. A region (about 50 mm^2) of interest (ROI) was placed in each slice of axial MDE images, and the signal intensity was acquired [mean + standard deviation (SD)]. The extent of LGE was calculated automatically in each slice, as well as the mass of LGE, and the proportion of total left ventricular mass, according to the formula (the threshold = mean + 6SD) (13), (*Figure 2A,B*). The last step was to check the extent of LGE, and made some adjustment by an experienced radiologist (more than five years' experience in CMR).

Statistical analysis

All data was presented as mean ± SD or percentage. *t*-test of independent samples was used to analyze the continuous data between the positive group and negative group. Non-parametric test was used to analyze the categorical variables. The correlation between variables was analyzed with Pearson correlation or Spearman correlation. The former one was for continuous data, and the latter one for categorical variables. Statistical analysis was performed using SPSS for windows (version 16.0; SPSS Inc., Chicago, IL, USA). P value <0.05 was considered statistically significant.

Results

In the 24 HCM patients, 16 patients were LGE positive, and eight were LGE negative. The incidences of diabetes mellitus, hypertension, family history, and NYHA class were not significant between two groups (*Table 1*). The indexes of LGE positive group such as $DVR_{10\text{-}40}$, DVR_{100}, ESV, ESVI and ESD were greater than LGE negative group. The indexes of, FS, NPFR, SV, SVI, EF, CO, CI and FS were

Table 1 Patients characteristics

	LGE positive	LGE negative	P
Gender (m/f)	9/16	4/8	0.772
Age (y)	49.75±13.96	55.62±13.71	0.339
BSA (m^2)	1.75±0.15	1.64±0.13	0.079
Family history	1	1	0.529
Hypertension	4	3	0.525
Diabetes mellitus	1	1	0.602
Coronary heart disease	2	2	0.439
NYHA class	1.38±0.72	1.88±1.13	0.198
ECG (LV diastolic dysfunction)	7	5	0.386

LGE, late gadolinium enhancement.

Table 2 The difference of structure and clinical function between LGE positive and LGE negative group

	LGE positive [16]	LGE negative [8]	P
EDV (mL)	141.89±38.61	137.26±22.16	0.758
ESV (mL)	45.79±31.61	20.78±5.16	0.039
SV (mL)	96.09±18.70	116.48±19.23	0.021
EDVI (mL/m^2)	80.80±18.72	83.71±14.37	0.704
ESVI (mL/m^2)	25.77±15.80	12.54±2.43	0.029
SVI (mL/m^2)	55.63±10.41	71.16±13.36	0.005
EF (%)	69.47±10.48	84.75±2.71	0.001
CO (mL/min)	6.79±1.22	8.03±1.18	0.027
CI (mL/min·m^2)	3.88±0.67	4.90±0.78	0.003
Mass (g)	179.67±57.39	197.59±24.65	0.411
FS (%)	39.50±8.16	43.38±3.16	0.001
WT (%)	23.32±14.90	16.63±4.83	0.118
EDD (mm)	51.19±6.69	46.38±5.32	0.091
ESD (mm)	30.94±7.20	23.23±3.07	0.010
WT (mm)	24.00±5.90	22.25±3.69	0.454
RWT	2.72±0.69	2.24±0.40	0.082
LVRI (g/mL)	1.30±0.37	1.46±0.24	0.288

LGE, late gadolinium enhancement; EDV, end diastolic velocity; ESV, end systolic volume; EDVI, end diastolic velocity index; EF, ejection fraction; FS, fractional shortening; RWT, relative wall thickness.

Table 3 The difference of indexes generated from left ventricular filling curve between LGE positive and LGE negative group

	LGE positive [16]	LGE negative [8]	P
PFR (mL/s)	356.90±115.58	521.87±113.66	0.003
NPFR (mL/s·mL)	4.80±1.18	6.55±1.25	0.003
TPFR (ms)	284.31±169.07	184.50±100.70	0.085
PER (mL/s)	511.58±157.95	583.23±91.36	0.251
NPER (mL/s·mL)	7.16±1.04	6.58±0.97	0.198
TPER (ms)	649.94±76.71	626.62±75.35	0.417
DVR_{10}	0.15±0.04	0.11±0.05	0.014
DVR_{20}	0.19±0.04	0.14±0.05	0.009
DVR_{30}	0.23±0.06	0.17±0.06	0.025
DVR_{40}	0.28±0.07	0.19±0.06	0.011
DVR_{50}	0.31±0.08	0.23±0.09	0.050
DVR_{60}	0.35±0.09	0.27±0.11	0.062
DVR_{70}	0.42±0.08	0.33±0.13	0.051
DVR_{80}	0.52±0.10	0.44±0.11	0.089
DVR_{90}	0.60±0.10	0.52±0.10	0.079
DVR_{100}	0.70±0.10	0.60±0.10	0.031

LGE, late gadolinium enhancement; PFR, peak filling rate; NPFR, normalized peak filling rate; TPFR, time to peak filling rate; PER, peak ejecting rate; NPER, normalized peak ejecting rate; TPER, time to peak ejecting rate; DVR, diastolic volume recovery.

smaller in LGE positive group, but the differences were still statistically significant (*Tables 2,3*). In the LGE positive group, the average LGE mass (ROI) was 20.78 g, the mean LGE proportion (ROI%) was 13.67% among 16 LGE positive patients. The correlation analysis between the extent of LGE and structural and functional indexes showed that LGE (ROI%) was correlated with ESV, EF, FS, PFR, TPER, DVR_{20-50}, DVR_{80}, all P values <0.05 (*Table 4*). The most correlative index was DVR_{40}, the correlation coefficient was 0.906. The LGE (ROI%) correlated with ESV, ESVI, EF well; the correlation coefficients were both greater than 0.7 (*Figures 3,4*).

Discussion

Our study highlights the potential of novel MR markers of diastolic function to provide additional, potentially prognostic data in patients with hypertrophic cardiomyopathy. Previous work has shown it feasible to evaluate heart diseases through the left ventricular filling curve (9,14,15). Currently, there is much interest in LGE in cardiomyopathies such as HCM seen on CMR (7,8,16). The correlation between LGE and the changes of structure and function also were seen in recent studies (15,17,18). The study of Choi *et al.* (17) revealed the extent of LGE

Table 4 The correlation between LGE and cardiac structure and function

	ROI	ROI%
ESV (mL)	0.816*	0.692*
SV (mL)	–0.042	–0.19
ESVI (mL/m^2)	0.811*	0.709*
SVI (mL/m^2)	–0.165	–0.215
ESD (mm)	0.639*	0.616*
EF	–0.766*	–0.718*
CO (mL/min)	0.064	–0.017
CI (mL/min·m^2)	–0.056	–0.017
FS	–0.46	–0.523*
PFR (mL/s)	–0.35	–0.534*
NPFR (mL/s·mL)	–0.316	–0.436
DVR_{10}	0.301	0.414
DVR_{20}	0.368	0.547*
DVR_{30}	0.349	0.544*
DVR_{40}	0.754*	0.906*
DVR_{100}	–0.009	0.206

*, means P<0.05; LGE, late gadolinium enhancement; ESV, end systolic volume; EF, ejection fraction; FS, fractional shortening; PFR, peak filling rate; NPFR, normalized peak filling rate; DVR, diastolic volume recovery.

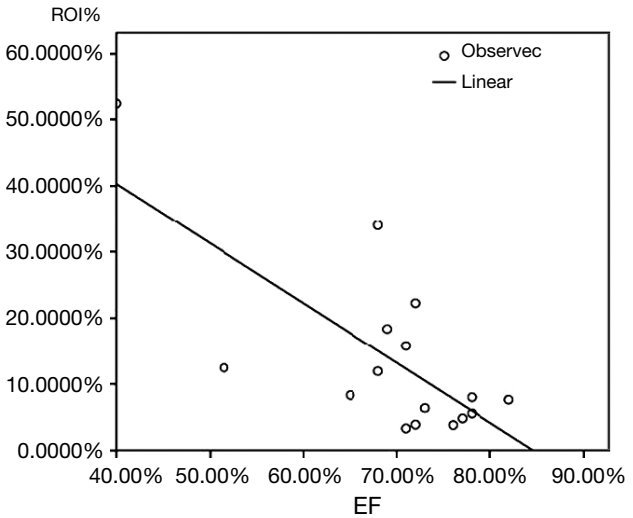

Figure 3 The correlation between ROI% and EF, the correlation coefficient was 0.718.

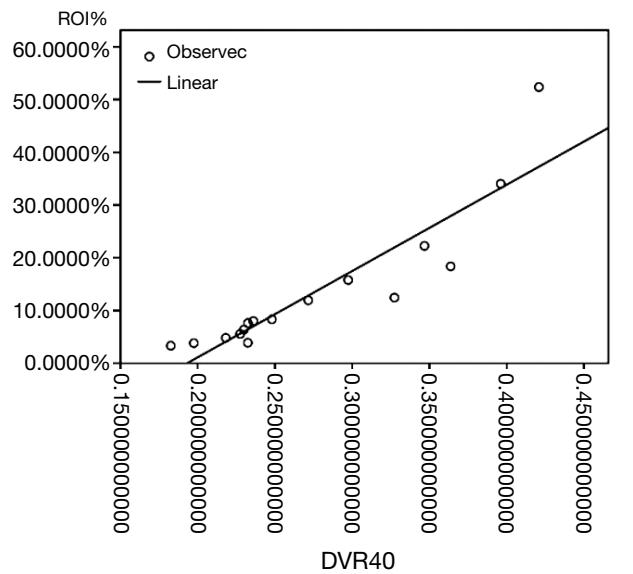

Figure 4 The correlation between ROI% and DVR40, the correlation coefficient was 0.906.

correlated with PFR, TPFR and NPFR. Another research done by Catalano *et al.* (15) showed the extent of LGE correlated with the size of left atrium. However, there were few studies on the correlation between DVR and the extent of LGE. In our study, a negative correlation between LGE and PFR was observed, and correlation between LGE and DVR was also found.

In contrast to the LGE negative group, indexes of the LGE positive group, such as ESV, $DVR_{10\text{-}40}$, DVR_{100}, ESV, ESVI and ESD were greater, and, FS, NPFR, SV, SVI, EF, CO and CI were smaller. It is possible that this is related to the extent of fibrosis revealed by LGE. We believed that the higher extent of fibrosis led to the more severely remodeling LV structure. Though EF and FS decreased more in the LGE positive group, the mean value of EF was still in normal range. Our study showed that the EF and FS was normal in LGE positive group, it was significantly lower than LGE negative positive group. The possible reason could be relative to the higher systolic function in HCM patients (higher EF and FS) compared normal individuals. The relations of LGE on diastolic function was suggested by changes in PFR, NPFR, $DVR_{20\text{-}40}$, DVR_{100}, with a decreased or increased of these indexes revealed the dysfunction of left ventricle. The ESV, ESVI, ESD were greater in LGE positive group, the probable reason may be correlated with thicker myocardium. The SV, SVI, CO, CI and FS were indexes of systolic function, and these indexes were smaller in LGE positive group. We considered the changes reflect the relations with LGE (main

reflection of myocardium fibrosis). PFR, NPFR, DVR_{10-40} and DVR_{100} were indexes of diastolic function. PFR, NPFR were smaller, DVR_{10-40} and DVR_{100} were bigger, DVR_{100} represented the total diastolic procedure, the prolonged of DVR_{100} showed the diastolic restriction. Moreover, the prolonged of DVR_{10-40} showed early diastolic restriction. This revealed the details of diastolic restriction.

Our results suggest that the extent of LGE is related to underlying pathology which alters diastolic function and structure remodeling and that the resulting altered dysfunction can be demonstrated by MR-derived markers. The correlation coefficients of ESV, ESVI and EF were both bigger than 0.7, which show the correlation were comparatively good. The decreasing of PFR generated from the filling curve showed left ventricular diastolic restriction, the left ventricular filling curve showed more detail of diastolic restriction. LGE (ROI%) had positive correlation with the indexes of DVR_{20} (r=0.547), DVR_{30} (r=0.544), DVR_{40} (r=0.906), DVR_{50} (r=0.908), DVR_{80} (r=0.608), but the differences of DVR_{50} and DVR_{80} between LGE positive group and LGE negative group were insignificant. This result meant diastolic restriction was represented in rapid filling period. We considered LGE influenced early diastolic volume recovery. The limitation and pitfalls mainly lied in the comparatively small sample size from a single center study. In addition, correlation of these MR-derived parameters with clinical outcomes is needed, in order to determine whether their use provides incremental or additional prognostic information compared to standard assessment of LGE on clinical CMR.

Conclusions

Our study demonstrated correlation of MR-derived markers of diastolic dysfunction with LGE on CMR. These parameters may provide further potential for CMR to provide prognostic information in patients with HCM.

Acknowledgements

We thank Philip Young for his technical assistance. This study was supported in part by the National Natural Science Foundation of China under Grant 30870671, and by the Natural Science Foundation of Zhejiang Province under Grant R207119, and by the Health and Family Planning Commission of Zhejiang Province under Grant 201463675. *Disclosure*: The authors declare no conflict of interests.

References

1. Maron MS. Clinical utility of cardiovascular magnetic resonance in hypertrophic cardiomyopathy. J Cardiovasc Magn Reson 2012;14:13.
2. Fluechter S, Kuschyk J, Wolpert C, et al. Extent of late gadolinium enhancement detected by cardiovascular magnetic resonance correlates with the inducibility of ventricular tachyarrhythmia in hypertrophic cardiomyopathy. J Cardiovasc Magn Reson 2010;12:30.
3. Aquaro GD, Masci P, Formisano F, et al. Usefulness of delayed enhancement by magnetic resonance imaging in hypertrophic cardiomyopathy as a marker of disease and its severity. Am J Cardiol 2010;105:392-7.
4. Nojiri A, Hongo K, Kawai M, et al. Scoring of late gadolinium enhancement in cardiac magnetic resonance imaging can predict cardiac events in patients with hypertrophic cardiomyopathy. J Cardiol 2011;58:253-60.
5. Appelbaum E, Maron BJ, Adabag S, et al. Intermediate-signal-intensity late gadolinium enhancement predicts ventricular tachyarrhythmias in patients with hypertrophic cardiomyopathy. Circ Cardiovasc Imaging 2012;5:78-85.
6. Boonyasirinant T, Rajiah P, Setser RM, et al. Aortic stiffness is increased in hypertrophic cardiomyopathy with myocardial fibrosis: novel insights in vascular function from magnetic resonance imaging. J Am Coll Cardiol 2009;54:255-62.
7. Motoyasu M, Kurita T, Onishi K, et al. Correlation between late gadolinium enhancement and diastolic function inhypertrophic cardiomyopathy assessed by magnetic resonance imaging. Circ J 2008;72:378-83.
8. Kawaji K, Codella NC, Prince MR, et al. Automated segmentation of routine clinical cardiac magnetic resonance imaging forassessment of left ventricular diastolic dysfunction. Circ Cardiovasc Imaging 2009;2:476-84.
9. Mendoza DD, Codella NC, Wang Y, et al. Impact of diastolic dysfunction severity on global left ventricular volumetricfilling - assessment by automated segmentation of routine cine cardiovascularmagnetic resonance. J Cardiovasc Magn Reson 2010;12:46.
10. Guerra M, Sampaio F, Brás-Silva C, et al. Left intraventricular diastolic and systolic pressure gradients. Exp Biol Med (Maywood) 2011;236:1364-72.
11. Alfakih K, Plein S, Thiele H, et al. Normal human left and right ventricular dimensions for MRI as assessed by turbo gradient echo and steady-state free precession imaging sequences. J Magn Reson Imaging 2003;17:323-9.

12. Schulz-Menger J, Abdel-Aty H, Rudolph A, et al. Gender-specific differences in left ventricular remodelling and fibrosis inhypertrophic cardiomyopathy: insights from cardiovascular magnetic resonance. Eur J Heart Fail 2008;10:850-4.
13. Harrigan CJ, Peters DC, Gibson CM, et al. Hypertrophic cardiomyopathy: quantification of late gadolinium enhancement with contrast-enhanced cardiovascular MR imaging. Radiology 2011;258:128-33.
14. Nojiri A, Hongo K, Kawai M, et al. Scoring of late gadolinium enhancement in cardiac magnetic resonance imaging can predict cardiac events in patients with hypertrophic cardiomyopathy. J Cardiol 2011;58:253-60.
15. Catalano O, Moro G, Perotti M, et al. Late gadolinium enhancement by cardiovascular magnetic resonance is complementary to left ventricle ejection fraction in predicting prognosis of patients with stable coronary artery disease. J Cardiovasc Magn Reson 2012;14:29.
16. Choudhury L, Mahrholdt H, Wagner A, et al. Myocardial scarring in asymptomatic or mildly symptomatic patients with hypertrophic cardiomyopathy. J Am Coll Cardiol 2002;40:2156-64.
17. Choi DS, Ha JW, Choi B, et al. Extent of late gadolinium enhancement in cardiovascular magnetic resonance and its relation with left ventricular diastolic function in patients with hypertrophic cardiomyopathy. Circ J 2008;72:1449-53.
18. Olivotto I, Maron BJ, Appelbaum E, et al. Spectrum and clinical significance of systolic function and myocardial fibrosis assessed by cardiovascular magnetic resonance in hypertrophic cardiomyopathy. Am J Cardiol 2010;106:261-7.

Cite this article as: Chen X, Hu H, Qian Y, Shu J. Relation of late gadolinium enhancement in cardiac magnetic resonance on the diastolic volume recovery of left ventricle with hypertrophic cardiomyopathy. J Thorac Dis 2014;6(7):988-994. doi: 10.3978/j.issn.2072-1439.2014.06.37

Original Article

Predictive value of lactate in unselected critically ill patients: an analysis using fractional polynomials

Zhongheng Zhang, Kun Chen, Hongying Ni, Haozhe Fan

Department of Critical Care Medicine, Jinhua Municipal Central Hospital, Jinhua Hospital of Zhejiang University, Jinhua 321000, China
Correspondence to: Zhongheng Zhang, MM. 351#, Mingyue Road, Jinhua 321000, China. Email: zh_zhang1984@hotmail.com.

Background and objectives: Hyperlactatemia has long been associated with poor clinical outcome in varieties of intensive care unit (ICU) patients. However, the impact of temporal changes in lactate has not been well established and there are some shortcomings in model building in previous studies. The present study aims to investigate the association of initial lactate and normalization time with hazard by using fractional polynomial Cox proportional hazard model.

Methods: A large clinical database named Multiparameter Intelligent Monitoring in Intensive Care II (MIMIC-II) was employed for analysis. Demographics, comorbidities, laboratory findings were extracted and were compared between survivors and non-survivors by using univariable analysis. Cox proportional hazard model was built by purposeful selection of covariate with initial lactate (L0) and normalization time (T) remaining in the model. Best fit model was selected by using deviance difference test and comparisons between fractional polynomial regression models of different degrees were performed by using closed test procedure.

Main results: A total of 6,291 ICU patients were identified to be eligible for the present study, including 1,675 non-survivors and 4,616 survivors (mortality rate: 26.6%). Patients with lactate normalization had significantly reduced hazard rate as compared to those without normalization (log-rank test: $P<0.05$). The best powers of L0 in the model were –2 and –1 with the deviance of 19,944.51, and the best powers of T were 0.5 and 3 with the deviance of 7,965.63. The adjusted hazard ratio for the terms $L0^{-2}$ and $L0^{-1}$ were 1.13 (95% CI: 1.09-1.18) and 0.43 (95% CI: 0.34-0.54); and the adjusted hazard ratio for the terms $T^{0.5}$ and T^{3} were 7.42 (95% CI: 2.85-19.36) and 3.06×10^{-6} (95% CI: 3.01×10^{-11}-0.31).

Conclusions: Initial lactate on ICU admission is associated with death hazard and the relationship follows a fractional polynomial pattern with the power of –2 and –1. Delayed normalization of lactate is predictive of high risk of death when it is measured within 150 hours after ICU admission.

Keywords: Fractional polynomial; lactate normalization; intensive care unit (ICU); mortality; critically ill

Submitted Apr 21, 2014. Accepted for publication Jun 17, 2014.
doi: 10.3978/j.issn.2072-1439.2014.07.01
View this article at: http://dx.doi.org/10.3978/j.issn.2072-1439.2014.07.01

Introduction

Lactate is the metabolic product of anaerobic glycolysis. In situations of low oxygen supply or tissue hypoxia, pyruvate will no longer enter into mitochondria for aerobic metabolism but will be reduced to lactate, leading to increases in arterial blood lactate concentrations (1,2). However, hyperlactatemia is not necessarily associated with hypoxia. There are varieties of medications that have been linked to hyperlactatemia, such as nucleoside reverse transcriptase inhibitors, metformin, epinephrine and methanol (3,4). Lactate can be produced from all kinds of tissues, including skeletal muscle, brain, red blood cell and intestine. Critically illness is often associated with increased production of in lactate from lung, blood cells and splanchnic organs. On the other hand, because lactate is primarily cleared via liver and kidney, dysfunction of these organs during critical illness also contribute to the elevated lactate levels (5).

Due to the high prevalence of hyperlactatemia in

critically ill patients, its association with clinical outcome has been extensively studied over the past two decades (6). In the early 1990s, Abramson D and coworkers demonstrated that lactate levels were strongly associated with survival in a cohort study involving 27 patients (7). Thereafter, investigations on the association of lactate or lactate clearance with clinical outcome increase exponentially (8-10). Higher lactate value is consistently associated with adverse clinical outcomes and rapid lactate clearance after treatment is associated with improved outcomes. However, most of these studies are observational studies which, whether it is prospective or retrospective, are subject to confounding bias. As a result, these studies have employed multivariable regression analysis by assuming that the effect of lactate on mortality or other clinical outcomes were linear. Furthermore, these studies were limited in that they predefined a certain time point for lactate clearance, and the times varied across studies, making it difficult for clinicians to determine when lactate should be rechecked. In the current study, fractional polynomial Cox proportional hazards model were fitted to investigate the association of lactate levels and mortality. This model allows for more flexibility in the shape of the curve. Secondly, we will investigate how normalization time impacts the clinical outcome.

Methods

Database

Our study was an analysis of a large clinical database named Multiparameter Intelligent Monitoring in Intensive Care II (MIMIC-II, http://physionet.org/mimic2) (11). This database is a research archive of data collected from patients in intensive care unit (ICU) and is freely accessible for the public. The data contained in MIMIC-II was collected at the ICUs of Beth Israel Deaconess Medical center in Boston from 2001 to 2008. The following data were available: demographics, laboratory test, vital sign recording, fluid and medical records. The establishment of MIMIC-II database was approved by the Institutional Review Boards of the Massachusetts Institute of Technology (Cambridge, MA, USA) and the Beth Israel Deaconess Medical Center. The patient records/information was anonymized and de-identified prior to analysis, and informed consent was not obtained from each participants. The database was continuously updated with the latest version of 2.6 that contained records from over 32,000 subjects. Our access to the database was approved after completing the NIH web-based training course "Protecting Human Research Participants" by the author Z.Z. (Certification Number: 1132877). Data acquisition was completed by using Structural Query Language (12).

Study population

All patients contained in MIMIC-II clinical database were potentially eligible for the present analysis. Adult patients with initial arterial blood lactate >2 mmol/L were included. Exclusion criteria included: (I) neonates; and (II) patients with missing data on arterial blood lactate.

Data abstraction and management

Data on following aspects were extracted: age, gender, SAPSI-1, sequential organ failure assessment (SOFA), admission type (elective, emergency and urgent), comorbidities (congestive heart failure, paralysis, chronic pulmonary disease, complicated diabetes, renal failure, metastatic cancer), date of ICU admission, date of death, ICU mortality and hospital mortality. In order to protect health information of individual patients, the database had obscured real ages for those aged over 90 years. All of them appeared to be 200 years old on first admission. The median age for these patients was 91.4 and we use it as a surrogate age for them. For patients who discharged alive, we obtained the date of death from the Social Security Death Index (SSDI) to determine out-of-hospital mortality. All measurements of arterial blood lactate and associated time were obtained. Lactate normalization was achieved when there was at least one measurement of lactate dropped below 2 mmol/L. Normalization time was the time interval between ICU admission and the time point when lactate normalization occurred.

Statistical analysis

Data were expressed as mean and standard error, or median and interquartile range as appropriate. Variables were compared between patients with and without lactate normalization with univariate analysis. Data of normal distribution were compared using t test and skewed data were compared using Wilcoxon rank-sum test. 28-day mortality was used as the primary end point and variables were compared between survivors and non-survivors.

The Cox proportional model was built by using

Table 1 Characteristics of included patients by lactate normalization categories

Variables	Total (n=6,291)	Normalization (n=3,311)	Non-normalization (n=2,980)	P value
Age (years)	63.2±17.9	63.0±17.7	63.5±18.1	0.32
Gender (male, %)	3,610 (57.62)	1,889 (57.17)	1,721 (58.12)	0.448
SAPS-1	17 [13-21]	18 [14-21]	16 [12-21]	<0.001
SOFA	8 [5-12]	9 [6-12]	8 [4-11]	<0.001
Admission type, n (%)				<0.001
Elective	891 (15.13)	446 (13.95)	445 (16.52)	
Emergency	4,776 (81.09)	2,649 (82.88)	2,127 (78.95)	
Urgent	223 (3.79)	101 (3.16)	122 (4.53)	
Comorbidity, n (%)				
Congestive heart failure	1,349 (22.95)	837 (26.25)	512 (19.04)	<0.001
Paralysis	69 (1.17)	39 (1.22)	30 (1.12)	0.703
Chronic pulmonary disease	836 (14.22)	476 (14.93)	360 (13.39)	0.092
Complicated diabetes	283 (4.82)	157 (4.92)	126 (4.69)	0.670
Renal failure	418 (7.11)	223 (6.99)	195 (7.25)	0.703
Metastatic cancer	285 (4.85)	130 (4.08)	155 (5.76)	0.003
28-day mortality, n (%)	1,675 (26.63)	617 (18.63)	1,058 (35.50)	<0.001
90-day mortality, n (%)	2,011 (31.97)	854 (25.79)	1,157 (38.83)	<0.001
ICU mortality, n (%)	1,121 (17.88)	438 (13.24)	683 (23.06)	<0.001
Hospital mortality, n (%)	1,438 (24.41)	600 (18.77)	838 (31.44)	<0.001

purposeful selection of covariates. Variables with P<0.2 in bivariate analysis and those considered to be clinically relevant were included to establish the initial multivariable model. The later included the severity scores and age. Variables in the initial model would be deleted if P>0.1 from the Wald test. If the removed covariate produced a significant change (>20% change) in the coefficient of lactate, it was thought to be a confounder and would be remained in the model. Any variable excluded should be added back to the model to confirm that it was neither statistically significant nor an important confounder. The process continued until no covariate could be deleted, and the preliminary main effects model had been built up to this point (13). To overcome the obstacle in model building that the relationship between outcome and predictor might be non-linear, the next step was to determine the scale of lactate by using fractional polynomials (14,15). We first determined the best fitting fractional polynomial regression model of second-degree (FP2) by choosing power transformations from the set –2, –1, –0.5, 0, 0.5, 1, 2, 3, where 0 denoted the log transformation. The best fitting model was determined using a deviance difference test. With closed test procedure (15), the deviance of FP2 was compared to deviances of the function with omitted variable, linear function and FP1. Statistical significance of the deviance difference was tested by using χ^2 test. Statistical analyses were performed using software package Stata 12.0 (College Station, Texas 77845 USA). Conventional P<0.05 was considered to be statistically significant.

Results

A total of 6,291 patients were identified to be eligible for the present study, including 3,311 patients with lactate normalization and 2,980 of non-normalization (*Table 1*). There were no statistically significant differences between normalization and non-normalization groups in age, gender, comorbidities of paralysis, chronic pulmonary disease, complicated diabetes and renal failure. Non-normalization was associated with significantly increased risk of death irrespective of the time frame for the definition of mortality: 28-day mortality (35.50% *vs.* 18.63%; P<0.001), 90-day mortality (38.83% *vs.* 25.79%; P<0.001), ICU mortality (23.06% *vs.* 13.24%; P<0.001) and hospital mortality (31.44% *vs.* 18.77%; P<0.001). *Figure 1* displays the Kaplan-Meier survival curves for 28- and 90-day mortality. The

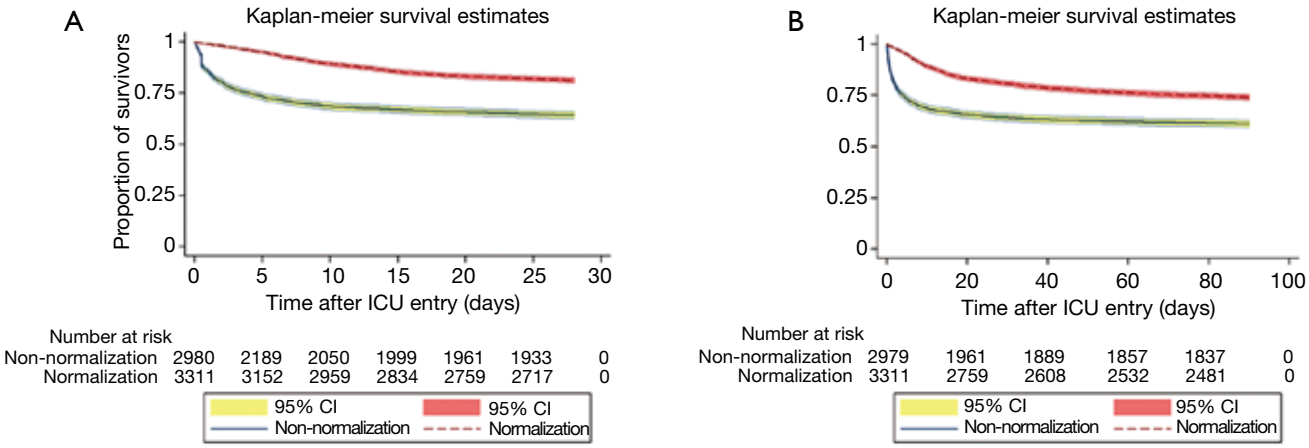

Figure 1 Kaplan-Meier survival curves of 28-day (A) and 90-day (B) for patients with and without lactate normalization. Patients with lactate normalization showed significantly lower hazard (P<0.05).

Table 2 Characteristics of survivors and non-survivors in 28 days

Variables	Total (n=6,291)	Survivors (n=4,616)	Non-survivors (n=1,675)	P value
Age (years)	63.2±17.9	61.5±17.9	67.9±16.9	<0.001
Gender (male, %)	3,610 (57.62)	2,676 (58.28)	934 (55.83)	0.083
SAPS-I	17 [13-21]	16 [13-20]	20 [16-24]	<0.001
SOFA	8 [5-12]	8 [5-11]	11 [7-14]	<0.001
Admission type, n (%)				
Elective	891 (15.13)	825 (18.71)	66 (4.46)	<0.001
Emergency	4,776 (81.09)	3,426 (77.70)	1,350 (91.15)	<0.001
Urgent	223 (3.79)	158 (3.58)	65 (4.39)	0.385
Comorbidity, n (%)				
Congestive heart failure	1,349 (22.95)	943 (21.42)	406 (27.53)	<0.001
Paralysis	69 (1.17)	53 (1.20)	16 (1.08)	0.713
Chronic pulmonary disease	836 (14.22)	636 (14.45)	200 (13.56)	0.398
Complicated diabetes	283 (4.82)	219 (4.98)	64 (4.34)	0.323
Renal failure	418 (7.11)	261 (5.93)	157 (10.64)	<0.001
Weight loss	207 (3.52)	138 (3.13)	69 (4.68)	0.005
Metastatic cancer	285 (4.85)	152 (3.45)	133 (9.02)	<0.001
Initial lactate (mmol/L)	4.21±2.65	3.76±2.04	5.43±3.59	<0.001
Lactate normalization, n (%)	3,311 (52.63)	2,694 (58.36)	617 (36.84)	<0.001
Time for normalization (hours)	20.7 (9.6-43.2)	19.9 (9.3-40.7)	24.7 (11.5-56.8)	<0.001

result showed that lactate normalization was associated with significantly longer survival time.

Among the 6,291 included patients, there were 1,675 non-survivors and 4,616 survivors within 28 days (*Table 2*; overall mortality rate: 26.6%). Non-survivors appeared to be older (67.9±16.9 *vs.* 61.5±17.9; P<0.001), had higher first SAPS-I (20 *vs.* 16; P<0.001) and SOFA scores (11 *vs.* 8; P<0.001). Patients admitted to ICU electively were more likely to survive (18.71% *vs.* 4.46%; P<0.001), whereas those admitted emergently were more likely to die (91.15% *vs.* 77.70%; P<0.001). With respect to comorbidities, patients with congestive heart failure (27.53% *vs.* 21.42%;

Table 3 Variables included in the Cox proportional hazard regression model

	Model 1†		Model 2‡	
	Hazards ratio	95% CI	Hazards ratio	95% CI
L0-2	1.13	1.09-1.18	–	–
L0-1	0.43	0.34-0.54	–	–
T-2	–	–	7.42	2.85-19.36
T-1	–	–	3.06×10^{-6}	3.01×10^{-11}-0.31
Age (with each one year increase)	1.015	1.011-1.019	1.016	1.010-1.022
Sex (male as the reference)	1.07	0.96-1.20	1.06	0.89-1.27
SAPSI-1	1.07	1.05-1.08	1.05	1.03-1.07
SOFA	1.09	1.07-1.11	1.05	1.02-1.08
Elective	0.25	0.17-0.36	0.38	0.19-0.75
Emergency	1.14	0.87-1.49	1.69	0.97-2.94
Congestive heart failure	0.97	0.82-1.07	0.95	0.78-1.15
Renal failure	1.04	0.85-1.27	1.40	1.05-1.87
Weight loss	1.08	0.83-1.40	0.97	0.65-1.45
Metastatic cancer	2.96	2.44-3.59	2.41	1.71-3.89

†, Deviance: 19,944.51. Best powers of L0 among 44 models fit: –2; –1. The FP2 model significantly improved model fit relative to that without lactate in the model (Deviance Difference =76.1, P value <0.001), the linear model (Deviance Difference =11.2, P value =0.011) and the FP1 model with the power of 0.5 (Deviance Difference =10.5, P value =0.005). ‡, Deviance: 7,965.63. Best powers of time among 44 models fit: 0.5; 3. The FP2 model significantly improved model fit relative to that without normalization time in the model (Deviance Difference =17.9, P value =0.001), the linear model (Deviance Difference =16.0, P value =0.001) and the FP1 model with the power of 0 (Deviance Difference =6.6, P value =0.037). L0 refers to the initial measurement of lactate after ICU entry, and the notation "–1" and "–2" indicates the first and second power of the fractional polynomials. Time refers the time it takes for lactate normalization, and the notation "–1" and "–2" indicates the first and second power of the fractional polynomials.

P<0.001), renal failure (10.64% *vs.* 5.93%; P<0.001), weight loss (4.68% *vs.* 3.13%; P=0.005) and metastatic cancer (9.02% *vs.* 3.45%; P<0.001) were more likely to die within 28 days.

All variables with P<0.2 were entered into proportional hazard model for covariate selection. Two models were established: one included initial lactate (L0) and the other included the time for lactate normalization (T). Fractional polynomials of second degree were applied. After model fitting, the best powers of L0 among 44 models were -2 and -1 with the deviance of 19,944.51 (*Table 3*). The FP2 model significantly improved model fit relative to that without L0 in the model (Deviance Difference =76.1, P value <0.001), the linear model (Deviance Difference =11.2, P value =0.011) and the FP1 model with the power of 0.5 (Deviance Difference =10.5, P value =0.005). The best powers of T among 44 models were 0.5 and 3 with the deviance of 7,965.63. The FP2 model significantly improved model fit relative to that without T in the model (Deviance Difference =17.9, P value =0.001), the linear model (Deviance Difference =16.0, P value =0.001) and the FP1 model with the power of 0 (Deviance Difference =6.6, P value =0.037). *Figure 2* displays the fractional polynomial functions adjusted for covariates. The results showed that the hazard increased with the increase in initial lactate level. The slope was most steep from 3 to 8 mmol/L, and after 10 mmol/L the slope tempered. With respect to the normalization time, the hazard increased with increases in normalization time before 150 hours, after that the hazard begin to decrease but with wide uncertainty as reflected by the wide 95% confidence interval.

Figure 3 displays contour plot showing the relationship between normalization time, initial lactate and mortality stratified by quartiles of SOFA score. The results showed that while the higher initial lactate was consistently associated with higher mortality, longer normalization time appeared to be associated with higher mortality in patients with SOFA >12.

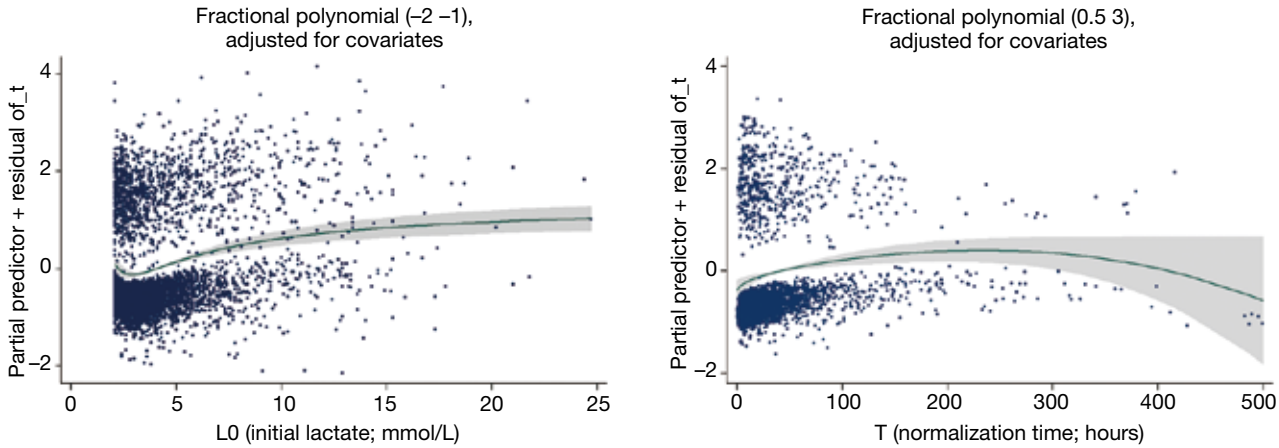

Figure 2 Fractional polynomials adjusted for covariates for initial lactate (L0) and normalization time (T). The best powers of L0 among 44 models were –2 and –1 with the deviance of 19,944.51, and the best powers of T among 44 models were 0.5 and 3 with the deviance of 7,965.63.

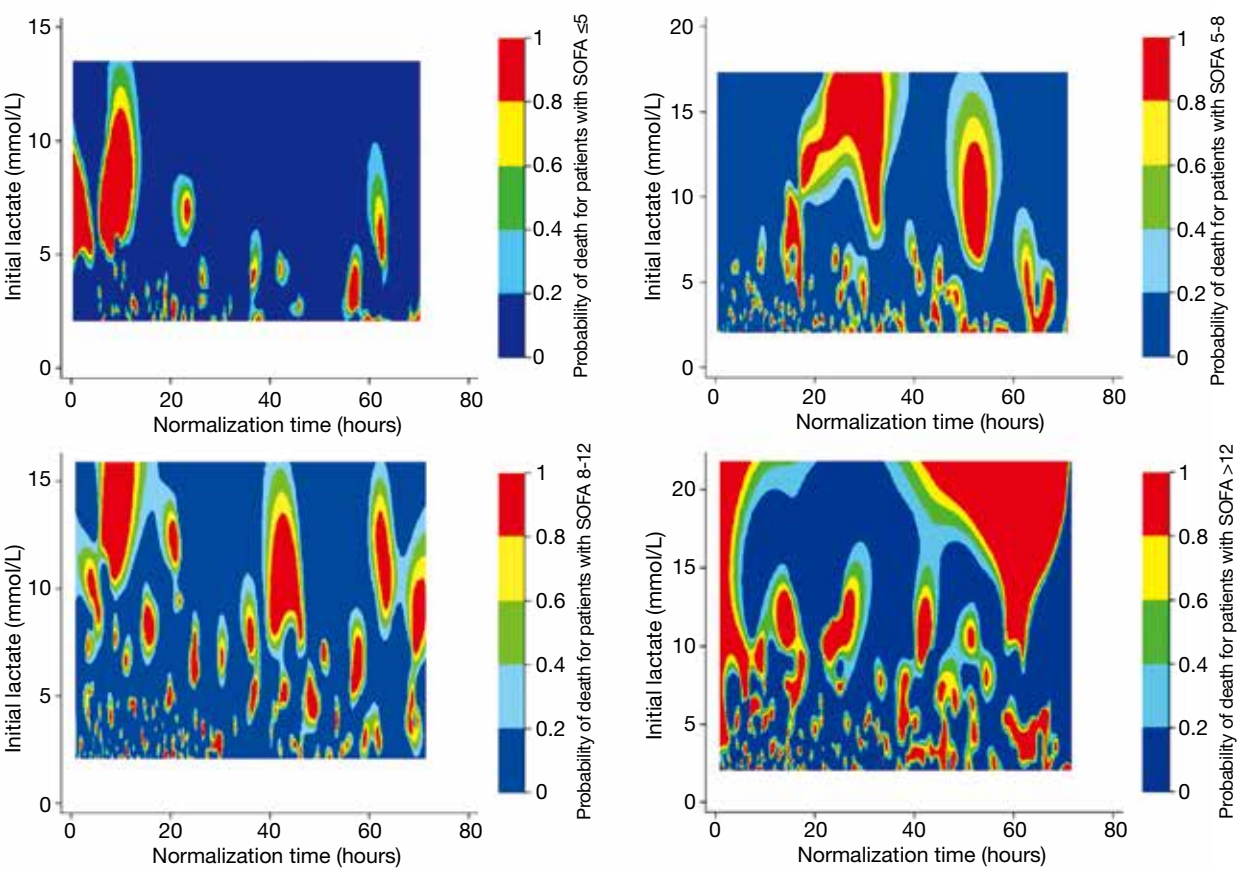

Figure 3 Contour plot showing the relationship between normalization time, initial lactate and mortality stratified by quartiles of SOFA score. The vertical axis represents initial lactate level in unit of mmol/L, and the horizontal axis represents the normalization time in hours. The results showed that while the higher initial lactate was consistently associated with higher mortality, longer normalization time appeared to be associated with higher mortality in subset with SOFA >12.

Discussion

The study showed that both initial lactate and normalization time were significantly associated with increased risk of death in ICU patients. Higher initial lactate and longer normalization time were associated with increased hazard of mortality. Commonly employed normalization time for predicting mortality ranged from 6 to 72 hours in literatures (7,9,16,17), because any prolongation of the time frame may be irrelevant for both risk stratification and resuscitation guidance. In our study we showed that normalization time within 100 hours was positively associated with the hazard.

Our study confirmed previous finding that initial lactate was able to predict clinical outcome (18). In patients underwent cardiothoracic surgery, Maarslet and colleagues (19) found that an increased initial lactate >4.5 mmol/L resulted in an odds ratio of 8.4 (95% CI: 1.5-46.1) for mortality. Lactate level measured at 6 hours after ICU admission was also found to be an independent predictor of complications after major cardiothoracic surgery (20). Some investigators have compared the predictive value of lactate to complex physiological scores in a cohort of cardiothoracic surgery patients. They found that the diagnostic performance of lactate was significantly superior to these scores, as reflected by an area under curve (AUC) of 0.88 for lactate versus 0.83, 0.79 and 0.76 for SOFA, SAPS II and APACHE II, respectively (21). However, these studies used mortality as a binary outcome and ignored the survival time, which may be biased in situations such as when both groups have the same mortality rate but the time to death is significantly different. Furthermore, that study is limited by the small sample size and the percentage of patients with the target event death was only 3.9%, which may potentially increase the risk of type I error. In our analysis, we employed Cox-proportional hazards model to account for the time to event variable, instead of simply dichotomizing the outcome as alive or death (22).

One strength of the present study is that fractional polynomials model was employed to account for the potential non-linear relationship between lactate and hazard. An important shortcoming in previous studies investigating lactate and mortality lies in that the fact that none of them examined the model adequacy by testing the linear assumption of the covariates with logit function. If the linear assumption is violated, the regression model will be invalid and odds ratio obtained from the model may not be hold true across full ranges of lactate value (14-23). Therefore, we used fractional polynomials model to identify the best fit model. Our result showed PF(2) with the power of –2 and –1 had the smallest deviance. As compared with other models (model without lactate, linear, FP1), the deviance difference of FP(2) was statistically different from others. The result confirmed our hypothesis that the relationship between initial lactate and hazard was non-linear. As shown in *Figure 2*, the slope of the function is steep between 4 to 10 mmol/L, and after that the steepness gradually attenuates. This finding suggest that resuscitation bundle aiming to improve tissue perfusion and entailing lactate clearance can benefit the most for patients with lactate level between 4 and 10 mmol/L. For patients with very high lactate beyond 15 mmol/L, the probability of survival may be small and strenuous resuscitation may add little benefit. However, due to the observational nature of the present study, this finding is hypothesis-generating and requires further validation.

To the best of our knowledge, this was the first study investigated the association of normalization time with death hazard, and the time was incorporated into the model as a continuous variable. Previous studies that have explored the time for lactate clearance commonly predefined a certain time point at which the lactate value was rechecked and subjects were dichotomized into groups with and without lactate normalization. This time points were defined arbitrarily and varied across studies ranging from 6 to 72 hours (7,24-26). This time point was chosen probably because this is a time window in which aggressive resuscitation strategy may provide benefit. In our study, we found that: (I) lactate normalization was an indicator of better outcome as compared with those without lactate normalization; (II) among patients with lactate normalization, the longer it takes for normalization, the worse the clinical outcome would be. The second notion holds true when normalization time was less than 150 hours, and after that the regression model became unstable as reflected by a wide confidence band. However, 150-hour is long enough for both medical decision making and risk stratification in real clinical practice. Nevertheless, limitations in analyzing normalization time needs to be acknowledged. Because this was an analysis of a large clinical database that was not specifically designed for the investigation of lactate normalization time, the frequency of lactate measurement was completely determined by the treating physician. Bias could be introduced in situations when one has actually normalized lactate but failed to be measured. As a result, such patients were grouped as non-normalization. One way to address this shortcoming is

to conduct a well-designed prospective study, by predefining the frequency and time points of lactate measurements.

Conclusions

In aggregate, our study confirmed previous finding that initial lactate was independent predictor of mortality in unselected ICU patients. What's new in our study is that we used fractional polynomials to fit the Cox proportional hazard model, allowing for more flexibility in the shape of the regression line. Secondly, it is for the first time that we provided empirical evidence on association of normalization time with death hazard. Our study demonstrates that normalization time was positively associated with death hazard within 150 hours.

Acknowledgements

Disclosure: The authors declare no conflict of interest.

References

1. Fall PJ, Szerlip HM. Lactic acidosis: from sour milk to septic shock. J Intensive Care Med 2005;20:255-71.
2. Okorie ON, Dellinger P. Lactate: biomarker and potential therapeutic target. Crit Care Clin 2011;27:299-326.
3. Vecchio S, Giampreti A, Petrolini VM, et al. Metformin accumulation: lactic acidosis and high plasmatic metformin levels in a retrospective case series of 66patients on chronic therapy. Clin Toxicol (Phila) 2014;52:129-35.
4. Gjedsted J, Buhl M, Nielsen S, et al. Effects of adrenaline on lactate, glucose, lipid and protein metabolism in the placebo controlled bilaterally perfused human leg. Acta Physiol (Oxf) 2011;202:641-8.
5. Fuller BM, Dellinger RP. Lactate as a hemodynamic marker in the critically ill. Curr Opin Crit Care 2012;18:267-72.
6. Gunnerson KJ, Saul M, He S, et al. Lactate versus non-lactate metabolic acidosis: a retrospective outcome evaluation of critically ill patients. Crit Care 2006;10:R22.
7. Abramson D, Scalea TM, Hitchcock R, et al. Lactate clearance and survival following injury. J Trauma 1993;35:584-8; discussion 588-9.
8. Lee TR, Kang MJ, Cha WC, et al. Better lactate clearance associated with good neurologic outcome in survivors who treated with therapeutic hypothermia after out-of-hospital cardiac arrest. Crit Care 2013;17:R260.
9. Puskarich MA, Trzeciak S, Shapiro NI, et al. Whole blood lactate kinetics in patients undergoing quantitative resuscitation for severe sepsis and septic shock. Chest 2013;143:1548-53.
10. Liu XW, Ma T, Qu B, et al. Prognostic value of initial arterial lactate level and lactate metabolic clearance rate in patients with acute paraquat poisoning. Am J Emerg Med 2013;31:1230-5.
11. Saeed M, Villarroel M, Reisner AT, et al. Multiparameter Intelligent Monitoring in Intensive Care II: a public-access intensive care unit database. Crit Care Med 2011;39:952-60.
12. Scott DJ, Lee J, Silva I, et al. Accessing the public MIMIC-II intensive care relational database for clinical research. BMC Med Inform Decis Mak 2013;13:9.
13. Bursac Z, Gauss CH, Williams DK, et al. Purposeful selection of variables in logistic regression. Source Code Biol Med 2008;3:17.
14. Royston P, Altman DG. Regression Using Fractional Polynomials of Continuous Covariates: Parsimonious Parametric Modelling. Appl Stat 1994;43:429-67.
15. Sauerbrei W, Meier-Hirmer C, Benner A, et al. Multivariable regression model building by using fractional polynomials: Description of SAS, STATA and R programs. Computational Statistics and Data Analysis 2006;50:3464-85.
16. Marty P, Roquilly A, Vallée F, et al. Lactate clearance for death prediction in severe sepsis or septic shock patients during the first 24 hours inIntensive Care Unit: an observational study. Ann Intensive Care 2013;3:3.
17. Murtuza B, Wall D, Reinhardt Z, et al. The importance of blood lactate clearance as a predictor of early mortality following the modified Norwoodprocedure. Eur J Cardiothorac Surg 2011;40:1207-14.
18. Borthwick HA, Brunt LK, Mitchem KL, et al. Does lactate measurement performed on admission predict clinical outcome on the intensive care unit? A concisesystematic review. Ann Clin Biochem 2012;49:391-4.
19. Maarslet L, Møller MB, Dall R, et al. Lactate levels predict mortality and need for peritoneal dialysis in children undergoing congenital heart surgery. Acta Anaesthesiol Scand 2012;56:459-64.
20. Hajjar LA, Almeida JP, Fukushima JT, et al. High lactate levels are predictors of major complications after cardiac surgery. J Thorac Cardiovasc Surg 2013;146:455-60.
21. Badreldin AM, Doerr F, Elsobky S, et al. Mortality prediction after cardiac surgery: blood lactate is indispensible. Thorac Cardiovasc Surg 2013;61:708-17.
22. Altman DG, Bland JM. Time to event (survival) data. BMJ 1998;317:468-9.

23. Schmidt CO, Ittermann T, Schulz A, et al. Linear, nonlinear or categorical: how to treat complex associations in regression analyses? Polynomialtransformations and fractional polynomials. Int J Public Health 2013;58:157-60.
24. Husain FA, Martin MJ, Mullenix PS, et al. Serum lactate and base deficit as predictors of mortality and morbidity. Am J Surg 2003;185:485-91.
25. McNelis J, Marini CP, Jurkiewicz A, et al. Prolonged lactate clearance is associated with increased mortality in the surgical intensive care unit. Am J Surg 2001;182:481-5.
26. Arnold RC, Shapiro NI, Jones AE, et al. Multicenter study of early lactate clearance as a determinant of survival in patients with presumed sepsis. Shock 2009;32:35-9.

Cite this article as: Zhang Z, Chen K, Ni H, Fan H. Predictive value of lactate in unselected critically ill patients: an analysis using fractional polynomials. J Thorac Dis 2014;6(7):995-1003. doi: 10.3978/j.issn.2072-1439.2014.07.01

Brief Report

Intrapulmonary recurrence after computed tomography-guided percutaneous needle biopsy of stage I lung cancer

Young-Du Kim[1], Bae Young Lee[2], Ki-Ouk Min[3], Chi Kyung Kim[1], Seok-Whan Moon[1]

[1]Department of Thoracic and Cardiovascular Surgery, [2]Department of Radiology, [3]Department of Hospital Pathology, College of Medicine, The Catholic University of Korea, Seoul, Korea

Correspondence to: Seok-Whan Moon, MD. Department of Thoracic and Cardiovascular Surgery, St. Paul's Hospital, College of Medicine, The Catholic University of Korea, 222 Banpo-daero, Seocho-gu, Seoul 137-701, Republic of Korea. Email: swmoon@catholic.ac.kr.

Abstract: Tumor seeding, along the needle tract after percutaneous needle biopsy, is a rare condition and most of the reported cases are implantation metastasis, which occurred in the chest wall or the pleura. We present a case of implantation metastasis that occurred in the pulmonary parenchyma, after a computed tomography-guided percutaneous needle biopsy (CT-PNB) of stage I lung cancer.

Keywords: Computed tomography (CT); lung cancer; biopsy; recurrence

Submitted Jan 06, 2014. Accepted for publication May 16, 2014.
doi: 10.3978/j.issn.2072-1439.2014.06.32
View this article at: http://dx.doi.org/10.3978/j.issn.2072-1439.2014.06.32

Introduction

Computed tomography-guided percutaneous needle biopsy (CT-PNB) is a useful diagnostic procedure that is used for the evaluation of pulmonary nodules, and is regarded as a relatively safe procedure. Although tumor seeding along the biopsy needle tract after CT-PNB is an extremely rare complication with a reported incidence of 0.06% in Japan (1), it can lead to unnecessary procedures or fatal outcomes. Most of the reported cases of implantation metastasis after CT-PNB were about the tumor seeding, which occurred in the chest wall or the pleura (2,3); however, we present here a case of intrapulmonary recurrence after CT-PNB.

Case presentation

A 70-year-old woman was admitted to our hospital for the evaluation of a growing lung mass. She had undergone a thoracoscopic lobectomy of the right upper lobe 17 months ago, after CT-PNB, using a 22-gauge needle, which had confirmed the lung mass as an adenocarcinoma (*Figure 1*). She was discharged uneventfully and had been followed-up without additional treatment because there was no evidence of metastasis to the lymph nodes or to the distant organs (pT2aN0M0). On the follow-up according to our protocol for stage I lung cancer, a CT scan of the chest revealed a small lung nodule (0.5 cm in the longest diameter), which was located in the superior segment of the right lower lobe. Six months later, a repeat CT scan of the chest showed that the nodule had grown up to 1.2 cm (*Figure 2*). On admission, we performed successful CT-PNB of the lesion of the right lower lobe, and pathologic examination revealed an adenocarcinoma, which took the same characteristics as the previous diagnosis from the right upper lobe, which suggested a recurrence (*Figure 3*). We suspected implantation metastasis, and reviewed the previous biopsy procedures. Finally, we found that the biopsy needle had passed through the superior segment of the right lower lobe to target the right upper lobe lesion, and concluded that the new lesion might be an implantation metastasis, as a result of tumor seeding along the biopsy needle tract. She underwent segmentectomy of the superior segment of the right lower lobe, because there was no evidence of distant metastasis. She recovered well and was followed-up without additional treatment as before.

Discussion

Although tumor seeding along the needle tract after PNB of lung cancer is a rare condition and there are several reports

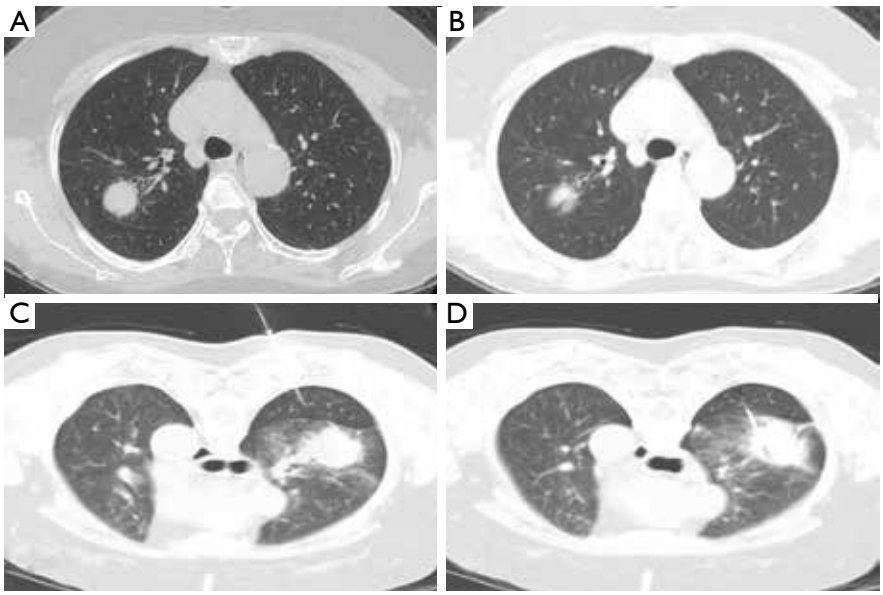

Figure 1 (A,B) Computed tomography (CT) of the chest showing that the primary lesion was located deeply and the scapula interfered with the anterior approach while performing percutaneous needle biopsy. However, there was no evidence of synchronous or metastatic nodules in the superior segment of the RLL; (C,D) CT-guided percutaneous needle biopsy (CT-PNB) of the primary lesion: the biopsy needle passed through the superior segment of the right lower lobe to target the right upper lobe mass.

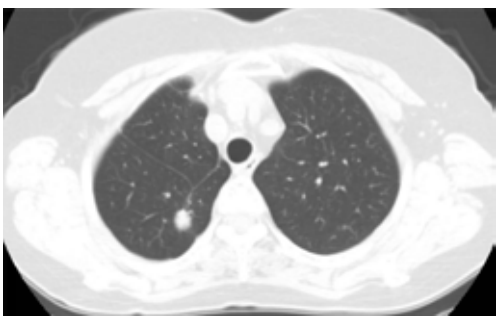

Figure 2 Follow-up computed tomography (CT) of the chest showing a round mass in the superior segment of the right lower lobe.

on metastasis in the chest wall or the pleura (2,3), pulmonary parenchymal implantation has not been documented in the English literature. However, the true incidence of pulmonary parenchymal implantation metastasis, after CT-PNB, might be underestimated, due to its difficulty in differentiating a procedure-related implantation from a local recurrence. Moreover, many patients would die before the diagnosis of intrapulmonary recurrence, and more commonly, it might have been removed with the primary lesion, during the curative anatomical resection (4,5). On reviewing the biopsy procedure in this case, the patient was in a prone position because the scapula bone interfered with the anterior approach on the supine position (*Figure 1*), and the biopsy needle was targeted to the right upper lobe lesion, while passing through the superior segment of the right lower lobe. Therefore, we assumed that the new mass was an implantation metastasis that was related to the CT-PNB procedure rather than a local recurrence or a second primary tumor, because the mass was located in the parenchyma of the RLL, which was far from the pleura, and the biopsy needle had passed through the superior segment of the RLL during the first CT-PNB, where the new mass was supposed to be developed. This was confirmed by a pathologic examination, including an immunohistochemical staining of oncoprotein *p53* (*Figure 3*).

Unfortunately, preventive measures against tumor seeding along the needle tract, while performing CT-PNB, such as the smaller size of the needle, co-axial system of puncture technique, and cauterization of the needle tract using radiofrequency pulses (4), are lack of conclusive proofs. Although they were not tried in this case, innovative bronchoscopic techniques, such as radial probe-endobronchial ultrasound and electromagnetic navigation bronchoscopy, may be safer than CT-PNB because the biopsy tract can be confined only in the parenchyma of the tumor-bearing lobe (6). We present here a lesson from

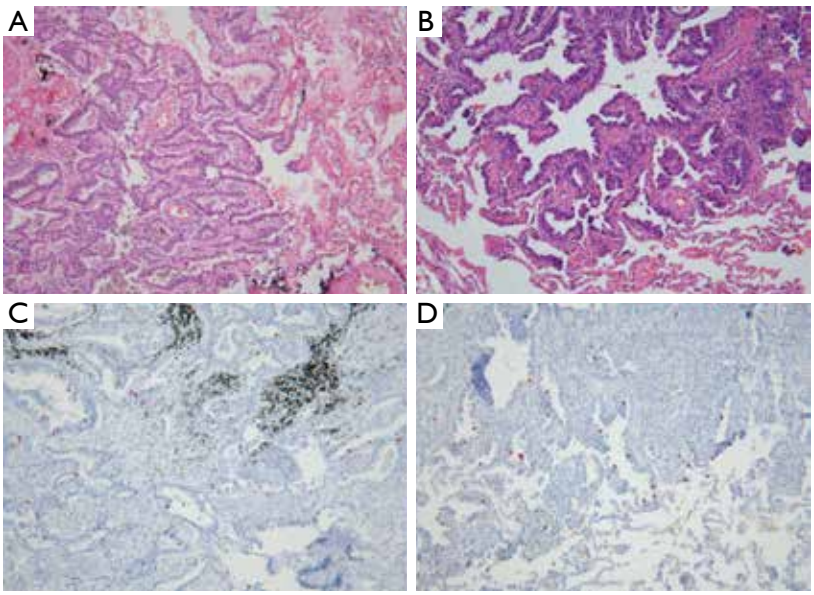

Figure 3 Histopathological sections of the initial mass in the RUL (A,C) and the recurrent mass in the RLL (B,D). Hematoxylin and eosin (A,B) and immunohistochemical (C,D) stains show same pathological characteristics, which are moderately differentiated adenocarcinoma and same degree of positivity for *p53* between the initial mass and the recurrent mass.

this case that the biopsy needle should not pass through different anatomical compartments other than the target compartment, and this strategy should be kept in mind, especially, when the lesion is located deeply.

Acknowledgements

Disclosure: The authors declare no conflict of interest.

References

1. Tomiyama N, Yasuhara Y, Nakajima Y, et al. CT-guided needle biopsy of lung lesions: a survey of severe complication based on 9783 biopsies in Japan. Eur J Radiol 2006;59:60-4.
2. Kim JH, Kim YT, Lim HK, et al. Management for chest wall implantation of non-small cell lung cancer after fine-needle aspiration biopsy. Eur J Cardiothorac Surg 2003;23:828-32.
3. Inoue M, Honda O, Tomiyama N, et al. Risk of pleural recurrence after computed tomographic-guided percutaneous needle biopsy in stage I lung cancer patients. Ann Thorac Surg 2011;91:1066-71.
4. Wiksell H, Schässburger KU, Janicijevic M, et al. Prevention of tumour cell dissemination in diagnostic needle procedures. Br J Cancer 2010;103:1706-9.
5. Robertson EG, Baxter G. Tumour seeding following percutaneous needle biopsy: the real story! Clin Radiol 2011;66:1007-14.
6. Leong S, Shaipanich T, Lam S, et al. Diagnostic bronchoscopy--current and future perspectives. J Thorac Dis 2013;5:S498-510.

Cite this article as: Kim YD, Lee BY, Min KO, Kim CK, Moon SW. Intrapulmonary recurrence after computed tomography-guided percutaneous needle biopsy of stage I lung cancer. J Thorac Dis 2014;6(7):1004-1006. doi: 10.3978/j.issn.2072-1439.2014.06.32

Nursing for the complete VATS lobectomy performed with non-tracheal intubation

Li Wang, Yidong Wang, Suihong Lin, Pengying Yin, Yanwen Xu

Operation Room, The First Affiliated Hospital of Guangzhou Medical University, Guangzhou 510120, China

Correspondence to: Li Wang, RN. Operation Room, The First Affiliated Hospital of Guangzhou Medical University, No. 151, Yanjiang Rd, Guangzhou 510120, China. Email: wangligfy@126.com.

Abstract: Video-assisted thoracoscopic surgery (VATS) has without doubt been the most important advance in thoracic surgery. The general anesthesia before the tracheal intubation for VATS was often accompanied with tracheal mucosa and lung injuries, which were typically manifested as painful throat, nausea, vomiting, and other symptoms. However, the non-intubated anesthesia VATS can avoid these shortcomings due to its shorter anesthesia time, simpler steps, and quicker post-operative recovery. A total of 63 patients underwent VATS lobectomy under non-intubated anesthesia from July 2012 to July 2013. Good teamwork, proper pre-operative visit, and comfortable intra-operative position had ensured the success of these operations. In conclusion, adequate pre-operative preparation, careful nursing, and close cooperation can achieve a successful non-intubated anesthesia VATS.

Keywords: Video-assisted thoracoscopic surgery (VATS); anesthesia; non-intubated anesthesia; clinical nursing

Submitted Apr 10, 2014. Accepted for publication Jun 02, 2014.
doi: 10.3978/j.issn.2072-1439.2014.06.35
View this article at: http://dx.doi.org/10.3978/j.issn.2072-1439.2014.06.35

Introduction

In the past, lung surgery required a major open procedure, known as a thoracotomy. In order to gain access to the lungs, this approach involves making a large incision and spreading the ribs apart with retractors. With new technological developments, it is now possible to perform lung surgery via a less invasive approach, known as "minimally invasive pulmonary resection", including two forms of minimally invasive or "key-hole" thoracic surgery: video-assisted thoracoscopic surgery (VATS) and robotic surgery (1). VATS has without doubt been the most important advance in thoracic surgery. No other single innovation has so totally revolutionized the way thoracic surgeons perform their craft, or so greatly improved the surgical experience for patients undergoing thoracic operations worldwide (2,3). The general anesthesia before the tracheal intubation for VATS was often accompanied with tracheal mucosa and lung injuries, which were typically manifested as painful throat, nausea, vomiting, and other symptoms (4,5). In contrast, the non-intubated anesthesia can avoid these shortcomings due to its shorter anesthesia time, simpler steps, and quicker post-operative recovery (6,7). Nevertheless, adequate pre-operative preparation, careful nursing, and close cooperation were also required for a successful non-intubated anesthesia VATS. Thus, it is critically important to translate the "minimally invasive operation" into an integrated "minimally invasive process" that also involves both anesthesia and nursing.

Surgical cooperation

Pre-operative visit

One day before the surgery, a circulating nurse should review the medical records in the ward, learn the surgical plan, conduct pre-operative visit, introduce herself, and learn the patient's physical and mental status. Also, she should explain the advantages of the non-intubated anesthesia and the VATS as well as the backgrounds of surgeons and anesthesiologists that will be involved in this surgery. Other information including the operating room environment, surgical position, surgical procedures, and precautions should also provided. She should share other successful stories with the patient, so as to relieve his/her

mental stress, stabilize emotion, and enhance confidence. The non-intubated anesthesia allows the patients to receive the surgery when they are waking, so as to alleviate their pre-operative anxiety.

Intra-operative preparation

The surgery needs to be done in a relatively large room, in which more instruments, equipment, and instrument tables can be installed and thus facilitate timely observations and salvage. The temperature and humidity of the operation room should be suitably adjusted. Lateral positioning cushion (90 degrees) should also be prepared.

Preparation of equipment and instruments

Before the surgery, the following equipment and items are prepared: 30 degree lens, thoracoscopic surgical instruments, monitors, camera and lighting systems, and high-frequency electric knife, multiple electrocautery hooks with different lengths, ultrasonic scalpel, suction cautery, and pleural automatic cutter & stapler with sufficient staple cartridges. Each surgical equipment and item must be carefully checked before the surgery.

Cooperation of the circulating nurse

The circulating nurse must carefully check the patient in the patients' waiting area before admitting him/her into the operation room. She should assist the patient to be moved onto the operation table, and establish intravenous access at the ipsilesional upper extremity. The patient is asked to take a 90 degree lateral position. A Gel cushion was put under the 4th to 5th ipsilesional thoracic ribs, so as to enlarge the intercostal space and reduce the intercostal nerve compression. The ipsilesional upper extremity is fixed with a hand bracket. Thoracic holders are placed at the pubic symphysis and sacral part to fix the patient. Patients under non-endotracheal anesthesia can have spontaneous breathing and may also move during the operation. The fixing brackets can accommodate one finger, so as to avoid any intra-operative injury.

Cooperation of the equipment nurse

Making incisions

The surgical approaches of the nonintubated VATS surgeries are same as the conventional thoracoscopic surgery. Lobectomy is performed using two or three ports. The observation port is mainly located between the 6th-7th intercostal cartilages, whereas the operating port between the 4th-5th intercostal cartilages. In addition, the auxiliary port is located at the same cartilage as the observation port, forming an isosceles triangle with the other two ports. Under the assistance of the equipment nurse, an incision protection sleeve is attached to each port in the presence of lubricants. Along with a 30° thoracoscope, almost the whole thoracic cavity can be visualized. Once the incision is made, the equipment nurse hands a gauze pad to the operator (with a toothed oval clamp holding 1/4 of the pad) expose the surgical site by pressing the lung tissue.

Nerve block

Intrathoracic vagus nerve block is performed to suppress the cough reflex caused by the traction of lung tissue during the thoracoscopic operations. Under direct thoracoscopic vision, 3-5 mL 1% Lidocain was injected near the vagus nerve beneath the mediastinal pleura. The equipment nurse hands a endoscopic needle connected with a syringe containing 1% Lidocain to the operator, who then performs the vagus nerve block. Both the nurse and the operator must check the concentration and dosage of the drug.

Surgical procedures

During the surgery, the equipment nurse hands the operator a gauze pad and oval clamp for exposing the lung tissue. Also, the equipment nurse hands the endoscopic siphon head to the assistant to facilitate the exposure. The operator uses right angle clamp, fissure pliers, electrocautery hooks or ultrasonic scalpel to dissect the incomplete fissures. The nurse installs the Johnson & Johnson pleural automatic cutter & stapler and then hands it to the operator, who separates the incomplete fissures. During the lower lobe resection, ultrasonic scalpel is handed to the operator to separate the inferior pulmonary ligament, so as to slowly expose the inferior pulmonary vein. electrocautery hooks are handed to the operator to open the venous or artery sheath, thus skeletonizing the vessels. Thoracoscopic forceps are handed to the operator to finalize the vascular exploration. The pleural automatic cutter & stapler are handed to the operator to disconnect the inferior pulmonary artery and vein. Also, the lower lobe bronchus is disconnected with the cutter. During the resection of other lung lobes, the equipment nurse hands the vessel-separating clamps of different lengths and different radians to the operator in accordance with the operation steps; in addition, different

types of cartridges are selected based on the thickness of the lung tissues. After the lobectomy, endosurgical extraction bag is handed for collecting body tissues. Systematic lymphadenectomy is performed (or not) based on the frozen section pathological results. Leak testing is conducted following the anastomosis by injecting the prepared warm salt solution into the thoracic cavity. Chest tubes and chest drainage bottles are also prepared. The amounts of equipment, blood pads, and gauzes are routinely counted. If the results are correct, close the incision.

Cleaning and maintenance of equipment and instruments

The equipment and instruments used for VATS are sophisticated and relatively expensive. Proper maintenance can not only prolong the service lives of these equipment and instruments but also ensure their performances. Therefore, all these equipment and instruments must be kept in special counters and routinely maintained by specially assigned personnel.

Results

A total of 63 patients underwent VATS lobectomy under non-intubated anesthesia in our hospital from July 2012 to July 2013. Good teamwork, proper pre-operative visit, and comfortable intra-operative position had ensured the success of these operations. During the surgery, appropriate instruments were handed according to the surgical requirements. After the surgery, all the thoracoscopic equipment and instruments were properly cleaned, disinfected, and maintained. In 2 of these 63 patients, the non-ideal lung collapse affected the operations; resulting in the change in anesthesia mode; in another patient, endotracheal intubation was adopted due to intra-operative bleeding. In the remaining 60 cases, shrinking of the lungs was achieved by artificial pneumothorax and the exposure of the surgical fields was satisfactory. The surgery was smooth.

Discussion

Although VATS lobectomy under non-intubated anesthesia has still not been widely applied in China, it has demonstrated to be a safe and feasible technique (8). Due to the small operation space under the thoracoscope, the operator must be highly skillful and have rich clinical experiences (3,9). In addition, the surgery has minimally invasive approaches, and the types and lengths of the endoscopic equipment often differ (2). Thus, nurses in the operation room must be highly skillful, and good communication is required among the medical team.

The operations of VATS are mainly performed under the thoracoscope, and the camera is equivalent to the surgeon's eyes. Thus, there are some specific requirements for the camera holder. A clear surgical field is the prerequisite for a successful operation. The thoracoscope needs to be soaked with hot brine before it enters the thoracic cavity. During the surgery, the equipment nurse must carefully protect the optical fiber and camera system of the thoracoscope and prevent any turnover. The contaminated lens must be soaked timely, so as to ensure the clearness and brightness of the surgical field.

Under non-intubated anesthesia, the operator needs to use specific instruments to compress the normal lung tissue to expose the surgical field, during which the equipment nurse will hand a folded gauze pad to the operator using a toothed oval clamp. Such a gauze pad can expose the lung tissue, and thus minimize any potential injury to the lung tissue; also, when used for compressing the bleeding site, it can temporarily stop bleeding. During the intrathoracic vagus nerve block, since the endoscopic puncture needle is longer than the conventional puncture needle, it may be less stable. Thus, we connect the endoscopic puncture needle, connecting tube, and a syringe; during the surgery, the nurse hands the whole system to the operator. By doing so, we increased the coherence of surgery, reduced post-puncture bleeding, and lowered the failure rate.

In conclusion, adequate pre-operative preparation, careful nursing, and close cooperation can achieve a successful non-intubated anesthesia VATS.

Acknowledgements

Disclosure: The authors declare no conflict of interest.

References

1. Cao C, Manganas C, Ang SC, et al. A systematic review and meta-analysis on pulmonary resections by robotic video-assisted thoracic surgery. Ann Cardiothorac Surg 2012;1:3-10.
2. He J, Yan TD. Video-assisted thoracoscopic surgery. J Thorac Dis 2013;5:S173.
3. Carrott PW Jr, Jones DR. Teaching video-assisted thoracic surgery (VATS) lobectomy. J Thorac Dis 2013;5:S207-11.
4. Kim JH, Park SH, Han SH, et al. The distance between the carina and the distal margin of the right upper lobe

orifice measured by computerised tomography as a guide to right-sided double-lumen endobronchial tube use. Anaesthesia 2013;68:700-5.
5. Campos JH, Massa FC, Kernstine KH. The incidence of right upper-lobe collapse when comparing a right-sided double-lumen tube versus a modified left double-lumen tube for left-sided thoracic surgery. Anesth Analg 2000;90:535-40.
6. Chen JS, Cheng YJ, Hung MH, et al. Nonintubated thoracoscopic lobectomy for lung cancer. Ann Surg 2011;254:1038-43.
7. Chen KC, Cheng YJ, Hung MH, et al. Nonintubated thoracoscopic lung resection: a 3-year experience with 285 cases in a single institution. J Thorac Dis 2012;4:347-51.
8. Guo Z, Shao W, Yin W, et al. Analysis of feasibility and safety of complete video-assisted thoracoscopic resection of anatomic pulmonary segments under non-intubated anesthesia. J Thorac Dis 2014;6:37-44.
9. Petersen RH, Hansen HJ. Learning curve associated with VATS lobectomy. Ann Cardiothorac Surg 2012;1:47-50.

Cite this article as: Wang L, Wang Y, Lin S, Yin P, Xu Y. Nursing for the complete VATS lobectomy performed with non-tracheal intubation. J Thorac Dis 2014;6(7):1007-1010. doi: 10.3978/j.issn.2072-1439.2014.06.35

Surgical Technique

Uniportal complete video-assisted thoracoscopic lobectomy with systematic lymphadenectomy

Guang-Suo Wang, Zheng Wang, Jian Wang, Zhan-Peng Rao

Shenzhen People's Hospital, Second Affiliated Hospital, Medical College of Ji'nan University, Shenzhen 518020, China

Correspondence to: Zheng Wang. Department of Thoracic Surgery, Shenzhen People's Hospital, Second Affiliated Hospital, Medical College of Ji'nan University, Shenzhen 518020, China. Email: wgswy01@163.com.

Abstract: Video-assisted thoracoscopic surgery (VATS) has permeated our thoracic surgical practice and now will develop in depth towards a next level of minimally invasive surgery (MIS). Irrespective of generation gaps and diversified perception within thoracic community, more and more surgical teams are adapting to the uniportal lobectomy. This video demonstrates a case undergoing uniportal VATS lobectomy with systematic lymphadenectomy for lung cancer. We here describe our technique for uniportal approach by using a combination of double-jointed and endoscopic instruments to combat the four major obstacles: (I) interference of the thoracoscope, stapler and the instrumentation in and out of the thoracic cavity? (II) whether the field of vision is enough or not without the other 1-3 ports to improve the exposure? (III) the optimal stapler introduction angle especially for upper and middle lobes resection? (IV) more importantly, the oncologic validity of uniportal procedures as well as the reduction of postoperative morbidity? We believe, uniportal VATS lobectomy with systematic lymphadenectomy is technically safe and feasible and alternative approach to conventional thoracoscopic lobectomy in lung cancer treatment. The issues of patient acceptability, the cosmetic and oncologic results, and cost-effectiveness remain to be determined in the future through multi-institution randomized controlled trials and long-term follow-up.

Keywords: Complete video-assisted thoracoscopic surgery (cVATS); uniportal; biportal; lobectomy; lung cancer; systematic lymphadenectomy; multiple nodules; oncologic outcome

Submitted May 10, 2014.Accepted for publication May 26, 2014.
doi: 10.3978/j.issn.2072-1439.2014.06.41
View this article at: http://dx.doi.org/10.3978/j.issn.2072-1439.2014.06.41

Introduction

When it comes to perspectives in complete video-assisted thoracoscopic surgery (cVATS), it has become a consensus in thoracic community that is to further reduce the number and the length of the incisions (1). In Jun 2011, Gonzalez Rivas first report uniportal cVATS lobectomy which becomes a milestone in the development history of VATS lobectomy (2). Perhaps the demand for increasingly more minimally invasive surgical approaches is even more important within the Chinese culture, uniportal VATS development has grown in popularity in mainland recently.

However, uniportal approach poses several major challenges to cVATS lobectomists (2): (I) interference of the thoracoscope, stapler and the instrumentation in and out of the thoracic cavity? (II) whether the field of vision is enough or not without the other 1-3 ports to improve the exposure? (III) the optimal stapler introduction angle especially for upper and middle lobes resection? (IV) more importantly, the oncologic validity of uniportal procedures as well as the reduction of postoperative morbidity? This video demonstrates a case undergoing uniportal cVATS lobectomy with systematic lymphadenectomy for lung cancer. We here describe our technique for uniportal approach by using a combination of double-jointed and endoscopic instruments.

Clinical data

A 64-year-old female presented with a 2.0 cm × 2.0 cm × 1.0 cm

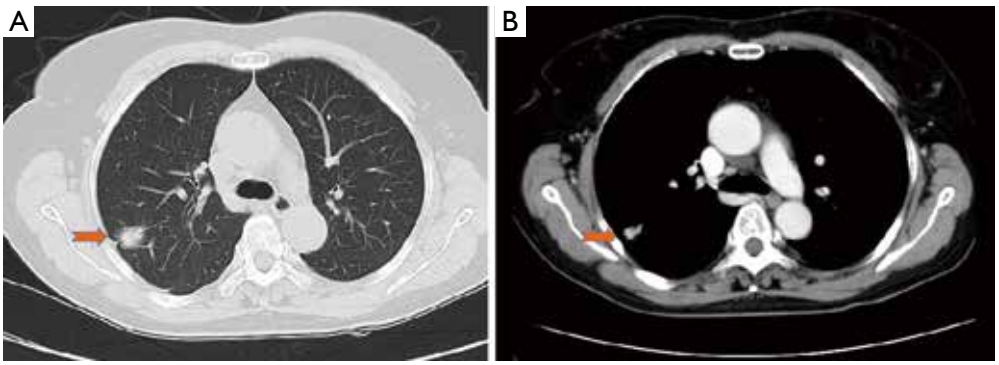

Figure 1 (A,B) A shadow in the right upper lobe.

Figure 2 A GGO in the left upper lobe. GGO, ground glass opacity.

Figure 3 Uniportal cVATS lobectomy for lung cancer (3).

nodule in posterior segment of right upper lobe and a ground glass opacity (GGO) in the left upper lobe on computed tomographic (CT) (*Figures 1,2*) was admitted in our institute on March 16th, 2014. The patient underwent preoperative staging and cardiac and pulmonary function assessment. PET-scan indicates no signs of metastasis. Under general anesthesia with double lumen tube, the patient underwent uniportal cVATS lobectomy for right upper lung tumor on March 19th, 2014 (*Figure 3*). The final pathologic TNM staging is T1aN0M0 (IA). Regular follow up was initiated for the GGO in the left upper lobe.

Operative techniques

Patient positioning, placement of the single incision

The patient is positioned in full lateral decubitus position with slight flexion of the table at the level of the mid-chest, which allows slight splaying of the ribs to improve exposure in the absence of rib spreading. This is similar to conventional VATS procedures. All lobectomies and segmentectomies were underwent via the 5th intercostal space about 3.5-4.5 cm long. Plastic wound protector was not used now and soft tissues are retracted by silk only to prevent the lung from expanding when suction is used. The 30° 10 mm thoracoscope (5 mm ever used) is placed in the posterior part of the above incision and fixed by a rubber band (*Figure 4*).

Different stance for the operating personnel and instruments

We now use a combination of endoscopic and double-jointed instruments and some specially adapted for uniportal cVATS including long and short curved suction tube and ring forceps (*Figure 5*). An articulating endoscopic linear cutter is preferred.

The operator and the scope holder always stand anterior to the patient whether the operator stands caudally or cranially varies depending on the procedures in the lower or upper thoracic cavity. The first assistant stands

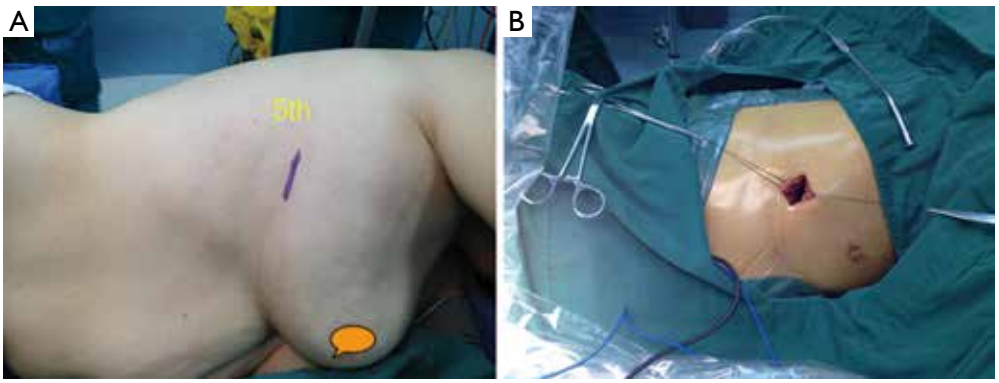

Figure 4 (A,B) The single incision is located in the fifth intercoastal space and retracted by silk.

Figure 5 A combination of double-jointed and endoscopic instruments.

Figure 6 The intraoperative outer view showing different stance for operation personnel and instruments.

posteriorly responsible for the macro exposure. The surgeon always holds suction tube in the left hand for micro and dynamic exposure while in the right hand almost are the electrocautery or harmonic scalpel. From posterior to anterior at the incision level lies in turn the scope, the long curved ring forceps containing gauze for macro exposure, the energy devices and the suction tube (*Figure 6*).

Exploration

We begin the procedure with an exploration of the pleural cavity. The tumor is identified in the posterior segment of the right upper lobe. The frozen section analysis after wedge resection revealed infiltrating adenocarcinoma, so we proceed to right upper lobectomy with systematic lymphadenectomy.

Division and transection of truncus anterior artery

First cut open mediastinal pleura in the anterior hilum and underneath the arch of the azygos vein. Then dissect and indentify the gap between the superior pulmonary vein and truncus anterior artery. The lymph nodes are cleared at the same time. Dividing the truncus anterior artery first is often recommended in order to facilitate the insertion of the staplers for the upper lobe vein. We strongly recommend the use of silk ligation and hemolock in cases where the angle for stapler insertion is not optimal especially for the left upper lobectomy. The posterior ascending artery can be divided separately or at last together with the fissure.

Division and transection of superior pulmonary vein

The location of endostapler and the thoracoscope are interchangeable between two incisions in biportal approach. In uniportal approach, first dividing the artery is most commonly used. In unusual cases, dividing the superior vein following the truncus anterior artery and then the upper bronchus is used. Sometimes divide the minor fissure help first staple the superior vein from anterior and superior to

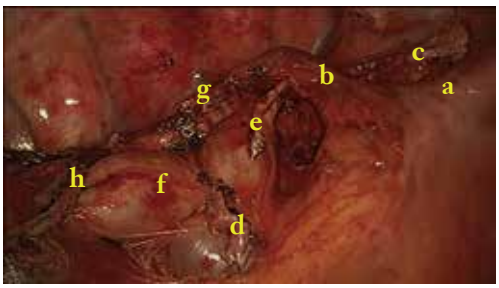

Figure 7 Surgical image after lobectomy and systematic lymphadectomy. a, superior vena cava; b, azygos vein; c, vagus nerve; d, stump of superior pulmonary vein; e, stump of truncus anterior; f, the pulmonary artery for middle and lower lobe; g, stump of right upper bronchus; h, the incisal margin of the fissure.

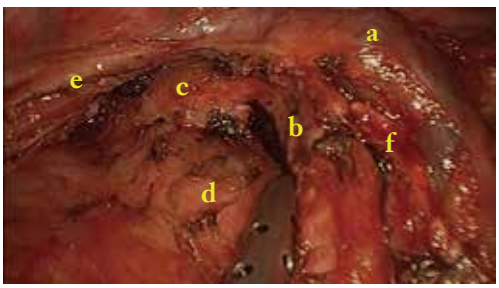

Figure 8 Surgical image after R7th lymph node dissection. a, azygos vein; b, right bronchus; c, left bronchus; d, left atrium; e, esophagus; f, stump of right upper bronchus.

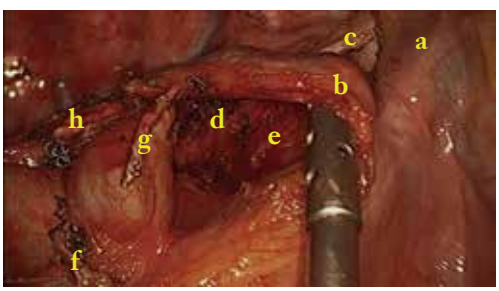

Figure 9 Surgical image after R2th and 4th lymph node dissection. a, superior vena cava; b, azygos vein; c, vagus nerve; d, trachea; e, aortic arch; f, stump of superior pulmonary vein; g, stump of truncus anterior; h, stump of right upper bronchus.

the posterior and inferior direction.

Division and transection of right upper lobe bronchus

Identifying and clearing the lymph nodes between the upper and intermediate bronchus first. The bronchus can be transected via anterior or posterior approach by a stapler while the former is more convenient because of no need to expose the lung anteriorly.

Figure 10 Single-chest tube placed in the posterior part of the incision up to the tip of the thoracic cavity.

Dissection of the horizontal fissure and the posterior halves of the oblique

The distal lymph nodes at the second carina should be dissociated to the distal end of the bronchus, and then removed *en bloc* with the right upper pulmonary lobe. The above fissures can be divided using stapler last. The lobe is extracted using a specimen retrieval bag.

Mediastinal lymph node (MLN) dissection

Move the operating table anteriorly. Systematic lymph node dissection using *en bloc* excision, instead of systematic sampling, is applied for the removal of 2, 4, 7, 8 and 9 MLNs. We use the same method as in the biportal approach (4). Cut open mediastinal pleura by a "∩" shaped incision for 7th, a "⊿" above azygos vein and "–" beneath azygos vein for 2th and 4th which greatly simplify the *en bloc* MLNs dissection (*Figures 7-9*).

Leakage testing, intercostals nerve blockade, insert drainage tube and incision closure

The lung is re-expanded for air leakage testing for the bronchial stump and the pulmonary resection margin. Finally a single 24$^{\#}$ chest tube with enough side holes is placed in the posterior part of the incision up to the tip of the thoracic cavity (*Figure 10*).

Comments

After sustaining and rapid evolution for more than two decades, VATS has permeated our thoracic surgical practice and now will develop in depth towards a next level of minimally invasive surgery (MIS) (5). Irrespective of generation gaps and diversified perception within thoracic community, more and more surgical teams are adapting to this new era. Since Diego from Spain optimize uniportal cVATS major pulmonary resections, uniportal approach development has become an increasingly popular approach to manage thoracic surgical diseases because of the reduced access trauma and better cosmesis, with several centres in Hong Kong, Taiwan, Singapore, Mainland China and Korea beginning to perform uniportal VATS major lung resections (5-9).

From June 2012, more than 160 cases of uniportal cVATS procedures have been accomplished in our center. On 16th August 2013, we performed the 1st uniportal left lower lobectomy for bronchiectasis; on 26th November 2013, the 1st bilateral same-stage single-port thoracoscopic right upper lobectomy for lung cancer and left lower lobectomy for destroyed lung caused by bronchiectasis; on 18th December 2013, the 1st uniportal right lower basilar segmentectomy; on 6th March 2014, the 1st combined uniportal right upper lobectomy and right lower superior segmentectomy for lung cancer. Until now, we have performed 33 cases of uniportal cVATS lobectomy and 16 cases of segmentectomy (unpublished).

After all, cVATS lobectomy through a single incision is a challenging technique for most thoracic surgeons especially those without experiences in biportal procedures. We surely believe Shenzhen People's Hospital experience partially combat the above obstacles and flatten the learning curve of uniportal approach.

(I) Interference of the thoracoscope, stapler and the instrumentation in and out of the thoracic cavity?

Initially, we use endoscopic and open-surgery instruments, 30° 5 mm thoracoscope and plastic wound protector. All the devices were crowded at the incision level and in and out of the thoracic cavity which require adequate patience and coordination between surgeon and camera person. Now, we abandon the use of plastic wound protector which leave much more space at the incision level. More importantly, certain modified tools are very helpful in the execution of uniportal procedures. The double-jointed and endoscopic instruments and articulating endostaplers contribute to avoid interference of the thoracoscope and the instrumentation. It is critical for adjust different stance for the operating personnel. The advantage of leaving the camera person in coordination with the surgeon anteriorly is that the vision is directed to the target tissue, bringing the instruments to address the target lesion from a straight perspective, thus we can obtain similar angle of view as for open surgery. Yet triportal VATS forces the surgeons to an unnatural eye to hand coordination compared to what they are used to in open surgery. The sagittal, caudo-cranial approach of uniportal cVATS amends this problem by letting the surgeon work along a plane he/she is mostly accustomed to in open (10). We have tried three cases of uniportal cVATS lobectomy via 3-dimension imaging system giving us the impression of raising one's head and operating "open" surgery.

(II) Whether the field of vision is enough or not without the other 1-3 ports to improve the exposure?

With experiences from biportal approach and uniportal approach for minor procedures, we learned that adequate exposure of the lung is mandatory in order to successfully access the interested lobe. The first assistant stands posteriorly responsible for the macro exposure. The surgeon always holds suction tube in the left hand for micro and dynamic exposure while in the right hand almost are the electrocautery or harmonic scalpel. The camera person leaves the scope displaying a close-up view of the target tissue. For all the team members and his devices, each does his part and work together and then contribute to good exposure.

(III) The optimal stapler introduction angle especially for upper and middle lobes resection?

Uniportal cVATS upper lobectomies are usually more difficult than lower obectomies in uniportal approach (11). The difficulty is mainly based on the sharp angles that are required to use instruments and staplers. Adjust the order for division of different hilar structures is conducive to access the target. For right upper lobectomy, the most common surgical steps are truncus anterior, upper vein, posterior ascending artery, upper bronchus and fissure which are similar to those of left upper lobectomy. The two strategies mentioned above for dividing superior pulmonary vein in unusual cases is helpful sometimes. But we strongly recommend placing hemoclips and ligation when there is no good angle for the stapler.

(IV) More importantly, the oncologic validity of uniportal procedures as well as the reduction of postoperative morbidity?

MLN dissection is the most critical point for lung

cancer and is a prevalent concern relates to the ability of thoracoscopic operations to achieve adequate staging (12). To my knowledge, long-term oncologic outcomes including lymph node dissection efficacy, local recurrence, and survival after uniportal approach for lung cancer are lacking. Based on our own experience (4,8) and review from the literature (2,6,7), we surely believe MLN assessment in patients who underwent uniportal cVATS lobectomy was as effective as in those who underwent traditional cVATS lobectomy in experienced centers, with no difference in number of N2 LN stations or total number of LN stations resected.

In conclusion, uniportal cVATS lobectomy with systematic lymphadenectomy is technically safe and feasible and alternative approach to conventional thoracoscopic lobectomy in lung cancer treatment. The issues of patient acceptability, the cosmetic and oncologic results, and cost-effectiveness remain to be determined in the future through multi-institution randomized controlled trials and long-term follow-up.

Acknowledgements

Disclosure: The authors declare no conflict of interest.

References

1. Rocco G. VATS and Uniportal VATS: a glimpse into the future. J Thorac Dis 2013;5:S174.
2. Gonzalez-Rivas D, Paradela M, Fernandez R, et al. Uniportal video-assisted thoracoscopic lobectomy: two years of experience. Ann Thorac Surg 2013;95:426-32.
3. Wang GS, Wang Z, Wang J, et al. Uniportal cVATS lobectomy for lung cancer. Asvide 2014;1:247. Available online: http://www.asvide.com/articles/259
4. Wang GS, Wang Z, Wang J, et al. Biportal complete video-assisted thoracoscopic lobectomy and systematic lymphadenectomy. J Thorac Dis 2013;5:875-81.
5. Ng CS. Uniportal VATS in Asia. J Thorac Dis 2013;5:S221-5.
6. Tam JK, Lim KS. Total muscle-sparing uniportal video-assisted thoracoscopic surgery lobectomy. Ann Thorac Surg 2013;96:1982-6.
7. Wang BY, Tu CC, Liu CY, et al. Single-incision thoracoscopic lobectomy and segmentectomy with radical lymph node dissection. Ann Thorac Surg 2013;96:977-82.
8. Wang GS, Wang Z, Wang J, et al. Uniportal complete video-assisted thoracoscopic surgery: a retrospective single-institution series of 106 cases. Chin J Endoscopy 2014;20:118-23.
9. Kang do K, Min HK, Jun HJ, et al. Single-port Video-Assisted Thoracic Surgery for Lung Cancer. Korean J Thorac Cardiovasc Surg 2013;46:299-301.
10. Bertolaccini L, Rocco G, Viti A, et al. Geometrical characteristics of uniportal VATS. J Thorac Dis 2013;5:S214-6.
11. Gonzalez-Rivas D, Fernandez R, de la Torre M, et al. Thoracoscopic lobectomy through a single incision. Multimed Man Cardiothorac Surg 2012;2012:mms007.
12. Amer K. Thoracoscopic mediastinal lymph node dissection for lung cancer. Semin Thorac Cardiovasc Surg 2012;24:74-8.

Cite this article as: Wang GS, Wang Z, Wang J, Rao ZP. Uniportal complete video-assisted thoracoscopic lobectomy with systematic lymphadenectomy. J Thorac Dis 2014;6(7):1011-1016. doi: 10.3978/j.issn.2072-1439.2014.06.41

Case Report

Non-intubated single port thoracoscopic procedure under local anesthesia with sedation for a 5-year-old girl

Jinwook Hwang[1], Too Jae Min[2], Dong Jun Kim[2], Jae Seung Shin[1]

[1]Department of Thoracic and Cardiovascular Surgery, [2]Department of Anesthesiology and Pain Medicine, Korea University Ansan Hospital, Korea University College of Medicine, Ansan, South Korea

Correspondence to: Jae Seung Shin. Department of Thoracic and Cardiovascular Surgery, Korea University Ansan Hospital, Korea University College of Medicine, 123, Jeokgeum-ro, Danwon-gu, Ansan-city, Gyeonggi-do 425-707, South Korea. Email: Jason@korea.ac.kr.

Abstract: Medical thoracoscopy is a feasible procedure for the diagnosis or treatment of thoracic diseases, and it can be performed under local anesthesia without tracheal intubation in cooperative adult patients. However, for younger than school aged patients, even simple procedures require general anesthesia with tracheal intubation. In this case report, we demonstrated the safe performance of a single port thoracoscopic procedure without tracheal intubation in a 5-year-old girl under local anesthesia and sedation. Local anesthesia around the site of a previous chest tube and sedation with intravenous (IV) dexmedetomidine and ketamine were applied. In the aspect of not only minimal injection of local anesthetics but also enhanced visualization of the thoracic structures, the non-intubated single port thoracoscopic surgery under local anesthesia with sedation was a good option for performing a simple thoracoscopic procedure in this 5-year-old patient.

Keywords: Thoracoscopy; non-intubated; single port; local anesthesia; sedation; bispectral index (BIS)

Submitted Feb 24, 2014. Accepted for publication Jun 16, 2014.
doi: 10.3978/j.issn.2072-1439.2014.06.36
View this article at: http://dx.doi.org/10.3978/j.issn.2072-1439.2014.06.36

Introduction

Medical thoracoscopy is a short and simple procedure for the diagnosis or biopsy of thoracic disease (1). In adult patients, it can be easily performed using local anesthetics with or without sedation under the cooperation of the patient (2). However, this is not feasible in pediatric thoracoscopy, which often requires general anesthesia (3). In pediatric patients less than 30 kg, carbon dioxide gas insufflation into the chest cavity through an air-tight port is needed to collapse the lung for operation (4).

In our case, we demonstrated the use of a non-intubated single port thoracoscopic procedure in a 5-year-old girl under local anesthesia with sedation for the management of a chest tube which was inadvertently sutured in the thoracic cavity.

Case report

A girl aged 5 years and 2 months (height 109 cm, weight 18.6 kg) experienced recurrent pneumonia over a 2-year period. Chest radiographs and computed tomographic (CT) scan showed extra lobar pulmonary sequestration in the left lower lung. Her vital signs were stable, and no other anomalies were detected during preoperative evaluation. We resected the lesion through an incision in the left lateral thoracotomy (length, 3 cm) along the fifth intercostal space, under general anesthesia with a single lumen tracheal tube (*Figure 1*). After resection of the sequestrated lung, a 16-Fr chest tube was inserted into the seventh intercostal space. The intercostal space was repaired using a 4-0 absorbable suture. After two days, the chest tube could not be withdrawn. It seemed to have been inadvertently sutured beneath the thoracotomy incision inside the thoracic cavity. At this point, we decided to perform the thoracoscopic procedure through the chest tube insertion site under sedation without tracheal intubation.

Sedation was achieved using Intravenous (IV) dexmedetomidine (1.0 μg/kg) for over 15 min before the

injection of local anesthetics, followed by 1 mg/kg of IV ketamine and dexmedetomidine 0.2-1.0 μg/kg/h IV (5). Oxygen at 6 L/min was administered via a pediatric face mask. The patient was monitored during sedation, and the bispectral index (BIS) was maintained between 45 and 65 during the procedure. The thoracoscopic procedure was performed in the right lateral decubitus position (*Figure 2A*). Local anesthesia was achieved around the hole where the chest tube was inserted, using a 2% lidocaine solution.

After the chest tube was pulled and shortened, a 2-mm thoracoscope was inserted through the chest tube site (5.5 mm incision) (*Figure 2*B). The ipsilateral lung was collapsed, during which the patient kept breathing with the contralateral lung. The intercostal suture material penetrating the middle part of the chest tube was found underneath the thoracotomy wound (*Figure 2B*). The suture was intrathoracically cut using 2-mm endoscopic scissor and grasper (*Figure 2C*), and the chest tube was removed. The new 16-Fr chest tube was inserted through the same hole, and anchored outside of the hole.

The patient's vital signs were stable during the entire operation (intraoperative mean arterial pressure, 85-90 mmHg; intraoperative heart rate, 90-92 beats/min; and intraoperative SPO_2, 99-100%). Ketamine 0.5 mg/kg (IV) was added as a bolus when involuntary movements or cough reflex occurred. The total operation time was 35 min, and the sedation time was 55 min. The IV dexmedetomidine infusion was discontinued at the end of surgery. After returning to the supine position, she was transferred to the recovery room.

The second chest tube was withdrawn immediately after checking the chest radiography. She was allowed to drink water one hour later, and was discharged after two days. No delayed complications were observed during the follow-up.

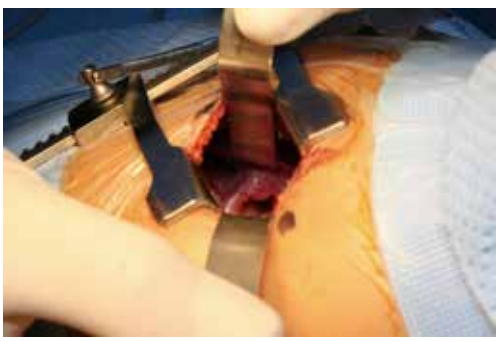

Figure 1 The extralobar type pulmonary sequestration with aberrant arterial pedicle from descending aorta was resected through a 3 cm thoracotomy incision.

Discussion

In thoracoscopic procedures for pediatric patients less than 30 kg, comprehensive visualization of the surgical field is

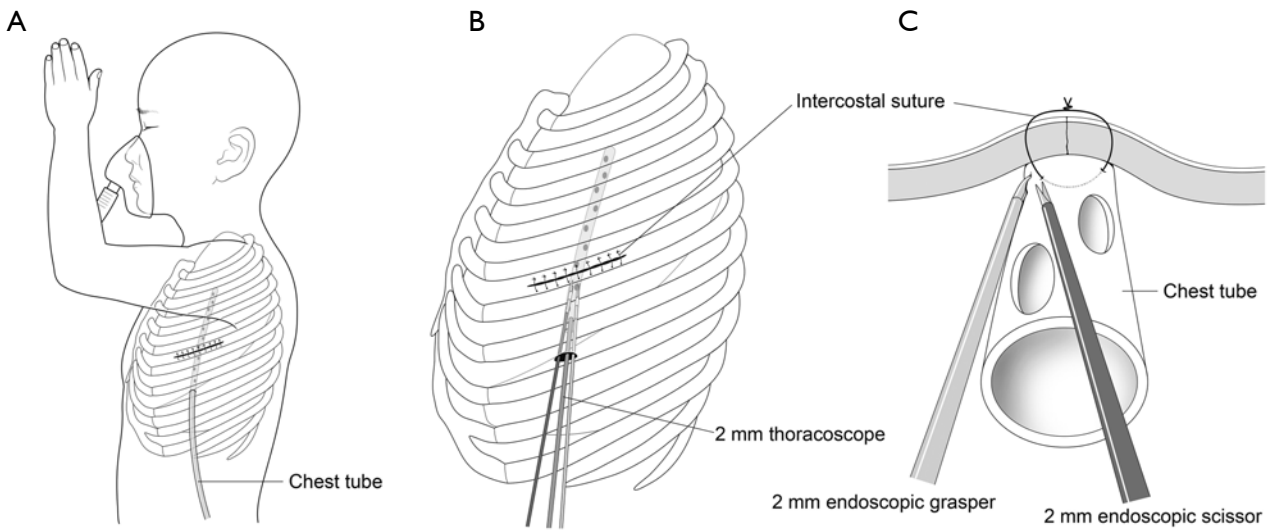

Figure 2 (A) The patient posed in the lateral decubitus position with oxygen supplied by facial mask, in deep sedation status; (B) the chest tube was shortened outside the thoracic cavity, and local anesthetic solution was injected around the chest tube site. A 2-mm-thoracoscope and other instruments were introduced through the chest tube site; (C) intercostal suture penetrated the chest tube underneath the thoracotomy incision. The suture material was cut using 2-mm endoscopic scissor and grasper under thoracoscopy.

quite difficult, even under general anesthesia (3,4). A collapse of the ipsilateral lung is essential for the surgeon to be able to perform a thoracoscopic procedure in thoracic cavities which have limited space. Because there are no appropriate double lumen tracheal tubes, which are used for selective one lung ventilation in adult patients, generally, single lumen tracheal intubation is generally applied in small pediatric patients, with carbon dioxide gas insufflations through air-tight ports into the thoracic cavity to collapse a lung (3,4).

In the present case, a self-ventilating thoracoscopic procedure under local anesthesia with sedation was planned. We considered that the repeat of general anesthesia in a patient who had undergone general anesthesia for the surgery just three days before may be harmful, especially for performing a short and simple procedure, such as cutting a suture material in the thoracic cavity. In addition, the ventilation of two lungs using a single lumen tracheal tube has no benefit in thoracoscopic surgery.

Active negative ventilation and opened thoracic cavity can collapse the ipsilateral lung, maintaining the ventilation of the contralateral lung under local anesthesia with sedation. Previous studies reported non-intubated thoracosopic bleb resections and lobectomies under sedation combined with various local anesthetic methods (1,6-9).

Sedation with IV ketamine and dexmedetomidine was available, and could provide a stable condition for uncooperative pediatric patients during the procedure. Even a simple procedure cannot be performed under local anesthesia without sedation in younger than school-aged patients because of their uncontrollable movement (4). This creates the necessity of deep sedation, which can often cause respiratory depression (3). We chose to combine IV ketamine with IV dexmedetomidine for our patient. Dexmedetomidine has been shown to produce stable sedation without respiratory depression (10), and provides analgesia and hemodynamic stabilization. In addition, it may prevent tachycardia, hypertension, and emergence phenomena associated with ketamine, while ketamine prevents bradycardia and hypotension, which have been reported with dexmedetomidine (11).

The procedure through the single hole from the previous chest tube, that is, the single port procedure was adjustable for an unconscious sedated patient. If possible, less irritation of the wound during the operation is better to maintain sedation. Compared with multiple port surgery, the stimulation of the port site can be reduced in single port surgery.

To the authors' knowledge, this report is the first report of a non-intubated single port thoracoscopic procedure under local anesthesia with sedation in a patient younger than school age. In the present case, non-intubated surgery improved the surgical view in pediatric thoracoscopic surgery, and single port surgery was effective under local anesthesia with sedation. However, our case was of a very short and simple procedure. Prospective randomized trials are required to determine the efficacy of non-intubated single port thoracoscopic surgery under local anesthesia and sedation in cases of complicated and long thoracoscopic procedures for pediatric patients.

Acknowledgements

Disclosure: The authors declare no conflict of interest.

References

1. Migliore M, Giuliano R, Aziz T, et al. Four-step local anesthesia and sedation for thoracoscopic diagnosis and management of pleural diseases. Chest 2002;121:2032-5.
2. Solak O, Cuhadaroglu S, Sayar A, et al. Thoracic surgical operations performed under local anesthesia and sedation for diagnosis and treatment. Thorac Cardiovasc Surg 2007;55:245-8.
3. McGahren ED, Kern JA, Rodgers BM. Anesthetic techniques for pediatric thoracoscopy. Ann Thorac Surg 1995;60:927-30.
4. Kumar K, Basker S, Jeslin L, et al. Anaesthesia for pediatric video assisted thoracoscopic surgery. J Anaesthesiol Clin Pharmacol 2011;27:12-6.
5. Tseng YD, Cheng YJ, Hung MH, et al. Nonintubated needlescopic video-assisted thoracic surgery for management of peripheral lung nodules. Ann Thorac Surg 2012;93:1049-54.
6. Nezu K, Kushibe K, Tojo T, et al. Thoracoscopic wedge resection of blebs under local anesthesia with sedation for treatment of a spontaneous pneumothorax. Chest 1997;111:230-5.
7. Pompeo E, Mineo TC. Awake operative videothoracoscopic pulmonary resections. Thorac Surg Clin 2008;18:311-20.
8. Rocco G, Romano V, Accardo R, et al. Awake single-access (uniportal) video-assisted thoracoscopic surgery for peripheral pulmonary nodules in a complete ambulatory setting. Ann Thorac Surg 2010;89:1625-7.
9. Katlic MR, Facktor MA. Video-assisted thoracic surgery

utilizing local anesthesia and sedation: 384 consecutive cases. Ann Thorac Surg 2010;90:240-5.
10. Levänen J, Mäkelä ML, Scheinin H. Dexmedetomidine premedication attenuates ketamine-induced cardiostimulatory effects and postanesthetic delirium. Anesthesiology 1995;82:1117-25.
11. Luscri N, Tobias JD. Monitored anesthesia care with a combination of ketamine and dexmedetomidine during magnetic resonance imaging in three children with trisomy 21 and obstructive sleep apnea. Paediatr Anaesth 2006;16:782-6.

Cite this article as: Hwang J, Min TJ, Kim DJ, Shin JS. Non-intubated single port thoracoscopic procedure under local anesthesia with sedation for a 5-year-old girl. J Thorac Dis 2014;6(7):E148-E151. doi: 10.3978/j.issn.2072-1439.2014.06.36

Case Report

Myelomatous pleural effusion as an initial sign of multiple myeloma—a case report and review of literature

Li-Li Zhang, Yuan-Yuan Li, Cheng-Ping Hu, Hua-Ping Yang

Department of Respiratory & Critical Care Medicine, Xiangya Hospital, Central South University, Changsha 410008, China

Correspondence to: Yuan-Yuan Li, MD. Department of Respiratory & Critical Care Medicine (Key site of National Clinical Research Center for Respiratory Disease), Xiangya Hospital, Central South University, No. 87 Xiangya Rd., Kaifu District, Changsha 410008, China. Email: leeround@163.com.

Objective: Discuss and improve the understanding of the clinical characters and diagnostic methods of myelomatous pleurisy, particularly of the patients with pleural effusion as an initial manifestation.

Background: A 53-year-old male, who had been misdiagnosed as tuberculous pleurisy in a local hospital, was diagnosed as multiple myeloma (MM) with pleural infiltration. We reviewed the literature on clinical manifestations, serum and pleural effusion characters, treatment and diagnostic options of this exceptionally rare presentation of MM.

Methods: We conducted a search of the published medical literature since 2000 in MEDLINE and PubMed using search criteria [("pleural effusion" and "MM") or "myelomatous pleural effusions"]. The search led to 64 case reports, and 16 cases with pleural effusion as an initial manifestation were included in this review. We have also searched for recent advances in diagnosis.

Results and conclusions: Myelomatous pleurisy is a rare complication of MM. Its clinical and laboratory findings are non-specific. Definitive diagnosis relies on the histopathology of pleural biopsy or pleural effusion. Thoracoscopic pleural biopsy is reliable, safe and effective. Chemotherapy is the mainstay of treatment for myelomatous pleural effusion. However, the response rate is low with an overall median survival time of 4 months.

Keywords: Multiple myeloma (MM); myelomatous pleural effusion; adenosine deaminase (ADA); extramedullary infiltration; thoracoscope technology

Submitted Mar 06, 2014. Accepted for publication Jun 06, 2014.
doi: 10.3978/j.issn.2072-1439.2014.06.48
View this article at: http://dx.doi.org/10.3978/j.issn.2072-1439.2014.06.48

Introduction

Multiple myeloma (MM) is one of the most common and represents 10% of all the malignant hematological diseases which mainly affects bone marrow although extramedullary tissues may be infiltrated as well. Pleural effusion may be a sign of thoracic involvement affecting about 6% of patients with MM (1), It is particularly rare (<1%) for MM patients to present myelomatous pleural effusion, especially for those with pleural effusion as an initial sign (2). Only 16 cases reported in English literature since 2000. We describe a case of MM presented initially as pleural effusion that was diagnosed and treated in our hospital, and reviewed the current literature on clinical manifestation, laboratory examination, diagnosis, treatment and prognosis.

Case report

A 53-year-old male presented with a 6-month history of dry cough, mild fever and night sweat. Two months prior to the admission, he was diagnosed as "Tuberculous pleuritis is possible" in the local clinic, and was given triple antituberculous treatment (isoniazide, rifampin and ethambutal) for 2 months. But his conditions did not change evidently. There was no chest pain, hemoptysis or palpitation. He was a chronic smoker for over 30 packs per years. Physical examinations only showed decreased breath sound, sporadic rhonchi and moist rale in the bilateral lower hemithorax. He preferred in sitting position. The patient's past history, social history, family history, and review of system were otherwise unremarkable.

Figure 1 Computed tomography (CT) of the thorax before the chemotherapy: initial image showed bilateral pleural effusions (red arrows) and distinctive nodular-like thickening of bilateral pleural with apparent enhancement (black arrows).

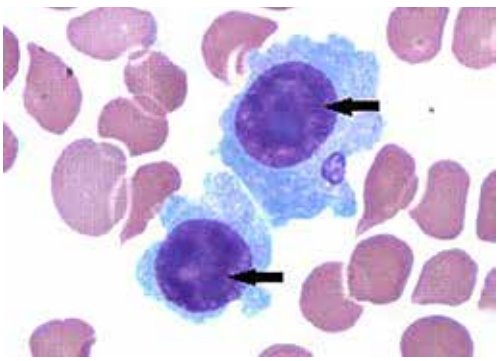

Figure 2 Giemsa-staining of the bone marrow: Malignant plasma cells were detected in the bone marrow. The cells have large eccentrically placed and pleomorphic nucleis and prominent nucleolis (arrows) (Wright-Giemsa, ×1,000).

Blood investigations revealed the following values: white blood cell (WBC) count: 2.5×10^9/L (40.7% neutrophils, 46.2% lymphocytes, 8.5% monocytes, 1.7% basophils and 0.0% eosinophils); hemoglobin, 76 mg/L; platelet count, 137×10^9/L; total protein, 93.1 g/L; albumin, 27.2 g/L; globulin, 65.9 g/L; blood calcium, 1.82 mmol/L (2.25-2.75 mmol/L), uric acid, 454.0 μmol/L; erythrocyte sedimentation rate (ESR), 43 mm/h; carcinoembryonic antigen (CEA), carbohydrate antigen 19-9 (CA19-9) are in normal range; thrombin time (TT), 24.3 s; D-dimer, 0.55 ng/L; T-SPOT.TB was negative. The serum light chain kappa: 4,210 mg/dL; the serum light chain lamda: 58.4 mg/dL. The serum immunoglobulin A: 351.00 mg/L, M: 153.00 mg/L, G: 52.7 g/L.

The pleural fluid was light yellow and highly cellular, in which 75% was mononuclear cells. Results from the analyses of the right side pleural fluid indicate an exudative type according to the Light criteria (3), which contained total protein 56.2 g/L, albumin 18.3 g/L, globulin 37.9 g/L, A/G 0.5, lactic dehydrogenase (LDH) 142.0 U/L, a-hydroxybutyrate dehydrogenase (aHBDH) 172.7 U/L, adenosine deaminase (ADA) 62.4 U/L. No acid-resistant bacilli were found. Computed tomography (CT) image of the chest (axial view) indicated bilateral sided pleural effusion and distinctive pleural nodular-like thickening as shown in *Figure 1*. The posteroanterior skull radiographs demonstrated low craniofacial bones density, and saccate transparent area could be seen without any signs of fractures. The posteroanterior view of pelvis was normal. The single photon emission computed tomography (SP-ECT) scan indicated metabolic disturbance of skull bones and elevated metabolism condition of the middle of left humerus.

The bone marrow aspiration biopsy showed that hyperplasia of original plasma cells (1.5%) and active hyperplasia of naïve plasma cells (15.5%) (*Figure 2*). A thoracoscopic pleural biopsy of right side through video-assisted thoracic surgery was performed. Multiple nodules of pleural surface and partial lung collapse could be seen (*Figure 3*). The pathology of the specimen revealed abnormal proliferation of plasmocytes on hematoxylin and eosin (HE) stains. The immunohistochemistry test of the specimen showed: CD31 (+), CD34 (+), Ki67 (50%+), CD138 (+), CD38 (+), Kappa (+), Lambda (–), MUM1 (+) (*Figure 4*).

The patient was finally diagnosed as MM with pleural infiltration, IgG-k type, stage II [ISS criteria (4)] based on the clinical manifestations, physical and laboratory examinations, radiographic findings, pathological and immunohistochemistry results. The patient was transferred accordingly to the Hematology Department for chemotherapy (bortezomib, dexamethasone and thalidomide) immediately. After two cycle of chemotherapy, the β-2 microglobulin dropped from 5.4 to 3.2 mg/L, the serum globulin dropped from 65.6 to 19.1 g/L. Chest CT showed that the bilateral sided pleural effusion was gone completely (*Figure 5*). The overall condition of the patient is good and currently under routine follow-ups.

Review criteria

We conducted a detailed search of the literatures in English published between 2000 and 2013 in MEDLINE and PubMed using search criteria [("pleural effusion" and "MM") or "myelomatous pleural effusions"]. The search led

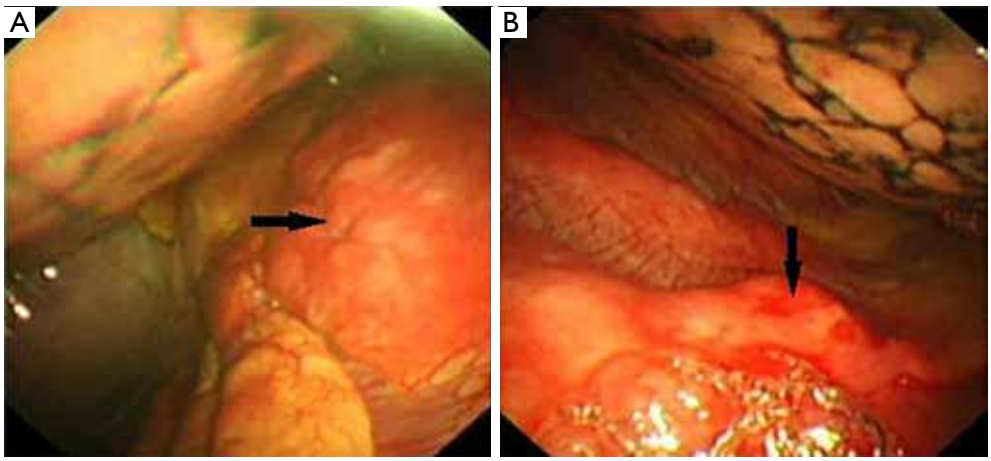

Figure 3 Video stills of right pleural during thoracoscopy. Multiple nodules of pleural surface (black arrows) and partial lung collapse could be seen.

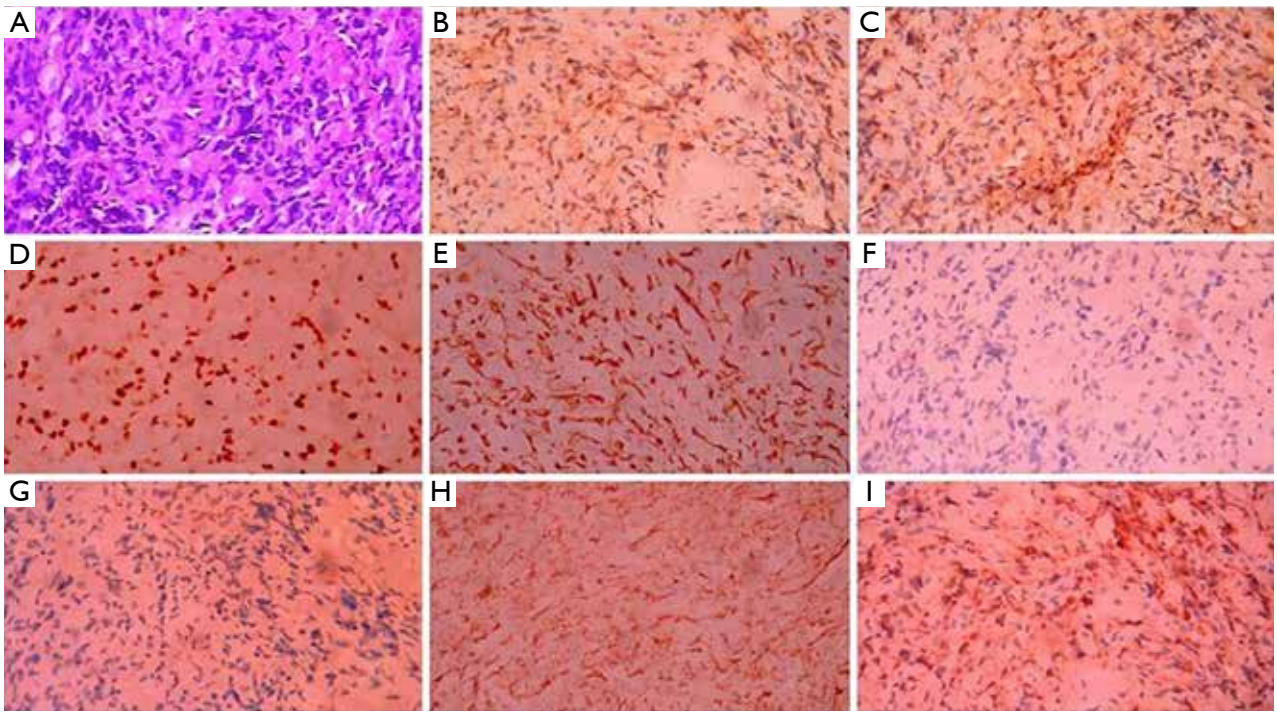

Figure 4 Pathology and immunohistochemistry of the pleural biopsy: (A) hematoxylin and eosin (HE) staining shows abnormal proliferation of plasmocytes. (B-I) are immunohistochemical staining including (B) CD138 (+), (C) Kappa (+), (D) Ki67 (50%+), (E) CD34 (+), (F) MUMI (+), (G) Lambda (–), (H) CD31(+), (I) CD38(+). CD138 and CD38 positive usually represent malignant plasmacyte disease; Kappa (+) and Lambda (–) means kappa light chain multiple myeloma. Ki-67 (50%+) represents the growth fraction of the cell population is over 50%. CD34 (+) here represents hematopoietic disorder. MUM1 is a key regulator of several steps in lymphoid, myeloid, and dendritic cell differentiation and maturation. CD31 (+) here represents malignant plasmacyte diseases. The magnifications are all of 400.

to 64 case reports of MM related pleural effusion including those from the relevant references. We read either the full texts or the abstracts thoroughly and finally decided to include 16 cases about MM of patients with the inclusion criteria: (I) the patients with MM presenting initially with pleural effusion; and (II) the patients are proved to have myelomatous pleural effusion by cytological biopsy of pleural effusion or pleural biopsy. We retrospectively

Figure 5 Computed tomography (CT) of the thorax after the chemotherapy: after two cycles of chemotherapy treatment, bilateral pleural effusion was completely absorbed.

reviewed these patients' data, including general information, laboratory indexes, diagnostic methods, managements, outcome and etc.

Results

The overall schematic general information, classification of MM, and clinical manifestations are shown in *Table 1*. Among the 17 cases in this review (including our case report), the mean age is 58.9-year-old (ranging from 40- to 76-year-old) with different gender distribution and the ratio of men to women is nearly 2:1.

Table 1 General characters of the cases

SN	First author	Year	Age/sex	Ig class	Extramedullary involvement	Osteolytic lesions	Diagnostic method of MPE	Treatment other than hospital care	Prognose (month)
1	Xu (2)	2013	54/M	Non-secretory	Yes	Yes	CT guided pleural biopsy	Yes	12
2	Oudart (5)	2012	62/F	k	Yes	Yes	Cyto and electrophoresis analysis of PE	NG	NG
3	Keklik (6)	2012	52/M	IgG-k	Yes	Yes	FCM of PE	Yes	NG
4	Dharan (7)	2010	54/M	IgA-k	Yes	Yes	Cyto of PE	Yes	4
5	Mehta (8)	2010	65/M	k	No	NG	pleural biopsy*	Yes	12
6	Ghoshal (9)	2010	61/F	k	Yes	Yes	Cyto of PE	Only hospital care	NG
7	Neuman (10)	2009	47/M	k	Yes	Yes	Cyto and immunohistology of PE	Only hospital care	NG
8	Kim (11)	2008	76/F	λ	Yes	No	Cyto of PE	Yes	1
9	Yokoyama (12)	2008	58/M	IgD-λ	Yes	No	pleural biopsy	Only hospital care	1
10	Usköl (1)	2008	56/M	IgG-k	Yes	No	pleural biopsy	Yes	18
11	Dhingra (13)	2007	40/M	IgG-k	Yes	Yes	Cyto of PE	NG	NG
12	Federici (14)	2007	78/M	IgG-k	Yes	Yes	Cyto and immunohistology of PE	Yes	2
13	Kamble (15)	2005	75/F	IgG-λ	Yes	Yes	FCM and Cyto of PE	Yes	50
14	Inoue (16)	2005	51/F	IgG-λ	Yes	NG	Cyto and immunohistology of PE	Yes	10
15	Deshpande (17)	2000	58/M	IgA-λ	Yes	Yes	Cyto of PE	Only hospital care	1
16	Kim (18)	2000	61/F	IgD-λ	Yes	Yes	Cyto of PE	Yes	1
17	Our case	NA	53/M	IgG-k	Yes	Yes	pleural biopsy under thoracoscopy	Yes	6

M, male; F, female; SN, serial number; Cyto, cytology; FCM, flow cytometry; PE, pleural effusion; NG, not given; *, pathology of pleural specimen demonstrated pleural amyloidosis.

Table 2 Laboratory indexes of MM

SN	Pleural effusion analysis						Current blood test		Current bone marrow
	Character	Property	Cytology	Location	ADA (IU/L)	LDH (IU/L)	B2M (g/dL)	Albumin (g/dL)	PC%
1	Pale yellow	Exudative	Negative	Bilateral	419	Normal	NG	4.1	0.76
2	Pale yellow	Exudative	Negative	Right	NG	NG	NG	NG	NG
3	Pale yellow	Exudative	Negative	Left	NG	NG	2.7	1.8	0.28
4	Bloody	Exudative	Positive	Right	NG	NG	NG	NG	0.6
5	Pale yellow	Exudative	Negative	Left	Normal	375	NG	NG	0.38
6	Bloody	Exudative	Positive	Left	142	Normal	NG	3.73	0.55
7	Pale yellow	Exudative	Positive	Left	Normal	Normal	2.4	NG	0.95
8	Pale yellow	Exudative	Positive	Right	Normal	2,281	NG	3.6	NG
9	Pale yellow	Exudative	Negative	Left	70	278	NG	2.92	NG
10	Pale yellow	Exudative	Positive	Left	Normal	Normal	NG	1.5	0.76
11	Pale yellow	Exudative	Positive	Bilateral	NG	NG	NG	NG	0.5
12	Bloody	Exudative	Positive	Left	NG	NG	NG	NG	0.29
13	Pale yellow	Exudative	Positive	Right	NG	NG	11	NG	0.8
14	Pale yellow	Exudative	Positive	Right	NG	NG	2.9	3.3	0.65
15	Pale yellow	Exudative	Positive	Bilateral	NG	NG	NG	NG	NG
16	Bloody	Exudative	Positive	Left	Normal	608	NG	2.5	0.53
17	Pale yellow	Exudative	Positive	Bilateral	62	Normal	5.4	1.83	0.17

Abbreviations: MM,multiple myeloma; SN, serial number; LDH, lactic dehydrogenase; ADA: adenosine deaminase; B2M, beta-2 microglobulin; PC%, plasma cell%.

In this series, IgG is the most common type of MM (7/17) in contrast to the IgA predominance in previous reports (19,20). The vast majority of patients presented with dyspnea (14/17) and the other symptoms include cough (4/17), chest pain (3/17), fatigue (3/17), back pain (2/17), mild fever (2/17), and expectoration (1/17). All of these symptoms are nonspecific and mainly caused by massive pleural effusion.

Some important laboratory indexes of MM including the analysis of pleural effusion, blood and bone marrow are shown in *Table 2*. Among the pleural effusions, eight were left-sided, five were right-sided, and four were bilateral sided and all of them were proved to be exudative. Four of the 17 cases had serosanguinous pleural fluid. Biochemical tests of pleural effusion were performed in ten patients.

Elevated ADA levels were proved in four patients (>70 IU/L), and elevated LDH levels were found in four patients. However, we did not find any evidence of pulmonary tuberculosis in the relevant literatures (see the detailed discussion). Some important laboratory evidence, such as anemia (hemoglobin <12 g/dL) was seen in 6 of the 17 patients and the serum beta-2 microglobulin and albumin were only both given in three case reports (*Table 2*). According to ISS criteria (4) and based on the available information, only three patients can be categorized as MM and all of them were at stage II.

Some medullary and extramedullary involvement proofs, diagnostic method, treatment and prognosis are also shown in *Table 1*. Six of the 17 patients were involved in nodular-like thickening of pleural, three cases had rib lyric lesions and two patients had spinal lyric lesions combined with mediastinal abnormalities. The overwhelming majority had osteolytic lesions (12/15) proved by either X-ray or SP-ECT and at the time of diagnosis, only one of the patients showed more than 80% of plasmacytosis in the bone marrow.

Nearly all of the patients (16/17) had associated pleural or chest wall plasmacytomas, and the final diagnosis of myelomatous pleural effusion was established by pleural biopsy in 4 patients, pleural cytology in 11 patients, immunohistochemistry method in 3 patients, flow cytometry (FCM) in 2 patients, and 1 patient's pleural fluid was originated from pleural amyloidosis.

Among all the reported case, the treatments described in this series of literature were quite complicated and most of the patients received chemotherapy (11/15) with two of them received radiotherapy after chemotherapy, and only one patient received blood stem cell transfusion. However, the positive response rate was less than 50% and the overall median survival time was 4 months (ranging from 3 to 50 months).

Discussion

MM is one of the most common and represents 10% of all the malignant hematological diseases which mainly affects bone marrow although extramedullary tissues may be infiltrated as well. Pleural effusion may be a sign of thoracic involvement affecting about 6% of patients with MM (1). Oudart and his colleagues (5) had summarized the six etiologic factors which lead to pleural effusion in MM, including congestive heart failure secondary to amyloidosis, chronic renal failure, nephritic syndrome secondary to renal tubular infiltration with paraprotein and development of glomerular damage, direct infiltration of pleural fluid from adjacent tissues, hypoalbuminemia, pulmonary embolism, secondary neoplasm, lymphatic drainage obstruction by tumor infiltration, infection and pleural myelomatous involvement. Of all these six factors listed above, myelomatous involvements of pleural and adjacent tissues were the most common one which brought about pleural exudates in our series.

About 80 reports about myelomatous pleural effusion have been reported so far and most of the symptoms were seen in a late stage of MM with a poor prognosis of the median survival time hardly exceeding 4 months (21). According to previous reports, left-sided pleural effusion is mostly seen (22). However, bilateral sided pleural effusion caused by pleural myelomatous is extremely rare and only three cases have been reported so far (2,13,23).

One noteworthy finding in our series is the high frequency of light chain kappa type of myeloma (24%) and high level in serum or pleural effusion. In the 2008 WHO classification, the light chain type usually less than 20% (24). In these light chain kappa subtype of myeloma patients, the k/λ ratios in the pleural effusion were all higher than that found in the serum, indicating a possible local synthesis of k light chain. Oudart *et al*. had proposed the ratio difference may be a reflection of variant clearance mechanism in the pleural fluid and blood (5).

Another noteworthy finding is the high ADA activities in pleural effusion. In our series, four cases were found with elevated ADA activities. High level of ADA activities in the pleural fluid strongly recommends tuberculous pleural effusion, and the sensitivity and specificity can reach 92% and 90%, respectively (25). The reported cutoff values of ADA activities to exclude tuberculous pleural effusion ranged from 40 to 60 IU/L (26-31). However, the elevated ADA activity had also been reported in other diseases, such as breast cancer, non-Hodgkin's lymphoma, and some malignant hematologic diseases (32-35). The ADA activities of the four patients reviewed in this paper exceeded the upper limit of the cutoff value. Since ADA is an enzyme expressed in activated T-lymphocytes, the elevation of ADA activity in the pleural effusion can be used as an indicator of active local inflammatory response (36,37). Therefore, since the ADA activity may indicate an activation or alteration of the immune system, and this also can be used to explain why most of the patients with elevated ADA activity in myelomatous pleural effusion also had enlarged lymph nodes, especially mediastinal lymph nodes. However, this hypothesis needs to be tested with more researches in the future.

The biochemistry tests of blood and fluid are important for giving good diagnostic orientations. The high quantitative of globulins, low levels of albumin and high levels of calcium suggest the possibilities of MM. When we consider about it, the blood and fluid investigation such as electrophoresis and immunofixation electrophoresis should be given to the patients. However, for those patients with pleural effusion as one of the first signs, mostly they visit respiratory department at first. Sometimes, their routine biochemistry tests of blood and fluid are non-specific. In this case, it is hard for a respiratory physician to take hematological malignancy into consideration and need to do some traumatic investigation to give final diagnosis.

Cytological identification of malignant plasma cells within the pleural effusion has been considered as the best diagnose method of myelomatous pleural effusion (38). However, due to the limited number of malignant plasma cells and potential in vitro degeneration, it may fail to make diagnosis. Since 4 of the 17 patients who were misdiagnosed as tuberculousis pleurisy and subsequently proven to be myelomatous pleural effusion by pleural biopsy, this indicates that pleural biopsy may also be the most efficient and reliable method in differentiating myelomatous and tuberculosis pleural effusion. It had been recommended that in patients with only pleural fluid appearance on CT scan and in those who may have benign pleural effusion, the primary method of diagnosis should

be medical thoracoscopy (21). Pleural infiltration of plasma cells is patchy sometimes and it is hard to find abnormal signs of pleural in CT images or B-ultrasonography, and it is unlikely to get positive result in CT/B-ultrasound guided pleural biopsy. However, with the development of thoracoscope technology, pleural biopsy under video-assisted thoracoscope is now not only a safe procedure but also could improve the diagnosis rate with both diagnostic sensitivity and specificity around 100% in pleural effusion from unknown origin (39,40). To our best knowledge, the case reported here is the first one whose pleural infiltration of MM was detected by pleural biopsy under video-assisted thoracoscope.

The overall median survival time for myelomatous pleural effusion is 4 months (ranging from 3 to 50 months), which is much less than 29 months, the median survival time of stage III MM (21). In our series, the treatment methods varied, the response rate was low, and survive time was short. Kamble *et al*. (15) had concluded that system chemotherapy combined with chest tube drainage or pleurodesis was an excellent palliation in most patients. However, there appears to be no advantage of radiotherapy, blood stem cell transfusion or other aggressive therapy. Therefore, newer drugs and palliation methods need to be developed in the future to prolong survival time and improve the quality of life for these patients.

Due to (I) the limited number of myelomatous pleural effusion cases as an initial clinical manifestation and (II) incomplete information from each individual cases, such as laboratory indexes of serum and pleural effusion, it is challenging at the present stage to establish the precise relationship between test indexes and prognosis of this disease. This not only prevented us from conducting evidence-based medicine but also limited our ability to provide any meaningful prognosis of this particular disease. This also indicates that further research in myelomatous pleural effusion is warranted.

Conclusions

Our review shows that myelomatous pleural effusion is rare. Its clinical and laboratory findings are non-specific. Definitive diagnosis relies on the histopathology of pleural biopsy or pleural effusion. Thoracoscopic pleural biopsy is reliable, safe and effective. Chemotherapy is the mainstay of treatment for myelomatous pleural effusion. However, the response rate is low with an overall median survival time of 4 months.

Acknowledgements

The author would like to thank Professor Dianzheng Zhang for the English language review.

Disclosure: The authors declare no conflict of interest.

References

1. Uskül BT, Türker H, Emre Turan F, et al. Pleural effusion as the first sign of multiple myeloma. Tuberk Toraks 2008;56:439-42.
2. Xu XL, Shen YH, Shen Q, et al. A case of bilateral pleural effusion as the first sign of multiple myeloma. Eur J Med Res 2013;18:7.
3. Light RW. The Light criteria: the beginning and why they are useful 40 years later. Clin Chest Med 2013;34:21-6.
4. Greipp PR, San Miguel J, Durie BG, et al. International staging system for multiple myeloma. J Clin Oncol 2005;23:3412-20.
5. Oudart JB, Maquart FX, Semouma O, et al. Pleural effusion in a patient with multiple myeloma. Clin Chem 2012;58:672-4.
6. Keklik M, Sivgin S, Pala C, et al. Flow cytometry method as a diagnostic tool for pleural fluid involvement in a patient with multiple myeloma. Mediterr J Hematol Infect Dis 2012;4:e2012063.
7. Dharan M. Unilateral pleural effusion as a presenting manifestation of plasma cell myeloma (multiple myeloma): a case report. Acta Cytol 2010;54:780-2.
8. Mehta AA, Venkatakrishnan R, Jose W, et al. Multiple myeloma presenting as eosinophilic pleural effusion. Asia Pac J Clin Oncol 2010;6:256-9.
9. Ghoshal AG, Sarkar S, Majumder A, et al. Unilateral massive pleural effusion: a presentation of unsuspected multiple myeloma. Indian J Hematol Blood Transfus 2010;26:62-4.
10. Neuman G, Denekamp Y. Dyspnea and pleural effusion as presenting clinical manifestations of multiple myeloma. Isr Med Assoc J 2009;11:118-9.
11. Kim YJ, Kim SJ, Min K, et al. Multiple myeloma with myelomatous pleural effusion: a case report and review of the literature. Acta Haematol 2008;120:108-11.
12. Yokoyama T, Tanaka A, Kato S, et al. Multiple myeloma presenting initially with pleural effusion and a unique paraspinal tumor in the thorax. Intern Med 2008;47:1917-20.
13. Dhingra KK, Singhal N, Nigam S, et al. Unsuspected multiples myeloma presenting as bilateral pleural effusion

- a cytological diagnosis. Cytojournal 2007;4:17.
14. Federici L, Blondet C, Andrès E. Aggressive form of multiple myeloma presenting with specific pleural effusion, neutrophilia, and eosinophilia. Eur J Intern Med 2007;18:348-9.
15. Kamble R, Wilson CS, Fassas A, et al. Malignant pleural effusion of multiple myeloma: prognostic factors and outcome. Leuk Lymphoma 2005;46:1137-42.
16. Inoue Y, Chua K, McClure RF, et al. Multiple myeloma presenting initially as a solitary pleural effusion later complicated by malignant plasmacytic ascites. Leuk Res 2005;29:715-8.
17. Deshpande AH, Munshi MM. Pleural effusion as an initial manifestation of multiple myeloma. Acta Cytol 2000;44:103-4.
18. Kim YM, Lee KK, Oh HS, et al. Myelomatous effusion with poor response to chemotherapy. J Korean Med Sci 2000;15:243-6.
19. Rodríguez JN, Pereira A, Martínez JC, et al. Pleural effusion in multiple myeloma. Chest 1994;105:622-4.
20. Cho YU, Chi HS, Park CJ, et al. Myelomatous pleural effusion: a case series in a single institution and literature review. Korean J Lab Med 2011;31:225-30.
21. Kamble R, Wilson CS, Fassas A, et al. Malignant pleural effusion of multiple myeloma: prognostic factors and outcome. Leuk Lymphoma 2005;46:1137-42.
22. Kintzer JS Jr, Rosenow EC 3rd, Kyle RA. Thoracic and pulmonary abnormalities in multiple myeloma. A review of 958 cases. Arch Intern Med 1978;138:727-30.
23. Makino S, Yamahara S, Nagake Y, et al. Bence-Jones myeloma with pleural effusion: response to alpha-interferon and combined chemotherapy. Intern Med 1992;31:617-21.
24. Sabattini E, Bacci F, Sagramoso C, et al. WHO classification of tumours of haematopoietic and lymphoid tissues in 2008: an overview. Pathologica 2010;102:83-7.
25. Liang QL, Shi HZ, Wang K, et al. Diagnostic accuracy of adenosine deaminase in tuberculous pleurisy: a meta-analysis. Respir Med 2008;102:744-54.
26. Light RW, Erozan YS, Ball WC Jr. Cells in pleural fluid. Their value in differential diagnosis. Arch Intern Med 1973;132:854-60.
27. Valdés L, Alvarez D, San José E, et al. Tuberculous pleurisy: a study of 254 patients. Arch Intern Med 1998;158:2017-21.
28. Valdés L, Alvarez D, San José E, et al. Value of adenosine deaminase in the diagnosis of tuberculous pleural effusions in young patients in a region of high prevalence of tuberculosis. Thorax 1995;50:600-3.
29. Villena V, Navarro-Gonzálvez JA, García-Benayas C, et al. Rapid automated determination of adenosine deaminase and lysozyme for differentiating tuberculous and nontuberculous pleural effusions. Clin Chem 1996;42:218-21.
30. Burgess LJ, Maritz FJ, Le Roux I, et al. Use of adenosine deaminase as a diagnostic tool for tuberculous pleurisy. Thorax 1995;50:672-4.
31. Ungerer JP, Oosthuizen HM, Retief JH, et al. Significance of adenosine deaminase activity and its isoenzymes in tuberculous effusions. Chest 1994;106:33-7.
32. Aghaei M, Karami-Tehrani F, Salami S, et al. Adenosine deaminase activity in the serum and malignant tumors of breast cancer: the assessment of isoenzyme ADA1 and ADA2 activities. Clin Biochem 2005;38:887-91.
33. Buyukberber M, Sevinc A, Cagliyan CE, et al. Non-Hodgkin lymphoma with high adenosine deaminase levels mimicking peritoneal tuberculosis: an unusual presentation. Leuk Lymphoma 2006;47:565-8.
34. Meier J, Coleman MS, Hutton JJ. Adenosine deaminase activity in peripheral blood cells of patients with haematological malignancies. Br J Cancer 1976;33:312-9.
35. Ohata M, Masuda I, Nonaka K, et al. Combination assay of IAP and ADA in hematologic malignancies. Rinsho Byori 1990;38:703-10.
36. Liu YC, Shin-Jung Lee S, Chen YS, et al. Differential diagnosis of tuberculous and malignant pleurisy using pleural fluid adenosine deaminase and interferon gamma in Taiwan. J Microbiol Immunol Infect 2011;44:88-94.
37. Light RW. Update on tuberculous pleural effusion. Respirology 2010;15:451-8.
38. Safa AM, Van Ordstrand HS. Pleural effusion due to multiple myeloma. Chest 1973;64:246-8.
39. Ng TH, How SH, Kuan YC, et al. Medical thoracoscopy: Pahang experience. Med J Malaysia 2008;63:298-301.
40. Metintas M, Ak G, Dundar E, et al. Medical thoracoscopy vs CT scan-guided Abrams pleural needle biopsy for diagnosis of patients with pleural effusions: a randomized, controlled trial. Chest 2010;137:1362-8.

Cite this article as: Zhang LL, Li YY, Hu CP, Yang HP. Myelomatous pleural effusion as an initial sign of multiple myeloma—a case report and review of literature. J Thorac Dis 2014;6(7):E152-E159. doi: 10.3978/j.issn.2072-1439.2014.06.48

Letter to the Editor

Moxifloxacin in acute exacerbations of chronic bronchitis and COPD

Wan-Jie Gu

Department of Anaesthesiology, the First Affiliated Hospital, Guangxi Medical University, Nanning 530021, China

Correspondence to: Wan-Jie Gu, MSc. Section Editor (Systematic Review and Meta-analysis) of Journal of Thoracic Disease, Department of Anaesthesiology, the First Affiliated Hospital, Guangxi Medical University, 22 Shuangyong Road, Nanning 530021, China. Email: wanjiegu@hotmail.com.

Submitted on Mar 13, 2014. Accepted for publication Jun 30, 2014.
doi: 10.3978/j.issn.2072-1439.2014.07.08
View this article at: http://dx.doi.org/10.3978/j.issn.2072-1439.2014.07.08

To the editor,

Liu and colleagues have conducted a systematic review and meta-analysis to evaluate the efficacy and safety of moxifloxacin in acute exacerbations of chronic bronchitis and chronic obstructive pulmonary disease (1). The searched databases were inconsistent. In the *Methods* subsection of *Abstract*, searched databases were PubMed, EMBASE, and the Web of Science; however, in the *Data sources and search strategy* subsection of *Text*, searched databases were PubMed, the Cochrane Central Database of Controlled Trials, and EMBASE.

(I) For the outcomes of clinical success and bacteriological eradication, it was inappropriate to use odds ratio for estimating the differences between moxifloxacin group and other antibiotics group, since the clinical success and bacteriological eradication rates were very high in both groups. In this case, relative risk should be used;

(II) In the *Study selection* subsection of *Text*, the authors stated that for this meta-analysis, we considered those randomized control trials (RCTs) that compared the clinical efficacy of moxifloxacin and another antibiotic in patients with AECB and AECOPD. In the *Statistical analysis* subsection of *Text*, the authors said that we computed pooled odds ratios (ORs) and 95% confidence intervals (CIs) from the adjusted ORs and 95% CIs reported in the observational studies. And then, I have to wonder why the authors computed pooled ORs from the observational studies rather than the included RCTs, even the adjusted ORs?

(III) In the *Statistical analysis* subsection of *Text*, there is no reason to select fixed-effects analysis when heterogeneity is less than 50% by I squared, since under those circumstances tau squared may still be greater than zero and random-effects models may still give wider confidence intervals. If there is zero heterogeneity (tau squared zero), then the random effects result will equal the fixed effects result;

(IV) In the second figure of that article, Wilson R 1999 accounts for nearly one-third (29.7%) of the total weight. Also, Wilson R 2012 accounts for nearly half (45.3%) of the total weight in the fourth figure of that article. The authors should performed sensitivity analysis by omitting the trial to test the robustness of their results;

(V) In the *Publication bias* subsection of *Text*, the authors found evidence of publication bias upon visual inspection of the funnel plot. Strictly speaking, it was incorrect to describe the result like this. The most important one is that the asymmetry of funnel plot does not mean the existence of publication bias. It would be more appropriate that evidence of small trial bias was found upon visual inspection of the funnel plot.

Acknowledgements

Disclosure: The author declares no conflict of interest.

References

1. Liu KX, Xu B, Wang J, et al. Efficacy and safety of moxifloxacin in acute exacerbations of chronic bronchitis and COPD: a systematic review and meta-analysis. J Thorac Dis 2014;6:221-9.

Cite this article as: Gu WJ. Moxifloxacin in acute exacerbations of chronic bronchitis and chronic obstructive pulmonary disease. J Thorac Dis 2014;6(7):E160. doi: 10.3978/j.issn.2072-1439.2014.07.08

Editorial

Individualized altered fractionation as a more effective radiotherapy for non-small cell lung cancer

Yi-Jen Chen

Radiation Oncology, City of Hope Medical Center, Duarte, CA 90603, USA

Correspondence to: Yi-Jen Chen, MD, PhD, Clinical Professor. Radiation Oncology, City of Hope Medical Center, Duarte, CA 90603, USA. Email: yichen@coh.org.

Submitted May 31, 2014. Accepted for publication Jun 04, 2014.

doi: 10.3978/j.issn.2072-1439.2014.06.39

View this article at: http://dx.doi.org/10.3978/j.issn.2072-1439.2014.06.39

Treating non-small cell lung cancer (NSCLC), it seems altered fractionations either by hypo- or hyper-fractionated radiotherapy (RT) improves overall survival as compared with conventional schedules (1). With innovative technologies of modern RT, altered fractionation can generally deliver higher biologically effective doses for a better clinical outcome without causing significant side effects. The technologies include imaging studies for tumor delineation, computerization of RT planning, intensity modulation RT, image guidance RT, respiratory motion assessment and stereotactic targeting technology. Today, stereotactic ablative RT (SABR) or stereotactic body RT (SBRT) is considered a standard treatment for patients with T1 or T2 N0 NSCLC when surgery is not an option due to refusal or comorbidities. In addition, since surgical metastectomy has been shown to cure patients with oligometastatic cancer to the lung, it is expected that SABR will play a major role for such patients in the future as well. Compared to surgical metastectomy, patients might favor to undergo SABR because it is non-invasive, out-patient treatment and likely more cost effective. It is however essential to understand that with the complexity and variation inherent in SABR, a potential catastrophic consequence could happen if mistakes in the process of implementation were not identified or corrected. Therefore, issues related to staffing training, simulation and planning technologies, equipment commissioning, and quality assurance must be addressed to ensure treatment efficacy and safety.

This special issue on hypo- and hyper-fractionated RT in NSCLC using cutting-edge technologies has been long awaited. Chang and Ruysscher are to be congratulated for being able to gather and compile nine reviews and one original article on the hottest subject related to hypo- and hyper-fractionated RT in NSCLC using cutting-edge technologies. All the authors are truly experts in the world on each topic. From biological, physical and clinical aspects, the authors discuss utilization of altered fractionated RT for early-stage and locally-advanced NSCLC and oligometastatic cancer to the lung. Followings are brief summaries for each article.

From preclinical laboratory studies to clinical trials, Prasanna *et al.* describe aspects from radiobiology point of view related to hyper- and hypo-fractionated RT for NSCLC. Novel concepts either by hyperfractionated or hypofractionated RT are presented. Other than discussing the classical 4-Rs (repair, re-assortment, re-oxygenation and re-population), unique phenomenon of hyper-radiation sensitivity at lower doses (0.1 to 0.6 Gy) combining with chemotherapy in hyperfractionated setting, and mechanisms underlying the effects of high-dose hypofractionated RT including abscopal/bystander effects, activation of immune system, endothelial cell death and effect of hypoxia with re-oxygenation are described. Molecular events in low dose hyperfractionated RT and impact of SABR are illustrated nicely in their article. In addition, clinical trials combining low doses hyperfractionated RT with chemotherapy in solid tumors are updated in details.

Challenges to treat patients with lung cancer from aspects of radiation physics include tumor motion, accurate dose calculation in low density media, limiting dose to nearby organs at risk, and changing anatomy over the treatment course. Glide-Hurst and Chetty nicely provide an overview of current state-of-the-art technologies regarding target volume definition, dose calculation, 4D dose accumulation, on-line IGRT, tumor tracking, and image-guided adaptive RT.

Accurate delineation and characterization of primary tumors and lymph nodes are prerequisites for successful RT. Van Elmpt *et al.* summarize the latest available imaging

techniques including FDG-PET/CT, hypoxia PET, MRI, dynamic contrast-enhanced CT, and dual energy CT (DECT) for target volume delineation and quantification, and SPECT/CT, CT, PET/CT, MRI, and DECT for normal tissue characterization.

It is believed that locoregional treatment of lung cancer is a critical starting point to cure a patient. For patients with locally advanced lung cancer, to increase RT therapeutic gain for a better locoregional control, hyperfractionated or accelerated RT provides promising ways for dose escalation. Haslett *et al.* provide a detailed overview of the current literature on hyperfractionated and accelerated RT in NSCLC. Novel concepts of "isotoxic" RT using hyperfractionated accelerated regimen and related trials are explained.

As mentioned, there is convincing evidence showing a clear radiation dose effect in NSCLC patients. The review article by Kong *et al.* is one of the highlight of this special issue. From the biological consideration point of view, issues related to radiation dose effect in locally advanced NSCLC are reviewed. As explained by the authors, although the benefit of using conventional dose/fractionation regimens for radiation dose escalation has been challenged by the preliminary results from RTOG0617, there are potential more effective approaches based on the sensitivity of tumor and critical organs of each individual patient. Promising ongoing trials including a European phase II PET-boost trial and RTOG1106 are presented.

Have the theoretical advantages of Bragg peak characteristics of proton particles been exploited on NSCLC for better results? From the point of view of dosimetric analyses and clinical analyses, in a review article of this special issue, Gomez and Chang nicely summarize the use of hypofractionated dose-escalated proton beam therapy for both early-stage and locally advanced NSCLC. Two ongoing trials using stereotactic body proton therapy for NSCLC are illustrated.

With advances in understanding of molecular biology of NSCLC, the treatment of NSCLC has started the era of personalized medicine. In the review article by McDonald and Popat, the concepts of combining targeted agents to isotoxic dose escalated accelerated RT are brought up. In addition, the authors concisely explain the molecular mechanisms of EGFR inhibitors related to treatment of NSCLC. Published studies in various clinical settings, including EGFR inhibitors with conventional fractionation RT alone, EGFR inhibitors with conventional fractionation sequential chemo-RT, EGFR inhibitors with conventional fractionation concomitant chemo-RT, and targeted agents with altered fractionation RT are discussed.

With more effective systemic therapy and advances in local therapy including minimally invasive surgery and SBRT, patients with oligometastatic lung metastases have now been considered as potential candidates for curative treatment and indeed, prolonged tumor local control rate and overall survival have been reported. Singh *et al.* in their original article in this special issue report their 34-case experiences utilizing SBRT in the treatment of oligometastatic cancer to the lung. Cases included patients with 1 to 5 lung metastases, tumor size <5 cm, and with locally controlled primary tumor. The median prescription dose was 50 Gy in 5 fractions. In parallel with experiences using SBRT for primary lung cancer, an excellent local control rate up to 80% in 3 years and no symptomatic pneumonitis were reported. This paper is surely original and important and it is expected to become a highly cited reference in the relevant field.

Radiologic lung changes occur in nearly all patients after SBRT. It is of paramount importance to distinguish between tumor recurrence and lung fibrosis after treatment for early intervention and therefore better results. In addition to summarize the current clinical approach for assessing response by conventional imaging modalities, such as CT or PET, Mattonen *et al.* focus their discussion on the emerging field of quantitative image feature analysis.

Lung cancer comprises of a heterogeneous group of tumor types and each type carries individualized genetic signature in multiple driver gene pathways. In addition to the conventional approach of surgical resection, chemotherapy, and RT, personalized approach to incorporate targeted treatment based on molecular abnormalities of the cancer has become a current trend and promising results have been reported. In the review article by Palmer *et al.*, lung cancer genetic aberrations and mechanisms of associated targeted therapy as well as novel biomarkers related to radiation pneumonitis are nicely elucidated.

Acknowledgements

Disclosure: The author declares no conflict of interest.

References

1. Mauguen A, Le Péchoux C, Saunders MI, et al. Hyperfractionated or accelerated radiotherapy in lung cancer: an individual patient data meta-analysis. J Clin Oncol 2012;30:2788-97.

Cite this article as: Chen YJ. Individualized altered fractionation as a more effective radiotherapy for non-small cell lung cancer. J Thorac Dis 2014;6(7):E161-E162. doi: 10.3978/j.issn.2072-1439.2014.06.39